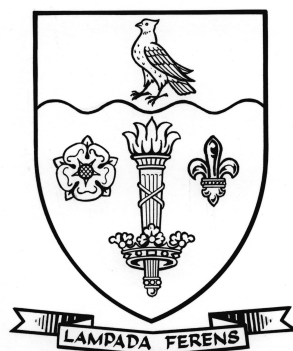


THE UNIVERSITY OF HULL



The Application of Continuous Flow Technology to the Expedient
Synthesis of Isotopically Substituted Compounds

being a Thesis submitted for the Degree of

Doctor of Philosophy

in [The University of Hull](#)

by

[Julian Hooper BSc \(Hons\)](#)

February 2008

*Dedicated to the loving memory of a talented geneticist whose PhD at
Cancer Research UK was cut short by the very disease that she was
working toward furthering an understanding of.*

Nicole Winkelmann BSc (Hons)

27th November 1978–28th September 2004

ACKNOWLEDGEMENTS

The following thesis, while an individual work, benefited from the insights and direction of many people.

Foremost thanks must go to my supervisor, Dr Paul Watts, for providing me with the opportunity to study for a PhD and also Dr. Charlotte Wiles whose time, tutelage and instructive comments have assisted greatly at every stage of the thesis process.

Of course accolades to members of the Department of Chemistry at The University of Hull are necessary, most notably Dr. Steve Clark for his assistance in device fabrication and Carol Kennedy for her help with elemental analysis. Additionally my thanks are extended to past and present colleagues from the micro-synthetic group for their continued friendship, help, comic relief and the occasional beer.

In addition to the people mentioned above I would also like to thank my family and in particular, my parents Nigel Anthony Hooper and Mary Fraser, who nurtured a passion for discovery and betterment which ultimately led me to undertake this work.

Lastly I must acknowledge my partner and best friend, Bridget Griffin whose love, encouragement, patience and support were critical in the successful completion of this project.

In conclusion, I recognize that this research would not have been possible without the financial assistance of The University of Hull and the EPSRC, and I express my gratitude accordingly.

ABSTRACT

ISOTOPICALLY modified compounds are of great importance to the scientific community owing to the large number of specific uses that exist for them; however, due to their low abundance associated costs are high. Once a small discrete isotopic precursor has been obtained, it must then be incorporated into a more complex molecule at the desired position which creates a major synthetic challenge owing to their limited availability. The difficulties encountered when obtaining isotopically enriched compounds result in phenomenal costs that mean even small quantities of simple molecules are extremely expensive to prepare; thus there is a need for expedient, cost effective and transferable syntheses involving isotopes.

In contrast to traditional synthetic techniques, continuous flow systems provide a superior route to the preparation of such molecules *viz* allowing the use of small, highly contained systems, stoichiometric quantities of reagents and generic methodology to deliver products in high yields and purities. The work contained herein exemplifies that by applying small scale, continuous flow technology to the traditional problems of synthesis involving isotopes, either stable or unstable, new developments can be realised which allow the rapid, efficient, controlled and contained preparation of labelled molecules.

General procedures have been developed which allow for the synthesis of isotopically substituted phenyl acetate, methoxybenzene, *N*-phenylacetamide and biphenyl derivatives in a timely manner using continuous flow systems. As proof of concept, small libraries comprising of compounds containing deuterium isotope labels were successfully prepared, generally in yields greater than 90% at a scale of 10's mg.

CONTENTS

Abstract	iii
Glossary of Terms	viii
1 Introduction	1
1.1 Isotopes	1
1.1.1 Isotope Effects	2
1.1.2 Sources of Isotopes	6
1.1.3 Uses of Isotopes	12
1.1.4 Issues Involving Synthesis with Isotopes	19
1.1.5 Isotope Analysis by Mass Spectrometry	19
1.1.6 Isotope Analysis by NMR Spectroscopy	20
1.2 Continuous Flow Reactors	22
1.2.1 Fabrication of Micro Reactors	23
1.2.2 Sealing Micro Reactor Channels	29
1.2.3 Fluidic Manipulation	30
1.2.4 Liquid Characteristics at Low Reynolds Numbers	32
1.2.5 Back Pressure	35
1.2.6 Micro Reactor Design Considerations	36
1.2.7 Continuous Flow Reactor Synthesis	38
1.2.8 Scale Out	45
1.3 Isotope Labelling In Continuous Flow Reactors	48

1.3.1	Literature Examples	48
1.3.2	Aims	52
2	C–O Bond Formation	53
2.1	Phenols and Carboxylic Acids	53
2.2	Acylation of Phenol Derivatives	54
2.2.1	Initial Micro Reactor Set Up	58
2.2.2	Solvent Studies within Micro Reactors	59
2.2.3	Further Reactions with <i>N,N</i> -Diethylethanamine	61
2.2.4	The Effect of Increasing Reactor Length	63
2.2.5	Acetylation in the Presence of DMAP	65
2.2.6	Effectiveness of Organic Bases in Acetylation Reactions	68
2.2.7	Inorganic Bases	68
2.2.8	Acetylation of Lithium Aryloxides	71
2.2.9	The Benzoylation of Phenol Derivatives	73
2.2.10	Summary of Acylation Reactions	76
2.2.11	Flow Synthesis of Deuterium Substituted Phenyl Acetate Derivatives	76
2.2.12	Analytical Considerations	77
2.3	Methylation of Phenol Derivatives	79
2.3.1	Preliminary Methylation Studies	80
2.3.2	Solvent Studies in Batch	81
2.3.3	Micro Scale Optimisation of Methylation Reactions	82
2.3.4	The Effect of Heating Micro Reactions	85
2.3.5	Flow Synthesis of Deuterated Methoxybenzene Derivatives	87
2.4	Methylation of Carboxylic Acids	89
2.4.1	Methods of Synthesis	89
2.4.2	Micro Reactor Methylation of Benzoic Acid	92
2.4.3	Alternative Methods of Methylation	93

2.4.4	Experiments with DMAP	93
3	C–N Bond Formation	95
3.1	Amides and Isotopes	95
3.1.1	Preparation of Labelled Amides	95
3.1.2	Methods of Synthesis	96
3.2	Acetylation of Primary Amines	97
3.2.1	The Schotten-Baumann Reaction	98
3.2.2	Evaluation of <i>N,N</i> -Diethylethanamine as a Base . . .	100
3.2.3	Optimising the Reactions for a Library of Amines . .	103
3.3	Benzoylation of Primary Amines	106
3.4	Synthesis of Deuterium Substituted Amides	107
3.5	Summary	108
4	C–C Bond Formation	110
4.1	The Suzuki-Miyaura Reaction	110
4.1.1	Reported Continuous Flow Methodology	111
4.2	Continuous Flow Set Up	115
4.3	Library Selection	116
4.4	Optimisation of Biphenyl Flow Synthesis	117
4.5	Library Generation	118
4.6	Revised Continuous Flow Set Up	118
4.7	Flow Synthesis of Biphenyl Derivatives	120
4.8	Synthesis of Deuterated Biphenyl Derivatives	122
4.9	Summary	124
5	Conclusions	125
5.1	Summary	125
5.2	Future Work	126
5.2.1	Potential Applications	127

6	Experimental Details	129
6.1	Materials	129
6.2	Instrumentation and Apparatus	130
6.3	Instrumental Methodology	131
6.3.1	GC-MS	131
6.3.2	GC-FID	132
6.3.3	HPLC	132
6.4	Batch Procedures	132
6.5	Micro Reactions	136
6.6	Preparation of Synthetic Standards	140
	References	164
A	Reactor Characteristics	179
A.1	Dimensions and Characteristics	179
A.2	Reynolds Numbers	181
A.3	Back Pressures	182
A.4	Fourier Numbers	183
A.5	Micro Reactor Data	183
B	CHN Analysis	188
C	Publications	191

GLOSSARY OF TERMS

Abbreviations

Acronyms

3-D	Three Dimensional	μTAS	Micro Total Analytical Systems
ADHD	Attention Deficit Hyperactivity Disorder	NMR	Nuclear Magnetic Resonance
AVLIS	Atomic Vapour Laser Isotope Separation	PET	Positron Emission Tomography
CAD	Computer Aided Design	RCY	Radiochemical Yield
CCD	Charge Coupled Detector	RF	Radio Frequency
CYTOS®	Continuously Operated System	RIE	Reactive Ion Etching
DRIE	Deep Reactive Ion Etching	RMD	Relative Mass Difference
EOF	Electroosmotic Flow	RSC	Royal Society of Chemistry
GC-FID	Gas Chromatography-Flame Ionisation Detector	RSD	Relative Standard Deviation
GC-MS	Gas Chromatography-Mass Spectrometry	RT	Room Temperature
HPLC	High Performance Liquid Chromatography	R _T	Retention Time
IR	Infra Red	SD	Standard Deviation
IR-MS	Isotope Ratio Mass Spectrometer	SEQUOS®	Sequentially Operated System
IUPAC	International Union of Pure and Applied Chemistry	SI	International System
LC-MS	Liquid Chromatography Mass Spectrometry	SPECT	Single Photon Emission Computed Tomography
LIGA	Lithographie Galvanoformung Abformung	TLC	Thin Layer Chromatography
mp	Melting Point	UK	United Kingdom
MS	Mass Spectrometry	USA	United States of America
		UV	Ultra Violet
		Vis	Visible

Punctuated Abbreviations

Ch.	Chapter	Ltd.	Limited
Conc.	Concentration	o.d.	Outer diameter
Ed.	Editor(s)	p.	Page
Edn.	Edition	pp.	Pages
Eq.	Equivalent(s)	Ref.	Reference
i.d.	Internal diameter	Sat.	Saturated
Inc.	Incorporated	Temp.	Temperature
Lit.	Literature	Vol.	Volume

Latin Abbreviations

<i>cf.</i>	<i>confer</i> (Compare)	<i>e.g.</i>	<i>exempli gratia</i> (For example)
<i>et al.</i>	<i>et alli</i> (And others)	<i>i.e.</i>	<i>id est</i> (That is to say)

Synonyms

Ar H	Aromatic proton	λ	Wavelength
br s	Broad singlet	M ⁺	Parent molecular ion
C ₀	Quaternary Carbon	m _U	Multiplet
d	Doublet	sep	Septet
δ_c	¹³ C-NMR chemical shifts	t	Triplet
δ_H	¹ H-NMR chemical shifts	t _{1/2}	Half life
Λ	Reflux		

Chemical Acronyms

Boc	<i>tert</i> -Butylformate	DMF	<i>N,N</i> -Dimethylformamide
Bu	Butyl	DMSO	Methylsulfinylmethane
DCC	<i>N,N'</i> -Dicyclohexylmethane-diimine	Et	Ethyl
DCM	Dichloromethane	FDG	2-Deoxy-2-fluoro-D-glucose
DMAP	<i>N,N</i> -Dimethylpyridin-4-amine	LSD	(8 β)- <i>N,N</i> -Diethyl-6-methyl-9,10-didehydroergoline-8-carboxamide

Me	Methyl	PIFA	(Pentafluorophenyl){bis-[(trifluoroacetyl)oxy]}- λ^3 -iodane
MeCN	Acetonitrile		
MeOH	Methanol	PTFE	Polytetrafluoroethylene
NMM	<i>N</i> -Methylmorpholine	TBAF	<i>N,N,N</i> -Tributylbutan-1-aminium fluoride
NMP	<i>N</i> -Methylpyrrolidone	TBAM	<i>N,N,N</i> -Tributylbutan-1-aminium methanolate
OAc	Acetate	TFA	2,2,2-Trifluoroacetic acid
OTf	Triflate	THF	Oxolane
PDMS	Dimethyl polysiloxane	TMS	Trimethylsilicon
PEEK™	Polyaryletheretherketone		
Ph	Phenyl		

Chemical Synonyms

Acamprostate	3-Acetamidopropane-1-sulfonic acid
Acetone	Propan-2-one
Aspirin	2-Acetyloxybenzoic acid
Carbon dioxide	Methanedione
Ciprofloxacin	1-Cyclopropyl-6-fluoro-4-oxo-7-piperazin-1-ylquinoline-3-carboxylic acid
Cocaine	Methyl (1 <i>R</i> ,2 <i>R</i> ,3 <i>S</i> ,5 <i>S</i>)-3- (benzoyloxy)-8-methyl-8-azabicyclo[3.2.1] octane-2-carboxylate
Doxorubicin	(7 <i>S</i> ,9 <i>S</i>)-7-[(2 <i>R</i> ,4 <i>S</i> ,5 <i>S</i> ,6 <i>S</i>)-4-amino-5-hydroxy-6-methyloxan-2-yl]oxy-6,9, 11-trihydroxy-9-(2-hydroxyacetyl)-4-methoxy-8,10-dihydro-7 <i>H</i> -tetracene-5, 12-dione
Eugenol	2-Methoxy-4-prop-2-enylphenol
K.2.2.2	4,7,13,16,21,24-Hexaoxa-1,10-diazabicyclo[8.8.8]hexacosane
D-Mannose triflate	1,3,4,6-Tetra- <i>O</i> -acetyl-2- <i>O</i> -trifluoromethanesulfonyl- β -D-mannopyranose
Melatonin	<i>N</i> -[2-(5-Methoxy-1 <i>H</i> -indol-3-yl)ethyl]acetamide
(\pm)-Oxomaritidine	(4 <i>aR</i> ,10 <i>bS</i>)-8,9-Dimethoxy-4,4 <i>a</i> -dihydro-3 <i>H</i> ,6 <i>H</i> -5,10 <i>b</i> -ethanophenanthridin-3-one
Paracetamol	<i>N</i> -(4-Hydroxyphenyl)acetamide
Pristane	2,6,10,14-Tetramethylpentadecane

Raclopride	3,5-Dichloro- <i>N</i> -[(1-ethylpyrrolidin-2-yl)methyl]- 2-hydroxy-6-methoxy-benzamide
Tamiflu	Ethyl (3 <i>R</i> ,4 <i>R</i> ,5 <i>S</i>)-4-(acetylamino)-5-amino-3-(1-ethylpropoxy)-cyclohex-1-ene-1-carboxylate
Taxol®	(2 α ,4 α ,5 β ,7 β ,10 β ,13 α)-4,10-Bis(acetyloxy)-13-[(2 <i>R</i> ,3 <i>S</i>)-3-(benzoylamino)-2-hydroxy-3-phenylpropanoyl]oxy-1,7-dihydroxy-9-oxo-5,20-epoxytax-11-en-2-yl benzoate
Toluene	Methylbenzene
Urea	Diaminomethanal
Vanillin	4-Hydroxy-3-methoxybenzaldehyde
Water	Oxidane

SI Unit Definitions

%	Percent	m	Metre(s)
"	Inch(es)	M	Mole(s) per litre
°	Degree(s)	mg	Milligram(s)
°C	Degree(s) centigrade	MHz	Megahertz
Å	Angstrom(s)	min	Minute(s)
cm	Centimetre(s)	ml	Millilitre(s)
cPa	Centipascal(ss)	mm	Millimetre(s)
Da	Dalton(s)	mM	Millimole(s) per litre
dm	Litre(s)	mmol	Millimole(s)
F	Farad(s)	mol	Mole(s)
fs	Femtosecond(s)	mPa	Millipascal(s)
g	Gram(s)	mV	Millivolt(s)
hr	Hour(s)	M Ω	Megaohm(s)
Hz	Hertz	N	Newton(s)
J	Joule(s)	ng	Nanogram(s)
K	Kelvin	nl	Nanolitre(s)
kg	Kilogram(s)	nm	Nanometer(s)
kJ	Kilojoule(s)	ns	Nanosecond(s)
kV	Kilovolt(s)	Ω	Ohm(s)
		Pa	Pascal(s)
		ppb	Part(s) per billion

ppm	Part(s) per million	μl	Microlitre(s)
s	Second(s)	μm	Micrometre(s)
V	Volt(s)	μmol	Micromole(s)
W	Watt(s)		

Mathematical Nomenclature

Notation

A	Area of cross section (m^2)	m/z	Mass to Charge Ratio (dimensionless)
D	Diffusion coefficient ($\text{m}^2 \text{s}^{-1}$)	n	Arbitrary non-negative integer (dimensionless)
E	Energy (J)	P	Pressure (Pa)
e	Irrational constant (≈ 2.718 , dimensionless)	p	Negative log (dimensionless)
F	Electric field strength (V m^{-1})	R	Resistance (Ω)
$ Fo$	Fourier number (dimensionless)	r	Radius (m)
G	Gibbs free energy (J)	Re	Reynolds Number (dimensionless)
H	Enthalpy (J)	R_T	Residence Time (s)
h	Planck's constant ($\approx 6.63 \times 10^{-34} \text{ J s}$)	S	Entropy (J K^{-1})
I	Spin quantum number (dimensionless)	S/V	Surface to Volume Ratio (m^{-1})
J	Coupling constant (Hz)	T	Temperature (K)
K	Equilibrium constant (units vary)	t	Time (s)
k	Rate constant (units vary)	V	Volume (m^3)
L	Length (m)	w	Width (m)
m	Mass (kg)	x	Arbitrary Distance (m)

Greek Letters

Δ	Difference	ζ	Zeta potential (V)
δ	Hydraulic diameter (m)	η	Dynamic viscosity (Pa s^{-1})
ϵ	Relative permittivity (units vary)	Θ	Circumference (m)

κ Constant (units vary)	ρ Density (kg m^{-3})
μ Reduced mass (kg)	σ Height/Depth (m)
ν Frequency (Hz)	Φ Flow Rate (units vary)
π Pi (dimensionless)	

Subscripts

a Species a	M Mask
AH Acid	max Maximum
B Boltzmann	o Free space
b Species b	s Spring
c Channel	T Tube
ϕ Flow	$TRANS$ Transmission
G Gas	V Volumetric
L Linear	

Superscripts

\ddagger Transition state

CHAPTER 1

INTRODUCTION

1.1 Isotopes

THE International Union of Pure and Applied Chemistry (IUPAC)¹ define isotopes as:

“Nuclides having the same atomic number but different mass numbers.”

From an atomic perspective the isotopes of an element, which occur in both stable and unstable forms, are one of two or more atoms that have the same number of protons, but a different number of neutrons. A stable isotope may be defined as a naturally occurring isotope of an element that exhibits no tendency to decay. Conversely unstable isotopes undergo spontaneous radio-degradation to more stable elemental forms, through the emission of α or β particles, or γ rays, which leads to a subsequent decrease in the atomic mass. The relative abundance of an element's isotopes is not constant, for example on earth the ratio of ^{13}C to ^{12}C atoms is approximately 1.1 : 98.9, but this is an average value and localised concentrations vary.

Hydrogen is the only element whose isotopes are given specific names and as an example their atomic structure is shown in Figure 1. The heaviest is tritium which contains one proton and two neutrons and is an unstable isotope whereas

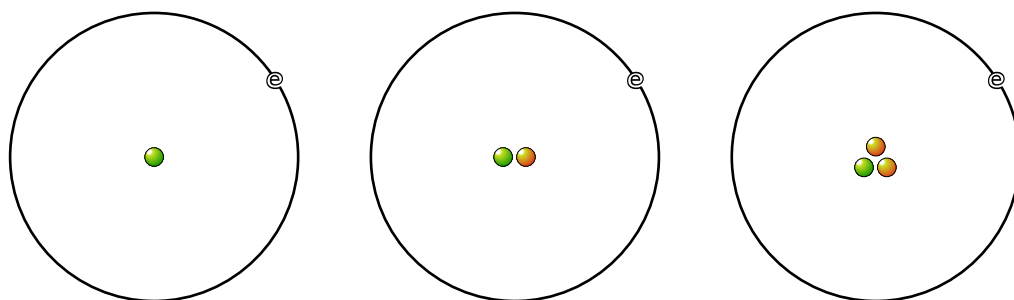


Figure 1. The isotopes of hydrogen; protium (left), deuterium (middle) and tritium (right).

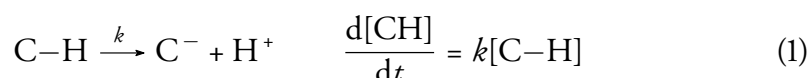
deuterium and protium* are stable. It is possible to separate deuterium from protium as it has a natural abundance of 0.015 % and although tritium also has a natural abundance, from sources such as nuclear reactions, it is commonly formed using techniques such as the neutron bombardment of protium.²

1.1.1 Isotope Effects

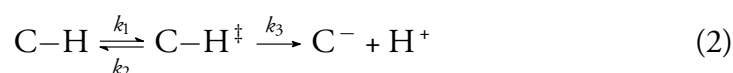
As defined by IUPAC,³

“The effect on the rate or equilibrium constant of two reactions that differ only in the isotopic composition of one or more of their otherwise chemically identical components is referred to as a kinetic isotope effect or a thermodynamic (or equilibrium) isotope effect, respectively.”

In order to explain this effect consider the cleavage of a C–H bond



with respect to transition state theory.⁴ When viewed as proceeding through an activated complex the process may be broken down into a two step concerted process as follows:



As Figure 2 illustrates the activated complex, C-H^\ddagger , represents the potential energy maximum of the reaction coordinate and is considered to be in equilibrium with the reactant which allows an equilibrium constant, K^\ddagger , for the first step of

*It should be noted that protium is itself normally referred to as hydrogen.

the reaction to be expressed as:

$$K^\ddagger = \frac{k_1}{k_2} = \frac{[\text{C-H}^\ddagger]}{[\text{C-H}]} \quad (3)$$

In a similar way the rate of the second step of the reaction is expressed by:

$$\frac{d[\text{CH}^\ddagger]}{dt} = k_3[\text{C-H}^\ddagger] = k_3 K^\ddagger [\text{C-H}] \quad (4)$$

The transition state rate constant, k_3^* , may also be expressed from a statistical viewpoint as follows:

$$k_3 = \frac{\kappa_B T}{h} \quad (5)$$

where κ_B is the Boltzmann constant ($\approx 1.381 \times 10^{-23} \text{ J K}^{-1}$), T is the temperature (K) and h is Planks constant ($\approx 6.63 \times 10^{-34} \text{ J s}$). Substitution of (5) into (4) gives the modified rate expression

$$\frac{d[\text{CH}^\ddagger]}{dt} = \frac{\kappa_B T}{h} K^\ddagger [\text{C-H}] \quad (6)$$

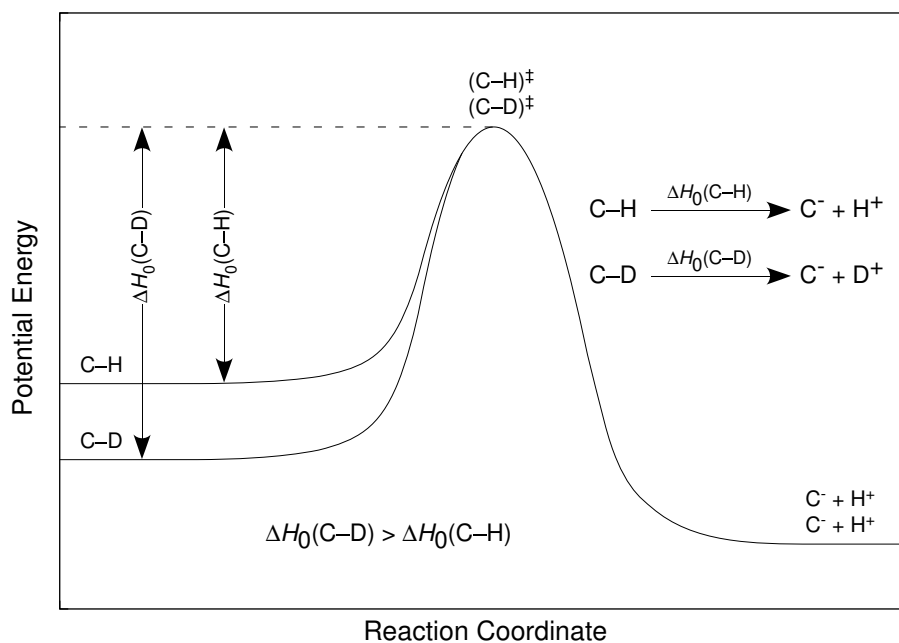


Figure 2. Differences in the reaction coordinate according to isotope discrimination. The potential energy of the activated complex, C-H^\ddagger is not altered to any appreciable degree because the force constant for such a species is so low.

*The transition state constant, k_3 , is considered to be equal to the product of the vibrational frequency, ν and the transmission constant, κ_{TRANS} , which is assumed to be equal to 1. For the purposes of this explanation however it is sufficient to represent it without further expansion.

which will also be equal to the overall rate of reaction,

$$\frac{d[\text{CH}]}{dt} = k[\text{C-H}] \quad (7)$$

Therefore by combining (6) and (7) an expression for the overall rate constant, k , is derived as:

$$k = \frac{\kappa_B T}{h} K^\ddagger \quad (8)$$

Thermodynamically the equilibrium constant, K^\ddagger , is related to the Gibbs free energy by:

$$K^\ddagger = e^{\frac{-\Delta G^\ddagger}{\kappa_G T}} \quad (9)$$

where the Gibbs free energy, ΔG^\ddagger , is composed of the standard free energy of activation, ΔH^\ddagger , and entropy, ΔS^\ddagger , equal to:

$$\Delta G^\ddagger = \Delta H^\ddagger - T\Delta S^\ddagger \quad (10)$$

Combining (9) and (10) gives:

$$K^\ddagger = e^{\left(\frac{\Delta H^\ddagger}{\kappa_G T}\right)} e^{\left(\frac{\Delta S^\ddagger}{\kappa_G}\right)} \quad (11)$$

which, when substituted into (8) yields the Eyring equation:

$$k = \frac{\kappa_B T}{h} e^{\left(\frac{\Delta H^\ddagger}{\kappa_G T}\right)} e^{\left(\frac{\Delta S^\ddagger}{\kappa_G}\right)} \quad (12)$$

As can be seen from Figure 2 the value of ΔH is greater for a heavier isotopologue and thus the rate of reaction, given by (12) is reduced accordingly. The reason for this lies within quantum mechanical theory.⁵ The vibrational frequency of a diatomic molecule, approximated for a simple harmonic oscillator is given by;

$$\nu = \frac{1}{2\pi} \sqrt{\frac{\kappa_s}{\mu}} \quad (13)$$

where ν is the vibrational frequency (s^{-1}), κ_s is the spring constant (N m^{-1}) and μ is the reduced mass (kg). The value of μ is an approximation which allows a diatomic system to be treated as a whole of its constituent parts and may be

subsequently broken down as;

$$\mu = \frac{m_a m_b}{m_a + m_b} \quad (14)$$

where m_a and m_b are the masses (kg) of atoms a and b respectively. The kinetic isotope effect becomes apparent when one considers the quantum mechanical equation for the energy of an n^{th} level harmonic oscillator,

$$E_n = h\nu \left(n + \frac{1}{2} \right) \quad (15)$$

where E_n is equal to the individual bond energy (J), h is Planck's constant ($\approx 6.63 \times 10^{-34}$ J s), ν is the vibrational frequency (s^{-1}) and n is the harmonic oscillation level ($\lim_{n \rightarrow +\infty} n$). Classically it then follows that a heavier atom with greater reduced mass, μ , will have a lower vibrational frequency, ν , and hence the zero point energy (*i.e.* where $n = 0$) will be lower, as shown in Figure 2, leading to a greater value for ΔH and a slower rate of reaction, according to the derived Equation 12.

Whilst the described effect is true of all isotopes, it is not usually noticeable and is most pronounced in cases where the relative mass difference (RMD) of the isotopes is at its greatest. As a result, where ^{12}C is replaced with ^{13}C only an 8.0% mass increase occurs and since the relative mass change is small, labelling a molecule with ^{13}C atoms is intrinsically safe with respect to mammalian studies since the isotopic substitution does not alter the molecules reactivity *in-vivo*; it may be expected to act in an analogous way to its isotopically unmodified counterpart.⁶ In contrast the RMD for protium/deuterium substitution is 100%, although in reality the effect of deuterium substitution in a labelled biomolecule will only lead to toxic side effects when the levels of deuteration are in excess of 15.0% of body water, possible only after consuming purely deuterated water for a number of days and thus extremely unlikely to ever occur with administered drugs.⁷

In conclusion, it should be noted that the work carried out for this project involved the substitution of C–H moieties for C–D moieties. In this case, the isotopic

substitution does not give rise to any observable difference in the rate of reaction, since the hydrogen isotopologues were located at unreactive positions which played no part in bond breaking or formation during a reaction. Thus it was possible to optimise reactions using the cheaper, protonated precursors, prior to isotope labelling by substitution of protium for deuterium.

1.1.2 Sources of Isotopes

It is common for radioisotopes to be manufactured directly, for example by the neutron bombardment of a suitably purified target material, whereas stable isotopes are most often obtained by the concentration or 'fractionation' of naturally occurring compounds which contain a mixture of isotopes. Generally speaking it is possible to separate isotopes using any physical or chemical process and there exists a number of methods to obtain enriched isotopes, depending upon the particular properties of the element in question. The separation process can be somewhat difficult to achieve since any two isotopes of an element exhibit very similar chemical properties. However using techniques exploiting differences in electromagnetic, centrifugal or diffusion coefficients, separation based on atomic weight may be achieved.⁸ Similarly, many common chemical separation methods take advantage of differences in reaction rates or nuclear resonances (*e.g.* by way of laser excitation). Industrially the large scale separation of isotopes is carried out *via* a series of cascading steps whereby sequential increases in purity occur and un-enriched partitions are recycled to ensure maximum process efficiency.⁹ Due to these factors, obtaining purified isotopes is a time and energy intensive process, contributing greatly to their high cost. This then adds to the need for synthesis with isotopes to be highly efficient, thus offsetting some of the cost associated with work of this nature.

Distillation Although conventional distillation allows the separation of components with boiling points differing by about $\pm 10^\circ\text{C}$, it is necessary for the process to be much more selective in the case of isotopic enrichment since the isotopologues differ in boiling point by only tenths of a degree. Consider the phase diagram illustrating the concept of distillation that is shown in Figure 3. As the

temperature composition of the liquid and pressure phases of two isotopologues is so similar, the difference between them is small meaning that the number of steps, or theoretical plates required to enrich an isotopic mixture is extremely large. As such, a distillation column, up to 213 m in length,^{*} containing a wettable packing compound is required. Heating the top and cooling the bottom of the tower establishes a constant equilibrium between vapour and liquid phases which, over time, become steadily enriched in the lighter and heavier isotopes respectively and partitioning of the isotopologues is achieved. It is possible to take advantage of the differing boiling points of D₂O and H₂O (101.4°C and 100.0°C respectively), however the low natural abundance of deuterium in water (< 200 ppm) makes deuterium enrichment by this method alone impractical as a huge amount of energy is required in return for the enrichment obtained.¹⁰ Isotopic distillation works well for compounds which are relatively light and gaseous, for example separation of isotopes such as ¹²C and ¹³C from carbon monoxide and ¹⁴N and ¹⁵N from nitric oxide or nitrogen dioxide is possible using cryogenic methods, where low temperatures cause condensation of these gases.¹¹

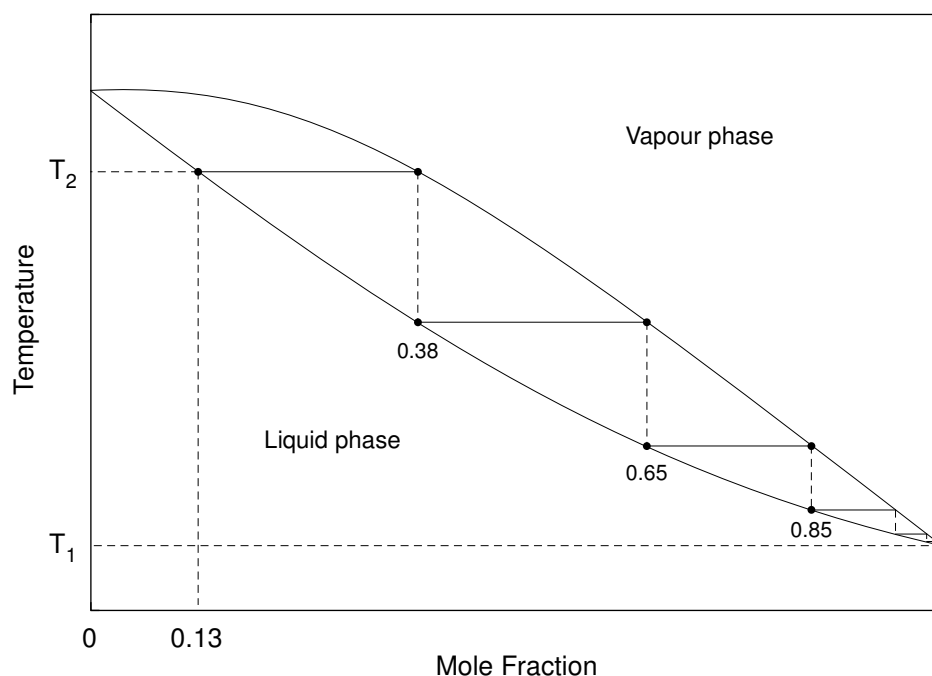


Figure 3. A phase diagram illustrating the concept of distillation over a number of boiling and condensation steps (theoretical plates) which sequentially leads to a greater mole fraction of the more volatile component being obtained.⁴

^{*}Required when separating isotopes of carbon from CO.

Plasma Separation Plasma separation is another technique which may be used to enrich stable isotopes in potentially large quantities.¹² The modern process works by bombarding a metallic feed target with microwaves causing the formation of a plasma. Heated electrons result in the generation of ions which are accelerated by an applied magnetic and electric field causing them to travel down a vacuum chamber with helical momentum. Collector plates are placed specifically at the other end of the chamber and selectively catch the ions such that isotopic separation is achieved. Although first reported in 1971 by Bonnevier,¹³ the widespread use of plasma separation is still in its infancy, although the possibility for specific large scale production will ensure its continued development and uptake by both the industrial and scientific community.

Cyclotron Production Cyclotrons, conceived by Ernest O. Lawrence in 1939, for which he was awarded the Nobel prize in physics,¹⁴ permit the formation of short lived radioisotopes, in particular for use within medicinal, diagnostic and research applications. They are a type of particle accelerator and as opposed to linear units, nucleons are forced to travel with a spiralling trajectory by a magnetic field so an applied accelerating voltage is encountered many times. In this way high speeds are achieved in return for a relatively small instrument size. When the high energy particles formed within the cyclotron unit reach the edge of the carousel they are directed into a chamber which contains a stable isotope. Bombardment of the target by the high energy beam initiates nuclear reactions and it is thereby converted into a corresponding radioactive isotope.

Electromagnetic Separation Calutrons are capable of extremely specific isotopic separation for literally any element and are, in essence, extremely large mass spectrometers.¹⁵ Representing the contentious side of isotope research the name derives from the early evolution of the California University cyclotron which was used to enrich uranium for weapons development as part of the famed Manhattan Project during the 1940's. Taking advantage of the differing mass to charge ratios of one or more isotopes within the confines of an electric field, electromagnetic separation is achieved through the varying deflection paths of such ions, as illustrated in Figure 4. Although capable of exceptionally high purity enrichment,

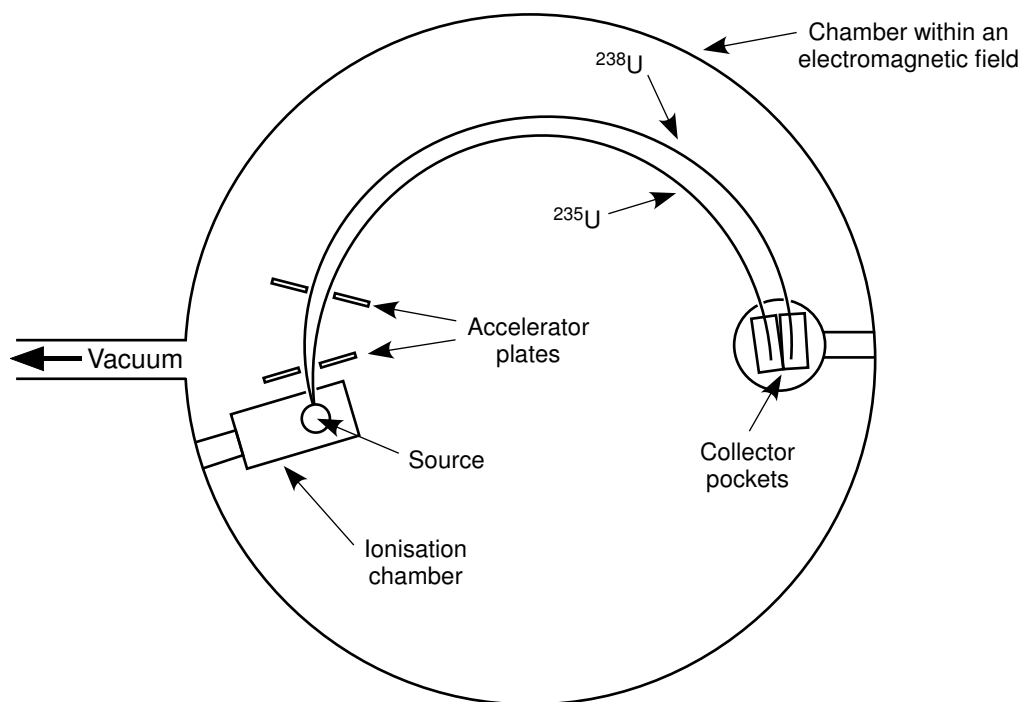


Figure 4. A schematic of the calutron conceived by E. O. Lawrence to separate mixtures of uranium isotopes, adapted from the original patent application.¹⁶

in modern times calutrons are rather inefficient and larger commercial units are being phased out due to the inflated costs associated with running them—ions must be neutralised by electrons which requires large energy expenses in return for a relatively low throughput.¹³

Laser Isotope Separation Laser based separation may be achieved using either atomic or molecular methods which allow the direct manufacture of isotopes by the irradiation of a suitable species at a specifically tuned frequency.¹⁷ The technique is not currently in widespread use and has only emerged recently, being complemented by advances in laser technology since the 1970's and Americas uranium atomic vapour laser isotope separation program; established in 1973 to find a way of enriching the ore at lower cost than either gaseous diffusion or gas centrifugation. Generally a unenriched mixture is introduced to the system as a vapour or gas where a finely tuned laser is set to excite and ionise a specific isotope, which is then separated by the application of an electric field. In addition to uranium enrichment one other example is the separation of ${}^6\text{Li}$ and ${}^7\text{Li}$, which has been achieved to a high degree of selectivity.¹⁸ In practice laser isotope

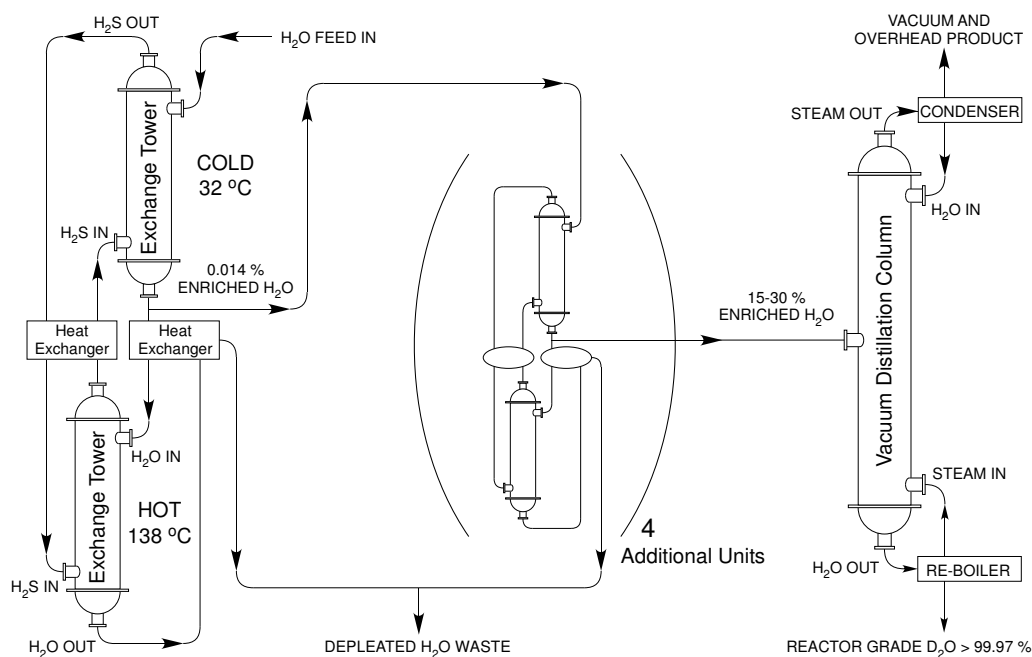


Figure 5. Commercial production of D_2O by the Girdler–Sulfide process.⁹

Electrolysis Research into electrolytic methods of isotope separation began in 1932 when Washburn and Urey¹⁹ reported that water obtained from commercial electrolytic cells contained increased concentrations of deuterium. The process is possible by way of the kinetic isotope effect and is not thermodynamically controlled as many other separation processes are. If a solution is electrolysed to produce a gas from one of the elements of that mixture the rate of dissociation from the bulk solution will differ according to the mass of the particular isotope. In this way when water undergoes electrolysis it is possible to produce D_2O since the dissociation of H_2O proceeds at a faster rate, so becoming steadily enriched in the heavier isotope. After reducing feed water by about 25 000 times, 99.9% D_2O may be obtained however in practice a cascade system is difficult to implement since liberated gases must be re-combined which becomes an energy intensive process. For this reason industrial isotope enrichment by electrolysis is not very efficient and its main use is in the final stage purification of heavy water.²⁰

Diffusion Either gaseous or thermal methods may be exploited for the enrichment of isotopes by the mode of diffusion.⁸ The process relies on the fact that, according to their masses, two discrete isotopes exhibit slightly different diffusion

coefficients. Although the magnitude of the difference is small process refinements such as the application of pressure allow the speed of separation to be greatly enhanced. Principally, forcing a fluid (typically a gas) through a membrane with a small pore size (10 nm to 100 nm), achieves isotopic separation since statistically the lighter isotope is more likely to find its way past the resistive barrier. As the mass difference is small, so too is the degree of separation but applying a cascade of steps negates this problem and allows high levels of isotopic purity to be attained. For these very reasons however, the process itself is expensive but may nonetheless be extensively applied since many simple compounds exhibit the potential for such isotopic diffusional partitioning.

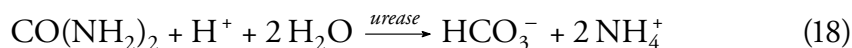
Summary In summary, the aforementioned examples illustrate some of the techniques that are available to obtain isotopically labelled molecular precursors. However given that all are extremely expensive processes the isotopes thus obtained must be incorporated into desired targets as efficiently as possible. For this reason the aim of this work is to develop such techniques through the investigation of novel labelling methodologies.

1.1.3 Uses of Isotopes

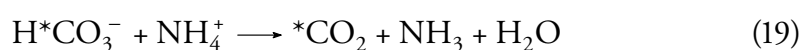
Many uses for isotopes now exist within modern research including medicinal, diagnostic and biosynthetic studies. There follows a short introduction to the most common of these areas, all of which employ isotopes as specific markers. As explained earlier, the extra mass of an isotope does not necessarily alter the chemistry or properties of the compound to which it belongs. Exploitation of this unique property is wide ranging, providing a valuable tool with which to probe the workings of specific systems.

Diagnosis Both stable and radio isotopes are utilised within a medicinal setting as a tool to provide diagnostic and non-invasive internal imaging. The urea breath test is an elegant example of the former and allows the detection of *helicobacter pylori*, a bacterium linked to stomach ulcers and certain cancers, which lives in the human stomach and intestine.²¹ The test is based upon the fact that urease,

an enzyme used by the bacteria to control the pH of its local environment, will be present in the stomach. This enzyme catalyses the conversion of urea into hydrogencarbonate and ammonium as follows:



If ^{13}C or ^{14}C labelled urea is administered to a patient and the bacteria is present it will be broken down and the isotope will find its way into the blood stream where it is incorporated into labelled carbon dioxide, $^*\text{CO}_2$, as shown by Equation 19.



Therefore, analysis of the patients breath by Isotope Ratio-Mass Spectrometry (IR-MS) or using a β -counter ~ 30 min after ingestion will reveal if the bacteria is present and an appropriate diagnosis can then be made.

PET The use of radioactive isotopes in diagnostic and imaging techniques is perhaps most well known and widespread in Positron Emission Tomography (PET).²² Here a biologically active molecule is labelled with a short lived radioisotope, the most common example being 2-deoxy-2- ^{18}F fluoro-D-glucose (^{18}F FDG) **1** ($t_{1/2} \approx 110$ min), which is illustrated in Figure 6. It is extensively used within oncology to image cancerous tumours²³ since, when glucose labelled in this way is administered to a patient, the ^{18}F FDG **1** concentrates within the tumour cells with greater density than the surrounding tissue. The patient is then placed in a PET scanner, which is essentially a large cylinder made from a scintillating material such as bismuth germanate,²⁴ that allows imaging to be undertaken. When one of the ^{18}F atoms undergoes β^+ radio decay a positron is emitted which has a short lifetime and, after travelling a couple of millimetres,

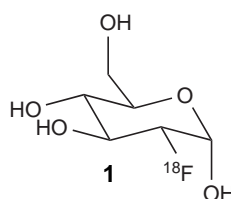


Figure 6. The structure of ^{18}F FDG **1**.

combines with an electron emitting two high energy photons which travel with equally opposite trajectories. When these hit the scintillator, an electrical signal is generated which is processed by a micro computer. Photons arriving more than 10's ns apart are ignored and in this way the point of origin may be resolved by comparing the flight times of those with an angle of incidence that is exactly 180°. Over time, after detecting many such events, an accurate three dimensional image is constructed which can greatly aid in locating and diagnosing cancers.

Imaging *via* PET is not only an extremely helpful technique where complex surgery is required, but also in understanding the functioning of the human body. For example, imaging areas within the brain that isotopically modified cocaine **2** concentrates has furthered an understanding of the action of this often abused drug.²⁵ In a similar way raclopride **3** has also been labelled, using ¹¹C, in order to assess the degree of binding to dopamine receptors, along with their distribution and density within the human brain.²⁶ This has provided a valuable method by which Parkinson's disease, Huntington's disease, tardive dyskinesia* and schizophrenia may be studied, thus enabling the more timely development of new treatment methods.

SPECT Single Photon Emission Computed Tomography (SPECT) is another computerised scanning technique which supplies similar information to PET, but relies instead on the detection of γ radiation to provide the mode of imaging.²⁷ After admission of a suitable imaging agent, a gamma camera is rotated around a scanning stage on which the patient is placed. The total angle of rotation and number of images or 'projections' that are taken depends on the type of scan being undertaken. Once acquired these are then processed by micro computer to render a 3-D representation of the imaged region which, in a similar way to PET, can be used to diagnose diseases and directly probe processes as they occur *in-vivo*. One radioisotope that has found particular use within this field of research is ^{99m}Tc which is a metastable isotope. It decays rapidly to ⁹⁹Tc *via* the emission of γ rays, allowing for a scan of the patient to be undertaken and then more slowly by the emission of softer β rays. The short half life ($t_{1/2} \approx 6$ hr) therefore makes it

*A condition that is caused by the long term use of drugs prescribed for psychiatric disorders.

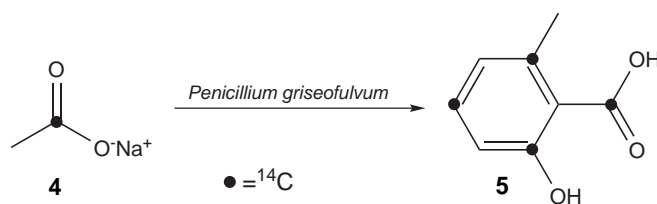
a useful isotope for medicinal applications since both SPECT and PET data may be collected whilst radiation exposure to the patient is minimised.

Radiotherapy Another application of radioisotopes within the field of nuclear medicine is for the non-invasive, *in-vivo*, therapeutic treatment of cancers *via* ionising radiation, chemotherapy perhaps being the most well known example.²⁸ The premise is simple and relies on the same targeting principles as those applied to molecular imaging, introduced above. If a vector carrying a radionuclide can sufficiently localise within a tumour and the degree (of penetration) of nuclear energy can be controlled, then it is possible to specifically target certain areas within the body and kill off unwanted cells, without the need for painful, complicated and time consuming invasive surgery.

Molecular Targeting The delivery of a particular isotope in the field of nuclear medicine relies on a number of different methods.²⁸ For example the isotope can be directly incorporated into the molecule of interest and thus localise on the receptors of interest, as occurs with [¹⁸F]FDG **1**. In the case of metal based isotopes, the mode of delivery is usually achieved by binding the metal to a chelator and then linking the resulting complex to a vector which may be a protein or antibody. One problem with this approach is the time taken by the vector to reach its target; diffusion of such large structures through cellular membranes can take days, not the ideal situation when working with short lived radioisotopes. One approach to circumvent this problem is to allow for the slow delivery of a pre-targeting agent to the receptor which, once bound, provides a secondary target thus allowing for fast delivery of the radionuclide.

Biosynthetic Studies Within a laboratory orientated setting, another good example of isotope use is for tracer analysis, exploited in the 1950's to elucidate biosynthetic pathways, in particular within plants and bacteria.²⁹ The real uptake of this area of research however came in the 1970's when NMR spectroscopy became more accessible and allowed the study of natural products containing isotopic labels (see Section 1.1.6).³⁰

One example of biosynthetic labelling, shown in Scheme 1, is the use of sodium

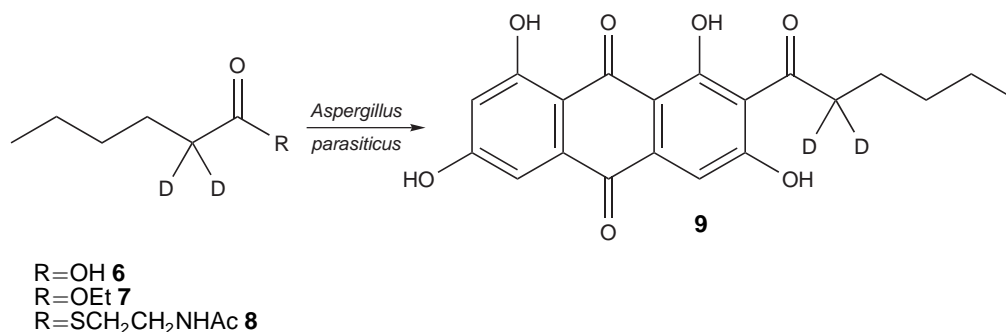


Scheme 1. The incorporation of sodium [1- ^{14}C] acetate **4** into 2-hydroxy-6-methyl[2,4,6- ^{14}C]benzoic acid **5**.³¹

[1- ^{14}C]acetate **4** to prove the hypothesis that polyketone chains could cyclise to form phenolic products. The biosynthetic head to tail linkage of sodium acetate groups and subsequent ring formation to afford the cyclic product, 2-hydroxy-6-methyl[2,4,6- ^{14}C]benzoic acid **5**, was determined when the labelled acetate **4** was fed to *Penicillium griseofulvum*.³¹ The metabolite was found to have ^{14}C labels incorporated into multiple positions, helping to confirm the validity of the proposed polyacetate mechanism.³² An important aspect of the research outlined above is that sodium acetate is a small and readily available molecule, so such work may be conducted at a low cost and in a timely fashion. However this is not always the case and when undertaking biosynthetic studies more complicated labelled molecules are often required, which must be synthesised on demand, purchased, or custom ordered from a specialist chemical supplier.

Biosynthetic experiments undertaken by Mc Keown *et al.*³³ illustrate one example of the need for more complex pre-metabolites. Feeding of [2- D_2]hexanoate, in the form of the free acid **6**, ethyl ester **7** and the *N*-acetylcysteamine thioester **8**, to cultures of *Aspergillus parasiticus* concluded that the compounds were all incorporated into the metabolite **9**, to differing degrees, according to the route shown in Scheme 2. The point to be emphasised in this example is that the precursors were structurally more complex than sodium [1- ^{14}C]acetate **4**, mentioned previously, and the labelled compounds **6–8** had to be obtained with the same core, but differing functionalities—a more expensive and time consuming requisite.

Metabolic Studies Deducing the fragmentation of a bioactive molecule and its fate in metabolic systems, is also possible through the use of incorporated

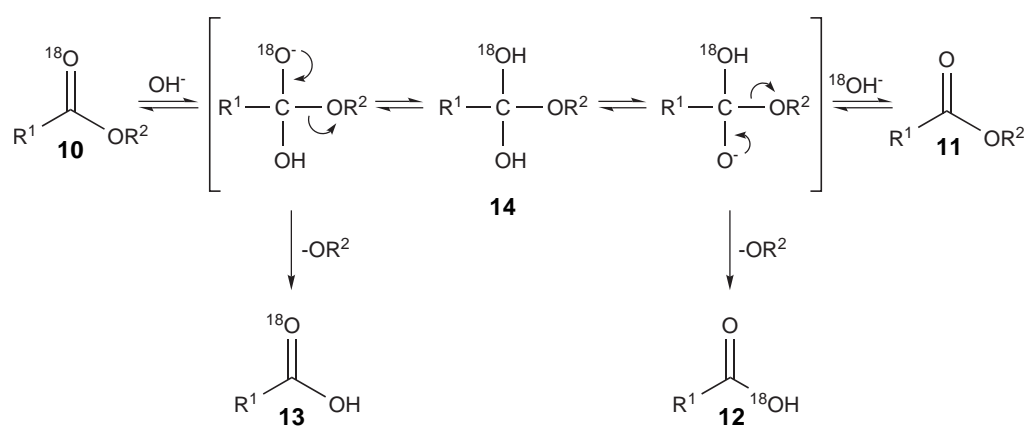


Scheme 2. The incorporation of three deuterium labelled hexanote derivatives into metabolite **9** after feeding cultures of *Aspergillus parasiticus*.³³

isotope labels.³⁴ An elegantly simple example is the doubly labelled water method developed in 1949 by Lifson *et al.*³⁵ The study allows the energy expenditure of an animal to be determined through the premise that ^{18}O in labelled water appears as $[^{18}O]CO_2$ exhaled by the animal. Incorporating an additional label by replacing H with D results in eliminated water becoming deruterated. By measuring and comparing the difference between the elimination rates of D_2O and $[^{18}O]CO_2$ the carbon dioxide production rate may be calculated which in turn can be converted into energy expended. This early example highlights the effectiveness of incorporating double labels as an accurate way of determining the fractional absorption of a molecule. Techniques such as this are desirable within a clinical setting since only one test and sample (blood or urine) is required in order to make a diagnosis or determination and as a result the doubly labelled water method is still used to this day for human studies.

Mechanistic Elucidation Furthering an understanding within the chemical sciences by discovering the mechanism by which a reaction proceeds can help improve yields through better management of the conditions under which it is performed. In order to elucidate such a pathway studies involving isotopes, which take advantage of the kinetic isotope effect (Section 1.1.1), are undertaken.³⁶ One example of particular relevance (see Chapter 2) is the tetrahedral transition state formed during certain acylation and hydrolysis reactions which is known to exist because of investigations conducted in 1951 by Bender,³⁷ involving the stable isotope ^{18}O , as shown in Scheme 3. It was noticed that when partially hydrolysing esters labelled with ^{18}O (at the carbonyl group **10**) under alkaline conditions, the

proportion of compound that contained the isotope label decreased. A similar result was also seen when undertaking an analogous study under acidic conditions. As a result, mixtures of ^{16}O and ^{18}O containing esters (**11** and **10** respectively) and hydrolysis products (**12** and **13** respectively) were obtained, the analysis of which made it possible to determine the level of isotopic substitution that occurred during the reaction. The investigation concluded that the only way this can occur is *via* the formation of a tetrahedral intermediate **14**, since from this structure reversion to the original starting material is possible through the loss of either oxygen.



Scheme 3. The formation of a tetrahedral intermediate **14** and its reversion to labelled **10** and unlabelled carboxylic acid derivative **11**.³⁷

Authentication The production of counterfeit drugs by clandestine operations is a particular problem for the pharmaceutical industry.³⁸ When a large capital expenditure is invested into the development of an active compound, for which the optimal synthetic route is patented, it is obvious that a profit should be made in order for the company to successfully continue in business. Additionally consumer confidence may be damaged if clandestine drugs find their way to the open market which can have detrimental effects for the company involved. Stable isotopic labelling of pharmaceuticals is an emerging use of labelled molecules which provides a simple tool for product security and authenticity. Incorporating labels to act as a combination lock allows the unique identity and origin of a particular batch to be determined.* Since the cost to exactly reproduce a

*It is not always necessary to actually carry out labelling since the exact fingerprint of a batch is likely to differ due to localised natural abundance regardless.

combination of isotopes would be far more expensive than purchasing the product commercially this method of security helps circumvent the emergence of counterfeit pharmaceuticals.³⁸

1.1.4 Issues Involving Synthesis with Isotopes

It should be emphasised that production of drugs suitable for the types of molecular imaging or therapy discussed, is difficult due to the short half lives of radioisotopes necessitated by the techniques. For this reason a cyclotron capable of producing the radioisotope needs to be located close to a hospital offering such a service. As the post-production time increases radioactive decay and sample degradation (*via* radiolysis) results in a greater volume of the drug being administered. Whilst chelation of metals relies on simple chemical methods which are themselves rapid (to the extent that they have become known as ‘shake and bake’), the need for shielding and mechanisation is still an issue. Although the work presented herein has used stable isotopes, the rapid synthesis and potential for automation lends itself well to transfer of the technology for use in radio pharmaceutical synthesis (see Section 1.3).

1.1.5 Isotope Analysis by Mass Spectrometry

The isotopic constituents of a sample may be determined using a number of methods and is necessary in order for any related research area to be effective in its work. The chosen technique depends on the information required as both qualitative or quantitative analysis is possible. For example, an IR-MS is an instrument capable of measuring precise mixtures of stable isotopes by comparison of an analyte’s isotopic composition with a standard.³⁹ This is possible through the use of dual inlet instruments which employ a changeover valve to alternate the gaseous sample and reference streams, allowing for continually repeated measurements. In addition they contain a number of Faraday cups so that different mass fragments (isotopes) may be simultaneously analysed.

More usefully with regard to the research presented herein, when labelling or-

ganic compounds the incorporation and position of an isotope label may also be determined by conventional mass spectrometry. In the former case the molecular weight of the isotopically enriched compound should be observed by the presence of the molecular ion (M^+) peak. The position of a label can be determined by examination of the fragmentation pattern for that molecule. The point at which the fragment that contains the isotope label is lost from the parent ion will be indicated by a return of the remaining fragment to its normal un-enriched molecular weight, thus it is possible to determine the fragment to which the isotope label belongs. Although the exact position may still be difficult to elucidate, when this is the case, further analytical methods would be necessary in order to provide a definitive answer.

When undertaking stable isotopic labelling it is generally accepted that the desirable mass increase for a molecule should be ≥ 3 Da, because there will be contributions to an unlabelled molecule's molecular ion from a combination of naturally occurring isotopes such as D, ^{13}C , ^{15}N or ^{18}O .⁴⁰ However, once beyond the mass of the $M^+ + 3$ peak these effects become negligible (due to the low abundances of the isotopes mentioned above), so a molecule labelled such that a corresponding increase of at least 3 Da is attained will not exhibit any underlying effects from naturally occurring combinations of other stable isotopes, thereby removing any experimental ambiguity.

1.1.6 Isotope Analysis by NMR Spectroscopy

All atoms have an intrinsic spin which in turn gives rise to a magnetic moment. Thus by applying a magnetic field of appropriate magnitude around a molecule, alignment occurs and it is this property that gives rise to nuclear magnetic resonance (NMR). Since the nuclear magnetic moment for an atom is dependent upon the spin of protons and neutrons, whose movement causes a dipole moment, it follows that altering the number of neutrons in an atom will change the NMR characteristics of an isotopologue. The effect of substituting an atom with one of its isotopes will alter both the observed chemical shift and coupling constant for that particular atom. This is a primary NMR isotope effect and those of a

secondary nature are also observed for other nuclei which are not sufficiently shielded from the isotope. Generally the magnitude of these changes is related to factors such as the change in mass when isotopic substitution occurs, the number of such atoms which have undergone substitution and the distance between them. With this in mind it follows that qualitative or quantitative determination of isotope substitution into molecules is possible *via* ^1H -NMR spectroscopy by the observation of such changes.⁴¹

Within this text one method of validating isotope incorporation into a molecule stems from the alteration in spin of different isotopes. When an NMR experiment is undertaken all of the atoms within a system that have a specific spin are probed so their related signals can be observed. However coupling between all of the spin active nuclei within a molecule occurs and so the signals are split according to the equation:

$$(2nI) + 1 \quad (20)$$

where it may be generalised that n is the number of equivalent nuclei that are attached, or adjacent to, the atom under observation and I is the spin quantum number. Both ^{13}C and ^1H have a spin $I = \frac{1}{2}$ so according to Equation 20 when a ^{13}C -NMR spectrum is recorded a CH_3 group should be present as a quartet. In practice only a singlet is observed because the spectrum is proton decoupled, which is necessary in order to remove the extraneous signals which would decrease the parent line intensities beyond practical levels to allow for timely spectrum acquisition.* However, if the CH_3 group were to be replaced with a CD_3 group then the carbon signal will be split and since deuterium has a spin $I = 1$ a septet is observed. Following the same logic a ^1H -NMR spectra will show a singlet for a CH_3 group as the three protons are equivalent and do not couple to one another, but on substitution of the three proton atoms for deuterium, the signal will disappear since only nuclei with $I = \frac{1}{2}$ are observed. Thus it is possible to confirm the incorporation of deuterium into an organic molecule by observing the multiplicity of peaks arising from the ^{13}C nuclei to which they are attached and the absence of expected signals in a ^1H -NMR spectra.

*Gated decoupled spectra where proton decoupling is only applied during the relaxation period is one way around the problem and allows ^{13}C - ^1H multiplicity and coupling constants to be determined.

Another consideration in ^{13}C -NMR spectroscopy is that substitution of an atom with an isotope causes an upfield shift in the signal, designated as α or β , according to the location of the substituent relative to the carbon being probed. This technique is often used in labelling studies where deuterium atoms are placed either directly on to, or one atom away from a ^{13}C reporter nucleus which enables determination of isotope label positions without the longer scan times that would otherwise be necessary.

1.2 Continuous Flow Reactors

Continuous flow micro reactors, such as the one shown in Figure 7, are best described as a network of interconnecting, micron sized ($10\ \mu\text{m}$ to $500\ \mu\text{m}$) channels etched into a solid substrate which are sealed such that fluids may be manipulated through them.⁴² However where the use of solid supported reagents, catalysts and scavengers are described the use of tubular reactors ($0.1\ \text{mm}$ to $3.0\ \text{mm}$) have primarily been reported.⁴³

Originally developed for use as μTAS (Micro Total Analytical Systems) or 'lab on a chip' devices,^{42,44} organic chemists soon started to take an interest in this new technology. From a synthetic standpoint micro reactors provide a method of achieving high throughput, large scale chemistry using identical methods to those developed in the laboratory. When comparing micro reactions to traditional batch preparations, the danger of a reaction exotherm increasing beyond a critical

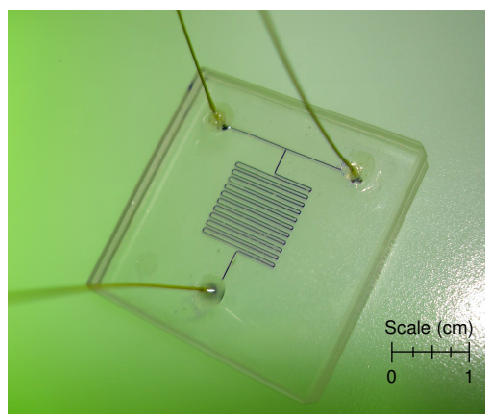


Figure 7. A photograph of a typical glass micro reactor filled with a purple dye.

temperature is significantly reduced by the high surface to volume ratio, which is often hundreds of times greater than conventional glassware, allowing rapid dispersion of heat through the channel walls. Efficient mixing regimes at these scales often result in excellent yields under easily controlled conditions. A single micro reactor generally has a typical volume in the nl to μl range and the resulting reduced working volumes of potentially hazardous materials, coupled with the higher containment of chemicals and solvents, means that handling, manipulation and exposure risks are kept to a minimum. The optimisation process for a reaction is commonly focused on minimising undesirable by-products and maximising productivity, typically achieved by varying concentrations, reactor designs and flow rates. The end product is an efficient system which, when coupled with the high containment and low volumes of chemicals is both safer and produces less waste. Transferring from laboratory to bulk scale production is then a simple process. Since scaling up the apparatus would alter the unique dimensions of the reactor, a parallel array of micro reactors can be employed, which retains the original methodology and significantly reduces lab-to-plant development time and cost.

1.2.1 Fabrication of Micro Reactors

There now exists a plethora of techniques for the transfer of complex and diverse channel designs to a large number of substrates such as glass, silicon, ceramics, metal and polymers.⁴⁵ These methods of fabrication may be divided into three main groups, according to the channel profile obtained, as illustrated in Figure 8. Channels that are always wider than they are deep, with curved walls, are produced using isotropic methods whilst anisotropic etching produces high aspect ratio (*i.e.* narrow and deep) channels with a trapezoidal or rectangular cross section. Lastly,

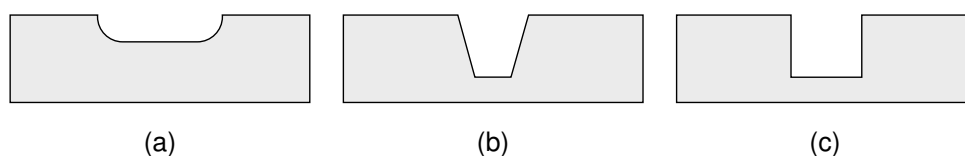


Figure 8. (a) Isotropic and (b and c) anisotropic channel profiles achievable using various micro fabrication methods.

a near perfect anisotropic etch will furnish a channel with perpendicular walls and high aspect ratios. The intended application, flexibility, reproducibility and production time for the micro structure predominantly influences the material and fabrication method of choice. There follows a brief overview on the main methods of micro reactor fabrication with particular emphasis placed on wet isotropic etching, the method used to produce the devices employed herein.

Wet Isotropic Etching The technique of wet etching is believed to have originated as far back as the 15th century for the purpose of creating decorative armour. In more recent times however it was developed for the manufacture of circuit boards and micromechanical elements. Transfer of designs into a substrate such as borosilicate glass or silicon produces economical and durable devices which exhibit excellent chemical resistance and heat latency.⁴⁶ As the name implies, isotropic etching is characterised by erosion of the substrate material at an equal rate in all directions, thus channels are always wider than they are deep and a curved channel profile results (Figure 8a). The substrate is usually etched at or above room temperature in aggressive acids such as HF, which require specialised handling and disposal protocols. One other drawback of this fabrication technique is that clean room facilities are required for more reproducible production, although it is possible to prototype devices, as used in this project, without such facilities.⁴⁷

As Figure 9 illustrates, one face of a glass plate is sputter-coated with a 0.5 μm to 2.0 μm layer of chromium and then spin coated with positive photoresist, which forms the means by which a channel network design may be transferred. Applying an accurately drawn mask (essentially a photo negative produced using CAD software) over the top of the prepared substrate and exposing it to UV light allows the channel design to be transferred by an appropriate developer solution. Subsequent immersion in a metal etchant solution removes the chromium layer and the glass is then hard baked in a furnace (120 °C, \sim 4 hr) before being etched in a mixture of 1% HF and 5% NH_4F^- . When in solution, the temperature is raised to 65 °C and the glass sonicated to ensure a constant replacement of etchant to the substrates surface. Following completion the channel (of typical resolution

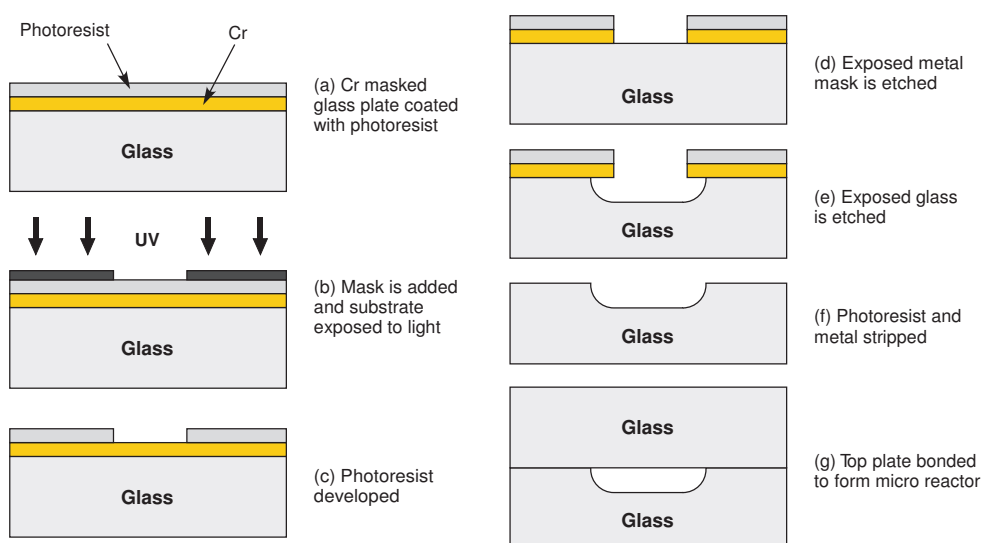


Figure 9. The photolithographic process described herein (note the under etching of the mask which causes a curved channel profile).⁴⁷

$\sim 0.5 \mu\text{m}$) is sealed by adding a top substrate layer as described in Section 1.2.2. Prior to bonding holes are pre-drilled into either the etched or top plate, which act as reservoirs to hold chemical solutions, or serve as an interface for fluidic connections.

Wet Anisotropic Etching Anisotropic wet etching is possible with silicon based substrates which have a well defined single plane crystalline structure, free from defects. The etchant erodes the substrate directionally along the exposed plane of the crystal lattice at a rate which varies according to the atomic density. A thin film of SiO_2 or Si_3N_4 is first applied to the top of the silicon substrate to which a masked design may be transferred by, for example, atom bombardment or with a layer of photoresist by initial isotropic etching of the SiO_2 . The substrate is then exposed to a basic solution such as 25% KOH and the temperature is increased to around 70°C to 80°C .⁴² This initiates surface reactions with the substrate and the exposed regions are etched. The design is thus transferred according to the mask layout, whilst the channel profile is dependent on the crystallographic orientation of the silicon. Whilst high aspect ratio micro channels may be obtained using such methods there are still drawbacks, for example when sharp corners are required common convex or concave channel profiles can prove problematic.

Laser Micro Machining Laser ablation was reported in 1997 by Roberts *et al.*⁴⁸ for polymeric micro diagnostic applications but today it is also used to micro machine materials such as ceramic, glass, metal and silicon. Irradiating a substrate with a laser at high flux causes photochemical degradation and at the correct wavelength chemical bonds break directly. Longer wavelengths cause thermal decomposition but pulses rapidly remove substrate material, which minimises localised heat deposition.⁴⁹ The rate of ablation is fast, being affected by pulse width, whilst depth of focus and beam shape also determine the feature size and aspect ratio respectively. Surface roughness varies between the μm (Nd:Yag lasers) to nm range (fs, Ti:Sapphire lasers) and in contrast to more traditional micro machining methods there is no direct contact, making micro fabrication of fragile materials possible. Although a large capital investment is required, the overall running costs and environmental impact of laser micro machining are low and automation is readily achieved through micro computer control. In addition, unlike other more indirect methods of fabrication that involve numerous production steps, no masks,* clean rooms or other special techniques need be employed. Subsequently the potential for flexible and rapid prototyping of complex designs in a variety of substrates has become a particular attraction of laser micro machining, especially in high turnover research dominated environments.

Plasma Etching In order to create a plasma that is useful for micro fabrication, gas molecules are introduced to an evacuated chamber and an oscillating electric field is applied which has the effect of accelerating free electrons. Collisions with neutral gas molecules cause ionisation, more electrons are released and the process continues until a steady state is reached—the plasma. In the case of reactive ion etching (RIE), electrons within the chamber are absorbed onto its walls and the plasma subsequently generates a positive charge. The formation of a large potential difference causes ions to drift towards a wafer platter and positioning a substrate within their path results in kinetic and chemical interactions at the surface which initiates etching. The more common and adaptable deep reactive ion etching (DRIE) incorporates an additional microwave power source and

*Parallel, batch processes use a mask but conventional serial modes write directly to the substrate.

magnetic field to transfer extra energy to the electrons.* Factors such as chamber pressure, stage position, temperature and the production of gaseous by-products all need to be considered. As an example, DRIE of Pyrex® glass is possible using a plasma of SF₆ gas.^{50,51} The channel design is initially transferred to a substrate using photolithographic techniques which is then exposed to a plasma rather than wet chemicals, producing channels with a high (> 10) aspect ratio and low (nm) surface roughness. The process does not suffer from mask undercutting and as with laser ablation there is an excellent level of control, but capital outlay is high due to the specialised equipment required.

Powder Blasting Traditionally used for cleaning or decorative effects, powder blasting is performed by the erosion of a brittle material such as ceramic, glass, or silicon using ultra fine particles.^{52,53} A powder of resolution in the range 10's μm, such as oxo-oxoalumanyloxyalumane (Al₂O₃), is introduced *via* a nozzle to a compressed air flux and then directed through a metal mask to the underlying substrate. Factors such as the powder velocity, particle size and angle of incidence (of the powder beam) heavily influence the final geometric features. High etch rates are possible (100's μm min⁻¹) and although the surface roughness is significantly greater (10's μm) when compared to other techniques (caused by the comparatively high erosion resolution and its direct physical impact), the degree of control on the channel profile is far superior. Whilst prototyping is rapid and safer than wet etching techniques depth and secondary impact limitations are pertinent with this method of fabrication and the surface roughness obtained has been demonstrated to greatly influence flow that is governed by electroosmotic flow (EOF, Section 1.2.3); Solignac *et al.*⁵⁴ have reported that liquid mobility properties are altered under EOF control when compared to channels produced by standard HF wet etching. Rapid broadening of electrophoretic plugs and a decrease in electroosmotic mobility in channels fabricated through powder blasting suggests the fabrication technique is only practical for micro reactors under hydrodynamic control.

*The two processes are differentiated by their etch rate; RIE ~ 1 μm min⁻¹; DRIE 5 μm min⁻¹ to 10 μm min⁻¹.

Moulding Employing a master (or positive relief), produced *via* a suitable lithographic technique, moulding or casting provides a way of rapidly transferring a channel design to a soft substrate, most often ceramic or polymer, which is then hardened to form a practical device. One common micro moulding technique uses dimethyl polysiloxane (PDMS) which provides a rapid route to prototyping as the time consuming photolithographic process, which slows wet etching techniques, need only be carried out once to produce the master.⁵⁵ After casting the PDMS, cross linking is thermally induced and a low cost, durable device with a smooth surface is produced. It is common to use silicon masters as demonstrated by Shah *et al.*⁵⁶ as they can be etched anisotropically (Figure 8) to produce high aspect ratio moulds, which are easily removed from the final substrate and consequently undergo repeated use. The somewhat more exotic low pressure injection moulding, combined with stereolithography, has also been used to fabricate micro reactors made of ceramics using silicon moulds.^{57,58}

LIGA The acronym LIGA derives from the German words Lithographie, Galvanoformung and Abformung which translate to lithography, electroforming and casting respectively and relate to the three main steps in the LIGA process.⁵⁹ At the heart of the technique is lithography; electron, ion beam and UV based methods are all possible. However, the most common example is deep X-ray lithography, which allows the precise etching of extremely high aspect ratio micro structures.⁶⁰ Synchrotron radiation transfers the design of an X-ray mask to a layer of photoresist which is then developed. The positive structure created in the photoresist is then copied to a metal mould by electroforming, that is, electrodeposition of metal from an electrolytic solution on to a base plate. From this metal master duplicates of the original design are fabricated using injection and casting techniques, resulting in micro structures of excellent surface quality and precision in materials such as ceramics, metals and polymers.

Other Fabrication Methods Of course there exists a greater number of ways to realise micro reactor structures than have been introduced here. For example surface cutting, embossing, sacrificial layer etching, electro discharge machining, punching and laminating have all been demonstrated as practical ways to carry

out micro fabrication and the list will inevitably grow as the field of micro reactor research matures.

1.2.2 Sealing Micro Reactor Channels

A micro reactor fabricated by one of the methods described in Section 1.2.1 only consists of a channel network etched into a given substrate. In order to be fully utilised, a closed channel network must be formed which allows for connection in some way to its external environment. Thus the design of a micro reactor also requires reservoirs capable of holding chemical solutions, or connectors to integrate with pumps, which in turn must connect to the channels of the micro reactors. These design features are realised through a second element of the reactor, in the form of a top plate. The use of adhesives is not very amenable to realising a closed channel as anything but homogeneous contact will cause leakage from the channels between the two plates. In addition this mode of sealing leads to deposition of adhesive within the channel network which is less than ideal. There exists two main methods by which substrate wafers may be bonded together when a sealed micro reactor channel is required after initial etching.

Fusion Bonding The first of these is known as direct or fusion bonding. The two substrate layers are brought together under a contact force causing them to be held together under Van der Waal forces and, more significantly for glass, hydrogen bonding.* Annealing the plates at high temperature (515 °C to 1000 °C) then forms a solid, durably bonded micro reactor.

Electrostatic Bonding The second type of wafer bonding is known as anodic or electrostatic bonding. An electric field is applied across a combination of silicon and Pyrex® at a temperature of around 25 °C to 450 °C. Ion diffusion then causes a space charge region to form, resulting in a strong electrostatic force between the wafers. This closes the gap, oxidation occurs and a bond is formed.

*Brought about by the application of a drop of purified water onto one plate, prior to them being sandwiched together.

1.2.3 Fluidic Manipulation

The application of external force to a fluid, allowing controlled motion within channels, is an obvious necessity of continuous flow technologies. The biggest hinderance to current technology is that although the reactor devices used to perform syntheses or analyses are small in size, the corresponding manipulation units are relatively large. Efforts are ongoing to improve this situation and shrink the units in question, resulting in some unique and exotic designs such as ‘heart’,⁶¹ bubble,⁶² capillary⁶³ and bacteria⁶⁴ driven pumps. In spite of these advances there are currently two common methods by which fluid movement within the channels of chemical reactors is achieved—electroosmotic and hydrodynamic flow. Both have their corresponding advantages and disadvantages with the chosen method commonly dictated by the intended application for the device under development.

Electroosmotic Flow To induce EOF, a high potential difference (typically ~ 1.5 kV) is applied to a closed circuit, formed by positioning electrodes across a channel which has been filled with the liquid to be mobilised. The inner glass channel walls hold a negative charge when the silanol groups have been dissociated and a diffuse double layer (the Gouy–Chapman layer)* forms to counteract this, as illustrated by Figure 10. When an electric field is present the diffuse layer of positive ions is pulled towards the anode, in turn causing a mass transfer of the liquid itself with a relatively flat velocity profile (except within nm of the channel wall).^{65,66} The magnitude of the velocity, Φ_v (m s^{-1}), is therefore determined by

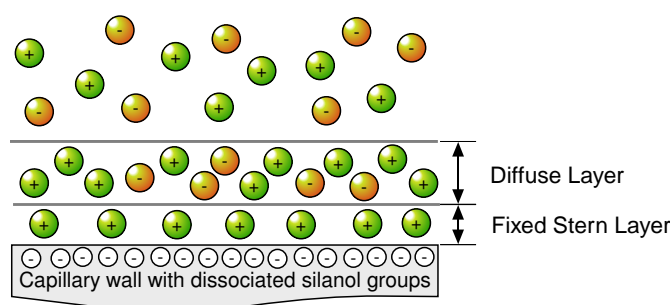


Figure 10. The attraction of charged ions in a solution to a negatively charged surface.⁶⁵

*The potential difference between the Guoy–Chapman layer and the Stern double layer is termed the ‘zeta potential’, ζ .

a number of factors and is quantified by

$$\Phi_v = - \left(\frac{F\epsilon\epsilon_0\zeta}{\eta} \right) \quad (21)$$

where F is the electric field strength (V m^{-1}), ϵ is the relative permittivity of the liquid (dimensionless), ϵ_0 is the permittivity of free space ($\approx 8.854 \times 10^{-12} \text{ F m}^{-1}$), ζ is the zeta potential (V) and η is the liquid viscosity (Pas).

Experimental variables include the magnitude of applied voltage, reagent concentrations, solution pH and choice of solvent. Influences arising from both the viscosity and dielectric constant of a liquid will determine its EOF properties.⁶⁷ A solvent with low or no polarity such as dichloromethane (DCM), toluene or hexane have low dielectric constants which leads to extremely low or no electroosmotic flow at all. Of course the addition of a suitable electrolyte will overcome this problem but the purity of the flow stream will consequently be compromised, an outcome dependant on the systems end application. Alternatively however good choices of solvent include the more polar organics, acetonitrile (MeCN), *N,N*-dimethylformamide (DMF) or methanol (MeOH). Another consideration that arises when effecting liquid mobility *via* EOF is that of electrophoretic separation, which has long been used within the analytical disciplines. This is not necessarily a hindrance as George *et al.*⁶⁸ demonstrated with the *in-situ* purification of peptides synthesised in an EOF based micro reactor.

Manipulating fluids by EOF in micro reactors gives the benefits of no moving parts and automated manipulation of multiple reagent streams under micro computer control using reservoirs to hold the various reactants and collect products. Care must be exercised to counteract pressures arising from differences in reservoir heights, for example through the integration of silica frits⁶⁹ or pressure resistant channel restrictions⁷⁰ into the reactor design. Alternatively leakage from one channel to another by hydrodynamic or diffusion effects can be counteracted as demonstrated by Seller *et al.*⁷¹ by the controlled application of potential differences. Perhaps one of the greatest advantages of EOF is that no fluidic connectors are required, minimising the risk and problems associated with blockage and leakage.

Hydrodynamic Infusion Hydrodynamic flow within micro channels is achieved by applying an external, mechanical force, upon the fluid to be manipulated. Commonly this is achieved using syringe drivers or infusion pumps (*e.g.* HPLC pumps) which are programmed to deliver fluid at a chosen flow rate or volume. In the former case gas tight syringes are filled with fluid, loaded into the syringe driver and connected to the micro reactor *via* tubing and commercially available HPLC fittings. The syringe plungers are then pushed by a back plate connected to a worm driver which operates at calibrated speeds to ensure the accurate delivery of fluids. Pumping by hydrodynamic means is a simple operation but the back pressures generated by the technique are high (see Section 1.2.5) which can prove problematic. In addition syringe driver units are expensive and bulky, often dwarfing the micro reactor units themselves. The velocity profile obtained by hydrodynamic pumping is parabolic in nature which can cause the broadening of plugs and streams. However the technique does provide a closed system and is extremely desirable for some applications, and as such is the reason hydrodynamic pumping has been exclusively employed during this project; when working with labelled compounds and in particular radioisotopes, it is obvious that loss of reagent through evaporation or degradation in air is an undesirable situation which should be avoided.

1.2.4 Liquid Characteristics at Low Reynolds Numbers

Laminar Flow Laminar flow, as opposed to turbulent flow, means that fluids flow adjacent to one another in defined layers with an orientation that is parallel to the bulk fluid flow. It is characterised by the dimensionless Reynolds number, Re , which represents the relationship between inertial and viscous forces of a fluid. It is governed by the viscosity and density of a fluid (liquid or gas) and within a cylinder defined by

$$Re = \frac{\rho \delta_r \Phi_L}{\eta} \quad (22)$$

where ρ is the fluid density (kg m^{-3}), δ_r is the hydraulic diameter (m), Φ_L is the linear velocity (m s^{-1}) and η is the viscosity (Pa s). Thus, in a given channel, if a fluid exhibits a large enough viscosity then the resultant value of Re is low (< 100),

its flow will be laminar dominated and occur without turbulent disruptions such as eddy currents or swirling vortices; the point at which this occurs is at a value of $Re = 2\,000$ for a cylinder. It therefore follows that within the channels of micro reactors, where δ is small, Φ_L would have to be excessively large to initiate turbulent flow. Thus laminar flow is predominantly observed, even for liquids of extremely low density and viscosity; consequently mixing between parallel flowing streams occurs exclusively by diffusional processes.

Diffusional Mixing Nature presents an elegant way to transfer molecules with relatively low molecular mass (*e.g.* $< 5\,000$ Da) over short distances—diffusion. In the absence of external flow or pressure, transport in fluids is diffusion orientated and the time it takes to achieve a homogeneous mixture will depend entirely upon the size of the molecular species, temperature and diffusion distance, quantified by the Fick's second law of diffusion⁴ as

$$x = \sqrt{4Dt} \quad (23)$$

where x is the displacement distance (m), D is the diffusion coefficient (m^2s^{-1}) and t is time (s). Since, for a given molecule, the relationship between distance travelled, x , is related to the square root of the only other variable, time, diffusion over a short distance ($100\text{'s}\mu\text{m}$) occurs rapidly, as illustrated in Figure 11. The diffusion coefficient, D , for a given molecule is dependent on many factors such as its activity coefficient, viscosity and molecular radius. Thus for molecules with large molecular weight (such as proteins) transport by diffusion is relatively slow. For the purposes of organic synthesis however, it is an ideal way for mixing to occur providing there is a fine level of control on the process. It is this fact that is exploited within micro reactors because, as a result of laminar flow profiles the mixing of two reaction components within a channel will occur exclusively by diffusion perpendicular to the bulk fluid flow. Thus an ideal channel design is one which affords a narrow interface between lamina, providing the shortest possible diffusion distance between the reactant partitions.

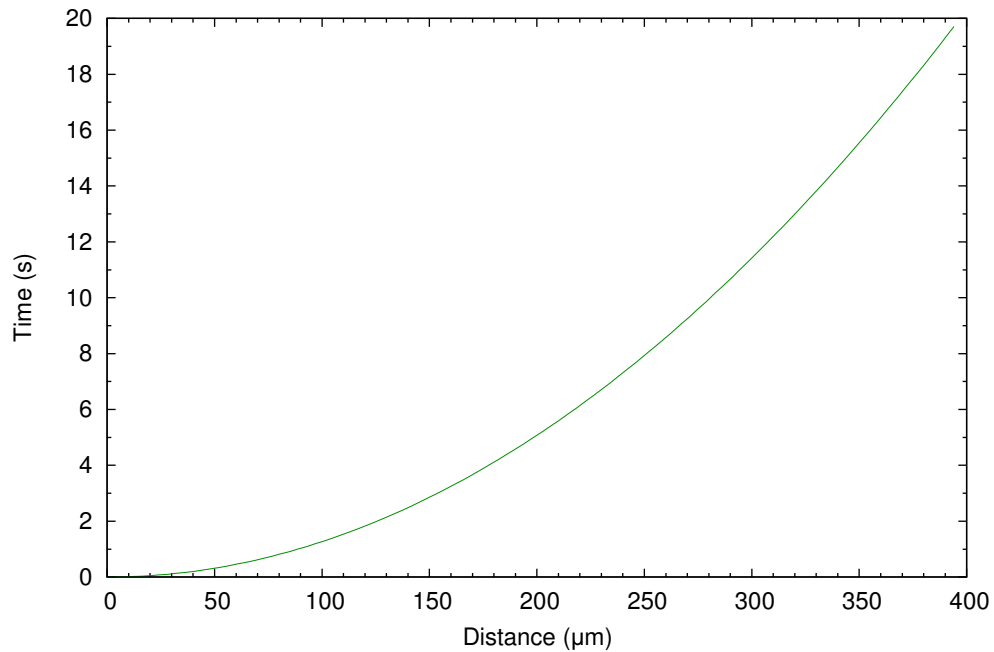


Figure 11. A graph illustrating the time it takes for aniline **15** to diffuse a given distance when dissolved in benzene at infinite dilution at 25°C according to Fick's second law of diffusion.^{4,72}

Fourier Numbers A Fourier number, Fo , is a dimensionless value which may be used to estimate the degree of mixing after a specific amount of time.⁷³ Within a micro reactor channel it is dependent upon the inherent dimensions, the residence time and the diffusion coefficient of the species under observation, calculated using the following equation:

$$Fo = \frac{Dt}{x^2} \quad (24)$$

where D is the diffusion coefficient ($\text{m}^2 \text{s}^{-1}$), t is time (s) and x is the distance over which the molecule diffuses (m). As the upper limit for mixing within a micro reactor channel is governed by the time it takes to diffuse over the distance of the largest channel dimension (*i.e.* the channel width, w_c , for isotropically etched channels) the value of Fo which relates to a homogeneously mixed solution within the channel may be calculated in the following way. Firstly Equation **23** is rearranged to determine the time taken to diffuse over the channel width:

$$t = \frac{w_c^2}{4D} \quad (25)$$

When considering Equation **24** the characteristic diffusion distance, x , will be constant for a particular micro reactor channel and, for a given channel with two

equally distributed laminar flow streams, will be equal to half channel dimension perpendicular to the direction of flow (*i.e.* the width). This is the case since each flow stream only needs to traverse half of the channel in order to have undergone complete displacement. With this assumption in mind substitution of (25) into (24) determines the Fourier number which relates to a completely inter-diffused mixture.

$$Fo = \frac{Dt}{x^2} = \frac{Dw_c^2}{4D(\frac{1}{2}w_c)^2} = 1 \quad (26)$$

By using the same equation (24) the Fourier number for a particular micro reactor based on the residence time, $R\tau$, may be calculated providing the diffusion coefficient, D , is known. This serves as a quantifiable method of estimating the degree of mixing within the device since any micro reactor that returns a value > 1 will have a completely mixed flow stream upon exiting the channel in question. Appendix A details the Fourier numbers for each micro reactor used within this text based upon the model described, using the diffusion coefficients of acetic acid in ethyl acetate (EtOAc) and aniline **15** in benzene as example systems.

1.2.5 Back Pressure

For Newtonian fluids flowing under laminar conditions within a cylinder (*i.e.* where $Re < 2000$) the volumetric flow rate may be approximated by dividing the pressure difference (the back pressure) with the viscous resistance, as quantified by Poiseuille's law:

$$\Phi_v = \frac{\Delta P}{R_\phi} \quad (27)$$

where Φ_v is the volumetric flow rate (m^3s^{-1}), ΔP is the pressure difference across the cylinder (Pa) and R_ϕ is the flow resistance (Pam^{-3}), determined by the length and radius of the cylinder and viscosity of the fluid using the Poiseuille equation in the following way:

$$R_\phi = \frac{8\eta L_r}{\pi r_r^4} \quad (28)$$

where η is the liquid viscosity (Pas), L_r is the cylinder length (m) and r_r is the cylindrical radius (m). Thus, as is done when calculating Reynolds numbers, Re ,

within isotropically etched channels (see Appendix A) making the channel radius

$$r_c = \frac{2A_c}{\Theta_c} \quad (29)$$

where A_c is the channels cross sectional area (m^2) and Θ_c is the wetted perimeter of the channel cross section (m) the previous equations (27–29) may be combined and rearranged which then allows for the back pressure, P , within an isotropically etched micro reactor channel to be calculated in the following way:

$$P = \frac{\Phi_v \eta L_c \Theta_c^4}{2\pi A_c^4} \quad (30)$$

Application of this equation using the dimensions of the micro reactors employed within this thesis yields the pressure changes across the chip that are given in Appendix A.

1.2.6 Micro Reactor Design Considerations

A plethora of micro reactor designs have been reported to date which are aimed at solving particular problems, or increasing the mixing efficiency. However one of the most common and useful of these is perhaps also the simplest, commonly known as the T reactor, illustrated in Figure 12. Two reagents are brought together and flow down the channel with a laminar partition, each occupying half of the channel. At the mid line between reagents diffusion occurs rapidly and the solutions reach their final concentration relatively quickly. For example from Figure 11 it can be seen that aniline **15** will take 0.16s to diffuse 25 μm when dissolved in benzene at infinite dilution at 25 °C. However as the diffusion distance

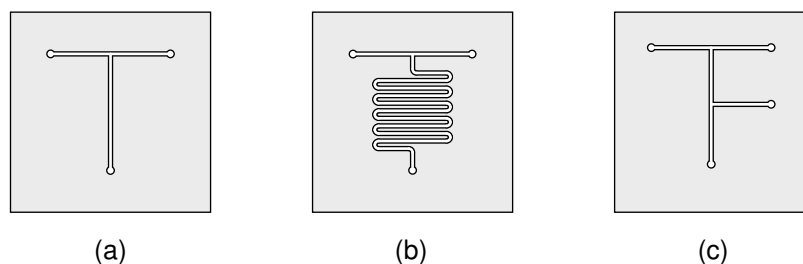


Figure 12. A top down view of selected micro reactor designs (a) T, (b) serpentine and (c) double T.

increases towards the wall of the channel, so too does the time taken to reach the final concentration, determined by the diffusion coefficients of the species involved. Moving along the main channel the mixture becomes increasingly homogeneous until, at a given reactor length complete inter diffusion is realised. Based on the rules of diffusion discussed in Section 1.2.4, the ideal mixer will have a small channel width and a large depth, which maximises the contact space of the two fluids, whilst providing a short diffusion distance. However, as introduced in Section 1.2.1 this is not always possible with fabrication methods such as isotropic wet chemical etching, which constrain the ratio between channel dimensions. If complete diffusion is not realised within a micro reactor the residence time of the solutions must be increased, either through slowing the flow rate or increasing the length of reactor. Figure 12b shows a design with a meandering, serpentine like channel which is significantly longer than the simple T (Figure 12a) and a double T reactor (Figure 12c) which enables multicomponent reactions to be performed within an integrated system. In the case of these relatively more complex designs (*i.e.* the meandering serpentine and the double T reactor), an increase in back pressure would be observed and this is another important consideration when designing micro reactors for practical use under hydrodynamic control, since the operational efficiency of pumps must be taken into account.

The Manz Mixer One option to circumvent this problem is the ‘Manz mixer’⁷⁴ which sequentially splits the input stream into gradually smaller channels thus reducing the diffusion distance. Poiseuille’s law (Equation 27) introduced earlier may be viewed in an analogous way to an electrical circuit where the potential difference is equivalent to the pressure change, ΔP , the current is equivalent to the volumetric flow rate, Φ_v and the electrical resistance is equivalent to the flow resistance, R_ϕ . It follows that the total resistance for a series arrangement of micro reactor channels will be equal to the summation of the individual resistance for each channel. In other words, if the arrangement in Figure 13 is considered we may write:

$$R_\phi(tot) = R_1 + R_2(tot) + R_3(tot) + R_4(tot) \quad (31)$$

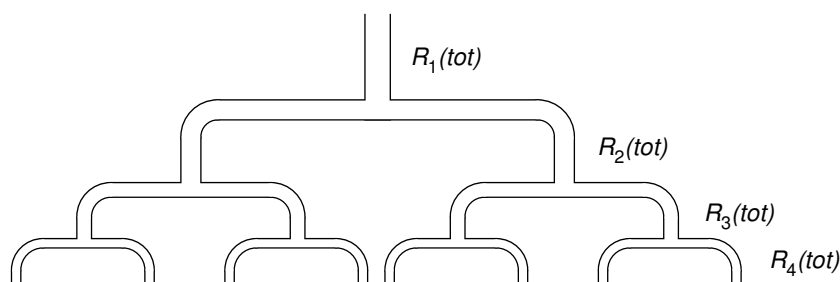


Figure 13. A top down view of the generalised design for a Manz mixer where an initial channel is sequentially split into channels of smaller dimensions.

As each segment of the channel network is comprised of a parallel arrangement of n channels of equal dimensions the reciprocal of the total resistance of each segment will be equal to the summation of the reciprocal resistance of each individual channel, denoted herein as $R_{(\frac{1}{\log_n 2} + 1)}$. This means, for example, that the total resistance for the third segment, $R_3(tot)$, may be expressed as:

$$\frac{1}{R_3(tot)} = \frac{1}{R_3} + \frac{1}{R_3} + \frac{1}{R_3} + \frac{1}{R_3} = \frac{4}{R_3} \quad (32)$$

Applying this treatment to Equation 31 for all of the segments shown in Figure 13 results in the modified expression for the total flow resistance:

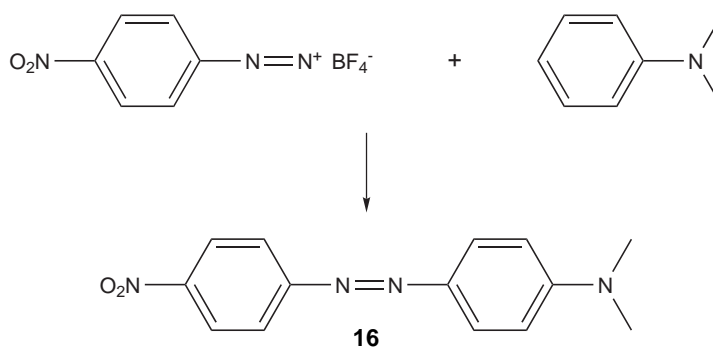
$$R_{\phi}(tot) = R_1 + \frac{R_2}{2} + \frac{R_3}{4} + \frac{R_4}{8} \quad (33)$$

which clearly indicates that the back pressure arising from such a design is less than that of a single, larger channel. This design can therefore prove to be a useful solution not only in situations where rapid diffusion is required but also when high back pressures, P , are experienced.

1.2.7 Continuous Flow Reactor Synthesis

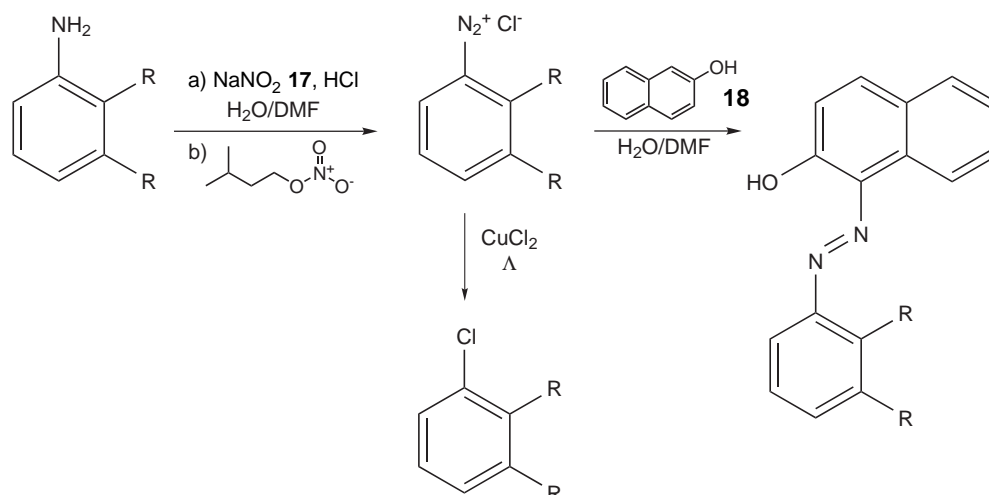
From its establishment around a decade ago the field of micro reactor synthesis continues to see a steady rise in the number of publications relating to undertaking conventional reactions within such devices. There follows a review of some reported syntheses, the more recent of which exemplify the level of complexity that is currently being achieved.

Diazo Coupling An early application of micro reactors to organic synthesis was reported by Salimi-Moosavi *et al.*⁷⁵ in 1997. The authors employed an electroosmotically driven micro reactor manufactured from Pyrex® glass to bring about the synthesis of a red dye **16** which was shown to occur in both protic (MeOH) and aprotic (MeCN) solvents according to Scheme 4. Reaction efficiency was shown to be 37 % and 22 % respectively and whilst the aim of the study was not to optimise conversions, this was the first example of synthesis and manipulation within a micro reactor set up operated by EOF.



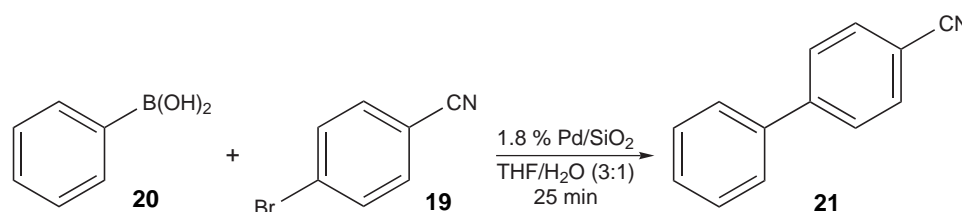
Scheme 4. The synthesis of red dye, dimethyl-[4-(4-nitro-phenylazo)phenyl]-amine **16** as carried out within a micro reactor under EOF control.⁷⁵

***In-situ* Formation of Diazonium Salts** The group of de Mello⁷⁶ have also reported on the use of a glass micro reactor under hydrodynamic control to generate a number of azo dyes. In contrast to the method presented by Salimi-Moosavi and co-workers,⁷⁵ the reactive diazo intermediates were formed *in-situ* by the concurrent introduction of aniline derivatives and sodium nitrite **17** at a micro channel intersection. Introduction of naphthalen-2-ol **18** to a third inlet then brought about formation of the corresponding diazonium products, as shown in Scheme 5. The authors highlight the significant safety features of an integrated system such as the one described, since there is need to store or transport unstable diazonium salts. The work has since been further extended to demonstrate chlorination reactions of diazonium salts, also shown in Scheme 5, within an identical micro reactor.⁷⁷ In addition the analysis of diazotisation products *via* on-line Raman spectroscopy was demonstrated in order to highlight the potential for expedient reaction optimisation when compared to employing alternative methods such as GC analysis.



Scheme 5. A generalised reaction scheme showing the routes used by the group of de Mello^{76,77} to form azo dyes (a) chloroarenes (b) within micro fluidic reactors.

The Suzuki-Miyaura Reaction The Suzuki coupling brings about C–C bond formation through the reaction of an aryl or vinyl halide with an aryl or vinyl boronic acid in the presence of a Pd⁰ catalyst. This particular reaction has received a great deal of attention within continuous flow systems in a bid to improve its efficiency and a more complete review is given in Chapter 4. One example, reported by Greenway *et al.*,⁷⁸ is the coupling of 4-bromobenzonitrile **19** and phenylboronic acid **20** (Scheme 6) within a micro reactor T under EOF control. The reaction was undertaken at room temperature in the presence of the catalyst (1.8 % Pd) which was immobilised on a silica frit, within a 3 : 1 mixture of oxolane (THF) and water, in order to ensure electroosmotic mobility (since EOF for pure THF it is poor). It was reported that a continuous flow of the reagents did not produce any significant amounts of product **21**. As a result, slugs of **19** were injected into a continuously flowing stream of the boronic acid **20** and the effect of varying slug volume, frequency and flow rate of the boronic acid

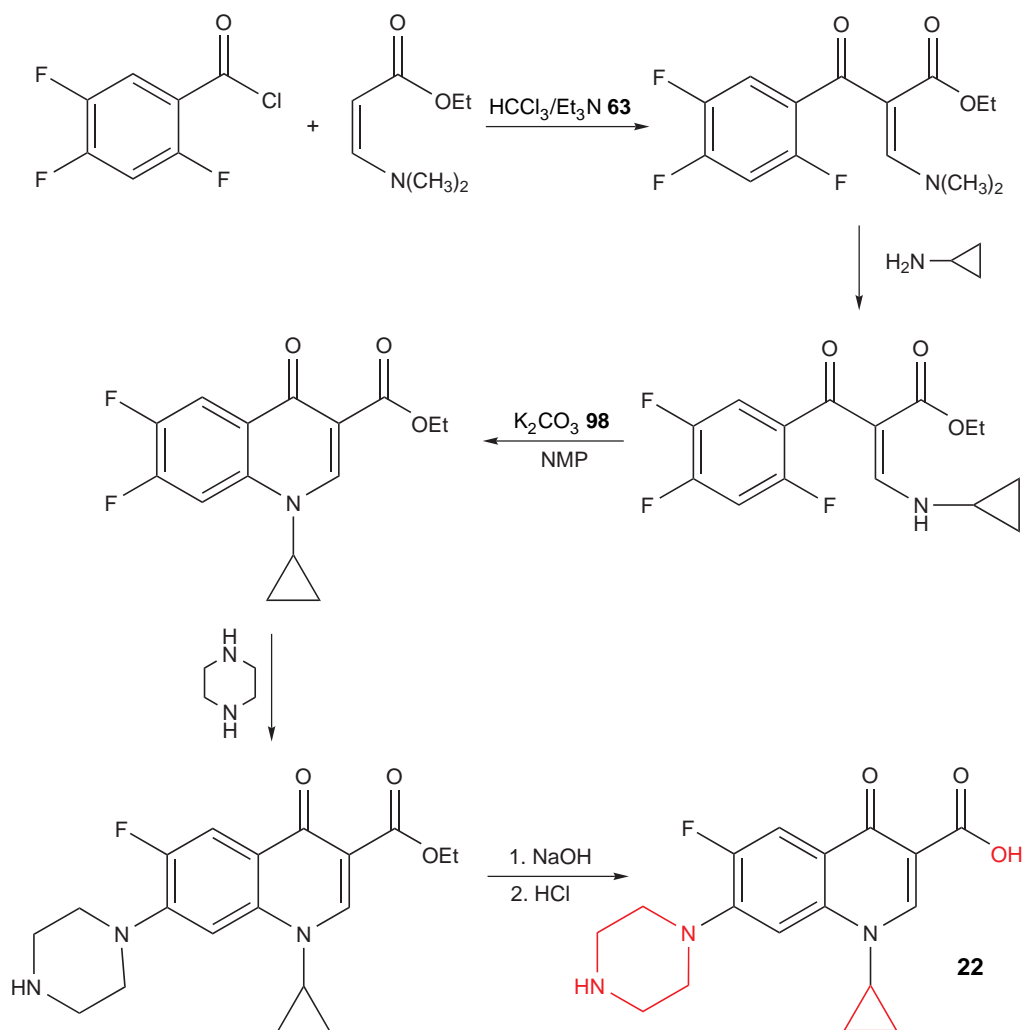


Scheme 6. The reaction between 4-bromobenzonitrile **19** and phenylboronic acid **20** to afford biphenyl-4-carbonitrile **21**.⁷⁸

20 were also studied. It was reported that the addition of a base, traditionally required for Suzuki reactions, was not required and at optimum conditions a 67% yield was obtained (5 s injection time at a frequency of 25 s and a flow rate of $0.8 \mu\text{l min}^{-1}$). The rate of Pd leaching was also determined to be low (1.2 ppb to 1.6 ppb) and there was no decrease in catalytic activity. To provide a comparison, batch reactions were carried out which only produced a 10% conversion after 8 hr. In addition, it was also necessary to heat the mixture to between 75°C and 85°C and add disodium carbonate as a base in the batch reaction.

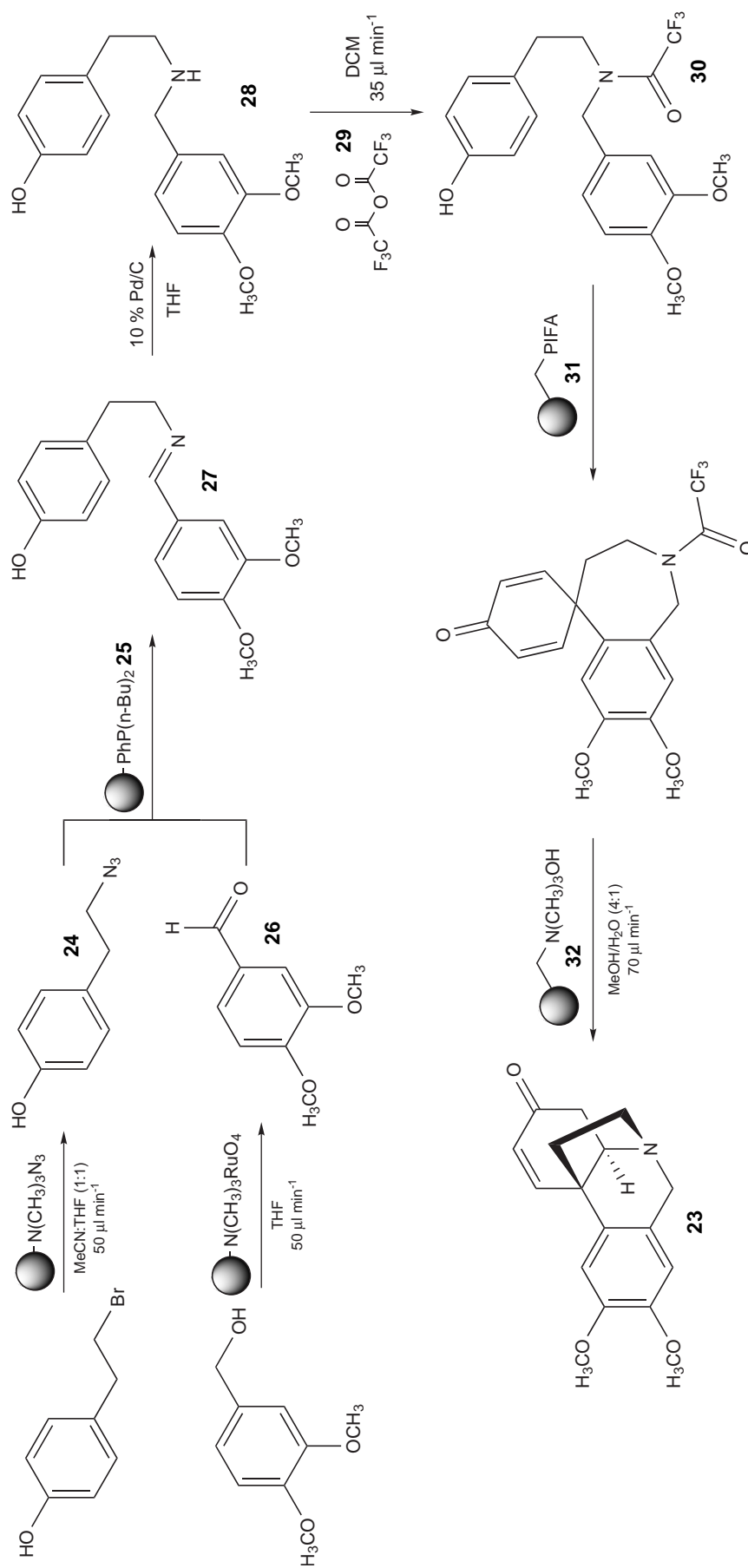
Combinatorial Pharmaceutical Synthesis The use of micro reactors in producing combinatorial libraries of pharmaceutical analogues has been demonstrated by Schwalbe and co-workers.⁷⁹ Ciprofloxacin **22**, is a common antibiotic that is used to treat many types of bacterial infection, so derivation of the core structure using combinatorial techniques is a likely way to identify new lead compounds. In order to prove the applicability of continuous flow methodology in speeding up and automating the generation of such libraries, the authors adapted a stainless steel CYTOS®(or SEQUOS®) micro reactor system to deliver plugs of reactants *via* an automated switching valve, employing a fraction collector at the outlet to deliver the synthesised compounds into discreet collection vials. In this way the successful synthesis of 28 Ciprofloxacin analogues was demonstrated following the route that is exemplified in Scheme 7. It should be noted that each of the reaction steps were worked up before re-introduction of the generated intermediates back into the reactor system.

Synthesis of Natural Products Baxendale *et al.*⁸⁰ have also undertaken a multi-step synthesis of natural product, commonly known as (\pm)-oxomaritidine **23**, a cytotoxic alkaloid, as shown in Scheme 8. The majority of the seven reaction steps were brought about using solid-supported reagents, catalysts or bases and this was achieved by packing them into cylindrical glass Omnifit® columns through which the reaction mixture was passed. Synthesis of the azide **24** occurred quantitatively and the product stream was then passed directly through another column which was packed with a polymer supported phosphine **25**, causing the azide **24** to become bound as an aza-Wittig intermediate. The second step of the



Scheme 7. The route by which Ciprofloxacin **22** and **28** core derivatisations were prepared in a CYTOS[®] micro reactor system, achieved by variations at the indicated positions (red).⁷⁹

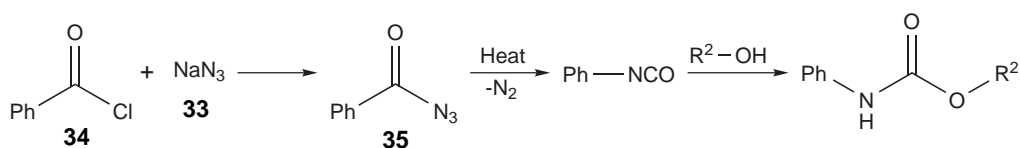
reaction, formation of aldehyde **26**, also occurred quantitatively and this stream was then passed over the prepared aza-Wittig column to furnish imine **27**. After the next reaction step, catalytic hydrogenation of the imine **27** using a Thales H-Cube[®] hydrogenator fitted with a 10% Pd/C cartridge, it was necessary to employ a solvent evaporator in order to exchange THF for DCM. The acetylation of the secondary amine intermediate **28** was undertaken with the concurrent introduction of 2,2,2-trifluoroacetic acid (TFA) **29** into a conventional glass micro reactor which was heated to 80 °C. The newly formed amide **30** was then passed over polymer supported phenyl{bis[(trifluoroacetyl)oxy]}- λ^3 -iodane (PIFA) **31**, causing oxidative phenolic coupling and ring formation. Finally the reaction mixture was passed through a further column containing polymer supported



Scheme 8. A scheme to illustrate the synthesis of the natural product (±)-oxomaritidine **23**, as undertaken by Baxendale *et al.*⁸⁰ within micro reactor systems.

base **32** to affect cleavage of the amide bond and formation of (\pm)-oxomaritidine **23**. Using the presented methodology the authors state that overall synthesis of the product at $\geq 40\%$ was achieved within a single day, compared to the 4 days it would normally take using conventional laboratory techniques. However, considering that each of the steps were carried out individually (as opposed to a fully integrated system) it should be possible to decrease this synthesis time by an even greater degree.

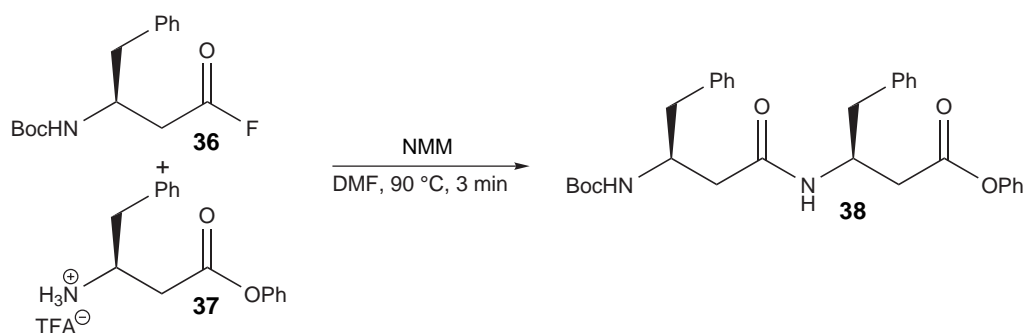
‘Online’ Multi-step Synthesis A recent example by Sahoo *et al.*⁸¹ demonstrates the multi-step, parallel synthesis of three carbamates, as illustrated by Scheme 9. The first step of the reaction was performed within a glass coated silicon micro reactor under phase transfer conditions whereby the sodium azide **33** was introduced as an aqueous solution and benzoyl chloride **34** as an organic solution (in toluene). A separation reactor, fabricated with a fluoropolymer membrane (pore size 0.1 μm to 1.0 μm) then ensured the exclusive diffusion of the organic phase and resulted in phase separation. The next micro reactor was packed with a solid acid catalyst and heated (90 °C) which caused conversion of benzoyl azide **35** to its corresponding aryl isocyanate. The nitrogen released as a result of this step (Curtius⁸² degradation) was then removed utilising another micro separation reactor containing a membrane through which the gas could diffuse. The parallel synthesis of three carbamates was demonstrated at the last step by feeding the outlet of the second separation reactor into a small vial and connecting this reservoir into three discrete reactors into which methanol, ethanol or phenylmethanol were also introduced. Post optimisation the reactions produced quoted yields of the carbamates in the range 96% to 99% at a throughput of 80 mg day^{-1} to 120 mg day^{-1} . The important feature of this work was the ability to change solvents at different stages within a continuous flow system, something which



Scheme 9. A generalised scheme of the route to carbamate derivatives which was successfully followed within a micro reactor based flow system.⁸¹

has previously hindered the further development of self contained, multi-step, fully functional miniaturised flow systems, as in the case of the synthesis of (\pm)-oxomaritidine **23** by Baxendale *et al.*,⁸⁰ summarised above.

Synthesis of β -Peptides A preparation for the synthesis of useful amounts ($\sim 3 \text{ g day}^{-1}$) of β -peptides, shown in Scheme 10, has recently been reported by Flögel and co-workers.⁸³ Using a silicon micro reactor capable of operating within the temperature range -80°C to $+150^\circ\text{C}$ the coupling of *tert*-butylformate (Boc) protected acyl fluoride **36** and primary amine **37** (as its TFA salt) to form β -dipeptide **38** was successfully demonstrated at an optimal temperature of 90°C when the residence time was 3 min. Following this success the synthesis of tripeptides and tetrapeptides was performed utilising the same set up. Formation of the sterically more demanding structure was brought about at elevated temperatures (120°C) where yields in excess of 81% were achieved. The effectiveness of the technique was evaluated by comparison with traditional solution and solid phase couplings and in all cases the micro reactor synthesis out performed the other methods, proving it to be a synthetically useful approach.



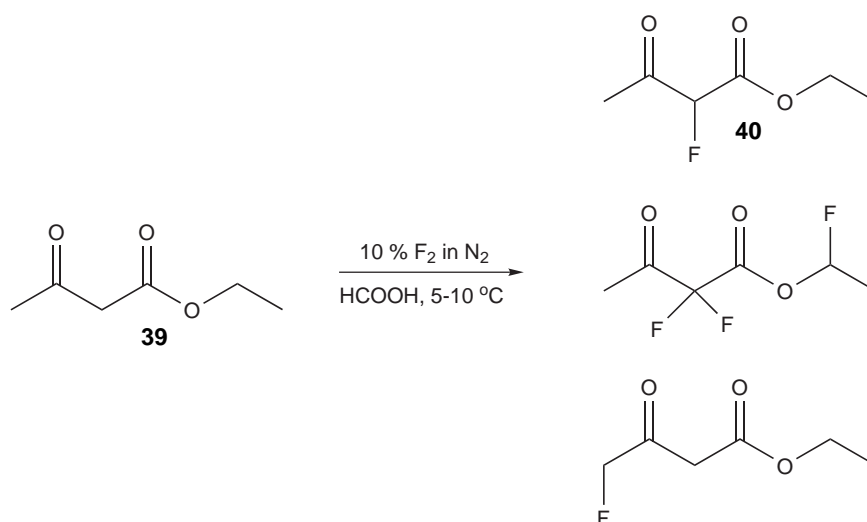
Scheme 10. The synthesis of β -peptide **38** which was successfully undertaken on a 3 g day^{-1} scale using a silicon micro reactor.⁸³

1.2.8 Scale Out

One of the unique benefits attributed to undertaking chemical synthesis within micro reactors is that once a particular process has been optimised it is possible to take a parallel approach to the mass production of a product. To produce a larger quantity of product, channel designs are thus replicated the desired number

of times and, as this process retains the original dimensions, reaction protocols remain unchanged which reduces the time, development and operational costs normally associated with migration to pilot plants.

Scale out may be achieved by either the direct replication of a previously optimised prototype, utilising multiple reactors, or the fabrication of multiple channels within a single micro reactor device. One example of the latter is the fluorination reactions that were undertaken by Chambers and co-workers.⁸⁴ After initially designing a nickel and polymer micro reactor, successful fluorination reactions, such as the one shown in Scheme 11 were performed by ‘pipe’ flowing a stream of F_2/N_2 through the center of a liquid stream to be reacted. In an effort to develop the reactor at a scale suited to industrial preparation it was redesigned; multiple channels were fabricated on replaceable stainless steel plates and fed from single reservoirs in a modular fashion. Using the developed system a 9 or 30 channel plate was used to bring about the fluorination of ethyl 3-oxobutanoate **39** which, when optimised led to 100 % conversion and predominant formation of the mono-fluorinated product **40**. This system was capable of producing $\sim 300 \text{ g day}^{-1}$ which the authors postulated could easily be increased to $\sim 3 \text{ kg day}^{-1}$ by employing a 60 channel plate and running 10 such reactor systems in parallel; equivalent to pilot plant scales but at significantly reduced cost. The same authors then went on to undertake the fluorination of diketones within the same micro reaction

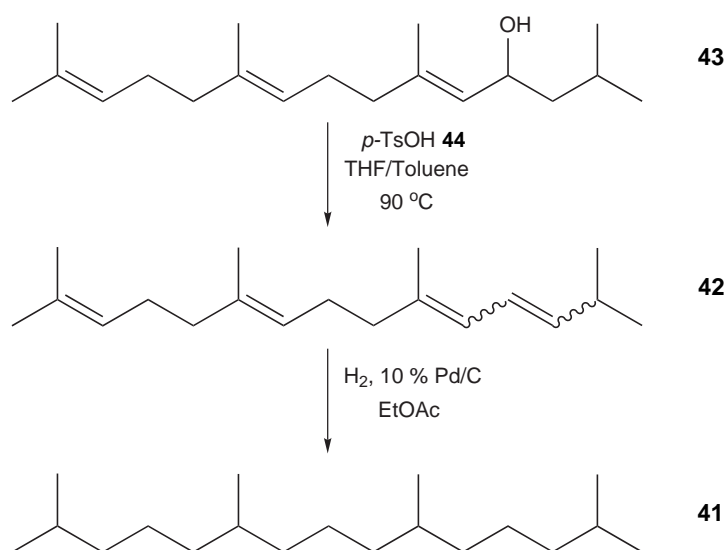


Scheme 11. Several of the products obtained on a large scale by the fluorination of ethyl 3-oxobutanoate **39** within a multichannel steel micro reactor system.^{84,85}

system to produce quantities in the range 1.6 g to 20.8 g.*⁸⁵

A more recent example of large scale micro reactor production is the preparation of a natural product pristane **41**, shown in Scheme 12, which has been reported by Tanaka and co-workers.⁸⁶ Used to conduct animal studies, pristane **41** has been in short supply since the basking shark, the main source of the compound, was listed as an endangered species in 2002. Thus a ready supply of the compound has been in demand, but attempts to batch scale the dehydration step to 100 g only produced the allylic hydrocarbon **42** in < 20% yield, due to the formation of polymeric by-products. To alleviate by-product formation a commercially available micro mixer was employed for the dehydration of **43** in the presence of 4-methylbenzenesulfonic acid **44** at a flow rate of 200 $\mu\text{l min}^{-1}$. Subsequent hydrogenation of the resulting alkene **42** brought about the natural product pristane **41** in an overall yield of 93% compared to 51% that was achieved in small scale (typically 100 mg) batch reactions. Operation of 10 micro mixers in parallel allowed the production of sufficient intermediate **42** to generate 5 kg of pristane **41** per week, enough to meet the current demand of 200 kg year^{-1} .

It should be noted that in the majority of situations, where the synthesis of



Scheme 12. The synthesis of precursor **42** which was undertaken on a large scale within a micro reactor and used to further synthesise pristane **41**.⁸⁶

*These amounts were produced in single runs (times not given) and final products isolated by fractional distillation of the pooled reaction streams.

molecules labelled with either stable or unstable isotopes is undertaken, an internal reactor scale out would produce sufficient compound for the majority of the applications introduced earlier (see Section 1.1.3). For example synthesis with radioisotopes usually occurs on the ng scale whereas for metabolic studies involving stable isotopes amounts in the order of mg are commonly required, both necessitated by, and as a consequence of, the rarity and activity of the atoms in question.

1.3 Isotope Labelling In Continuous Flow Reactors

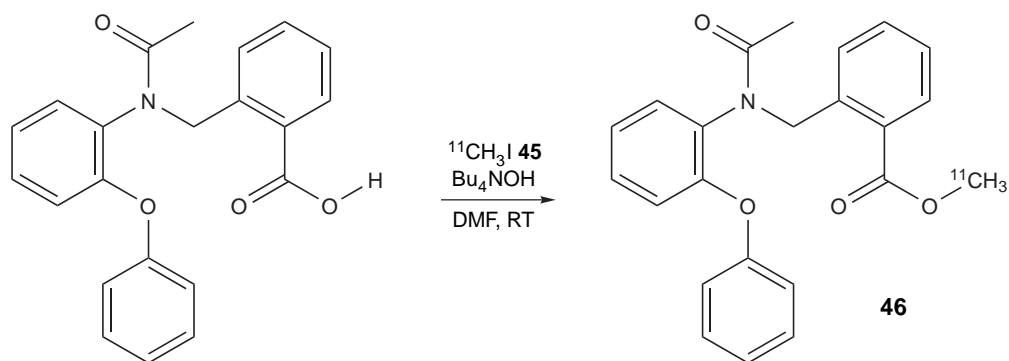
1.3.1 Literature Examples

Although the field is in its infancy, recent years have seen a steady rise in the number of papers published that employ continuous flow reactors as a tool with which to undertake isotope labelling. Limited at first to a single patent application⁸⁷ there is now a growing interest in the coalition of these two disciplines. The following gives a brief review of successful isotope labelling that has been undertaken within micro reactors and published to date.

Labelling with ^{11}C and ^{18}F The first scientific paper that reported the synthesis of isotopically labelled compounds within micro reactors was published by Lu *et al.*⁸⁸ in 2004 and described the production of carboxylic esters which were radiolabelled with ^{11}C and ^{18}F within a glass T micro reactor. A number of compounds were prepared from either iodo[^{11}C]methane **45** or 2-[^{18}F]fluoroethyl 4-methylbenzenesulfonate following reaction optimisation. An example of one of the compounds that was labelled with ^{11}C using the micro reactor system is the compound **46**, a potential brain imaging agent (Scheme 13). Following reaction optimisation with unlabelled MeI **47** the system was operated at a flow rate of $1\ \mu\text{l}\ \text{min}^{-1}$ which produced the radiolabelled compound **46**, in 65 % radiochemical yield (RCY).

Synthesis of Radiotracers Micro reactor based labelling of a number of relevant radiotracers has also been published recently by Gillies *et al.*^{89,90} Employing a

1.3 ISOTOPE LABELLING IN CONTINUOUS FLOW REACTORS



Scheme 13. The labelling of a PET brain imaging agent **46** with ^{11}C as carried out within a micro reactor.⁸⁸

multi layered polycarbonate micro reactor consisting of a mixing vortex chamber and micro channels, the incorporation of radioisotopes ^{124}I , $^{99\text{m}}\text{Tc}$ and ^{18}F into a number of compounds, such as those illustrated in Figure 14, was successfully demonstrated. The anti cancer drug analogue of doxorubicin **48** was radioiodinated within the micro reactor with the isotope ^{124}I by introduction of the tin-butyl precursor with an oxidising agent, *N*-chlorosuccinimide, and the labelling agent, $^{124}\text{I}]\text{NaI}$. Analysis of the reaction mixture by radio TLC showed that after 20s of mixing the product, **48**, had formed and that after 60s the labelling efficiency had reached 80% which was comparable to the conventional batch strategy but provided the potential for automation.

The metastable SPECT radioisotope $^{99\text{m}}\text{Tc}$ has been complexed with hydroxyl

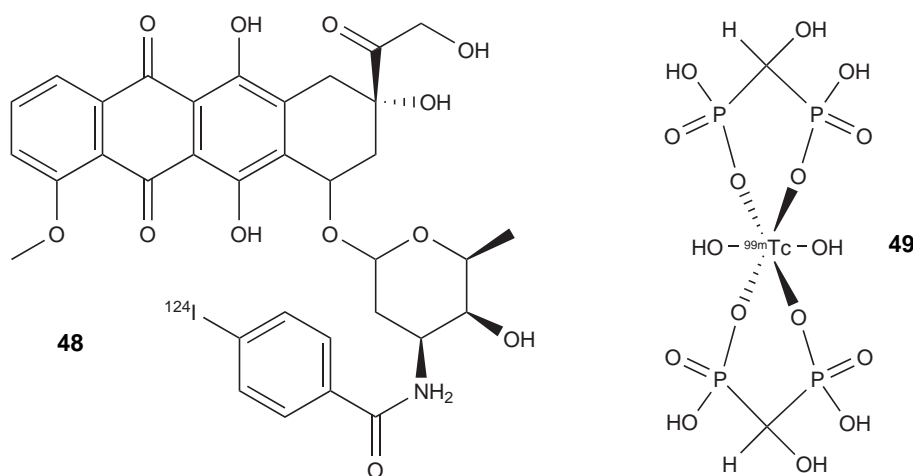


Figure 14. Two of the radiolabelled compounds that were prepared within micro reactors by Gillies and co-workers.^{89,90}

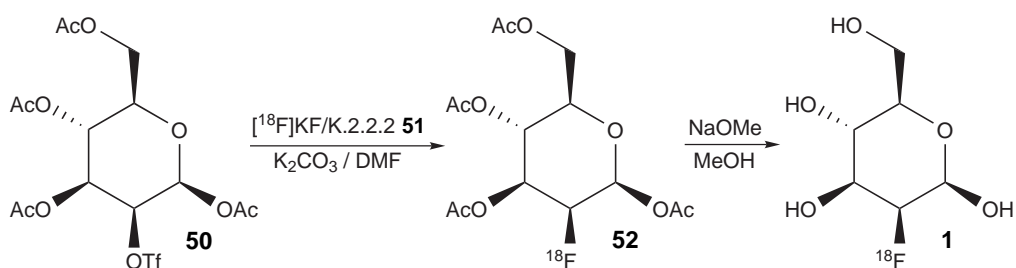
1.3 ISOTOPE LABELLING IN CONTINUOUS FLOW REACTORS

diphosphinate oxidronate **49** using the micro reactors with a RCY of $\sim 85\%$ being achieved at a residence time of 4 s. Although this aqueous complexation reaction occurs extremely rapidly by conventional methods, the ability to automate the synthesis when dealing with radioisotopes is clearly an advantage.

Micro flow synthesis of $[^{18}\text{F}]\text{FDG}$ **1** was also undertaken according to Scheme 14, this time using two identical micro reactors which were coupled together. Within the first reactor initial fluorination of D-mannose triflate **50** occurred by the concurrent introduction of pre-prepared $[^{18}\text{F}]\text{KF}$ entrapped in K.2.2.2 **51** whereby the outlet was fed into the second reactor which allowed for deprotection *via* hydrolysis to afford the final, radiolabelled $[^{18}\text{F}]\text{FDG}$ **1**. The RCY of the product was 50% and although unreacted intermediate **52** and $[^{18}\text{F}]\text{F}^-$ remained in the mixture, the on-chip reactions were completed within 4 s to 6 s.

Integrated Synthesis of $[^{18}\text{F}]\text{FDG}$ An automated PDMS micro flow reactor operated under digital control containing integrated micro valves has also been used to demonstrate the timely synthesis of $[^{18}\text{F}]\text{FDG}$ **1**.⁹¹ Normally such synthesis, when undertaken with commercially available automated units takes up to 50 min, but by applying the same synthetic route as is depicted in Scheme 14 to the developed system this was reduced to 14 min. The protocol for the micro reactor synthesis followed 5 integrated steps:

1. Concentration of ^{18}F using a micro sized ion exchange column.
2. Entrapment of $[^{18}\text{F}]\text{KF}$ into K.2.2.2 **51**.
3. Solvent exchange; evaporation of water and replacement by MeCN, achieved by heating the micro reactor device.



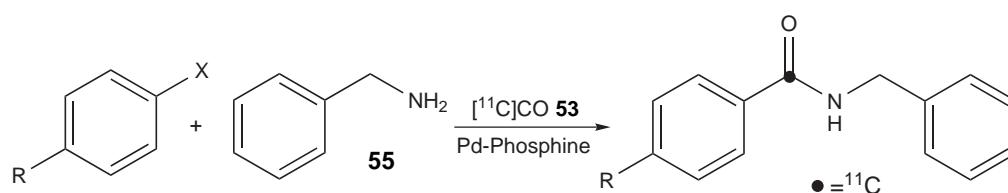
Scheme 14. The route by which $[^{18}\text{F}]\text{FDG}$ **1** was synthesised within two microfluidic reactors.^{89,90}

4. Fluorination of the D-mannose triflate **50** precursor.
5. Solvent exchange; MeCN evaporation through PDMS and replacement with water.
6. Acid hydrolysis of the intermediate **52** to afford [¹⁸F]FDG **1**.

Clinical use of synthesised [¹⁸F]FDG **1** was then successfully demonstrated by undertaking PET imaging of a tumour infected mouse. Although similar to the microfluidic synthesis reported by Gillies *et al.*^{89,90} the developed reactors integrated characteristics and the capability for solvent exchange and automation provide several key advantages. Most importantly these include the reduction in conventional (total) synthesis time and the cost saving that can be achieved when using an integrated reaction system; *i.e.* the cost is mostly associated with design and development, rather than the reproduction of such systems.

Micro Reactor Labelling via [¹¹C]CO Recently Miller *et al.*⁹² reported the use of a micro tube reactor packed with Pd-phosphine catalyst to bring about the synthesis of amides with [¹¹C]CO **53**, thus providing a rapid route to the introduction of this particular isotope into such compounds. Reagents were introduced to the reactor through a mixing tee which was connected to a CO mass flow controller and a syringe pump coupled to a substrate injector and infused through the reaction column at a flow rate of 10 $\mu\text{l min}^{-1}$ for a period of 12 min, before being flushed off at a flow rate of 200 $\mu\text{l min}^{-1}$. Yields that were achieved during optimisation of the reactions (with non-radioactive CO) were much higher when compared to their batch equivalents (23% to 72% improvement). Following this, [¹¹C]CO **53** was produced with a cyclotron, trapped in a stainless steel loop packed with molecular sieves and cooled using liquid nitrogen. Subsequent warming and controlled infusion of nitrogen through the loop then allowed the radiolabelled reactant **54** to be introduced into the micro reactor system where the reaction between phenylmethanamine **55** and four aryl halides was undertaken as illustrated in Scheme 15. Over two runs for each compound the system showed reasonable reproducibility ($\geq 22\%$ difference between runs), good radiochemical purity and comparable RCY to the ‘cold’

1.3 ISOTOPE LABELLING IN CONTINUOUS FLOW REACTORS



Scheme 15. A generalised scheme to illustrate the labelling of secondary amides *via* ^{11}C CO which was successfully performed within individual micro tube reactors.⁹²

synthesis, all within one half life (20 min) of the ^{11}C CO **53** being released from the trap.

1.3.2 Aims

As mentioned when the concept of PET was introduced (Section 1.1.3), and exemplified by the work published within the field to date, continuous flow synthetic methods are well suited to synthesis with radioisotopes, in particular because of the small device dimensions which lead to easy shielding and potential for the design of fully integrated reaction units, such as the one described in Section 1.2.7. In contrast the work carried out herein is undertaken with stable isotopes and although there is potential for the same reactions to be undertaken with radiolabelled precursors the application of the methods that will be presented lie directly within the realms of stable labelling applications. The overall aim of this work was to investigate isotope substitution using various reactions as models, and to transfer the procedures to micro reactors in a bid to improve the overall reaction efficiency.

CHAPTER 2

C–O BOND FORMATION

2.1 Phenols and Carboxylic Acids

WHEN examining the structure of phenol derivatives, such as those shown in Figure 15, it is not difficult to see that their name stems from the characteristic OH group bonded directly to a phenyl ring. Although these compounds resemble alcohols, they should in fact be viewed very differently since they are at least one million times more acidic. The proton belonging to the hydroxyl group is able to dissociate more readily due to resonance stabilisation of the conjugate anion, a mesomeric effect which leads to lower pK_{aH} values when compared with aliphatic alcohols.⁹³ In contrast, carboxylic acids are less dissociated in solution since they hydrogen bond to one another, forming dimers. However, weakening of the OH bond by the presence of the carbonyl group and corresponding stability of the conjugate base, caused by resonance effects, ensures as the name suggests that these compounds too are partially dissociated when in solution.⁹⁴

The two classes of reactions that were carried out using phenolic substrates, with the aim of introducing deuterium isotope labels into the corresponding products, were acylations (Section 2.2) and methylations (Section 2.3). The former leads to products which contain an ester functional group and the latter a methyl ether (if performed on alcohols or phenols) or a methyl ester (if performed on a carboxylic acid). These are important moieties, exemplified by their presence within many

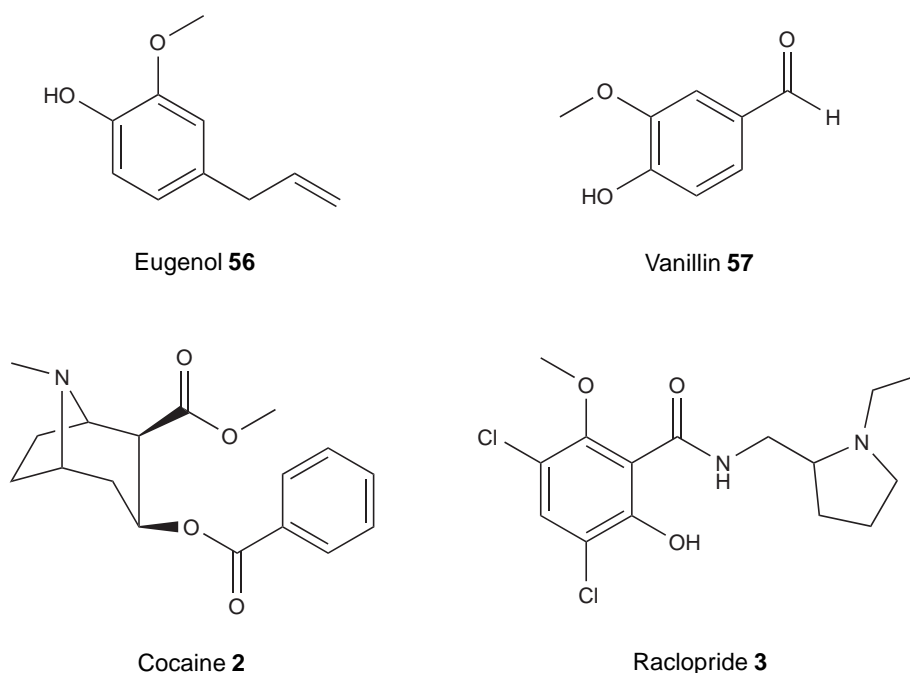


Figure 15. Examples of compounds containing phenol, ester and methyl ether functional groups.

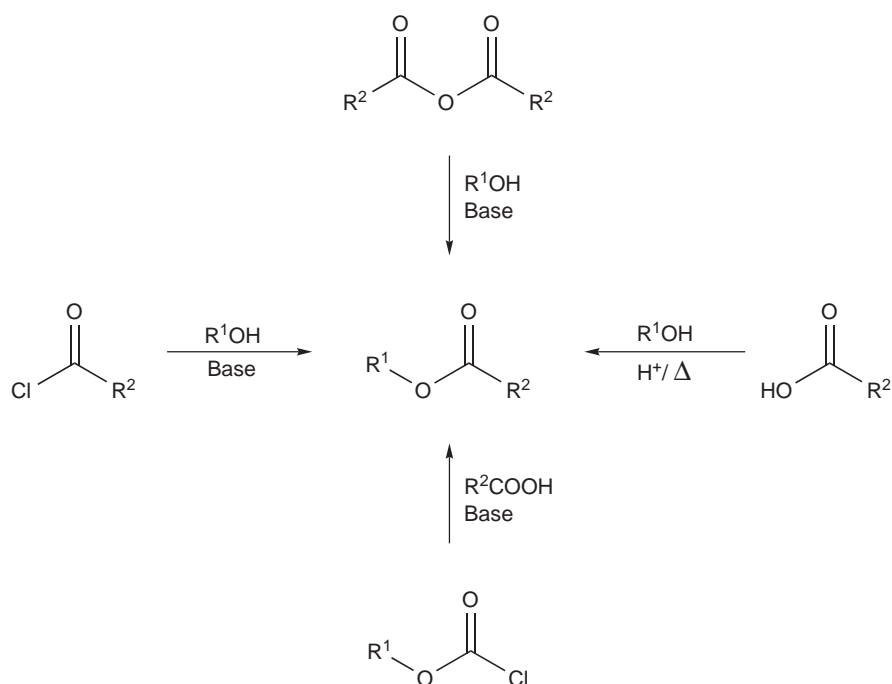
natural products and pharmacologically relevant compounds with eugenol **56**, vanillin **57**, cocaine **2** and raclopride **3** (Figure 15) being particular examples.

2.2 Acylation of Phenol Derivatives

The introduction of an acyl group into a compound results in esters which are found in compounds ranging from polyesters to fats, oils, lipids (which are important natural acids) and foodstuffs.⁹⁵ They also find use as protecting groups in organic synthesis⁹⁶ but more importantly for this project, they are distinctive functional groups in a large number of pharmaceuticals. For example, the common analgesic 2-acetyloxybenzoic acid (aspirin) contains an ester group and the previously mentioned cocaine **2** (Figure 15) contains two different ester groups. For this reason it is clear that the development of novel methods to enable the efficient, controlled incorporation of isotopes into ester moieties, *via* the reaction of phenol derivatives with isotopically substituted acyl groups, are extremely useful techniques to establish.

Esterification reactions may be carried out *via* a number of routes such as those illustrated in Scheme 16. The well known Fischer esterification⁹⁷ is an acid

2.2 ACYLATION OF PHENOL DERIVATIVES



Scheme 16. Common methods by which esters may be synthesised.⁹⁵

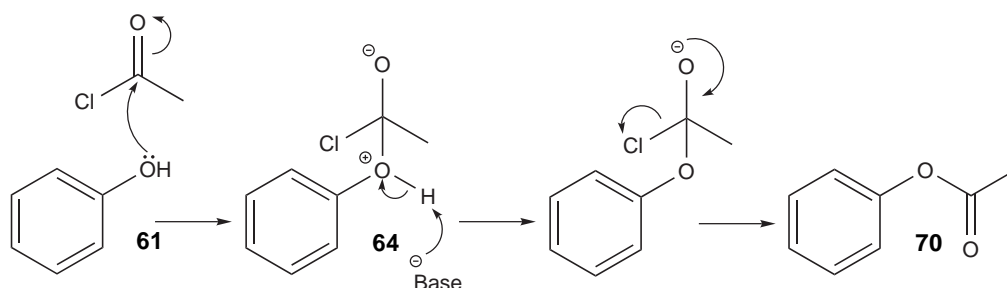
catalysed reaction between an alcohol and carboxylic acid which involves heating the reagents and pushing the equilibrium in favour of the product by using one reagent in excess, generally the least expensive, or removing water under Dean-Stark conditions.⁹⁸ This particular approach is ideally avoided within the realms of isotopic labelling, since it is desirable to achieve full label incorporation, thus minimising costs of expensive labelled precursors. In addition, employing stoichiometric quantities of reagents simplifies purification procedures. With this in mind another possible route to ester formation is the reaction between an alcohol or phenol derivative with an acid anhydride, however using this method of synthesis one mole of carboxylic acid is generated for every mole of product formed. For the purposes of this project, where introduction of a label through the smaller, acyl portion of the molecule is desired, the resultant 'isotopic waste' that would be generated using a (cheaper) symmetrical acid anhydride, is undesirable. Another alternative is to react alcohol or phenol derivatives with acyl halides, which may be formed from their corresponding carboxylic acids by treatment, for example, with thionyl dichloride or trichlorophosphane.⁹⁹ This method has the advantage that it is possible to incorporate the complete molecule into the final product and that acyl chlorides are highly reactive, increasing the rate by

which reactions progress. Consequently it was decided to study the reaction of five selected phenols, optimising the reaction conditions prior to isotope labelling by the substitution of acetyl chloride **58** for its deuterated counterpart (D₃)acetyl chloride **59**.

Many specific examples may be found within the literature that pertain to the acylation of alcohols and phenols including catalysis by graphite bisulfate,¹⁰⁰ the use of immobilised acids,¹⁰¹ cobalt chloride,¹⁰² zeolites,¹⁰³ potassium fluoride on alumina,¹⁰⁴ zinc oxide,¹⁰⁵ ionic liquids,¹⁰⁶ organic bases such as *N,N*-dimethylpyridin-4-amine (DMAP) **60**¹⁰⁷ and other common inorganic bases such as sodium hydroxide.¹⁰⁸ Whilst it is also possible for the reaction to proceed without an added promoter at room temperature, especially in the absence of a solvent, the rate is well known to be enhanced with an organic base, which helps decrease the addition-elimination reaction time considerably.¹⁰⁸ Influenced by previously published results¹⁰⁹ involving the reaction of phenol **61** and 4-nitrophenol **62** with acetyl chloride **58**, in the presence of *N,N*-diethylethanamine (Et₃N) **63**, within a micro reactor under EOF control, this method was chosen as a starting point for labelling investigations. However, in contrast to the previously reported work, fluid infusion was controlled hydrodynamically which allows for greater conservation of isotopically modified precursors and products, since there are no open wells (as found within EOF based systems) which can lead to loss of reagents through evaporation.

The Solubility of Ammonium Salts in Organic Solvents

As illustrated by the mechanism shown in Scheme 17, when the reaction of phenol



Scheme 17. The mechanism of base action on the conversion of phenol **61** to phenyl acetate **70**.¹⁰⁸

2.2 ACYLATION OF PHENOL DERIVATIVES

61 and acetyl chloride **58** is undertaken in the presence of a base it abstracts a proton from the tetrahedral intermediate **64**. In the case of nitrogen containing organic bases, sequestering of the chloride ion also occurs and ammonium chloride salts are formed. As the solubility of this by-product was envisaged to be a problem, with respect to precipitation and consequent obstruction of flow within the micro channels, a suitable solvent system was sought for the acetylation reactions.

Protic solvents are an unsuitable medium in which to undertake reactions with acyl chlorides, since hydrolysis of such halogenated compounds in the presence of water to their corresponding carboxylic acids, or reaction with other species such as alcohols will occur. Since an aprotic solvent which avoided precipitation was required, the ideal choice was one with a high dielectric constant (polarity). After comparing the dielectric constants of a variety of solvents, summarised in Table 1, it can be seen that dimethylsulfoxide (DMSO, Entry 1) is the most polar. However, in comparison to other solvents, its viscosity is high and due to the back pressures generated when mobilising fluids hydrodynamically through micro channels (see Section 1.2.5, it was discounted on practicality grounds. MeCN (Entry 2), the next most polar solvent, was therefore selected as it is significantly less viscous, allowing for ease of manipulation within micro channels.

Table 1. The boiling point, dielectric constant and viscosity of various aprotic solvents (at 20 °C) arranged in order of dielectric constant.¹¹⁰

Entry	Solvent	Boiling Point (°C)	Dielectric Constant	Viscosity ^a (mPa·s)
1	DMSO	189.0	47.2 ^b	2.20
2	MeCN	81.6	37.5	0.34 (25)
3	DMF	153.0	36.7	0.92
4	Acetone	56.1	20.7 (25)	0.30 (25)
5	Pyridine	115.3	12.3 (25)	0.95
6	DCM	39.8	9.1	0.45 (15)
7	THF	64.8	7.6	0.55
8	EtOAc	77.1	6.0 (25)	0.46
9	Ethoxyethane	34.4	4.4	0.24
10	Benzene	80.1	2.3	0.65
11	Hexane	68.7	1.9	0.31

^a The numbers in parentheses indicate alternative temperatures (°C) at which readings were taken.

^b The cited value originates from the 86th edition (2005) of the CRC Handbook of Chemistry and Physics since the value as it appears within the reference¹¹⁰ is misquoted as being 4.7.

2.2.1 Initial Micro Reactor Set Up

All micro reactions reported herein were carried out using borosilicate glass micro reactors, fabricated in-house by photolithographic and wet etching techniques as described in Section 1.2.1.⁴⁷ The inherent dimensions and physical characteristics of all devices referred to within the text are provided in Appendix A. Combining standard HPLC fingertight fittings with 10.0 cm of polyaryletheretherketone (PEEK™) tubing (360 μm o.d., 150 μm i.d.) allowed the inlets to be interfaced with glass luer-lock syringes, which were driven by a syringe pump capable of simultaneously delivering a maximum of three solutions. The product stream was collected from the outlet, through a 5.0 cm length of PEEK™ tubing, into a small vial containing 50 μl of water, in order to quench reactions and ensure the % conversions reflected their occurrence within the micro reactor set up. Where two reactors were used in series, connection of one reactor outlet to another reactor inlet was achieved *via* a 5.0 cm length of PEEK™ tubing, as shown in Figure 16. Using such a modular approach is an effective way to optimise reactions when working at the prototyping stage, since swapping of individual reactor units is a facile procedure. After allowing sufficient time for the system to equilibrate at a set flow rate, typically 10 min to 15 min at $1 \mu\text{l min}^{-1}$, 10 μl of product solution was



Figure 16. A photograph of a typical micro reactor set up.

collected and analysed *via* HPLC. In order to determine accurate % conversions an appropriate calibration using synthetically prepared standards or commercially available chemicals was undertaken prior to the collection of data so that the relative responses of the compounds under investigation could be normalised.

Previous calibrations¹¹¹ utilising the same syringe pump and controller indicated that as the set flow rate was lowered, the actual (recorded) flow rate deviated to a greater degree. For example at $20\ \mu\text{l min}^{-1}$ using a 1 ml syringe the RSD was observed to be 0.89%, which rose to 8.10% at $1\ \mu\text{l min}^{-1}$. Thus it may be concluded that when operating at lower flow rates there is a greater influence on the error of recorded conversions/yields arising from this inconsistency. However, because the influence of infusion rate on results is reduced at lower flow rates (*i.e.* because mixing is complete and only kinetic limitations of the reaction are pertinent), the effect can be assumed as equally negligible (< 1% RSD) across all flow rates that were employed herein and the influence on final results small. The majority of error is thus introduced *via* the method of analysis which is in accordance with RSD's observed when calibrating instruments against synthetic standards (generally 2% to 4%).

2.2.2 Solvent Studies within Micro Reactors

Evaluation of the reaction of 4-nitrophenol **62** with acetyl chloride **58** in the presence of Et_3N **63** within a hydrodynamically controlled micro reactor system was selected as the initial reaction to study as the colour change which accompanied formation of the product **65** was helpful in allowing the reaction progress to be visualised *in-situ*. In accordance with the findings discussed earlier relating to solubility of by products and from the aforementioned publication,¹⁰⁹ MeCN was used as the solvent for the investigation. As shown schematically in Figure 17, the first micro reactor ($T_1 = 201\ \mu\text{m} \times 75\ \mu\text{m} \times 2.0\ \text{cm}$; width \times depth \times mixing channel length) combined the phenol derivative and Et_3N **63**, delivered as 100 mM solutions from two 500 μl syringes. The outlet of the first reactor was then connected to the inlet of a second reactor ($T_2 = 158\ \mu\text{m} \times 54\ \mu\text{m} \times 1.5\ \text{cm}$) where acetyl chloride **58** was introduced as a 50 mM solution from a 1000 μl

2.2 ACYLATION OF PHENOL DERIVATIVES

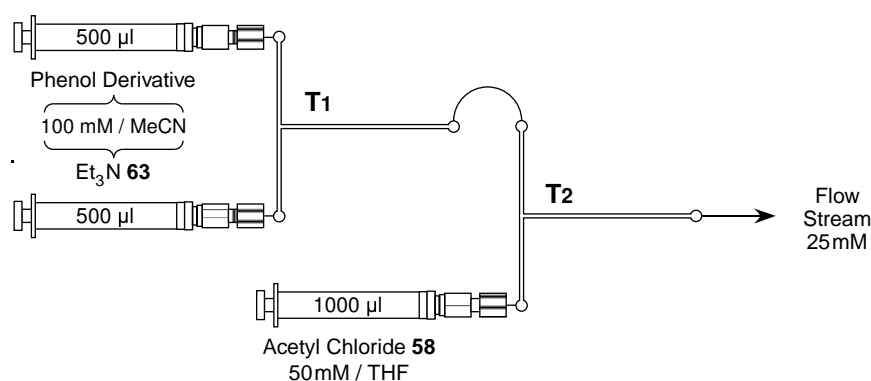


Figure 17. Schematic of the micro reactor set up T₁-T₂, used to investigate the reaction between phenol derivatives and acetyl chloride **58** in the presence of Et₃N **63** (note the differing syringe sizes and reagent concentrations; the overall effect gives rise to stoichiometric quantities of reactants when all syringes are driven at an equal flow rate).

syringe. It should be noted that the concentration of substrates delivered from the first reactor equates to 1 equivalent (eq.) of acetyl chloride **58** solution as pre-mixing the solutions would dilute them to 50 mM. Consequently this afforded a final product stream, assuming 100% reaction, of 25 mM for collection and analysis.

Initial experiments into the acylation of 4-nitrophenol **62** were undertaken within micro reactor set up T₁-T₂ and excellent results (> 90.0% conversion) were obtained, however it was apparent that the stability of the reagents was questionable, as gradually diminishing conversions were observed over the course of a day's experimentation. To confirm this observation, the system was run at a flow rate of 5 µl min⁻¹ which allowed for continual testing over a prolonged period without necessitating the reloading of syringes. A sample was collected from the flow stream every 15 min and analysed immediately over a period of 4.5 hr. As can be seen from the data presented in Figure 18, during this time there was a significant drop in conversion of 4-nitrophenol **62** to 4-nitrophenyl acetate **65** when the reagents were prepared as solutions in MeCN; the cause of which was attributed to the decomposition of acetyl chloride **58**, owing to its high reactivity. Selecting an alternative solvent in which to prepare the acetyl chloride **58** solution (the 4-nitrophenol **62** and Et₃N **63** still being dissolved in MeCN), the experiment was then repeated and in the case of THF, loss of activity was not found to occur to such a degree. The overlaid plot (Figure 18)

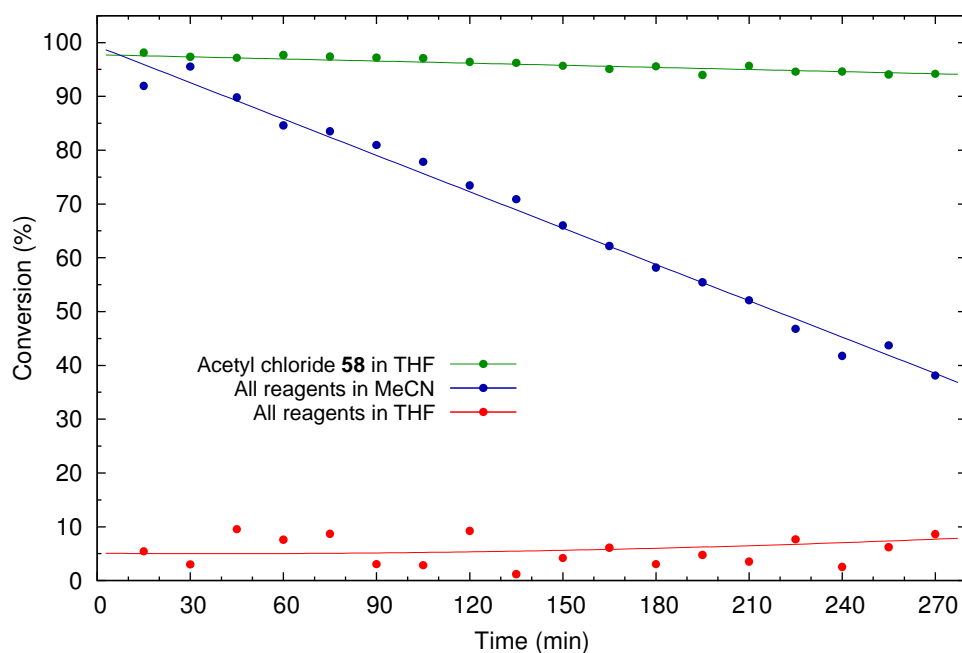


Figure 18. A time based study showing the effect of solvent composition on conversion when acetylating 4-nitrophenol **62** in the micro reactor set up T₁-T₂.

shows a significant improvement in the stability of the system however, as can be further seen, when reagents were prepared exclusively as solutions in THF, fluctuating low conversions were recorded. In the latter case these inconsistencies were caused by precipitation within the channel of the second micro reactor, T₂, of the reactions by-product, Et₃N·HCl **66**. For this reason a mixed solvent system was employed as the conversion of reactant to product, although showing a very slight decrease of 1.4% over the 4.5 hr period, remained consistently high indicating its suitability for the reactions under study.

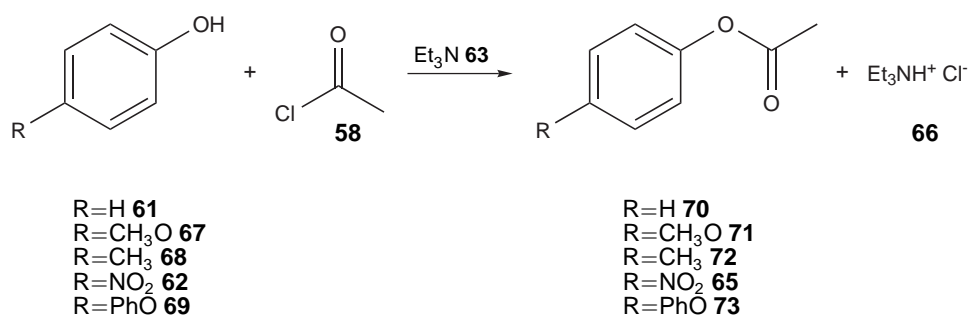
2.2.3 Further Reactions with *N,N*-Diethylethanamine

To expand the scope of the study the acetylation of five phenol derivatives was investigated using the optimised solvent system and identical micro reactor set up (T₁-T₂). In order to investigate reactivity as a function of flow rate phenol **61**, 4-methoxyphenol **67**, 4-methylphenol **68** and 4-phenoxyphenol **69** were also chosen to undergo micro reaction optimisation. For example, methoxy groups are electron donating and thus 4-methoxyphenol **67** was selected to undergo investigation whilst in contrast 4-phenoxyphenol **69**, which is a comparatively

2.2 ACYLATION OF PHENOL DERIVATIVES

larger moiety, may be expected to diminish reactivity. In addition phenol **61** served as a good, general starting point when investigating reactions and the nitro group is commonly used as a precursor to amines and is electron withdrawing making 4-nitrophenol **62** an important derivative to evaluate. Using the pre-determined optimal solvent conditions the synthesis of phenyl acetate **70**, 4-nitrophenyl acetate **65**, 4-methoxyphenyl acetate **71**, 4-methylphenyl acetate **72** and 4-phenoxyphenyl acetate **73** were studied, according to Scheme 18, in micro reactor set up T1-T2, previously illustrated in Figure 17.

At each set flow rate, a total of 10 repeat measurements were made in order to determine the reproducibility of the system. In all cases it was found to be excellent ($< 5.0\%$ RSD) and, as would be expected, when the flow rate was lowered the conversion of phenol derivatives to their corresponding phenyl acetate derivatives improved (Figure 19). This observation correlates with an increase in the residence time of reactants within the micro reactor, since they spend a longer time in contact with one another prior to quenching. As can be further seen, in comparison to the other phenol derivatives investigated, the reaction of 4-nitrophenol **62** was extremely fast and exhibited near quantitative conversion to its corresponding acetate **65**, regardless of the residence time (flow rate) of the reagents within the micro reactor channels. This was surprising since estimates of the Fourier numbers for acetic acid in EtOAc passing through the mixing channel of micro reactor T2 and exit tubing indicate that complete mixing ($Fo \geq 1$) is only achieved when the overall flow rate is $20 \mu\text{l min}^{-1}$ which equates to a set flow rate of $40 \mu\text{l min}^{-1}$. Based upon this estimation it may be assumed that



Scheme 18. The conversion of phenol derivatives to their corresponding phenyl acetate derivatives in the presence of Et₃N **63**.

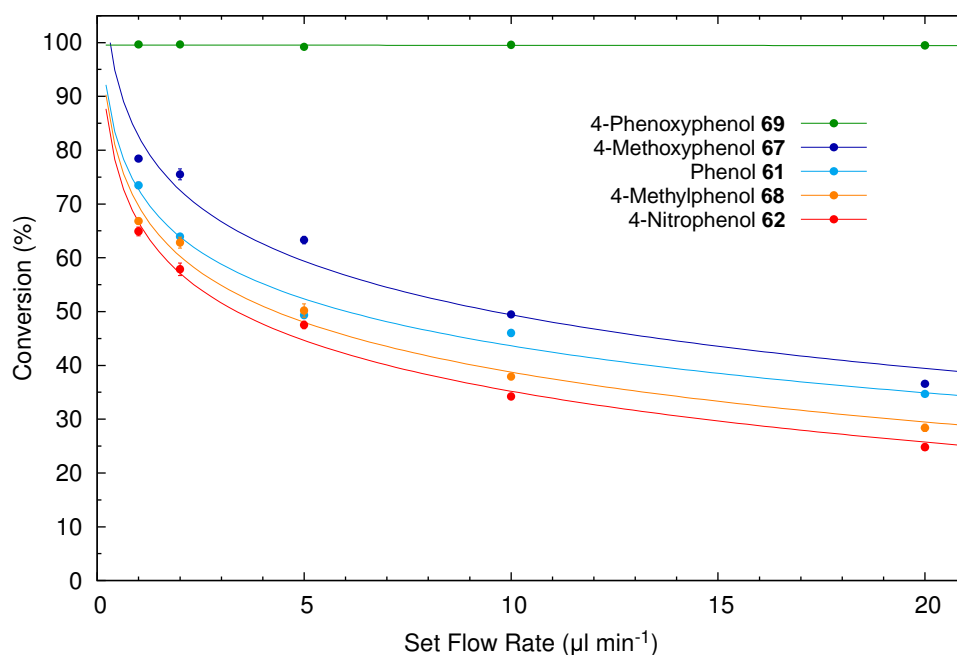


Figure 19. Results obtained for the acetylation of 5 phenol derivatives in micro reactor set up T₁-T₂ ($n = 10$).

at set flow rates lower than $10 \mu\text{l min}^{-1}$ the reactions are limited kinetically and extrapolation of the plot indicated that an extremely slow flow rate would produce a more complete reaction (*e.g.* higher conversions) however, it is proposed that the systems reproducibility at flow rates $< 1 \mu\text{l min}^{-1}$ would be questionable due to perturbations caused by the mechanical nature of the pump and observations made when conducting calibration studies. In addition, due to the low throughput that would be achieved from such a system, *i.e.* $4.2 \times 10^{-2} \text{ mg hr}^{-1}$ for the synthesis of phenyl (D₃)acetate **74**,* an alternative approach was sought in order to ensure suitable levels of productivity.

2.2.4 The Effect of Increasing Reactor Length

Lengthening the channels of micro reactors is an effective way to increase the degree of reaction that occurs within them, since complete mixing of the substrates occurs before the majority of a channel has been traversed and consequently reactants remain in contact for greater periods of time at equivalent flow rates. For this reason it was decided to substitute the reactors T₁ and T₂ for two serpentine micro reactors of longer channel length; S₁ = $150 \mu\text{m} \times 50 \mu\text{m} \times 12.1 \text{ cm}$ and S₂ =

*Throughput calculated assuming 100% conversion of phenol **61** to phenyl (D₃)acetate **74** at a set flow rate of $0.1 \mu\text{l min}^{-1}$.

176 μm \times 63 μm \times 12.1 cm. Using the new micro reactor set up S1-S2, depicted in Figure 20, the experiments were repeated at the same flow rates to determine if longer reaction channels offered any improvement in recorded conversions.

As Figure 21 illustrates, the results are similar to those obtained in shorter reactors and there was in fact only an average improvement of 5.6% conversion for the phenol derivatives that had failed to react sufficiently within reactor set up T1-T2. If the combined Fourier numbers at the fastest overall flow rate (40 $\mu\text{l min}^{-1}$) for the final stage reactor, S2, and exit tubing are evaluated ($Fo = 1.0$ for acetic acid in EtOAc) it may be inferred that the modified micro reactor set up, S1-S2, afforded complete mixing of the three reactants regardless of the flow rate employed. Considering the comparative increase in post mixing (reaction) time this set up affords, especially at slower flow rates, the improvement in conversions that was noted is extremely low and indicated that an alternative route may need to be contemplated in order to bring about the successful (high yielding) acetylation of the majority of phenol derivatives. Once again, the one exception was 4-nitrophenol **62** which reacted extremely well at all flow rates, as would be expected when considering the previous results that were obtained using the shorter micro reactor system.

To account for the different reactivity of 4-nitrophenol **62** in comparison to the other derivatives it is proposed that due to resonance stabilisation of 4-nitrophenolate **75**, which is illustrated in Figure 22, a greater proportion of the unbound anion exists in solution thus increasing its availability to react. This

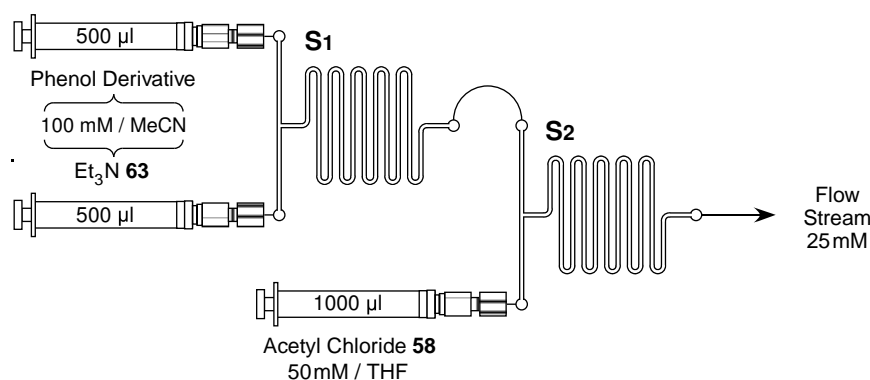


Figure 20. The micro reactor set up S1-S2, used to increase the residence time of phenol derivatives and acetyl chloride **58** in the presence of Et₃N **63**.

2.2 ACYLATION OF PHENOL DERIVATIVES

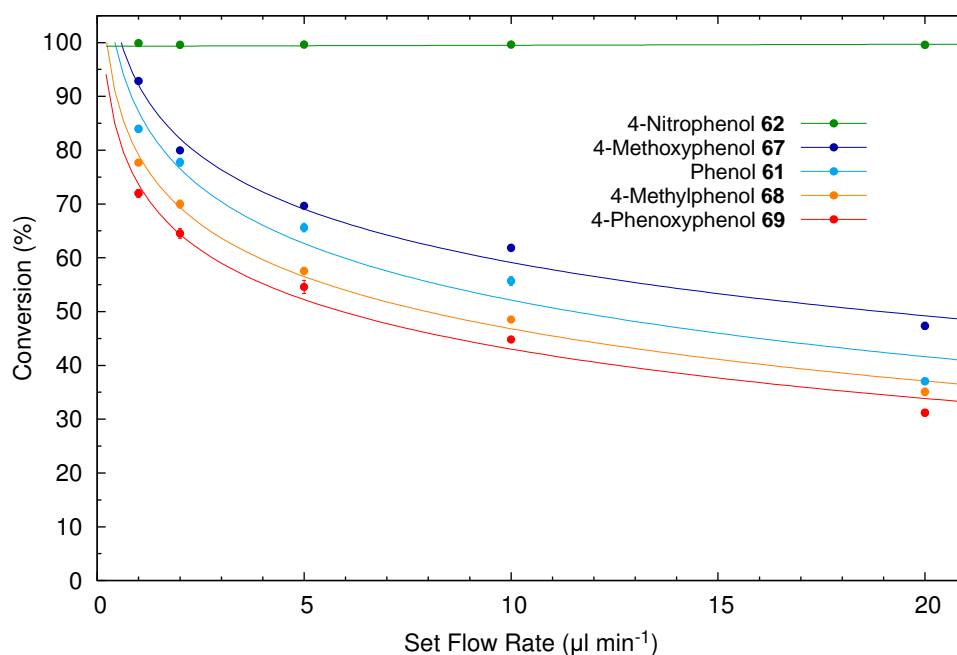


Figure 21. Results of acetylating 5 phenols within micro reactor set up S1-S2 ($n = 10$).

effect may be noted with the naked eye by mixing a solution of 4-nitrophenol **62** with a base such as Et_3N **63** and noting the distinct vivid yellow colour change that accompanies formation of the anion.

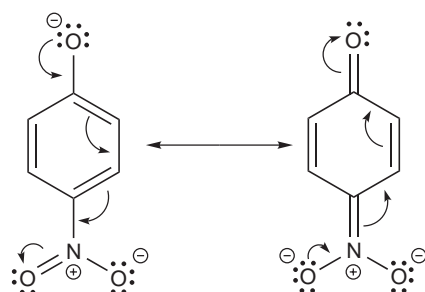


Figure 22. The resonance structure of 4-nitrophenolate **75**.

2.2.5 Acetylation in the Presence of DMAP

A natural solution to the requisite of increased residence times would have been to further lengthen the two reactors and continue experimentation in a likewise manner. There are however practical problems with this approach, such as increased back pressures, which can compromise the system integrity. Additionally, considering the small improvement in conversions observed when lengthening the micro reactors (Figure 19 *cf.* Figure 21) it seemed as though the Et_3N **63** was

simply not basic enough to afford full reaction of all the phenol derivatives. In consideration of these points the use of DMAP **60**, which is well documented as an acylation catalyst,^{107,112–114} in conjunction with Et₃N **63** was investigated.

Batch Reactions with DMAP

In order to evaluate any enhancement to the acetylation of phenol **61** in the presence of DMAP **60** small scale batch reactions using MeCN as the solvent were undertaken in the following way. To a small vial containing MeCN (0.5 ml) phenol **61** (50 μ l, 100 mM, 5.0×10^{-3} mmol) was added with an appropriate amount of Et₃N **63** base and DMAP **60** catalyst, as indicated in Table 2, followed immediately by acetyl chloride **58** (50 μ l, 100 mM, 5.0×10^{-3} mmol)*. The mixture was subsequently mixed on a carousel for 5 min and then analysed *via* HPLC method A, the results of which are shown in Table 2. As can be seen the addition of a stoichiometric amount of DMAP **60** to the reaction (Entry 6) in the absence of Et₃N **63** did not show any significant sign of improving previous conversions. However, even a catalytic amount of DMAP **60** (0.1 eq.) in the presence of a stoichiometric quantity of Et₃N **63** (Entry 5) affected the acetylation reaction considerably when compared to the reaction being conducted in its absence (Entry 2). Increasing the amount of DMAP **60** to a stoichiometric quantity did not appear to further enhance the conversions (Entry 8) and as such further investigations were conducted using 0.1 eq. of DMAP **60**.

Table 2. Experimental results obtained when testing the catalytic activity of DMAP **60** in the acetylation of phenol **61**.

Entry	DMAP 60 (10^{-3} mol)	Et ₃ N 63 (10^{-3} mol)	Conversion (%)
1	0.0	0.5	2.8
2	0.0	5.0	72.8
3	0.5	0.0	1.2
4	0.5	0.5	3.1
5	0.5	5.0	91.8
6	5.0	0.0	3.0
7	5.0	0.5	47.8
8	5.0	5.0	91.8

*Acetyl chloride **58** was prepared as a solution in THF to avoid degradation.

Micro Reactions with Catalytic DMAP

Following these results, the reaction was transferred to micro reactors for further experimentation and, having seen earlier that longer micro reactor channels were beneficial to the reaction with respect to mixing time, the micro reactor set up S_I-S₂ (Figure 20) was once again employed. A catalytic (10 mM) amount of DMAP **60** was added to the solution containing Et₃N **63** with all other reagents, solvents and concentrations remaining the same. The micro reactor set up was then run at a variety of set flow rates in order to determine the usefulness of DMAP **60** during the reaction of phenol **61** to phenyl acetate **70**.

As Table 3 illustrates, successful acetylations were achieved at the lowest set flow rate 1 $\mu\text{l min}^{-1}$ (Entry 5) whereby enhanced conversions to those demonstrated in the absence of DMAP **60** were attained. Although this result was within the range that was desired (> 90.0% conversion), the problem once again of a low throughput meant there remained no practical way to demonstrate the applicability of isotope labelling within a single micro reactor system. Scaling out would alleviate this problem, the requirement for larger volumes of solutions would, beyond a certain point, be a hindrance as production synthesis with isotopes is normally undertaken with small amounts of precursors. Due to the potential problems discussed previously, of high back pressure (upon increasing channel lengths) and precipitations (upon increasing reagent concentrations), evaluation of alternative organic bases was undertaken to determine if further improvements were possible.

Table 3. Experimental results obtained when testing the catalytic activity of DMAP **60** at a variety of flow rates in micro reactor set up S_I-S₂.

Entry	Set Flow Rate ($\mu\text{l min}^{-1}$)	Average Conversion ^a (%)	RSD ^b (%)
1	20	52.7 (37.0)	4.51
2	10	77.0 (55.7)	3.79
3	5	80.4 (65.6)	3.95
4	2	84.0 (77.8)	2.22
5	1	92.0 (84.0)	1.61

^a Numbers in parenthesis represent the conversions obtained within the same micro reactor set up without the addition of DMAP **60** catalyst.

^b $n = 10$.

2.2.6 Effectiveness of Organic Bases in Acetylation Reactions

In order to compare the suitability of ten alternative organic bases in assisting the acetylation reactions phenol **61** was chosen as a model for the study since previous experiments had identified that its reactivity lies between the other derivatives under investigation. A small scale batch study was again undertaken by dissolving an appropriate base (0.5 mmol) in 0.5 ml of 1 M phenol **61** solution (0.5 mmol in MeCN) and agitating the mixture by revolution on an automatic carousel for 1 hr, after which time acetyl chloride **58** (36 μ l, 0.5 mmol) was added to afford the corresponding product **70**. Following a further 1 hr mixing the mixture was quenched with water (0.5 ml) and analysed by HPLC; the results obtained are summarised in Table 4.

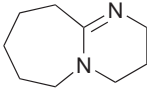
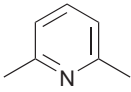
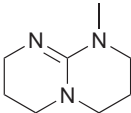
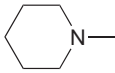
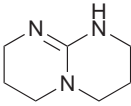
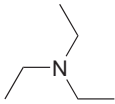
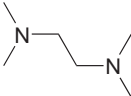
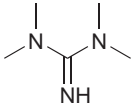
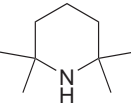
It may be inferred that no base managed to fully assist in the transformation of phenol **61** to phenyl acetate **70**, since none of the reactions were found to reach quantitative limits. From the data collected it can be seen that *N*-methylpyrrolidone (NMP) **76** (Entry 5) and 2,2,6,6-tetramethylpiperidine **77** (Entry 11) showed the most promising results (81.3% and 88.6% conversion respectively) however, in comparison to Et₃N **63** which promoted conversion to 87.0% itself (Entry 8) the improvement that would be gained here was not deemed worthy of further investigation. Due to the relatively high cost of stronger organic bases, such as phosphazenes,¹¹⁵ the use of inorganic bases was investigated instead.

2.2.7 Inorganic Bases

Acyl halides may also be reacted with alcohols or phenol derivatives in the presence of a strong inorganic base, such as sodium hydride **78** or BuLi **79**, which are employed to achieve activation of the nucleophile. Upon reaction with an acyl halide, inorganic salts are produced which, in a micro reactor environment, can readily block the small channels. With this in mind feasibility studies were performed on the reaction between commercially available sodium phenoxide **80** and acetyl chloride **58** within micro reactor T2. Since the by-product of the reaction, NaCl **81**, does not exhibit high solubility in organic solvents both

2.2 ACYLATION OF PHENOL DERIVATIVES

Table 4. Comparison of the effectiveness of various organic bases in aiding the synthesis of phenyl acetate **70** in batch at 100 mM in MeCN.

Entry	Base	Structure	Conversion (%)
1	1,4-Diazabicyclo[2.2.2]octane		66.2 ^a
2	2,3,4,6,7,8,9,10-Octahydropyrimido[1,2- <i>a</i>]azepine		76.8
3	2,6-Dimethylpyridine		76.0 ^a
4	1-Methyl-1,3,4,6,7,8-hexahydro-2 <i>H</i> -pyrimido[1,2- <i>a</i>]pyrimidine		69.5
5	1-Methylpiperidine 76		81.3
6	Pyridine		60.0
7	1,3,4,6,7,8-Hexahydro-2 <i>H</i> -pyrimido[1,2- <i>a</i>]pyrimidine		68.9
8	Et ₃ N 63		87.0 ^a
9	<i>N,N,N',N'</i> -Tetramethylethane-1,2-diamine		65.7 ^a
10	<i>N,N,N',N'</i> -Tetramethylguanidine		57.1
11	2,2,6,6-Tetramethylpiperidine 77		88.6 ^a

^a Precipitation formed upon addition of acetyl chloride **58**.

reagents were prepared as dilute (2 mM) solutions in MeCN and infused through the micro reactor at a flow rate of 5 $\mu\text{l min}^{-1}$. As the optical microscope image (Figure 23) clearly shows, a dark area of precipitate following a characteristic

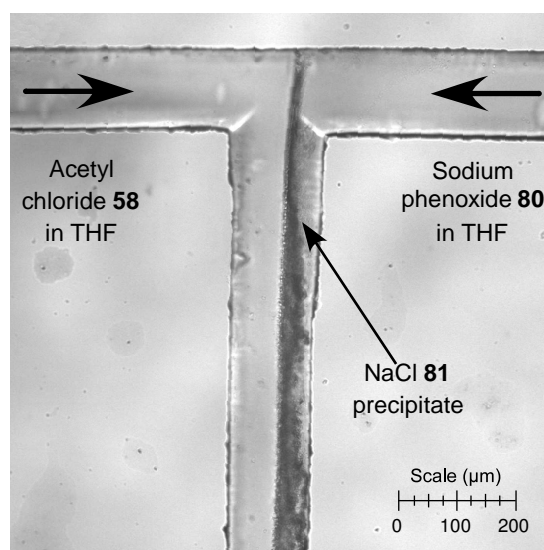


Figure 23. Optical microscope image of NaCl **81** precipitation within the central channel of micro reactor T2.

diffusion profile developed along one side of the reaction channel. This solid was attributed to the formation of NaCl **81** which exhibited extremely low solubility in a variety of organic solvents that were tested (see Table 5). As a result of this unavoidable precipitation, the micro channels were rapidly blocked and flow through the system was compromised. As it is also possible to react the corresponding lithium aryloxides with acyl chlorides to afford the desired phenyl acetate derivatives the feasibility of taking such an approach was therefore explored by testing the solubility of LiCl **82** in a variety of organic solvents.

Sodium and Lithium Chloride Solubility in Organic Solvents

Although literature is available pertaining to the solubility of LiCl **82** in organic solvents for the purposes of this project a comparison to the solubility of NaCl **81** was required and therefore carried out experimentally as follows. A saturated solution of metal chloride was prepared in the appropriate solvent by sonicating an excess of the salt for a period of 30 min. The solution was then filtered and 10.0 ml aliquots were concentrated *in-vacuo* and the inorganic residue subsequently weighed. As can be seen from Table 5 the results were rather pleasing since in all solvents LiCl **82** was found to be significantly more soluble when compared to its sodium counterpart. As THF was the most capable at dissolving

2.2 ACYLATION OF PHENOL DERIVATIVES

Table 5. Solubility of NaCl **81** and LiCl **82** within a variety of solvents at 21.5 °C.

Entry	Solvent	NaCl 81		LiCl 82	
		Weight ^a (mg)	Conc. (mM)	Weight ^a (mg)	Conc. (mM)
1	Acetone	4.5	7.8	115.6	272.6
2	EtOAc	5.6	9.6	16.0	37.8
3	MeCN	1.8	3.1	17.3	40.8
4	THF	22.7	38.8	670.0	1580.2

^a Weights reported as averages calculated from 5 repeat measurements of 10.0 ml aliquots.

LiCl **82** (Entry 4) and is also a common solvent to be used when carrying out lithiation reactions, it was subsequently selected for experimentation within micro reactor systems.

2.2.8 Acetylation of Lithium Aryloxides

Having found the solubility of LiCl **82** to be at its best in THF the reaction of lithium phenoxide **83** with acetyl chloride **58** was then attempted in the micro reactor set up S1-S2 (Figure 20). Lithium butane (BuLi) **79** (100 mM, THF) was substituted for Et₃N **63** with all other reagents and concentrations remaining the same, resulting once again in a final concentration of 25 mM. Initially the system seemed to indicate a good degree of reaction occurring (> 90.0%), although there appeared to be inconsistencies in the amount of product delivered within a set time period indicated by large differences in peak areas of the resultant chromatograms. As Figure 24 illustrates, upon examination of the intersection of micro reactor channel S1 with an optical microscope, precipitation at the

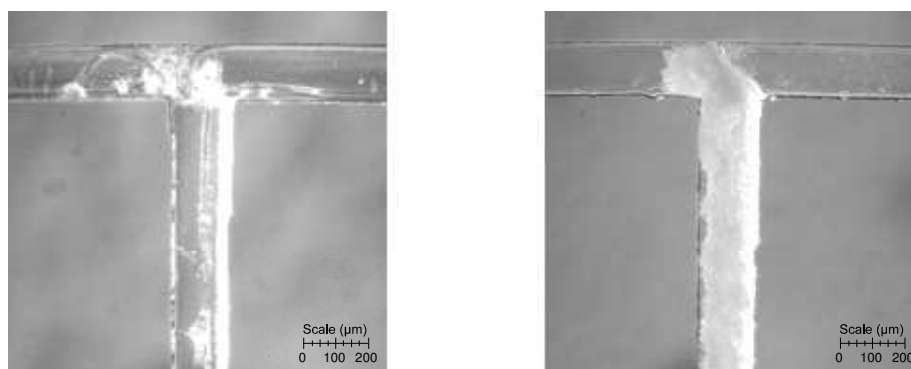


Figure 24. Precipitation observed at the interface of micro reactor channel S1 when phenol **61** and BuLi **79** were reacted in THF (left) and hexane (right).

2.2 ACYLATION OF PHENOL DERIVATIVES

channel interface could be clearly seen. Considering that lithium phenoxide **83** may be purchased as a 1 M solution in THF and that localised concentration within the micro reactor channel would be, at most, 100 mM this precipitate was attributed to other aggregates that could be forming as by-products, perhaps through reaction with the solvent, as occurs with the more reactive secondary or tertiary derivatives. Repeating the reaction with BuLi **79** solution prepared in hexane was found to increase the severity of the problem, due to the corresponding decrease in polarity between the two solvents and solubility of LiCl **82**.

Due to the problems encountered with the *in-situ* generation of lithium aryloxides the micro reactor system was simplified and lithium aryloxides were instead prepared 'off-chip'. One advantage to this approach is that since the lithiated precursors are prepared off-line, synthetic protocols may be established independently of the system that will carry out the isotope labelling. For example, a particular functional group may be pre-protected and undergo rapid on line deprotection post labelling, producing the target molecule in an expedient manner.

It was found that the most efficient way to obtain the lithium aryloxides was as ready to use solutions (100 mM), prepared by combining an appropriate amount of phenol derivative and BuLi **79** in THF as described in Section 6.4. To afford a greater amount of time for reaction, post mixing, a longer serpentine micro reactor ($S_3 = 170 \mu\text{m} \times 60 \mu\text{m} \times 23.6 \text{ cm}$, Figure 25) was commissioned ($Fo = 0.9$

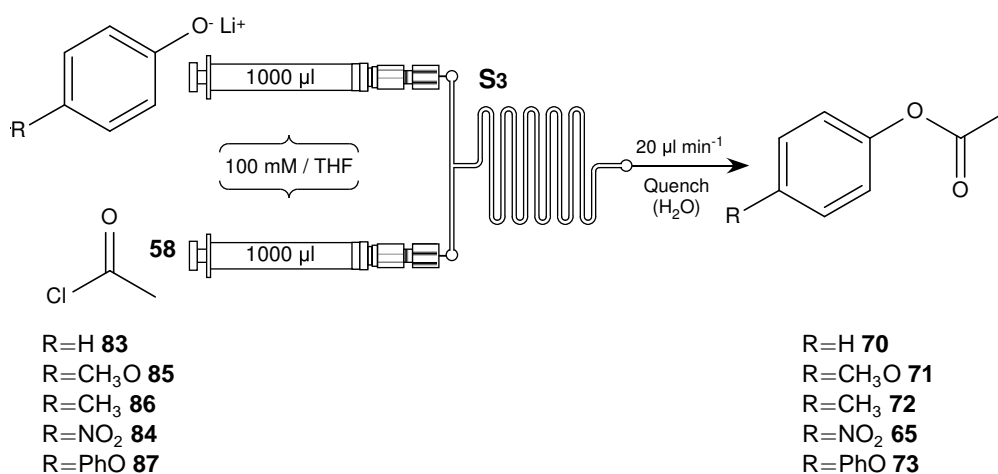


Figure 25. The micro reactor set up used to synthesise phenyl acetate derivatives from their corresponding lithium aryloxides.

2.2 ACYLATION OF PHENOL DERIVATIVES

for acetic acid in EtOAc at 40 $\mu\text{l min}^{-1}$). Introducing these solutions without further purification, to one inlet of S₃ and a solution of acetyl chloride **58** in THF (100 mM) to the other inlet the reaction of lithium phenoxide **83**, lithium 4-nitrophenoxide **84**, lithium 4-methoxyphenoxide **85**, lithium 4-methylphenoxide **86** and lithium 4-phenoxyphenoxide **87** to afford esters **70**, **65** and **71–73** respectively was brought about as illustrated in Figure 25.

It was pleasing to observe, as Table 6 shows, that when the syringe pump was set at the highest flow rate of 20 $\mu\text{l min}^{-1}$ the conversions achieved were high in the majority of cases. The one exception was found to be the lithium salt of 4-nitrophenol **62** (Entry 4) which exhibited comparatively lower conversions.

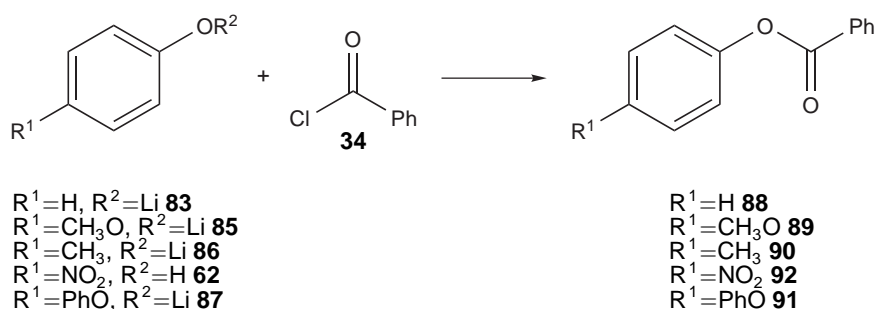
Table 6. Conversions achieved when acetylating a variety of pre-formed lithium aryloxides within the serpentine micro reactor S₃.

Entry	Product	Average Conversion (%)	RSD ^a (%)
1	Phenyl acetate 70	94.7	0.92
2	4-Methoxyphenyl acetate 71	96.3	1.33
3	4-Methylphenyl acetate 72	98.0	1.21
4	4-Nitrophenyl acetate 65	68.0	11.96
5	4-Phenoxyphenyl acetate 73	96.3	3.63

^a $n = 10$.

2.2.9 The Benzoylation of Phenol Derivatives

To expand the utility of the successful methodology it was decided to investigate the effect of replacing acetyl chloride **58** with benzoyl chloride **34**. To achieve this, the reaction between lithium phenoxide **83** and benzoyl chloride **34**, to afford phenyl benzoate **88**, was initially investigated, according to Scheme 19,



Scheme 19. Benzoylation of phenol derivatives performed in micro reactors.

employing micro reactor S₃.

Under the previously optimised conditions (set flow rate of 20 μlmin^{-1} and reagent concentration of 100 mM) it was found that conversion to the product **88**, was not as high as achieved when acetylating phenol **61** (49.2% *cf.* 94.7%), possibly due to the increased mixing and lower reaction time that would be caused by the larger benzoyl moiety. To account for this, the flow rate was subsequently lowered and, as can be seen from Table 7, there was no greatly significant effect on the conversion to phenyl benzoate **88**; surprisingly the best results were observed at a flow rate of 5 μlmin^{-1} .

To determine if other derivatives showed a similar reduction in conversions, the same set up was employed to benzoylate lithium aryloxides **85–87** to afford 4-methoxyphenyl benzoate **89**, 4-methylphenyl benzoate **90** and 4-phenoxyphenyl benzoate **91** respectively, according to Scheme 19. Although the optimal flow rate for the synthesis of phenyl benzoate **88** was found to be 5 μlmin^{-1} this was seen as an anomaly and experimentation was undertaken at the lowest flow rate, 1 μlmin^{-1} , as it was envisaged this would facilitate the maximum conversions in the other cases. Subsequently, when the benzoylation of the aforementioned lithium aryloxides was attempted under these conditions it was found that conversions were once again low, as indicated by the data presented in Table 8. As the nucleophile in these cases is the phenolate anion, which remains the same regardless of the type of acylation being conducted (*i.e.* acylations or benzoylations), it may be concluded that the lower reactivity observed when attempting benzoylation reactions stems directly from the presence of the phenyl ring on the acyl chloride. Because formation of the tetrahedral intermediate occurs through

Table 7. The effect of varying flow rate on the conversion of lithium phenoxide **83** to phenyl benzoate **88** within micro reactor S₃.

Set Flow Rate (μlmin^{-1})	Average Conversion (%)	RSD ^a (%)
20	49.2	8.86
10	62.8	6.23
5	73.7	7.57
2	64.5	6.60
1	63.1	8.22

^a $n = 10$

2.2 ACYLATION OF PHENOL DERIVATIVES

Table 8. The results obtained when benzoylating phenol derivatives within micro reactor set up S₃ at a set flow rate of 1 $\mu\text{l min}^{-1}$.

Entry	Product	Conversion (%)	RSD ^a (%)
1	Phenyl benzoate 88 ^b	73.7	7.57
2	4-Methoxyphenyl benzoate 89	53.2	10.59
3	4-Methylphenyl benzoate 90	28.6	42.29
4	4-Nitrophenyl benzoate ^c 92	81.4	23.83
5	4-Phenoxyphenyl benzoate 91	19.2	34.18

^a $n = 10$.

^b Result obtained at the optimal set flow rate of 5 $\mu\text{l min}^{-1}$.

^c Benzoylation of 4-nitrophenol **62** was carried out in the presence of Et₃N **63** using micro reactor set up S₁-S₂ at a set flow rate of 20 $\mu\text{l min}^{-1}$.

attack of the nucleophile at the Bürgi-Dunitz angle,¹¹⁶ 107° from the C=O bond, its approach will be sterically hindered by the larger phenyl ring when compared to the methyl group that is present on the acetyl derivative. Furthermore, the tetrahedral intermediate is stabilised by the presence of the adjoining phenyl moiety which means that its collapse to form the product is slowed. It may therefore be postulated that a combination of these effects greatly reduces the rate of reaction and leads to the lower conversions that were observed.

As was undertaken for the acetylation of 4-nitrophenol **62**, the reaction with benzoyl chloride **34** to afford 4-nitrophenyl benzoate **92** was then investigated using the organic base Et₃N **63** under the same conditions. Knowing that the reaction would be slower than the corresponding acetylation it was immediately attempted in the longer micro reactor set up S₁-S₂ at the lowest set flow rate of 1 $\mu\text{l min}^{-1}$. As can be seen from the results summarised in Table 8 (Entry 4) the results were in close agreement with those obtained when reacting lithium aryloxides, giving an overall conversion of 81.4% and confirming that the presence of the phenyl group limits the potential for successful benzoylation reactions within the micro reactor set ups described herein.

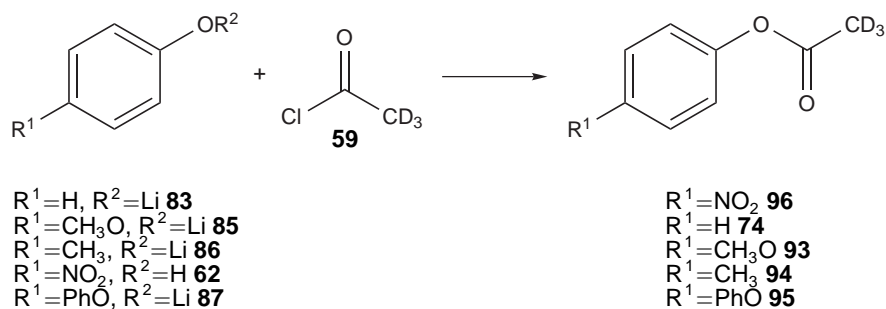
It is suggested that in order to successfully synthesise benzoylated products within micro reactors that a longer reactor may be beneficial. In addition raising the kinetics through heating the system may also produce higher conversions after equivalent residence times. Failing this, the suggested route would be to employ a better leaving group, such as bromine or iodine.

2.2.10 Summary of Acylation Reactions

After initially performing acetylation reactions in the presence of organic bases, it was encouraging to find a method that afforded high conversions. Although the 4-nitrophenol **62** derivative did not acetylate efficiently when attempting to react the corresponding lithium phenoxide, it exhibited behaviour that was opposite in nature to that of the other derivatives when employing an organic base, an observation that is attributed to its inherent mesomeric effects. Altering the acyl substrate by substituting acetyl chloride **58** for benzoyl chloride **34** also showed promising results, although slower flow rates, necessitated by the lower reactivity of the compound, were required.

2.2.11 Flow Synthesis of Deuterium Substituted Phenyl Acetate Derivatives

As high conversions had been achieved for all acetylations, the micro reactions of lithium aryloxides **83**, **85–87** and 4-nitrophenol **62** combined with Et₃N **63**, were thus repeated using (D₃)acetyl chloride **59** in place of its isotopically unmodified counterpart **58** to afford deuterium substituted esters phenyl (D₃)acetate **74**, 4-methoxyphenyl (D₃)acetate **93**, 4-methylphenyl (D₃)acetate **94**, 4-phenoxyphenyl (D₃)acetate **95** and 4-nitrophenyl (D₃)acetate **96** respectively, as illustrated by Scheme 20. Although the kinetic isotope effect is at its greatest in the case of hydrogen isotopes, it was expected that labelling reactions would exhibit the same high conversions under equivalent (optimised) conditions,



Scheme 20. Scheme illustrating the introduction of deuterium isotope labels into a library of phenyl acetate derivatives.

since the substituted label does not play a key role in the reaction.

Using the optimised micro reactor set ups, either S_I-S₂ (for 4-nitrophenol **62**) or S₃ (for the remaining phenol derivatives), 10 runs for each compound were performed in order to monitor the success of the isotope labelling. The data given in Table 9 illustrates the results of these experiments whereby the conversions and reproducibility achieved compared excellently to those obtained when using acetyl chloride **58**.

Due to this success, attention was focused on proving the successful incorporation of deuterium isotope labels. In order to produce enough labelled product for full characterisation, reactions were run for sufficient time (2.0 hr to ~ 5.0 hr) to collect 50 mg of product, after which a conventional aqueous work-up to remove residual phenol derivative, Et₃N·HCl **66** or inorganic salts was undertaken. Table 10 shows that following a work-up, isolated yields compared excellently to optimised conversions when employing both labelled and unlabelled reagents. The level of throughput achieved for the synthesis of each deuterium substituted phenyl acetate derivative was also high ($\geq 10.2 \text{ mg hr}^{-1}$) and in all cases analysis of isolated products by CHN, IR, NMR and MS confirmed that the isotope label had been successfully incorporated.

Table 9. Conversions achieved when introducing deuterium isotope labels into a small library of phenyl acetate derivatives using micro reactor S₃.

Entry	Product	Conversion ^a (%)	RSD ^b (%)
1	Phenyl (D ₃)acetate 74	92.8 (94.7)	0.57
2	4-Methoxyphenyl (D ₃)acetate 93	94.7 (96.3)	2.57
3	4-Methylphenyl (D ₃)acetate 94	95.3 (98.0)	2.33
4	4-Nitrophenyl (D ₃)acetate 96 ^c	99.2 (99.6)	0.53
5	4-Phenoxyphenyl (D ₃)acetate 95	94.6 (96.3)	3.27

^a Numbers in parentheses represent the % conversions obtained when undertaking reactions with the unlabelled derivative, acetyl chloride **58**.

^b $n = 10$.

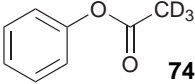
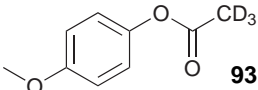
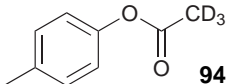
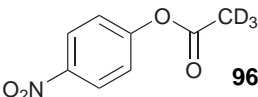
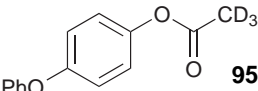
^c Acetylation was carried out in micro reactor set up S_I-S₂ using Et₃N **63** as a base.

2.2.12 Analytical Considerations

Incorporation of the isotope label into the molecule was confirmed using a variety of analytical techniques including NMR spectroscopy, MS and IR spectroscopy,

2.2 ACYLATION OF PHENOL DERIVATIVES

Table 10. Results obtained for the analytical preparation of deuterium labelled phenyl acetate derivatives in micro reactors at a set flow rate of 20 $\mu\text{l min}^{-1}$.

Product	Reactor Set Up	Residence Time (s)	Throughput (mg hr^{-1})	Conversion ^a (%)	Yield ^b (%)
 74	S ₃	4.6	15.5	97.8 (94.7)	93
 93	S ₃	4.6	19.2	96.9 (96.3)	95
 94	S ₃	4.6	17.1	96.1 (98.0)	93
 96	S ₁ -S ₂	12.0	10.2	95.0 (99.6)	92 ^c
 95	S ₃	4.6	26.6	98.0 (96.3)	96

^a Number in parentheses represents the % conversion under optimal conditions using acetyl chloride **58**.

^b Isolated Yield.

^c Acetylation of 4-nitrophenol **62** was carried out using Et₃N **63** as a base.

with CHN combustion analysis providing an excellent indication of purity. Care had to be taken when calculating expected values, since the instrument in use did not detect deuterium directly, but rather measured it as hydrogen. Consequently a treatise on the method used to calculate these values is given in Appendix B.

Examination of the ¹³C-NMR spectra in all cases showed splitting of the CD₃ signal into a septet ($J = 20.0 \text{ Hz}$), which relates to the three deuterium atoms attached to the carbon that is being probed. Since ¹³C-NMR are only proton decoupled the $2nI + 1$ rule (Equation 20) gives rise to the observed splitting, as explained previously in Section 1.1.6. In addition, upon examining the ¹H-NMR spectra there is an absence in each case of the singlet, attributed to the CH₃ group that was present in the un-deuterated counterpart. Another form of confirmation was also provided by the mass spectra, which in all cases exhibited the expected

parent ion peaks at a mass of 3 Da greater than the un-deuterated compounds.

2.3 Methylation of Phenol Derivatives

Many different routes exist to the synthesis of alkylated phenol derivatives, such as those illustrated in Table 11, however they all suffer from certain drawbacks when approached from the point of isotopic modification, where conservation of the label is the most important consideration. For example the use of $\text{KF}-\text{Al}_2\text{O}_3$ produces excellent results¹¹⁷ (Entry 2) but an excess of iodomethane (**47**) is required and the KF supported on alumina **97** does not act as a true catalyst,¹²² being consumed it is thus not applicable to a continuous flow process. In another example, the use of metal carbonates such as Li_2CO_3 or K_2CO_3 **98** in acetone¹²³ is not transferable to micro reactors due to their low solubility in organic solvents, meaning flow-ready solutions are impossible to obtain. Although methods that make use of bases such as KOH **99**¹¹⁹ or NaOH **100**¹²⁰ in DMSO (Entries 5 and 6 respectively) produce high yields, they also suffer from similar solubility problems. Taking these points into consideration experiments were undertaken using pre-formed lithium phenoxide **83**, as success with this method was previously demonstrated when carrying out the acylation of phenol derivatives (Section 2.2.8).

Table 11. Reported methods found to enhance the reaction of phenol **61** with MeI **47** at room temperature.

c1ccc(O)cc1 (**61**) + CI (**47**) $\xrightarrow[\text{Solvent}]{\text{Base}}$ COc1ccccc1 (**101**)

Entry	Base	Solvent	MeI 47 (eq.)	Time (hr)	Yield (%)	Ref.
1	$\text{CsF}-\text{Al}_2\text{O}_3$	DMF	2.0	1.0	100	117
2	$\text{KF}-\text{Al}_2\text{O}_3$	DMF	2.0	1.0	100	117
3	Cs_2CO_3	MeCN	5.0	5.0	39	118
4	K_2CO_3 98 ^a	MeCN	5.0	5.0	13	118
5	KOH 99 ^b	DMSO	2.0	5.0	83	119
6	NaOH 100	DMSO	2.0	0.5	90	120
7	$\text{Bu}_4\text{N}^+\text{F}^-$ 116	MeCN	1.0	0.5	98	117
8	$\text{Et}_4\text{N}^+\text{F}^-$	DMF	1.0	24.0	70	121

^a Reaction carried out under reflux conditions.

^b Reaction carried out at 19°C.

2.3.1 Preliminary Methylation Studies

Since use of THF as the solvent had proved successful to carry out acetylations a batch reaction between phenol **61**, BuLi **79** and MeI **47** to form methoxybenzene **101** was, at first, undertaken in the same way. It was found that conversions reached, at best, $\sim 50.0\%$ and efforts to improve this result by varying concentrations and temperature were not forthcoming, so it was decided to alter the conditions by undertaking a solvent study. Due to the reactivity of BuLi **79** the solvents with which it may be used (to carry out a synthesis) are limited, consequently it was necessary to isolate lithium phenoxide **83** in order to undertake these experiments. This was achieved by the treatment of phenol **61** in THF (-78°C) with an equimolar amount of BuLi **79**, followed by distillation of the solvent. Attempting a solvent exchange in this way proved problematic due to a number of obstacles which hindered the success of isolating lithium phenoxide **83** in suitable purity, these included:

- Heating of the reaction flask to drive off the solvent *in-vacuo* appeared to affect the purity of the product (discolouration was apparent).
- The properties of the compound itself were those of a semi solid, this waxy substance was difficult to work with when, for example, attempting to weigh it out.
- The compound was extremely air sensitive, fouling rapidly in air.

With these points in mind it was decided to investigate the corresponding sodium aryloxides to undertake methylation reactions. Although the by-product of the reaction with MeI **47** in this case is NaI, it seemed reasonable to assume that its high solubility in various solvents (Table 12) would not lead to any problems with regards to precipitation and blockage.

The *in-situ* generation of sodium phenoxide is possible within micro reactors if NaH **78** is employed to effect the deprotonation of phenol derivatives, however, due to the low solubility of NaH **78** in organic solvents the addition of crown

2.3 METHYLATION OF PHENOL DERIVATIVES

Table 12. Solubility of NaI and NaCl **81** in selected solvents at 25 °C.¹²⁵

Solvent	Solubility per 100 g of solvent (g)	
	NaI	NaCl 81
Water	184.0	3.6×10^1
MeCN	24.9	3.0×10^{-4}
Acetone	28.0	4.2×10^{-5}
DMF	3.7–6.4	4.0×10^{-2}

ethers is necessary in order to obtain a homogeneous reaction mixture, suitable for use in a flow reaction.¹²⁴ This approach would ultimately necessitate additional clean up of the flow stream which would adversely effect the speed of synthesis. Since the final purity of mixtures was considered to be an important issue, the use of pre-formed sodium aryloxides proved desirable.

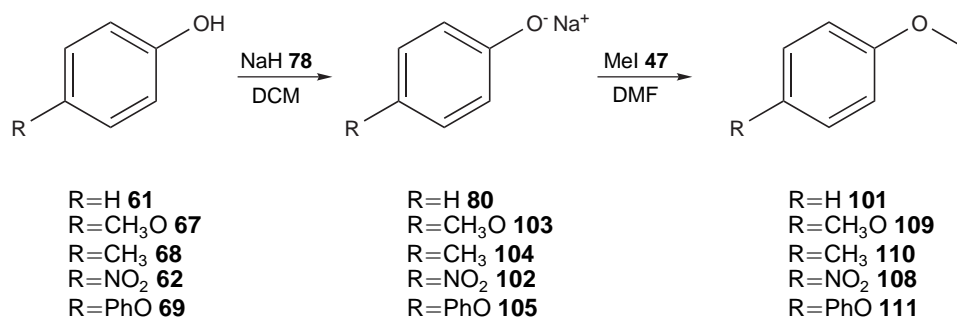
A successful protocol for the synthesis and subsequent purification of sodium aryloxides was developed, based upon the polarity of the formed salts within DCM. Upon treating a solution of each phenol derivative, **61**, **62**, **67–69**, in DCM with NaH **78** the respective products, sodium phenoxide **80**, sodium 4-nitrophenoxide **102**, sodium 4-methoxyphenoxide **103**, sodium 4-methylphenoxide **104** and sodium 4-phenoxyphenoxide **105** exhibited no solubility and consequently precipitated as finely divided solids from solution. Thus it was possible to separate the resultant sodium aryloxides from any unreacted phenol derivatives by a simple process of filtration, washing and vacuum drying.* The compounds obtained using this procedure proved to be significantly easier to work with when compared to their lithiated equivalents, attributed to the difference in characteristics of the solid and reduced hygroscopic nature of the alkali counter-ion.

2.3.2 Solvent Studies in Batch

Although the overall aim was to introduce deuterium labels into the same five phenol derivatives, *via* (D₃)MeI **106** (Scheme 21) using micro reactors, batch syntheses indicated that certain solvents would impede the reaction rate, so an investigation was undertaken.

*The same procedure was attempted to synthesise lithium phenoxide **83**, from phenol **61** and BuLi **79**, but the resultant slurry was so fine that filtration proved impossible.

2.3 METHYLATION OF PHENOL DERIVATIVES



Scheme 21. Scheme illustrating the conversion of phenol derivatives *via* sodium aryloxides to their corresponding methoxybenzene products.

The reaction of sodium phenoxide **80** with MeI **47** was initially studied under batch conditions to determine a suitable solvent with which to undertake micro reaction optimisation. Several solvents were thus selected based on their dielectric constant (Table 1), since formation of NaI as a by-product of the reaction could potentially block the reactor channels. The reactions were carried out in DMF, MeCN and THF as described. Sodium phenoxide **80** (117.1 mg, 1.0 mmol) was dissolved in the solvent (DMF, MeCN or THF) under investigation (150.0 ml) and then MeI **47** (69 μ l, 1.1 mmol) was added. At this point timing was initiated and in those cases where heating was performed, the mixture was brought to reflux. At the indicated time periods samples were collected from the reaction mixture and analysed immediately using HPLC method A.

As can be seen from the experimental data presented in Figure 26, THF was deemed the most unsuitable solvent in which to undertake the methylation reaction. Although the reaction fared well when refluxed in MeCN the best performing solvent was DMF which significantly increased the rate of reaction, even in the absence of heat. Based on this observation DMF was subsequently selected for micro reactor based experimental optimisation.

2.3.3 Micro Scale Optimisation of Methylation Reactions

As observed when acylating phenol derivatives, conversions were often improved when low flow rates were employed so a new micro reactor was commissioned to allow for the residence time of any set up to be easily increased. This residence time unit, denoted herein as R_tU , consisted of one inlet and a long serpentine

2.3 METHYLATION OF PHENOL DERIVATIVES

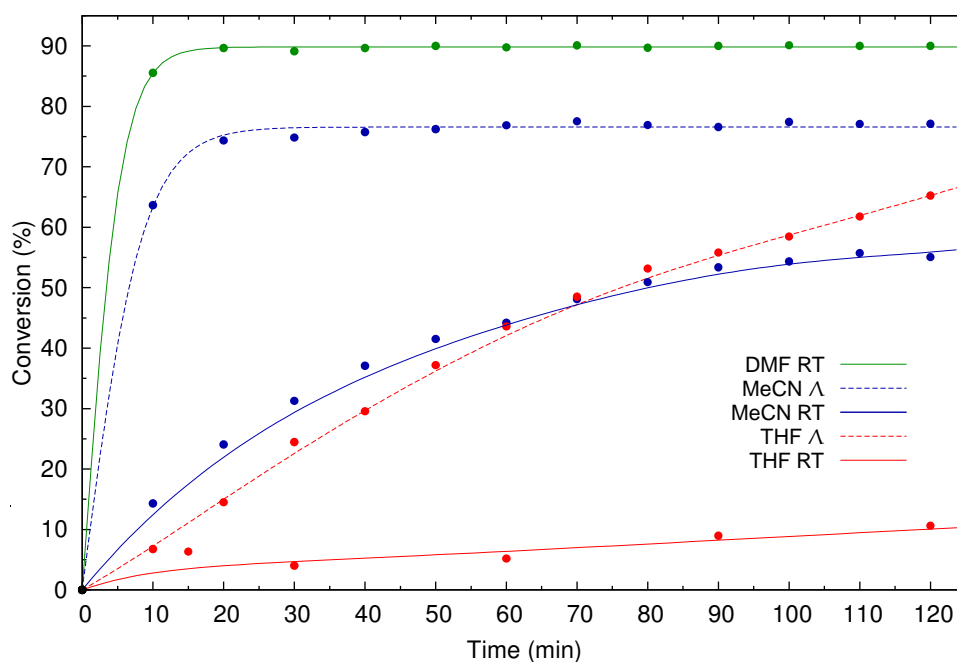


Figure 26. Effect of reaction solvent and temperature on the conversion of sodium phenoxide **80** to methoxybenzene **101** conducted in batch.

channel leading to an outlet ($R_TU = 195 \mu\text{m} \times 73 \mu\text{m} \times 45.1 \text{cm}$), so that it could be attached to any micro reactor in series. It should be noted that the reactor was etched to afford larger channels that would alleviate the increase in back pressure associated with its integration.

Having determined a suitable solvent in which to conduct methylations, the reaction of sodium phenoxide **80** and MeI **47** (as 100 mM solutions in DMF), to afford methoxybenzene **101** (Scheme 21), was studied in order to evaluate the dependence of conversions on residence time using a number of different micro reactor set ups, T_2 , S_3 and T_1-R_TU (Figure 27). HPLC analysis of the micro

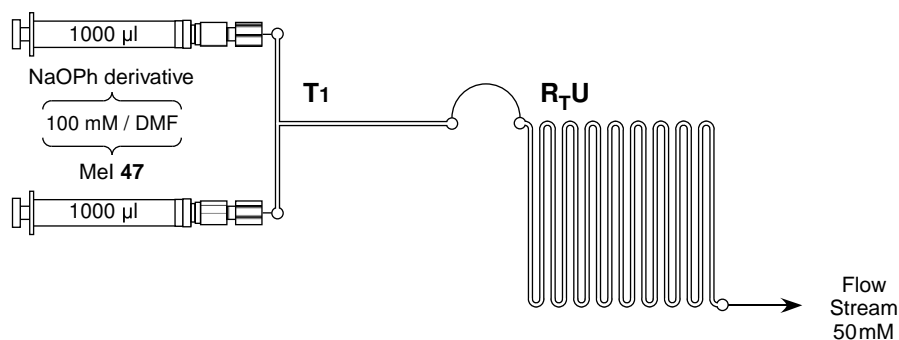


Figure 27. The micro reactor set up T_1-R_TU employed to methylate phenol derivatives (the two reactors were connected *via* 5.0 cm of PEEK™ tubing).

2.3 METHYLATION OF PHENOL DERIVATIVES

reaction at each flow rate was conducted a total of 10 times in order to confirm the integrity of the systems, collecting 10 μl of solution from the reactor outlet into a small vial which contained 50 μl of water to quench the reaction. The relative response of each phenol and methoxybenzene derivative was normalised by an appropriate calibration in each case.

As can be seen from Table 13, within all set ups when the flow rate was reduced there was an improvement in the conversion, as would be expected. An overall indication to the degree of reaction that was achievable was obtained at the lowest set flow rate of 1 $\mu\text{l min}^{-1}$ where $> 90.0\%$ conversion was obtained with the extended micro reactor set up S₃ and T_I-R_TU (Entry 5). Although this is a high value, the throughput of such a system would once again be low so in order to understand the reaction better it was decided to evaluate the results with respect to the residence time.

Figure 28 shows that when the obtained conversions (Table 13) are plotted with respect to the residence time the relationship between the two is not linear. For all set ups the residence time that is required to give a Fourier number of 1 varies according to the channel dimensions and PEEK™ tubing employed but is in all cases $\leq 3.7\text{ s}$ (when evaluated with respect to acetic acid dissolved in EtOAc), indicating that incomplete mixing was not the primary cause of the lower observed conversions. Above a residence time of $\sim 50\text{ s}$, the kinetic limitation of the reaction becomes apparent and, beyond this point, a relatively large increase in the residence time afforded a comparatively small improvement in the conversion. Although the addition of another residence time unit to the longer set up, T_I-R_T

Table 13. Results of experiments to investigate the effect of reactor dimensions on the conversion of sodium phenoxide **80** to methoxybenzene **101**, undertaken in DMF at a variety of flow rates.

Entry	Set Flow Rate ($\mu\text{l min}^{-1}$)	Conversion ^a (%)		
		T ₂	S ₃	T _I -R _T U
1	20	25.6 (1.28)	55.5 (1.04)	69.6 (1.03)
2	10	33.1 (1.09)	68.5 (1.01)	84.1 (0.91)
3	5	53.2 (1.10)	80.8 (0.65)	89.4 (0.60)
4	2	74.1 (2.23)	88.0 (0.47)	95.7 (0.80)
5	1	83.9 (1.40)	94.6 (0.71)	96.8 (0.43)

^a Numbers in parentheses represent the corresponding RSD ($n = 10$).

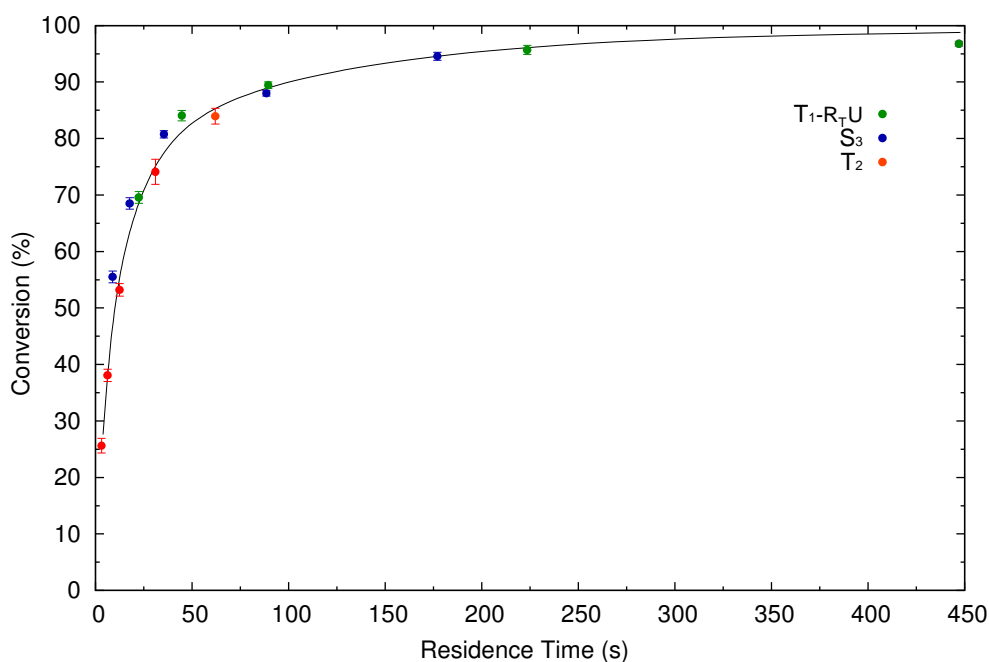


Figure 28. A plot illustrating the effect of residence time on the conversion of sodium phenoxide **80** to methoxybenzene **101** ($n = 10$).

U, was possible, the observed relationship indicated that attempting to improve the throughput in this way would not be a worthwhile concession for the longer synthesis time and increase in back pressure that would result. As such it was decided to investigate alternative methods of overcoming the observed limitations of the reaction, so that the synthesis of isotopically substituted methoxybenzene derivatives could be performed in an expedient manner.

2.3.4 The Effect of Heating Micro Reactions

In order to alleviate the encountered problem of low throughputs when synthesising labelled products (*e.g.* $< 0.67 \text{ mg hr}^{-1}$ *), it was decided to investigate the effect on conversion at higher flow rates when heating the micro reactor array. This was achieved by placing the two micro reactors into a shallow silicone oil bath which was heated using a standard laboratory hot plate. Although direct placement on to the hot plate was possible, employing an oil bath allowed the temperature to be monitored more efficiently (using a thermocouple) and heat to be distributed to the set up more evenly since the heat latency of the oil is high. Using

*Throughput calculated assuming 100% conversion of sodium phenoxide **80** to (D₃)methoxybenzene **107** at a set flow rate of $1 \mu\text{l min}^{-1}$.

2.3 METHYLATION OF PHENOL DERIVATIVES

this approach micro reactor set up T_1-R_TU was heated to 100°C (Figure 29) and the reaction of five sodium aryloxides, **80** and **102–105** with MeI **47**, to afford methoxybenzene **101**, 1-methoxy-4-nitrobenzene **108**, 1,4-dimethoxybenzene **109**, 1-methoxy-4-methylbenzene **110** and 1-methoxy-4-phenoxybenzene **111** respectively was investigated.

Table 14 shows that when using the set up show in Figure 29, in all but one case $> 90.0\%$ conversion of each derivative to its corresponding methoxybenzene product was obtained at the highest set flow rate of $20\ \mu\text{lmin}^{-1}$. Once again the exception was found to be sodium 4-nitrophenoxide **102** (Entry 4) which exhibited fluctuating, low conversions, due to its greatly decreased nucleophilicity, caused by the presence of the strongly electron withdrawing nitro group and the bound sodium metal ion.

Overall, the results were pleasing and compared well to those obtained for the acylation of phenol derivatives, with similar conversions being achieved (Table 6). It was disappointing not to have developed a successful protocol to methylate 4-nitrophenol **62** since the nitro moiety is a group that may be commonly found within organic molecules, particularly due to its use as an amine precursor when carrying out such addition reactions to O atoms. Although in the case of acylating

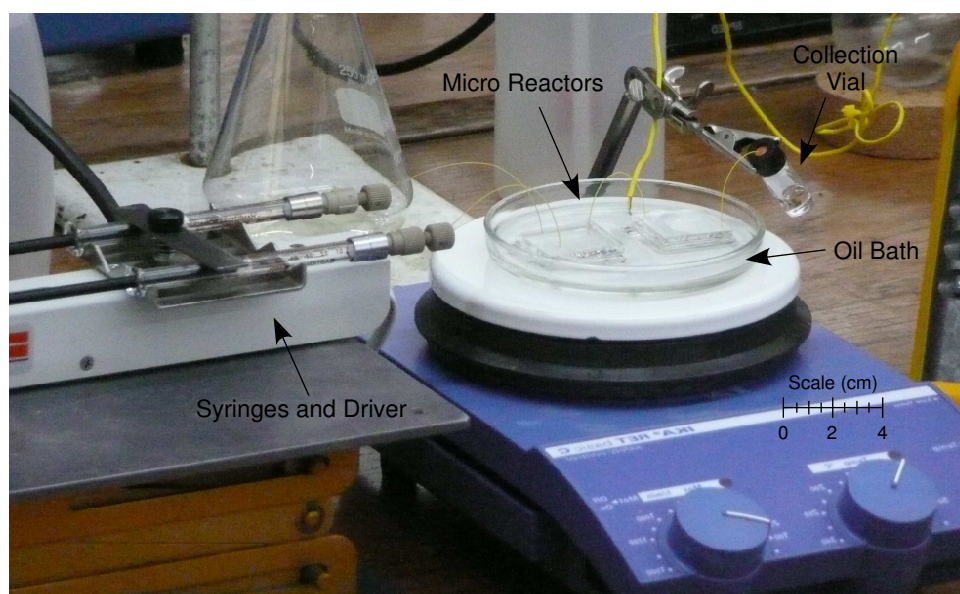


Figure 29. Micro reactor set up T_1-R_TU immersed in an oil bath for heating *via* a hot plate.

2.3 METHYLATION OF PHENOL DERIVATIVES

Table 14. Results obtained for the methylation of sodium aryloxides within the micro reactor set up T_I-R_TU (Figure 27) at a set flow rate of 20 μl min⁻¹.

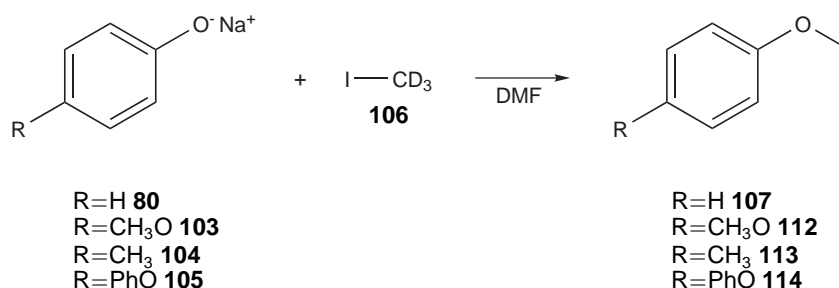
Entry	Product	Conversion (%)	RSD ^a (%)
1	Methoxybenzene 101	96.1	0.66
2	1,4-Dimethoxybenzene 109	91.4	0.68
3	1-Methoxy-4-methylbenzene 110	96.3	0.95
4	1-Methoxy-4-nitrobenzene 108	9.9	40.68
5	1-Methoxy-4-phenoxybenzene 111	90.5	1.62

^a *n* = 10

this derivative (**62**) it was possible to employ the organic base, Et₃N **63**, this approach is not feasible when attempting alkylations since the alkylating agent will also be consumed by a competing reaction with the amine and hence a large excess would be required; circumventing some of the advantages (*i.e.* stoichiometry) obtained by using micro reactors for isotope incorporation. In spite of this the methylation of most phenol derivatives had been achieved in high conversion using continuous flow techniques so it was decided to investigate the synthesis of isotopically modified methoxybenzene derivatives by undertaking the same reactions and substituting MeI **47** for (D₃)MeI **106**.

2.3.5 Flow Synthesis of Deuterated Methoxybenzene Derivatives

In a similar way as was presented for the acetylation reactions, attention was then turned to proving the concept of efficient isotope substitution *via* a series of methylations. The reactions of sodium aryloxides, **80** and **103–105**, were repeated under optimal conditions by the substitution of MeI **47**, for its tri-deuterated equivalent, (D₃)MeI **106**, as shown in Scheme 22. To confirm incorporation of the deuterium label into (D₃)methoxybenzene **107**, 1-(D₃)-methoxy-4-methoxybenzene **112**,



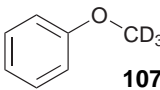
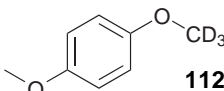
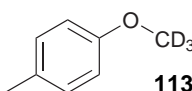
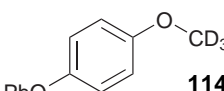
Scheme 22. The route by which selected isotopically substituted methoxybenzene derivatives were synthesised within micro reactor set up T_I-R_TU.

2.3 METHYLATION OF PHENOL DERIVATIVES

1-(D₃)-methoxy-4-methylbenzene **113** and 1-(D₃)-methoxy-4-phenoxybenzene **114**, sufficient time (~ 2 hr to 4 hr) was allowed for the synthesis of enough product (~ 50 mg) to carry out analysis post work-up. It was found to be necessary to flush the micro reactor array clean with water, acetone and DMF after every 1.5 hr of running to prevent channel blockages caused by the long term build up of precipitates.

When undertaking the isolation of products obtained from the reactions of phenol **61** and 4-methylphenol **68** (Table 15, Entries 1 and 3 respectively) was found to be problematic, due to an incompatibility with the solvents used during work-up. The methoxybenzene derivatives would not fully dissolve in either the DMF/water or hexane phase and due to the similarity in boiling point between products and the reaction solvent (*e.g.* 189 °C and 153 °C to 155 °C for DMF and (D₃)methoxybenzene **107** respectively¹²⁶), isolation by distillation on such a small

Table 15. Results for the analytical preparation of deuterium labelled methoxybenzene derivatives within micro reactor set up T₁-R₁U at 100 °C when operated at a set flow rate of 20 μl min⁻¹.

Entry	Product	Residence Time (s)	Throughput (mg hr ⁻¹)	Conversion ^a (%)	Yield ^b (%)
1	 107	11.4	12.4 ^c	93.7 (96.1)	–
2	 112	11.4	15.6	93.7 (91.4)	92
3	 113	11.4	14.5 ^c	96.2 (96.3)	–
4	 114	11.4	22.4	92.7 (90.5)	92

^a Numbers in parentheses represent conversions obtained for the reaction of sodium aryloxides with unlabelled MeI **47**.

^b Isolated yield.

^c Throughput for (D₃)-methylations calculated based on HPLC conversion, since no product was isolated post work-up.

scale is difficult. Consequently the confirmation of product formation within micro reactors was attained *via* HPLC, following synthesis of these compounds in batch reactions (using THF) and subsequent characterisation.

The results for all compounds correlated extremely well with the optimised conversions achieved when employing the isotopically unmodified substrate MeI **47** and where isolation was achievable, excellent yields (92%) were obtained. In addition the level of throughput that was attained for all compounds was in excess of 12.4 mg hr^{-1} , an extremely positive result given that a $10\times$ scale out of the prototype reactors would provide a sufficient amount of labelled product for most applications within extremely short time scales.

2.4 Methylation of Carboxylic Acids

Methyl esters may be formed by the substitution of the acidic proton on a carboxylic acid by a CH_3 group which, as noted by Johnstone and Rose,¹¹⁹ usually takes longer than with other compounds such as phenols, alcohols or amides. This reaction is often used to introduce isotope labels into compounds *via* a suitable isotopologue of MeI **47** as reported for the synthesis of (^{11}C)methyl 2-phenyl-2-piperidin-2-ylacetate.*¹²⁷ In addition, one of the ester moieties found within cocaine **2** (Figure 15) is an ester derived from a carboxylic acid, although in terms of isotopic modification it is usually the more labile primary amine that is reacted to afford the desired product.¹²⁸

2.4.1 Methods of Synthesis

The quickest route by which to obtain methyl esters from carboxylic acids would have been to replicate the protocol established for the methylation of phenols within micro reactors (Section 2.3), synthesise the corresponding sodium or lithium salts and then react with MeI **47** or (D_3)MeI **106**. However, upon taking this approach with benzoic acid **115** it was that these salts were extremely insoluble in all solvents evaluated, including DMSO. In order to determine if this effect

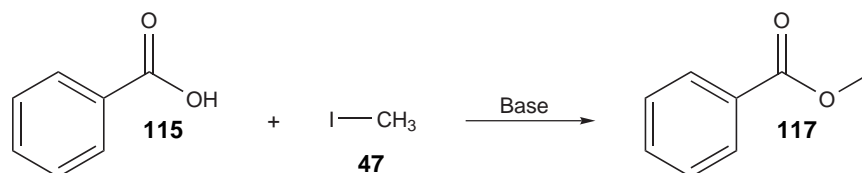
*Commonly known as Ritalin, a stimulant used to treat Attention Deficit Hyperactivity Disorder (ADHD).

was limited to benzoic acid **115** the procedure was repeated with the 4-nitro and 4-methoxy derivatives and again no appreciable dissolution occurred. For these reasons an alternative route to the products was sought.

There are numerous bases that are cited within the literature which promote the alkylation of carboxylic acids including Cs_2CO_3 , KO^tBu , KF, Li_2CO_3 and *N,N,N*-tributylbutan-1-aminium fluoride (TBAF) **116**.^{*†} Since the solubility of such bases (or, where relevant, the salts formed thereof) can be a problem when undertaking reactions within micro channels, small scale reactions between benzoic acid **115** and MeI **47** to form methyl benzoate **117** were undertaken in accordance with Scheme 23 within a range of polar solvents in order to determine the best combination to employ for micro reactions.

Benzoic acid **115** (50 μl , 100 mM, 5.0×10^{-3} mmol) in MeCN was added to a small vial containing solvent (0.5 ml) and an appropriate base was then added (5.0×10^{-3} mmol). The vial was mixed on the carousel for 30 min after which time MeI **47** (50 μl , 100 mM, 5.0×10^{-3} mol) was added. Stirring was continued for 2 hr before carrying out analysis *via* HPLC. Conversions were calculated following appropriate calibration based upon the amount of methyl benzoate **117** formed with respect to residual benzoic acid **115**.

The results of these experiments (Table 16), undertaken in DMF, MeCN and THF, show that the only viable base to pursue in a micro reactor was TBAF **116**. The remaining bases were not suitably soluble in any of the solvents and at best, fine suspensions were obtained which were not transferable to on-chip studies, since particulates rapidly settle within the syringes.



Scheme 23. The base assisted methylation of benzoic acid **115** to afford methyl benzoate **117**.

*It should be noted that TBAF **116** itself is a quaternary ammonium salt that is believed to be a source of anhydrous F^- ions which act as strong hydrogen bond acceptors.¹²⁹ Thus, as is done throughout, although TBAF **116** is commonly referred to as a base it is best viewed in terms of providing a base source when solubilised.

† See Table 11 for related references.

2.4 METHYLATION OF CARBOXYLIC ACIDS

Table 16. Results obtained in small scale batch reactions when methylating benzoic acid **115** with MeI **47** using an array of bases and solvent systems.

Base	Solvent		
	DMF	MeCN	THF
Cs ₂ CO ₃	66.4 ^a	6.6 ^a	0.0 ^a
TBAF 116	54.4	31.1	47.7
Li ₂ CO ₃	70.0 ^a	0.0 ^a	0.0 ^a
KO ^t Bu	35.6	6.3 ^a	0.0 ^b
KF	49.8 ^a	1.0 ^a	0.0 ^a

^a Base did not suitably dissolve in the solvent.

^b Base formed a fine suspension.

With these points in mind, further experiments were conducted in order to determine the optimal combination time for the carboxylic acid and base before addition of MeI **47** as follows. Benzoic acid **115** (50 μ l, 100 mM in THF, 5×10^{-3} mmol) and TBAF **116** (50 μ l, 100 mM in THF, 5×10^{-3} mmol) were added to a small vial containing THF (0.5 ml) and the mixture was rotated on the carousel for the specified time (see Table 17). MeI **47** (50 μ l, 100 mM in THF, 5×10^{-3} mmol) was then added and agitation continued in a likewise manner for a further 1 hr before analysis *via* HPLC. Conversions were calculated based on the amount of methyl benzoate **117** formed with respect to MeI **47** remaining in the reaction mixture.

It can be seen from the data in Table 17 that, within the bounds of experimental error, there appeared to be no effect on the conversion when the combination time of benzoic acid **115** and TBAF **116** was varied, so the reactions were transferred to the micro scale.

Table 17. Effect of varying the time benzoic acid **115** and TBAF **116** were allowed to mix before addition of MeI **47**.

Combination Time (min)	Conversion (%)
5	44.3
10	43.0
20	44.0
30	43.6
60	44.0
90	43.2
120	42.8

2.4.2 Micro Reactor Methylation of Benzoic Acid

Knowing that as long a residence time as possible would allow for a greater reaction time post mixing (where $Fo \geq 1$) and produce the best conversions, a double T micro reactor ($dT = 150 \mu\text{m} \times 50 \mu\text{m} \times 0.7 \text{cm} \times 0.7 \text{cm}$) with three inlets and one outlet was connected to the residence time micro reactor unit, R_TU , as shown in Figure 30. Benzoic acid **115** and TBAF **116** (100 mM in THF) were delivered through two inlets and flowed together down a 0.7 cm section of channel before being introduced to MeI **47** (100 mM in THF) where the resultant flow stream was delivered to R_TU via a further 0.7 cm of channel length and 5.0 cm of PEEK™ tubing. The syringe pump was set to the lowest flow rate $1 \mu\text{l min}^{-1}$ and 10 μl of sample was collected into a small vial containing 50 μl of H_2O in order to quench the reaction. Due to concerns regarding the consumption of MeI **47** by the base **116**, conversions were calculated based on the amount of methyl benzoate **117** formed with respect to the amount of MeI **47** that remained and to an internal standard (ethyl benzoate).

As can be seen from the results in Table 18, there was a significant difference in the conversions depending on the method by which the data was treated. It may be inferred from this difference that consumption of MeI **47** is occurring via unwanted side reactions since more of it reacts than is incorporated into the product **117**. This was viewed as a significant problem as the isotopic label would be incorporated into final products via the alkyl halide substrate. Since the data

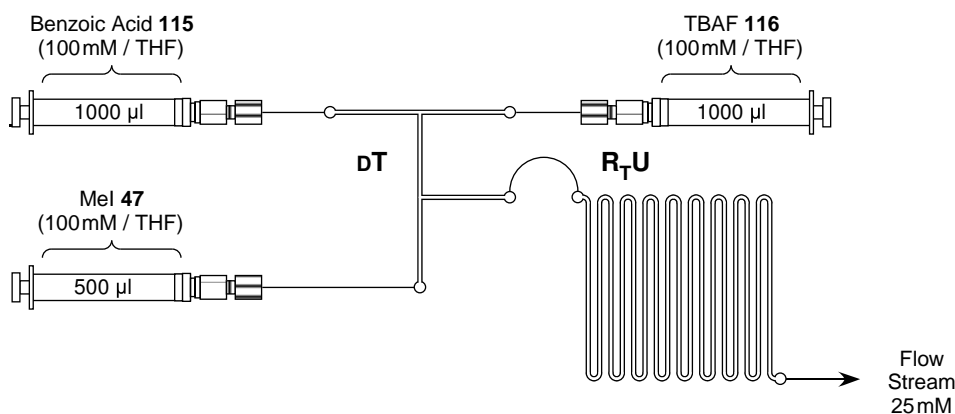


Figure 30. The experimental micro reactor set up dT - R_TU used to attempt the methylation of benzoic acid **115** in the presence of TBAF **116**.

Table 18. Conversions achieved in micro reactor set up dT-R_TU when attempting the methylation of benzoic acid **115** in the presence of TBAF **116**.

Method of Analysis	Conversion (%)	RSD ^a (%)
Methyl benzoate 117 <i>cf.</i> MeI 47	51.0	18.0
Methyl benzoate 117 <i>cf.</i> Ethyl benzoate	20.8	6.2

^a *n* = 10.

suggests that sub stoichiometric quantities of the alkyl halide would be available for reaction, this detracts from the benefits of using micro reactors to achieve high yielding reactions.

2.4.3 Alternative Methods of Methylation

Due to the competing reaction of MeI **47** and TBAF **116** the reaction between benzoyl chloride **34** and methanol was investigated as an alternative route to the incorporation of a label *via* (D₃)methanol. In small scale batch reactions it was found that the two components did not react together to any appreciable degree, which would be expected based on earlier results that had indicated the relative inactivity of benzoyl chloride **34**. In an attempt to increase the degree of conversion, the reactions were repeated in the presence of organic bases such as Et₃N **63** and pyridine **118**. Although it was found that a slight increase in conversion to methyl benzoate **117** occurred, the bases appeared to catalyse the formation of benzoyl benzoate as a by-product and no way around this problem could be found.

2.4.4 Experiments with DMAP

In a final attempt to successfully undertake the labelling of benzoic acid derivatives an adaptation of a reported synthesis, utilising DMAP **60**¹³⁰ was attempted in the following way; DMAP **60** (12 mg, 0.1 mmol) and methanol (40 μl, 1.0 mmol) were added to a stirred solution of benzoic acid **115** (122 mg, 1.0 mmol) in DCM (20.0 ml). *N,N'*-Dicyclohexylmethanediimine (DCC, 206 mg, 1.0 mmol) was added and stirring continued for 3 hr. A white precipitate formed, indicating that a reaction had occurred and the mixture was analysed after dilution in MeCN. Although the degree of conversion appeared to be good (90.4%) it

2.4 METHYLATION OF CARBOXYLIC ACIDS

was disappointing to see that there was a large amount of benzoyl benzoate formation which meant that the actual conversion was significantly lower than the calculated value (since it was determined based upon the amount of benzoic acid **115** consumed). As a result of this and the previously reported shortcomings identified for the methylation of benzoic acid **115**, it was decided to forgo further experimentation and, as such, label incorporation was not investigated.

CHAPTER 3

C–N BOND FORMATION

3.1 Amides and Isotopes

THE most well known pharmaceutical to contain the amide unit is undoubtedly paracetamol, however it is also found in many other naturally occurring and biologically active molecules. For example the basic core of all penicillin's contain the amide linkage, as does Taxol[®] which is used to treat cancerous tumors.¹³¹ As shown in Figure 31 the amide functionality is also found in Tamiflu **119** which is currently being stockpiled due to its inhibitory effects towards certain strains of influenza¹³² and in the famously misused, but highly active, (8β)-*N,N*-diethyl-6-methyl-9,10-didehydroergoline-8-carboxamide (LSD) **120**. Although diverse in their actions, it is clear that the ability to effectively label amides with isotopes is paramount in the development and evaluation of both lead compounds and known drugs so that their effects and metabolic fate *in-vivo* may be fully understood.

3.1.1 Preparation of Labelled Amides

Specific examples of preparing amides containing isotopic labels may be found within the literature, for example the photoinduced labelling of amides *via* [¹³C]CO has been reported with conversions of [¹³C]CO to final product being in the range 10.0% to 89.0%.¹³³ The labelling of melatonin, employing 1.5 eq.

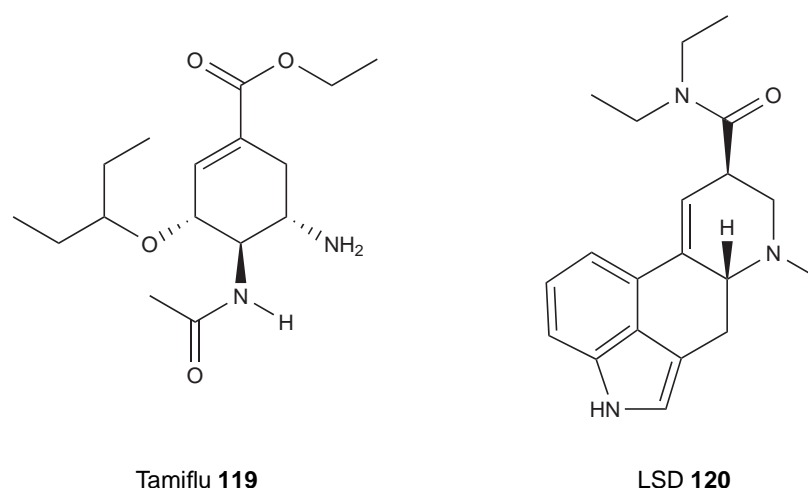


Figure 31. Two pharmaceutically active compounds which contain the amide functionality.

of $[D_3]$ acetyl chloride **59**, has been achieved at a quoted yield of 80.0% after 1.5 hr,¹³⁴ but the need for excess labelled reagent is clearly a disadvantage. Furthermore Courtyn *et al.*¹³⁵ published the synthesis of $[^{11}C]$ acamprosate using $[D_3]$ acetyl chloride, with the focus being primarily on biological studies using the radiolabelled compound. These are rare examples though, since, as highlighted by Shevchenko *et al.*,¹³⁶

“...preparing labelled amides using reagents such as acetyl acetate **121** or acetyl chloride **58** is difficult due to their high cost and volatility.”

The work covered within this Chapter aimed to address these issues through the use of hydrodynamically controlled micro reactors which are, for the most part, closed units which provide the ability to accurately control reagent delivery and consumption, thus circumventing some of the problems outlined above. In addition it was sought to improve the synthesis of isotopically modified amides to such an extent that the methodology developed may be applied to the above examples to improve their overall efficiency.

3.1.2 Methods of Synthesis

There exists a number of ways to synthesise amides with the most notable being the Schotten-Baumann reaction,^{137,138} Schmidt reaction,¹³⁹ one-pot Ugi synthe-

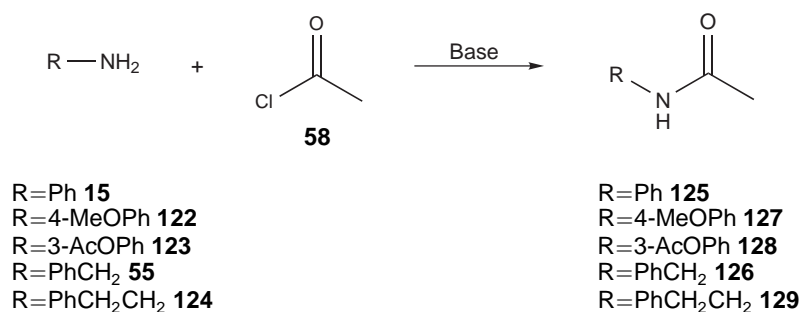
sis¹⁴⁰ and the Bodroux¹⁴¹ reaction. More exotic examples include the Chapman rearrangement to form di-aryl amides,¹⁴² and the Beckman rearrangement to form corresponding amide products from oximes.¹⁴³ Generally however amides may be prepared by reacting an amine with a carboxylic acid, acid anhydride or acyl chloride. As was the case when carrying out the acylation of phenol derivatives in Chapter 2 it was desired to incorporate the maximum amount of isotope label possible into the final products thus generating minimal waste. For these reasons the reaction of carboxylic acids was discounted, since it relies on the use of a catalyst or a coupling reagent (such as DCC), both of which would necessitate a work-up in order to purify the product. The use of acid anhydrides was also ruled out for reasons discussed earlier in Section 2.2. As acetyl chloride **58** is relatively accessible in a variety of isotopically substituted forms it was decided to study the incorporation of its protonated and deuterated isotopologues *via* reaction with primary amines to form series of secondary amides. Although the compound is volatile it was known from previous investigations (see Chapter 2) that the micro reactor systems to be employed would effectively prevent the loss of the valuable starting reagent.

When amides are prepared from amines and acyl chlorides, an equimolar amount of HCl is produced which can form a salt with another mole of the amine, thus necessitating an excess of the amine precursor to be employed. Although the reaction of only two compounds within a continuous flow system would have been operationally simple it was decided to investigate the stoichiometric reaction in the presence of a base to sequester the liberated HCl. This route was followed due to the potential of employing any successfully developed system to undertake the labelling of a complex and consequently expensive amine. Using a generic, readily available base is the best option in order to standardise the reaction conditions and minimise operational costs with respect to routine synthesis.

3.2 Acetylation of Primary Amines

In order to derive a library of compounds that would reflect a cross section of reactivity scenarios aniline **15**, 4-methoxyaniline **122**, 1-(3-aminophenyl)ethanone

123, phenylmethanamine **55** and 2-phenylethanamine **124**, were selected for initial experimentation with acetyl chloride **58** in accordance with Scheme 24. Percentage conversions for all reactions were calculated based on the amount of product (amide) present with respect to amine remaining upon analysis by HPLC. Retention times and relative responses of all components were determined using synthetic standards or commercially available materials.



Scheme 24. The acetylation of five primary amine derivatives with acetyl chloride **58** to afford their respective secondary amides.

3.2.1 The Schotten-Baumann Reaction

The Schotten-Baumann reaction, first described at the end of the 19th century,^{137,138} provides one method to overcome the problem of HCl production by neutralising it with NaOH **100**. However, since hydroxide ions can react with an acyl chloride to form a carboxylic acid a biphasic system is employed, whereby an aqueous solution of NaOH **100** and amine are combined with an immiscible solution of acyl chloride (*e.g.* in DCM). Diffusion of the amine into the organic layer initiates the reaction and the ammonium chloride salt which is formed may then dissolve within the aqueous layer where it is neutralised with NaOH **100**. The free amine then re-dissolves within the organic layer awaiting reaction, as illustrated in Figure 32.

Traditionally the reaction is carried out for prolonged periods of time, depending on the scale, in order to allow for completion of the multiple transfer processes which occur. Having the perfect way to solve this problem by monopolising on the properties of micro reactors, in which rapid bulk transfer across a defined interface occurs, it was decided to investigate the reaction. Potential advantages to

3.2 ACETYLATION OF PRIMARY AMINES

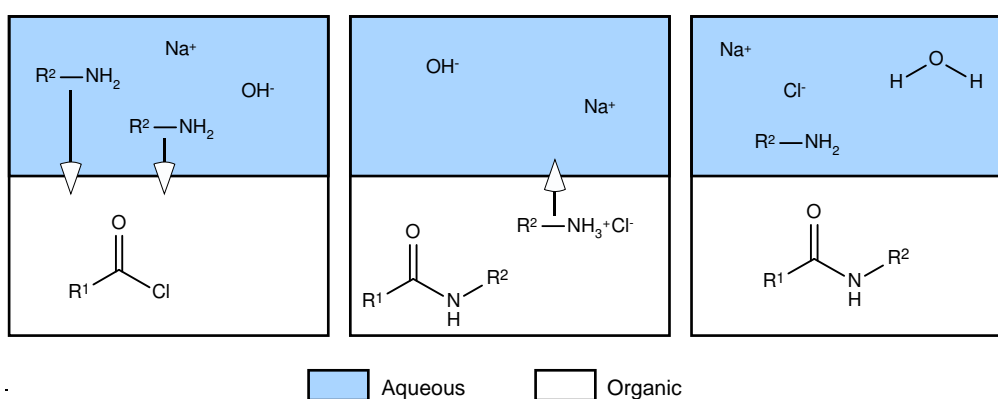


Figure 32. Diagram illustrating the phase transfer processes that occur when synthesising amides from amines and acyl chlorides under Schotten-Baumann conditions.^{137,138}

carrying out the Schotten-Baumann reaction within a micro reactor include mild reaction conditions, simplicity of using two inputs to the reactor system (since only an organic and an aqueous feed are required) and the biphasic nature of the system, which would permit simple in-line purification of the reaction products. In order to determine if amide forming reactions reported by Kikutani *et al.*¹⁴⁴ within a pile-up micro reactor could be transferred to the systems used herein the reaction of aniline **15** and acetyl chloride **58** to afford *N*-phenylacetamide **125** was investigated in a single micro reactor, S₃ (Figure 33). Introducing a solution of aniline **15** (100 mM) in aqueous NaOH **100** (100 mM) into one inlet and a solution of acetyl chloride **58** (100 mM) in EtOAc to the second inlet, the product stream was directed *via* 5.0 cm of PEEK™ tubing into a small vial for sufficient time to collect 10 μl, and was quenched in 50 μl of HCl (100 mM in 1 : 9 H₂O/MeCN); analysis was undertaken using HPLC method C.

After allowing sufficient time for the system depicted in Figure 33 to equilibrate, collection of 10 samples at each of the 5 set flow rates produced the results that are

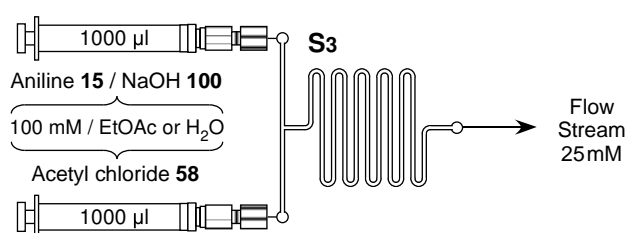


Figure 33. Schematic representation of the experimental set up used to investigate the Schotten-Baumann reaction, under continuous flow, in micro reactor S₃.

3.2 ACETYLATION OF PRIMARY AMINES

Table 19. Effect of flow rate on the conversions obtained for the acetylation of aniline **15** under Schotten-Baumann conditions within micro reactor S₃.

Set Flow Rate ($\mu\text{l min}^{-1}$)	Average Conversion (%)	RSD ^a (%)
20	46.2	11.84
10	46.5	8.65
5	51.7	5.22
2	53.6	5.88
1	48.9	8.62

^a $n = 10$

summarised in Table 19. As can be seen, the reaction did progress to some degree but the RSD's indicate fluctuation in the conversions obtained. Reducing the flow rate did not seem to effect the degree of conversion to the product, which is most likely due the diffusion of H₂O into the EtOAc stream, which occurs to some degree, allowing a significant amount of acetyl chloride **58** to undergo hydrolysis. This effect was not reported by Kikutani *et al.*,¹⁴⁴ possibly due the increased hydrolytic stability of aromatic acyl halides employed. As a result of these shortcomings it was felt that further investigation with this system was not warranted with respect to isotopic labelling.

3.2.2 Evaluation of *N,N*-Diethylethanamine as a Base

Knowing that an amine and acyl chloride could also be reacted in the presence of an organic base, and having previously developed a micro reactor system that would allow for rapid optimisation under such conditions, it was decided to divert the investigation in this direction. Employing Et₃N **63** as the chosen base would theoretically allow the preferential sequestering of any HCl evolved as Et₃N·HCl **66**, thus ensuring that the procedure would remain as cost effective as possible for reasons discussed earlier.

Micro Reactor Set Up

Based on findings obtained during the optimisation of the acetylation reactions (Section 2.2.3) it was decided to perform the amide synthesis using an analogous set up. As Figure 34 illustrates, the micro reactions were carried out within reactor set up T₁-T₂. The first reactor (T₁) was employed to mix the primary amine and

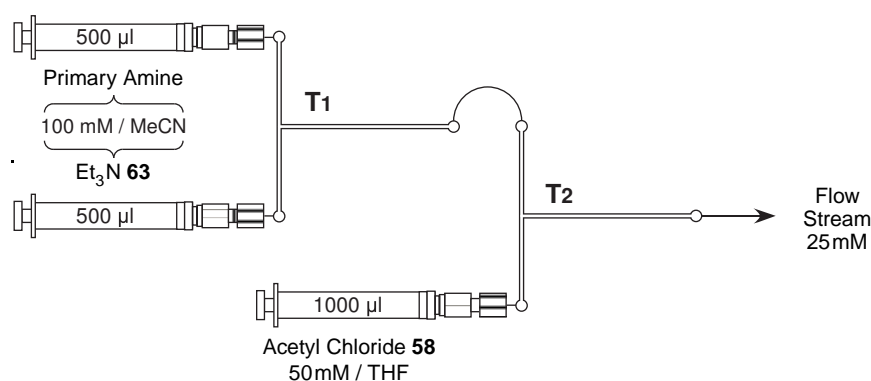


Figure 34. Schematic of micro reactor set up, T₁-T₂ which was used to undertake initial experimentation on the acetylation of primary amines.

Et₃N **63**, the outlet was connected *via* a 2.5 cm length of PEEK™ tubing to one inlet of the second stage reactor (T₂) which allowed for subsequent reaction with the acyl chloride derivative which was introduced through the second inlet. In order to analyse the flow reactions 10 µl of product solution was collected from the reactor outlet into a small vial containing 50 µl of quench agent (1.0% H₂O in MeCN) and analysed immediately by HPLC, thus enabling confirmation that the reaction had occurred within the flow set up rather than in the collection vial.

By once again employing a modular set up, comprising of two micro reactors, it was possible to rapidly optimise the reactions by interchanging the second stage reactor for one of longer channel length (S₃), as was later required.

Selection of Reaction Conditions

The reaction between aniline **15** and isotopically unmodified acetyl chloride **58** in the presence of Et₃N **63** to afford *N*-phenylacetamide **125** was thus investigated using the set up T₁-T₂, illustrated in Figure 34. Reactions were conducted at a concentration of 100 mM (aniline **15** and Et₃N **63**) and 50 mM (acetyl chloride **58**), which provided a final concentration of 25 mM on collection and correlates to a 1 : 1 : 1 ratio of reagents.

Although all synthetic standards had been successfully prepared in THF, previous studies (Section 2.2.2) had shown that the exclusive use of this solvent would cause Et₃N·HCl **66** to precipitate within the micro channels, leading to irreproducible

results. Drawing upon the knowledge that the polarity of MeCN was an effective solvent at avoiding precipitation of ammonium salts, and that THF is a suitable solvent for the daily storage of acyl chloride solutions, a mixed solvent system (MeCN/THF) was once again employed.

In addition, as the previous concentration range was found to be effective at avoiding the precipitation of solids, a problem which had now repeatedly shown itself to hamper any attempts at optimisation and reproducibility, reactions were also undertaken at analogous concentrations, providing a final flow stream of concentration 25 mM.

Continuous Flow Synthesis of *N*-Phenylacetamide

Using micro reactor set up T₁-T₂ under the aforementioned conditions the reaction of aniline **15** to form *N*-phenylacetamide **125** was then repeated. The syringe driver set to the following flow rates; 20, 10, 5, 2 and 1 $\mu\text{l min}^{-1}$, with each reaction repeated 10 times (at each flow rate) in order to determine system reproducibility. In all cases the RSD was observed to be < 5.0% and the relationship between flow rate and conversion can be seen in Figure 35. It was pleasing to observe

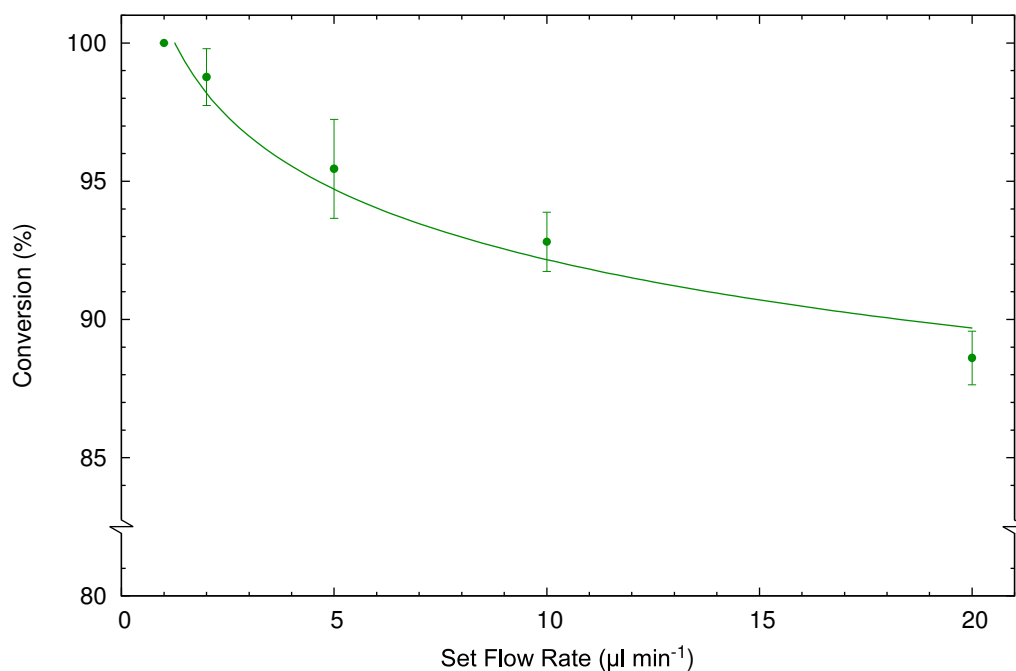


Figure 35. The effect of varying flow rate on the conversion of aniline **15** to *N*-phenyl acetamide **125** in micro reactor set up T₁-T₂ ($n = 10$).

that at the lowest investigated flow rate ($1 \mu\text{l min}^{-1}$) the complete conversion of aniline **15** to *N*-phenylacetamide **125** was attained.

Although maximum conversion was achieved at a low flow rate, leading to a low overall throughput, it was decided to evaluate the reaction of the other amine derivatives under the aforementioned conditions before deciding upon the best course of action to address the inevitable need for greater productivity.

3.2.3 Optimising the Reactions for a Library of Amines

Having determined using the set up T₁-T₂ at $1 \mu\text{l min}^{-1}$ that the quantitative conversion of aniline **15** to *N*-phenylacetamide **125** was possible, the acetylation of the four other amines, **55** and **122–124**, to afford the respective products *N*-(phenylmethyl)acetamide **126**, *N*-(4-methoxyphenyl)acetamide **127**, *N*-(3-acetylphenyl)acetamide **128** and *N*-(2-phenylethyl)acetamide **129** was investigated according to Scheme 24, within the same set up.

As Figure 36 illustrates, in all cases near quantitative conversions were achieved although a small drop in conversions was seen for the amines **55**, **122** and **124**,

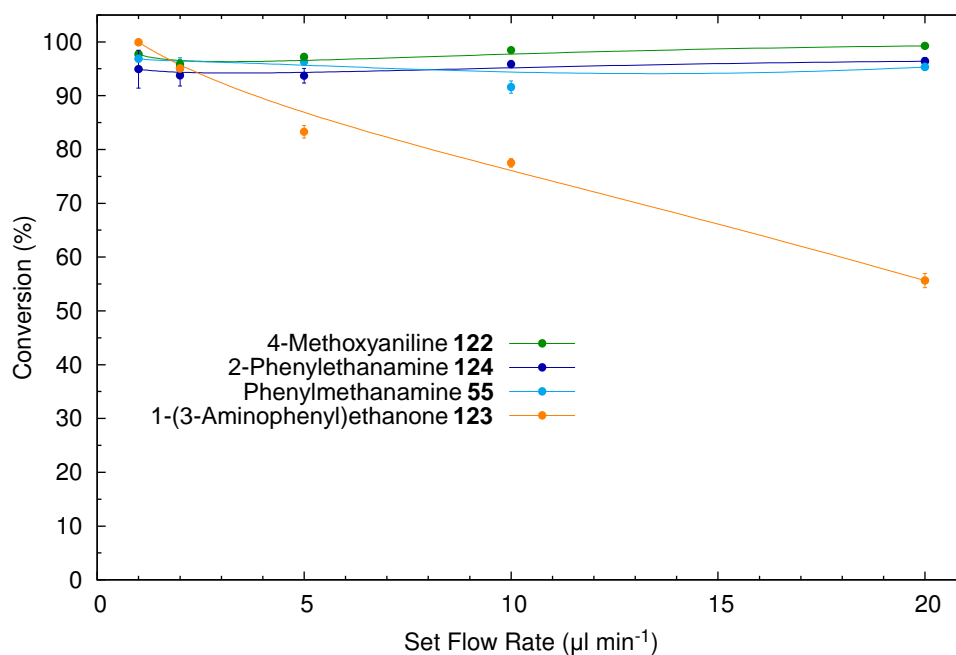


Figure 36. Reaction of amine derivatives **55** and **122–124** with acetyl chloride **58** to afford their corresponding amides in micro reactor set up T₁-T₂ at varying flow rates ($n = 10$).

which was attributed to a minimal amount of degradation of acetyl chloride **58** in THF solution, shown by Figure 18. As was observed previously for the acetylation of 4-nitrophenol **62** (Section 2.2.3) the near quantitative conversions recorded at a set flow rate of $20\ \mu\text{l}\ \text{min}^{-1}$ do not correlate with the theoretical Fourier number for the second stage reactor and PEEK™ tubing ($Fo = 0.6$ for acetic acid in EtOAc), which indicates that mixing is incomplete. It is suggested that the reduced viscosity of the mixed MeCN/THF solvent system (compared with EtOAc) and consequent effect on the true diffusion coefficient account for this difference and a completely mixed system ($Fo \geq 1$) is present at an overall flow rate of $40\ \mu\text{l}\ \text{min}^{-1}$ upon quenching from the micro reactor outlet. For the acetylation of aniline **15** and 1-(3-aminophenyl)ethanone **123** an increased residence time (achieved by employing a slower flow rate) was necessary to allow the reactions sufficient time to reach completion and two contributing factors may be attributed to this observation:

1. Resonance stabilisation of aniline **15** and electron withdrawing effects of the acetyl group, belonging to 1-(3-aminophenyl)ethanone **123**, which negatively affects the reactivity of the molecules, unlike the methoxy derivative **122** which is electron donating leading to an increase in the rate of reaction.
2. Both aniline **15** and 1-(3-aminophenyl)ethanone **123** are aromatic amines (*i.e.* molecules which contain NH_2 groups bonded directly to a conjugated ring system) thus it is reasonable to assume that this general feature diminishes the reactivity, since phenylmethanamine **55** and 2-phenylethanamine **124** both react readily at higher flow rates.

The Effect of Reactor Length on Conversion

In an effort to improve the productivity for the micro reactor synthesis of *N*-phenylacetamide **125** and *N*-(3-acetylphenyl)acetamide **128**, it was decided to substitute the second stage micro reactor (T2) for one of longer length, affording an increase in residence time at each particular set flow rate. As the internal channel volume of T2 ($0.11\ \mu\text{l}$) and exit tubing ($0.88\ \mu\text{l}$) was known, it was possible to calculate the minimum residence time required to allow for complete

conversion based upon the flow rates and corresponding conversions that had been determined for these particular compounds. This relationship, between conversion and residence time was therefore plotted, as shown in Figure 37, and the optimal time to achieve a theoretical quantitative conversion was thus estimated to be ~ 2.5 s. At a flow rate of $20 \mu\text{l min}^{-1}$ the residence time provided by micro reactor S₃ is ~ 6.1 s (see Appendix A) so it was consequently used in place of the shorter reactor, T₂.

Using the modified set up illustrated in Figure 38 the acetylation of aniline **15** and 1-(3-aminophenyl)ethanone **123** at a set flow rate of $20 \mu\text{l min}^{-1}$, was once again investigated. Although conversion to the corresponding products (**125** and **128**) had previously been measured as 88.6% and 55.6% respectively at the same flow rate it was pleasing to see that comparable results to those observed in the first system (T₁-T₂) at lower flow rates, were achieved. Quantitative conversion of aniline **15** was achieved whilst 1-(3-aminophenyl)ethanone **123** attained a conversion of 97.7% ($n = 10$) thus increasing the throughput when synthesising these particular amides on chip. Although an increase in throughput for the other amines may also have been possible by applying the same, lengthier set up to their syntheses, the higher flow rates that would be encountered led to

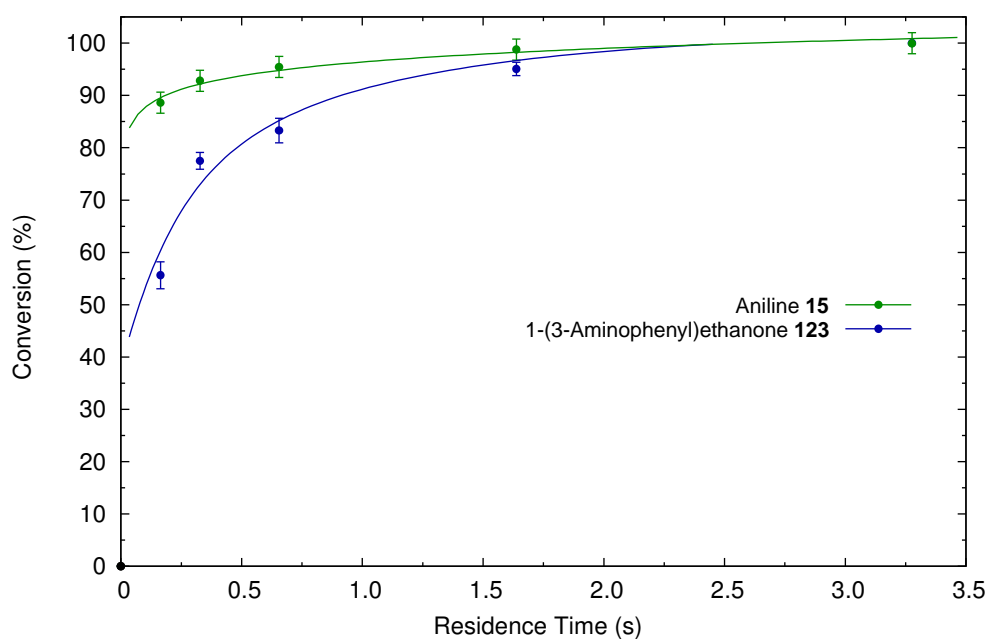


Figure 37. The relationship between residence time and conversion for aniline **15** and 1-(3-aminophenyl)ethanone **123** within micro reactor T₂ ($n = 10$).

3.3 BENZOYLATION OF PRIMARY AMINES

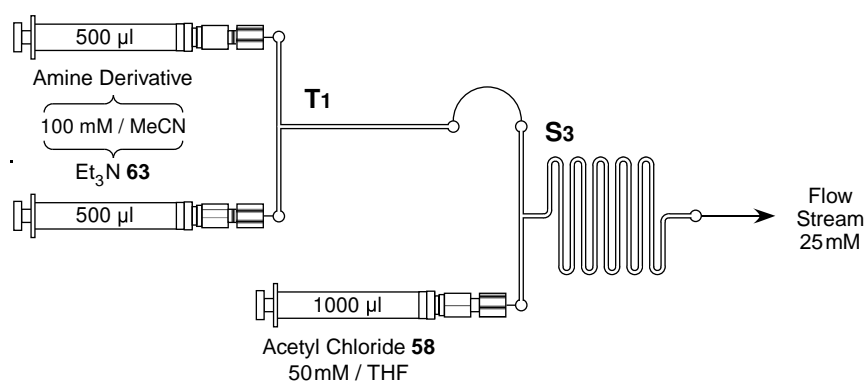
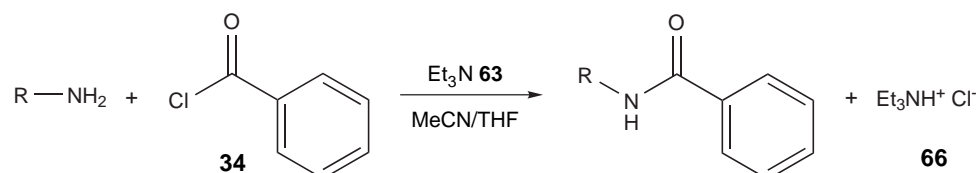


Figure 38. Schematic of the modified micro reactor set up, T1-S3, which was used to successfully acetylate aniline **15** and 1-(3-aminophenyl)ethanone **123** at a flow rate of $20 \mu\text{l min}^{-1}$.

uncertainties about the integrity of running such a system for prolonged periods of time, due to the increased back pressures that would be encountered. Since it was possible to achieve high conversions for all the amines at the top set flow rate it was envisaged that the optimised micro set ups could now be successfully utilised to demonstrate the feasibility of synthesising isotopically substituted amides within micro reactors.

3.3 Benzoylation of Primary Amines

As was the case for the acetylation of phenols, it was desired to expand the scope of the reaction by altering the acyl substituent and carrying out reactions with benzoyl chloride **34**. In accordance with Scheme 25, the reaction of the five amines, **15**, **55** and **122–124**, with benzoyl chloride **34**, to form *N*-phenylbenzamide **130**, *N*-(phenylmethyl)benzamide **131**, *N*-(4-methoxyphenyl)benzamide **132**, *N*-(3-



R=Ph **15**
R=4-MeOPh **122**
R=3-AcOPh **123**
R=PhCH₂ **55**
R=PhCH₂CH₂ **124**

R=Ph **130**
R=4-MeOPh **132**
R=3-AcOPh **133**
R=PhCH₂ **131**
R=PhCH₂CH₂ **134**

Scheme 25. The reaction of five primary amine derivatives with benzoyl chloride **34** in the presence of Et₃N **63** to afford an array of benzamide derivatives **130–134**.

3.4 SYNTHESIS OF DEUTERIUM SUBSTITUTED AMIDES

acetylphenyl)benzamide **133** and *N*-(2-phenylethyl)benzamide **134** respectively, was then investigated using the previously optimised micro reactor configurations and conditions (see above).

Although it had been found previously that upon substitution of acetyl chloride **58** with its benzoyl analogue **34** acylation reactions did not reach completion, in this case the results fared much better as can be seen from Table 20. The reduction in reactivity observed in the case of *N*-(3-acetylphenyl)benzamide **133** can be attributed to a combination of delocalisation across the ring between the amino and acetyl group, leading to stabilisation of the molecule, and the decreased reactivity of benzoyl chloride **34**, the net result leading to a lower conversion.

Table 20. Conversions obtained for the benzoylation of primary amines within a two stage micro reactor set up at a set flow rate of 20 $\mu\text{l min}^{-1}$.

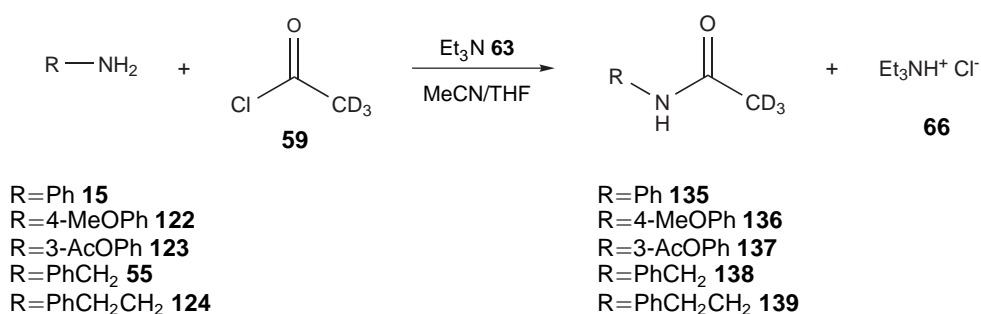
Product	Reactor	Conversion (%)	RSD ^a (%)
<i>N</i> -Phenylbenzamide 130	T _I -S ₃	90.5	4.91
<i>N</i> -(4-Methoxyphenyl)benzamide 132	T _I -T ₂	94.0	5.50
<i>N</i> -(3-Acetylphenyl)benzamide 133	T _I -S ₃	65.5	4.70
<i>N</i> -(Phenylmethyl)benzamide 131	T _I -T ₂	97.4	0.94
<i>N</i> -(2-Phenylethyl)benzamide 134	T _I -T ₂	91.9	2.46

^a $n = 10$

3.4 Synthesis of Deuterium Substituted Amides

Having successfully optimised the acetylation of five amine derivatives, the concept of employing the micro reactor systems to carry out efficient isotope labelling was then investigated. As was conducted for the synthesis of isotopically modified phenyl acetate derivatives (Section 2.2.11), acetyl chloride **58** was exchanged for its tri-deuterated isotopologue, (D₃)acetyl chloride **59**, and the reactions carried out under optimised conditions in accordance with Scheme 26.

The incorporation of deuterium labels into *N*-phenyl(D₃)acetamide **135**, *N*-(4-methoxyphenyl)-(D₃)acetamide **136**, *N*-(3-acetylphenyl)-(D₃)acetamide **137**, *N*-(phenylmethyl)-(D₃)acetamide **138** and *N*-(2-phenylethyl)-(D₃)acetamide **139** was confirmed by operating the appropriate micro reactor system for an extended period of time (2.5 hr to 3.0 hr) in order to prepare sufficient compound



Scheme 26. The synthesis of five isotopically substituted secondary amides as demonstrated within micro reactor systems.

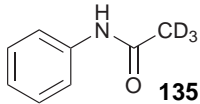
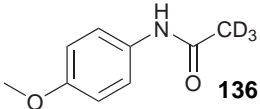
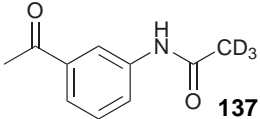
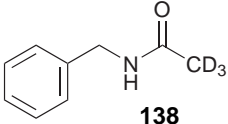
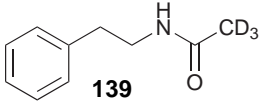
(~ 20 mg) for analysis, following work-up and recrystallisation to remove reaction by-products. As Table 21 shows, analogous results were obtained with the deuterated reagent and although there was slight variation, the reaction efficiency was found to be comparable to the pre-optimised conditions obtained with acetyl chloride **58**. In all cases the deuterium label was successfully incorporated into the final product and excellent isolated yields ($\geq 92\%$) were obtained at levels of throughput that enable the expedient synthesis of mg amounts of isotopically substituted amides.

3.5 Summary

The results obtained for the synthesis of isotopically modified amides were extremely pleasing since high yields were achieved and results compared well to those obtained when running the system under optimised conditions with unlabelled precursors. The purity of final products was also high as indicated by the elemental analysis results which in all cases correlated with theoretical values. It should be emphasised that the ability to obtain similar yields when substituting for the labelled reagent is a significant result, as this is often difficult to obtain in batch. Once again the work illustrates the applicability of micro reactor technology to carry out isotope labelling in a way that minimises cost and waste through efficient label incorporation. In particular the high conversions and yields lend themselves well to transference within a clinical setting when a minimum purity of a compound must be achieved; something that would be simple to address through on-line clean-up of the final product stream.

3.5 SUMMARY

Table 21. Summary of the results obtained for the incorporation of deuterium labels into amides within micro reactor systems.

Product	Reactor Set Up	Residence Time (s)	Throughput (mg hr ⁻¹)	Conversion ^a (%)	Yield ^b (%)
 135	T _I -S ₃	5.5	7.6	95.0 (100.0)	92
 136	T _I -T ₂	2.6	9.9	98.0 (97.7)	98
 137	T _I -S ₃	5.5	10.0	95.8 (99.9)	92
 138	T _I -T ₂	2.6	9.0	98.2 (91.6)	98
 139	T _I -T ₂	2.6	9.6	96.4 (94.9)	96

^a Number in parentheses represents the optimal % conversion when using acetyl chloride **58**.

^b Isolated Yield.

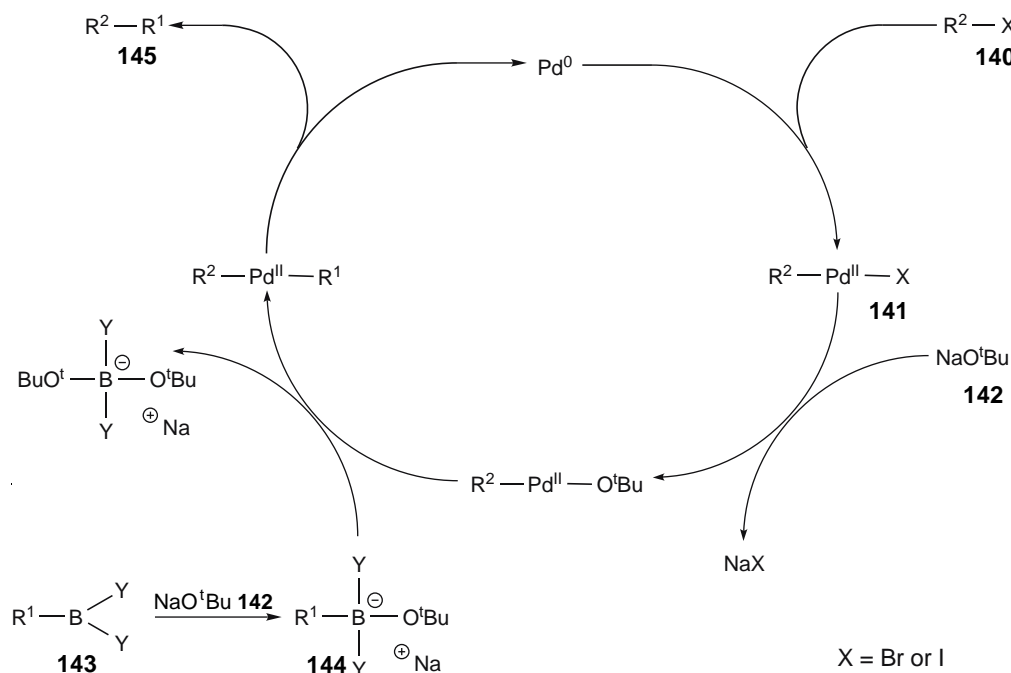
CHAPTER 4

C–C BOND FORMATION

4.1 The Suzuki-Miyaura Reaction

ONE particular example of C–C bond formation which has been widely studied within continuous flow systems is the Suzuki-Miyaura reaction or, as it is more commonly known the Suzuki coupling. Due to the potential for rapid optimisation based upon the wealth of published information available, along with the reactions tolerance to an array of functional groups, it was decided to investigate this reaction as a route to the preparation of a library of five deuterium substituted biphenyls.

The reaction was first reported in 1979 by Suzuki and Miyaura^{145,146} and has since grown into a well known and often used transformation to bring about C–C bond formation with the synthetic utility of the reaction demonstrated by the plethora of reviews on the subject.^{147–149} Although the mechanism^{150,151} is still not fully understood it can be seen from the example reaction cycle shown in Scheme 27 that initial oxidative addition of the aryl halide **140** forms a coupled Pd-aryl complex **141**, which is then stripped of halide *via* the addition of base **142**. The aryl or allyl portion of the boronic acid **143** then replaces the base **142**, after formation of an intermediary salt **144**, and finally a rapid reductive elimination releases the newly formed product **145** from the palladium centre.



Scheme 27. Reaction cycle of the Suzuki-Miyaura coupling reactions.⁷⁸

4.1.1 Reported Continuous Flow Methodology

As previously discussed, the Suzuki coupling is one of the most widely studied synthetic reactions within small scale, continuous flow systems. In addition to the example introduced in Chapter 1, reported by Greenway and co-workers,⁷⁸ a great deal of investigative work has been undertaken by other research groups and this is briefly reviewed below.

Catalytic Membranes An interesting example of the Suzuki-Miyaura reaction occurring within a micro reactor was demonstrated by Uozumi *et al.*¹⁵² who deposited a Pd containing polymer membrane **146** (Figure 39) at the laminar interface of a micro channel. Its position between a stream of reagents allowed it to

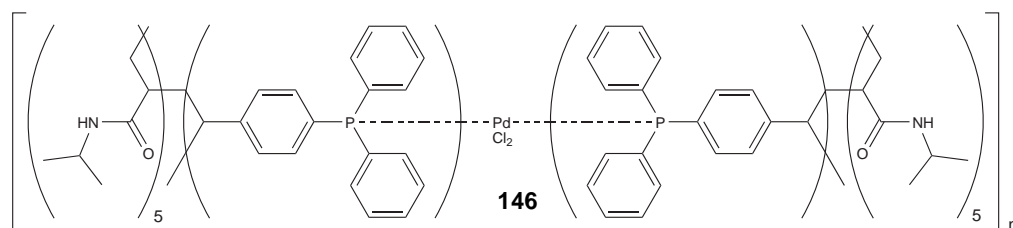
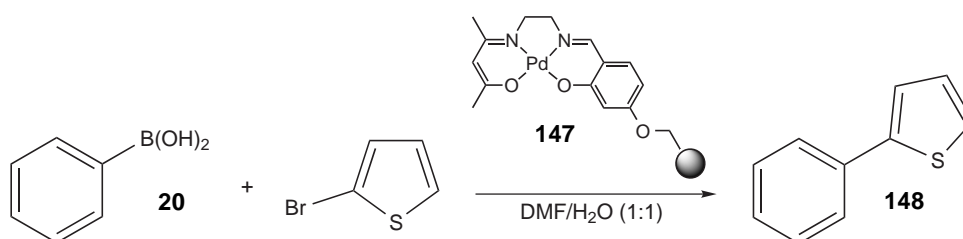


Figure 39. The metallo-crosslinked polymer which was formed within the channel of a micro reactor in order to catalyse Suzuki-Miyaura reactions.¹⁵²

4.1 THE SUZUKI-MIYAJURA REACTION

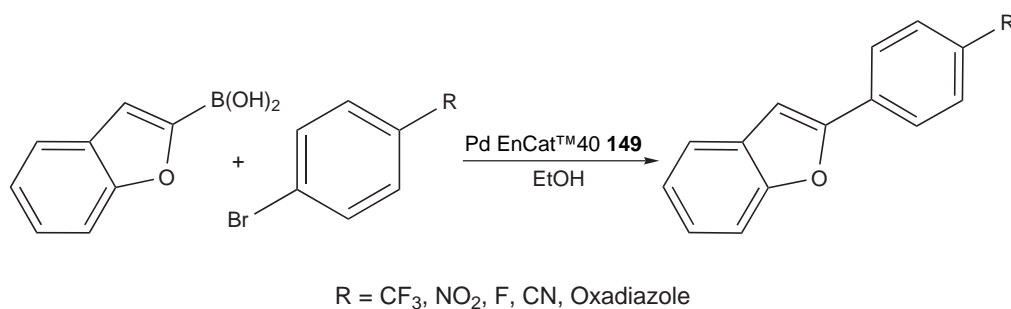
act as an *in-situ* phase transfer catalyst for the reaction between several aryl halides (in EtOAc/propan-2-ol) and boronic acids (in aqueous Na₂CO₃). High yields (88.0% to 99.0%) were reported within short time scales (4s) and, although the system required extra fabrication steps in order to form the polymeric membrane *in-situ*, the excellent results indicate the superiority of this micro reactor system over traditional batch techniques, particularly with respect to reaction time.

Polymer Supported Catalysis In contrast, Phan *et al.*¹⁵³ reported the use of a Merrifield® resin immobilised palladium salen complex **147** (Figure 28) as a catalyst in the reaction of various aryl and heteroaryl bromide derivatives with phenylboronic acid **20** in a flow reactor. The catalyst (110.0 mg) was packed into an Omnifit® column (25 mm i.d. × 3mm length), heated to 100 °C by a water bath and a mixture of reagents in DMF/water (1 : 1) was then mobilised through it by syringe pump. It was reported that at a flow rate of 6 μl min⁻¹ the synthesis of biphenyl derivatives containing alkyl, aldehyde, ester, ketone, nitrile and thio ester groups proceeded relatively well (65.0% to 77.0% conversion), as did the formation of several furan and thiophene containing compounds such as the one shown in Scheme 28. However the reaction exhibited low conversions when attempted with nitro, amino and amide aryl bromide derivatives, and some pyridine derivatives. Moreover it was necessary to employ an excess of phenylboronic acid **20** (1.50 eq.) to achieve these results, an undesirable situation if undertaking isotope labelling *via* this portion of the molecule. In spite of these shortcomings the work highlights the applicability of using miniaturised flow systems for the rapid screening of catalysts and reagents, in addition to the production of varied libraries of core derivatives.



Scheme 28. One of the heteroaryl biphenyl derivatives **148** that was synthesised under continuous flow conditions *via* the Suzuki-Miyaura reaction using an immobilised palladium salen complex **147**.¹⁵³

Microwave Assisted Reactions Elaborations on the reaction which utilise microwave power are certainly the most common and many permutations of this approach have been reported within recent years.¹⁵⁴⁻¹⁵⁷ For example the use of microwaves to enhance continuous flow Suzuki couplings has been demonstrated by Baxendale *et al.*¹⁵⁸ using an encapsulated palladium catalyst, Pd EnCat™ 40 **149**. According to Scheme 29 a library of biphenyl derivatives was successfully synthesised under optimal conditions using a U-shaped flow capillary which was packed with the catalyst **149** and inserted into a microwave cavity according to Figure 40. The reagents, solutions of aryl halide and boronic acid derivative (70 mM in EtOH) and the base, *N,N,N*-tributylbutan-1-aminium acetate (140 mM in EtOH) were infused using a pump, which was run at a flow rate of 1000 $\mu\text{l min}^{-1}$. After leaving the microwave cavity the resultant stream was passed over Amberlyst® 15 ion exchange resin in order to sequester any residual boronic acid salt and the base. The authors found that it was necessary to pulse the microwave irradiation at 50 W for 30 s and then 0 W for 18 s in order to avoid heating the metal catalyst to a point where the polymer melted and blocked the flow cell. The resulting product was then analysed without further purification by LC-MS and ¹H-NMR. Using this approach, yields ranged from 87 % to 92 % whilst purities were reported to be > 98.0 %, indicating the synthetic applicability of the technique, albeit requiring the use of specialist equipment to undertake reaction heating.



Scheme 29. The generalised route followed by Baxendale *et al.*¹⁵⁸ when undertaking microwave assisted Suzuki flow synthesis.¹⁵⁸

Encapsulated Pd Without Microwave Irradiation It is noteworthy to consider another piece of work, published by Lee and co-workers,¹⁵⁹ which utilised the

4.1 THE SUZUKI-MIYAJURA REACTION

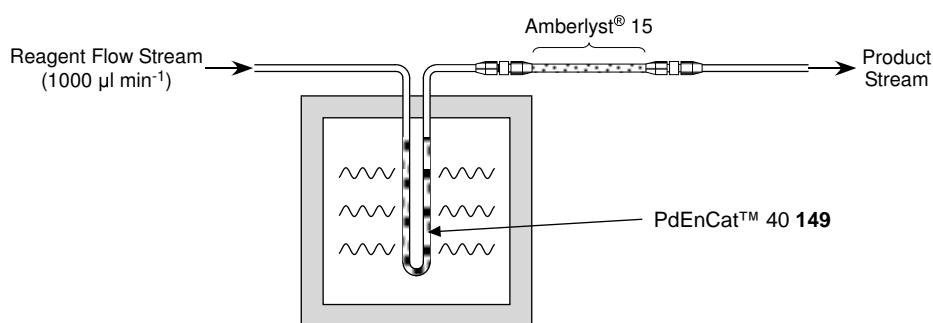
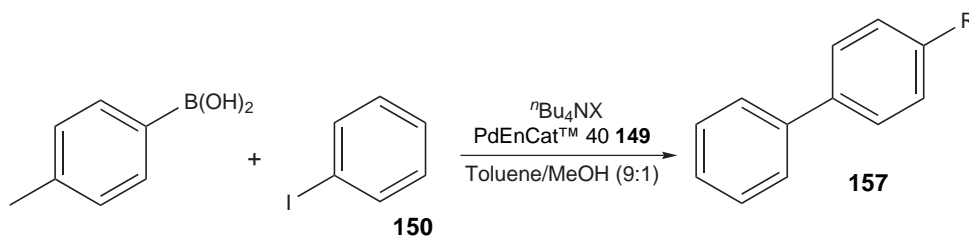


Figure 40. Schematic representation of the microwave set up employed by Baxendale *et al.*¹⁵⁸ for the flow synthesis of biphenyl compounds *via* the Pd EnCat™ 40 149 assisted Suzuki reaction.

same catalyst but did not require the application of microwave power. In this case, heat was supplied to a commercially obtained flow column (4500 µm i.d. × 5 cm) which had been pre-packed with the same Pd EnCat™ 40 149 catalyst, by immersion into a hot water bath. Using the reaction between (4-methylphenyl)boronic acid and iodobenzene **150** as an example, experimentation with a range of bases at 55 °C and 70 °C led the authors to conclude that an effective system utilising conventional heating methods was achievable. As Table 22 exemplifies, optimal results were achieved at 200 µl min⁻¹ when employing *N,N,N*-tributylbutan-1-aminium methanolate (TBAM) **151** as a base in conjunction with a 9 : 1 mixture of toluene and MeOH at 70 °C (Entry 5), affording 100 % conversion after a single pass through the flow system. The authors report that at a flow rate of 200 µl min⁻¹ and temperature of 70 °C, the coupling reaction occurred to give

Table 22. Reported conversions obtained after a given number of cycles when evaluating the effectiveness of organic bases in assisting a conventionally heated continuous flow Suzuki reaction.¹⁵⁹



Entry	<i>n</i> Bu ₄ NX	Temperature (°C)	Conversion (%)		
			Cycle 1	Cycle 2	Cycle 3
1	X = OAc	55	4.7	7.5	11.0
2	X = OH	55	3.1	13.0	70.0
3	X = OMe 151	55	12.0	48.0	85.0
4	X = F	55	36.0	40.0	55.0
5	X = OMe 151	70	100.0	–	–

100% conversion, determined by GC-FID, in a single pass through the packed bed. Based upon the positive observations concerning the use of Pd EnCat™40 **149** as a solid-supported catalyst, such as;

- Low rate of leaching (of palladium from the polymeric matrix).
- The ability to undertake the reaction without the need for specialist technology and techniques.
- Excellent and timely conversions.

It was decided to adapt the latter method and attempt the synthesis of a library of isotopically substituted biphenyl derivatives using (D₅)phenylboronic acid **152** as a precursor following unlabelled flow reaction optimisation in the presence of TBAM **151**. The ease by which the same apparatus (*e.g.* connectors and columns) may be acquired, especially by those without ready access to specialist fabrication facilities, and the simplicity of preparing such flow systems (*i.e.* ease of packing catalytic material) resulted in investigations being attempted using analogous techniques in order to develop methodology that maximised potential transferability.

4.2 Continuous Flow Set Up

In order to fabricate an analogous reactor to the one that was supplied to Lee *et al.*¹⁵⁹ by Astra Zeneca, a system comprising of a borosilicate glass capillary (3000 μm i.d. × 3 cm) was constructed and hand packed with 0.16 g of Pd En-Cat™40 **149** catalyst. In order to prevent displacement of the catalyst an Omnifit® connector, fitted with a small plug of cotton wool, was attached to the downstream end of the column, C₁, and a length of polytetrafluoroethylene (PTFE) tubing (584 μm i.d., 1/16" o.d.) so that it was possible to direct the product stream in to a suitable collection vessel. The other end of the column was interfaced to a 10.0 ml syringe *via* a further length of PTFE tubing, Omnifit® connector, syringe luer and HPLC connector (1/16") as shown in Figure 41.

As previously reported, it was necessary to supply heat to the column, which

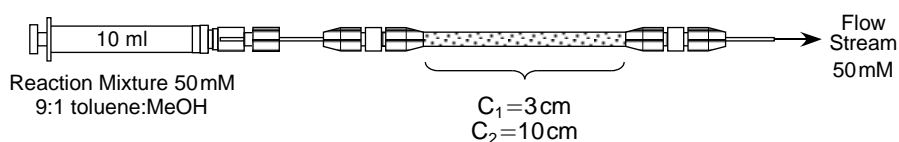


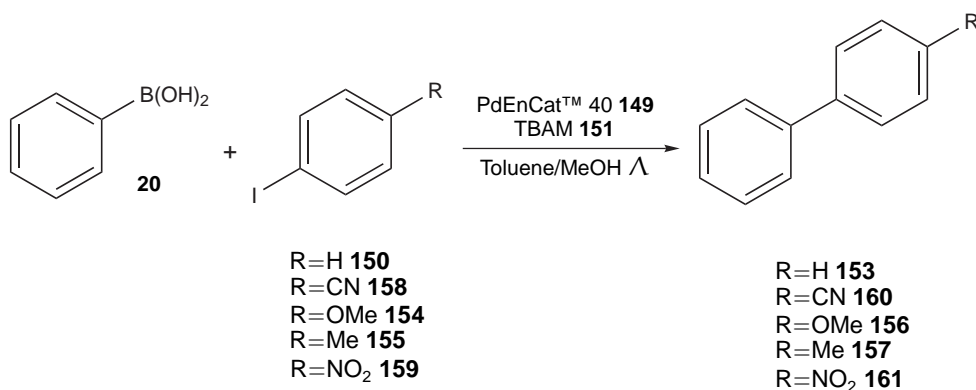
Figure 41. A schematic of the flow set up, C₁, which was used to study Suzuki-Miyaura couplings reported herein.

was achieved utilising a water bath, however rather than use this method of heating, which would necessitate regular topping up and monitoring of the heating medium, it was decided to substitute the water for silicone oil as it had proved a suitable method of heating when conducting previous work involving micro reactors (Section 2.3.4). The column was therefore submerged into an oil bath and was heated *via* a standard laboratory hot plate.

In order to prime the reactor and ensure a steady flow of reaction mixture was obtained, the syringe pump was operated for 60 min before sample collection and analysis was initiated. During the optimisation of all reactions, routine analysis was undertaken using GC-FID by comparing the peak areas of the biphenyl derivative with any aryl iodide that remained in the crude reaction mixture. Prior to conducting experimentation appropriate calibrations using synthesised or purchased standards were undertaken in order to normalise the relative response of the compounds under investigation.

4.3 Library Selection

In order to demonstrate the system, C₁, as a viable tool for the synthesis of isotopically substituted compounds, a variety of aryl iodide derivatives were selected to undergo reaction with phenylboronic acid **20**, as depicted in Scheme 30. Firstly experimental optimisation of reaction with iodobenzene **150** to afford biphenyl **153** was undertaken and in order to indicate how easily ring activated compounds would undergo reaction 1-iodo-4-methoxybenzene **154** and 1-iodo-4-methylbenzene **155** were selected to afford 4-methoxybiphenyl **156** and 4-methylbiphenyl **157** respectively. In an opposite manner, the deactivated derivatives 4-iodobenzonitrile **158** and 1-iodo-4-nitrobenzene **159** were also selected, to afford 4-phenylbenzotrile **160** and 4-nitrobiphenyl **161** respectively.



Scheme 30. The reaction of five aryl iodide derivatives with phenylboronic acid **20** to form the corresponding biphenyl products.

4.4 Optimisation of Biphenyl Flow Synthesis

As a general starting point, the operational conditions reported by Lee *et al.*¹⁵⁹ were used employing the synthesis of biphenyl **153** as a model. Using the aforementioned conditions, $\sim 70^\circ\text{C}$ and $200\ \mu\text{l min}^{-1}$, it was found that conversions did not compare well with those that had been reported (100%), an observation that can be attributed to the use of less catalytic material (0.16 g *cf.* 0.48 g). As can be seen from Table 23, an average conversion of only 0.7% was achieved so the flow rate was sequentially lowered until the highest conversion of 93.2% was observed at a flow rate of $10\ \mu\text{l min}^{-1}$.

Although the optimal flow rate was significantly lower than that achieved by Lee *et al.*¹⁵⁹ the result was nevertheless a positive one, confirming that high yields were attainable, so attention was turned to generating the library of isotopically unmodified biphenyl derivatives introduced earlier (Section 4.3).

Table 23. Conversions achieved for the synthesis of biphenyl **153** across a range of flow rates when heated to $70^\circ\text{C} \pm 5^\circ\text{C}$ in reactor C1.

Entry	Flow Rate ($\mu\text{l min}^{-1}$)	Conversion (%)	RSD ^a (%)
1	200	0.7	11.0
2	100	9.5	6.2
3	50	56.8	4.9
4	20	85.4	1.4
5	10	93.2	1.2

^a $n = 5$

4.5 Library Generation

The second derivative to undergo flow synthesis, 4-methylbiphenyl **157**, was attempted using isotopically unmodified precursors under the optimal conditions of $10\ \mu\text{l min}^{-1}$ at a temperature of $\sim 70^\circ\text{C}$. The experiments afforded an average conversion of 74.2%* which, reproducibility considerations aside, was significantly lower than the value obtained for the flow synthesis of biphenyl **153**. Considering this, an attempt to improve the conversions was made by increasing the temperature of the oil bath to 100°C , whilst keeping the flow rate set at $10\ \mu\text{l min}^{-1}$. Under these conditions, the results that were collected were much improved and an average conversion of 92.2% was obtained. The reproducibility also dramatically improved to 6.0% RSD ($n = 5$) however it was decided to run the system for a longer period of time in order to try and achieve greater stability and thus lower the RSD. Upon doing this it was found that the waste collection contained traces of oil and inspection of the Omnifit® connectors revealed that cracks had formed, thus revealing the source of the problem. Since it was essential to develop a system that was robust enough to be heated to 100°C on a regular basis, for prolonged periods of time and that fouling of the flow stream was a situation to avoid, it was decided to revise the set up and investigate alternative methods of providing heat to the capillary column, Cr.

4.6 Revised Continuous Flow Set Up

One of the biggest issues was the integrity of the connectors following prolonged, direct heating and whether or not the catalyst remained fully operational after spoiling by the entry of oil in to the packed capillary. Removal and washing of the catalyst (Hexane, MeOH) was possible, but also a time consuming process, especially if the situation regularly occurred and not suited to robust method development or prolonged and routine operation. Switching the system to one which incorporated a packed micro reactor channel would alleviate this problem by minimising interconnections, since previous heating *via* an oil bath had been

*RSD = 20.1%, $n = 5$

4.6 REVISED CONTINUOUS FLOW SET UP

successfully achieved (see Section 2.3.4). However the ease by which a column may be packed and operated in a continuous flow environment, the promising results achieved (Table 23) and the success reported by Lee *et al.*¹⁵⁹ were all deciding factors in retaining the same general methodology. In contemplating ways around the problems that had been encountered, the following solutions were considered:

- Use of water instead of oil as a heating medium, since successful application had been previously reported.^{153,159}
- Sourcing alternative connectors that could withstand higher temperatures.
- Provide a more direct method of heating.

The alternative option that was found to offer the best solution was to employ direct heating *via* the use of a chromatography column heater which contained aluminium blocks, that ensured dispersion of heat around the reaction column, but most importantly not the Omnifit® connectors (Figure 42). This approach allowed efficient dispersion of heat to the reactants within the flow system and it was found that the temperature could be much more precisely controlled using this apparatus, with fluctuations of only $\pm 2^{\circ}\text{C}$, overall a much more robust way



Figure 42. A photograph of the flow column, C2, within the chromatography column heater. Inset—A magnified view of the column *in-situ* with the top heating block removed.

of supplying heat to the reactor, C₁ (oil bath $\pm 10^\circ\text{C}$). In addition, the use of such equipment would prevent potential fouling of valuable catalyst material, were the connectors to leak.

Since an alternative system was being implemented, a new column was packed with fresh Pd EnCat™ 40 **149**, in order to allay any fears of the repeated catalyst fouling affecting future optimisation data. It was also decided to employ a longer borosilicate glass column (C₂ = 3 mm i.d \times 10 cm) so that the stream of reagents was exposed to a greater proportion of catalyst as it passed through the system. Using an analogous packing technique, the column was filled with 0.35 g of catalyst material, which was more comparable to the system employed by Lee and co-workers¹⁵⁹ (0.48 g). The reactor, C₂, was again interfaced to the syringe and collection vessel using PTFE tubing, Omnifit® and PEEK™ connectors in the same manner as was previously described, in accordance with the photograph shown in Figure 42.

4.7 Flow Synthesis of Biphenyl Derivatives

When the system was operated at 70°C , over a range of flow rates, the data shown in Figure 43 was obtained. It was surprising to find that, considering the additional catalyst material present, in comparison to flow reactor C₁, conversions were lower than had been observed at an equivalent flow rate and temperature. This observation was attributed to the fact that when the temperature had been controlled by the oil bath there were large fluctuations in the temperature (up to 10°C difference) and it would seem that with a stable temperature of 70°C there was simply not enough energy for the reaction to progress to such a degree, exemplified by the fact that additional catalyst did not promote any extra reaction. This observation is surprising considering the results published by Lee *et al.*¹⁵⁹ but nevertheless, in the case of the set up described herein, it seemed worthwhile to investigate the effect of raising the temperature to 100°C .

As can be seen from Table 24, when the reaction was repeated at the higher temperature of 100°C there was a significant improvement in conversions at all

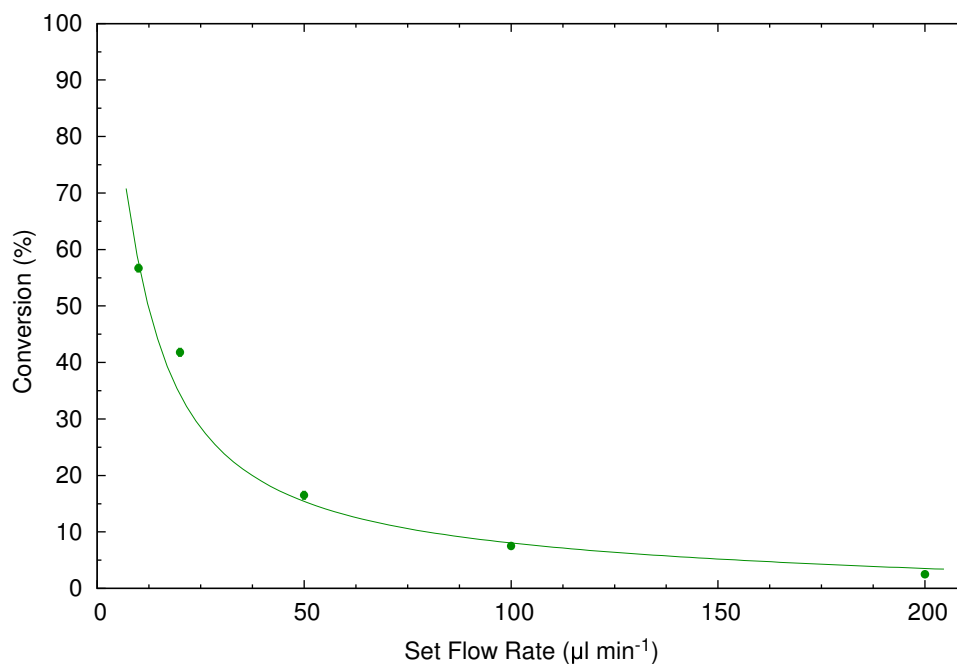


Figure 43. The results obtained when attempting the flow synthesis of biphenyl **153** at various flow rates when heated to 70°C using a chromatography column heater.

investigated flow rates and the results compared well to those obtained with the previous set up, C1. As had been observed previously, at the lowest investigated flow rate (10 µl min⁻¹), excellent conversions were obtained.

Following the development of a stable flow system for the synthesis of biphenyl **153**, generation of the full library of isotopically unmodified compounds, introduced in Section 4.3, was attempted under the aforementioned conditions. The data presented in Table 25 shows that for all compounds conversion and reproducibility was found to be excellent, which indicated that the synthesis of deuterium substituted biphenyl derivatives would now be possible, in an efficient way, using the developed reaction process.

Table 24. Conversions achieved for the synthesis of biphenyl **153** across a range of flow rates when heated to 100°C using a chromatography column heater and reactor C2.

Entry	Flow Rate (µl min ⁻¹)	Conversion (%)	RSD ^a (%)
1	200	37.2	18.4
2	100	69.8	0.9
3	50	76.7	1.6
4	20	82.9	3.0
5	10	91.1	0.8

^a $n = 5$

4.8 SYNTHESIS OF DEUTERATED BIPHENYL DERIVATIVES

Table 25. Conversions obtained for the flow synthesis of biphenyl derivatives at a flow rate of $10 \mu\text{l min}^{-1}$ and temperature of 100°C within reactor C2.

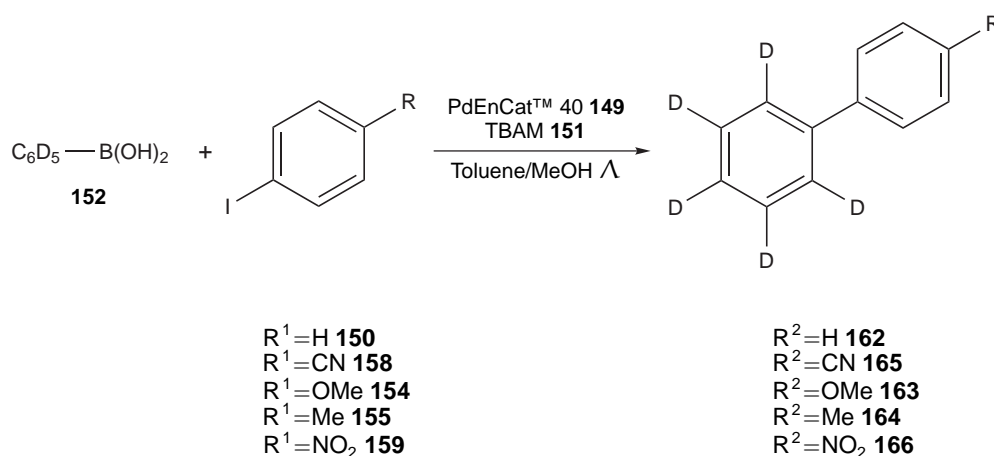
Product	Conversion (%)	RSD ^a (%)
4-Phenylbenzotrile 160	95.9	0.84
4-Methoxybiphenyl 156	97.9	0.70
4-Methylbiphenyl 157	95.0	2.10
4-Nitrobiphenyl 161	97.2	0.15

^a $n = 5$

4.8 Synthesis of Deuterated Biphenyl Derivatives

In order to demonstrate the synthesis of deuterium substituted biphenyl derivatives the optimised reactions were repeated with phenylboronic acid **20** substituted for its penta-deuterated isotopologue, (D_5) phenylboronic acid **152**, as shown in Scheme 31. Reaction of iodobenzene derivatives **150**, **154**, **155**, **158** and **159** in this way brought about the synthesis of (D_5) phenylbenzene **162**, 1-methoxy-4- (D_5) phenylbenzene **163**, 1-methyl-4- (D_5) phenylbenzene **164**, 4- (D_5) phenylbenzotrile **165** and 1-nitro-4- (D_5) phenylbenzene **166** respectively. The results of running the reactor C2 under optimal conditions for all biphenyl derivative can be seen in Table 26.

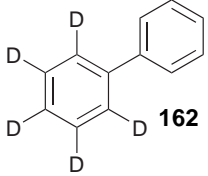
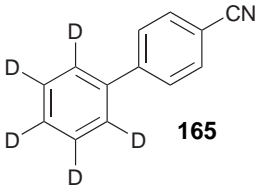
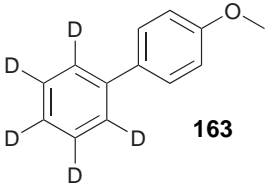
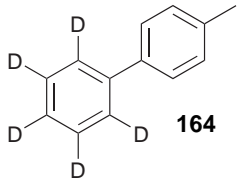
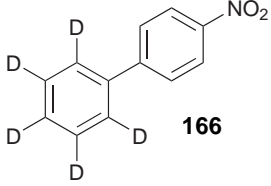
In all cases the flow system was operated for between 3.3 hr and 4.2 hr (prior to removal of the solvent *in-vacuo* and an aqueous work-up) in order to produce sufficient compound for analysis by NMR and MS, so that successful synthesis



Scheme 31. The five deuterium substituted biphenyl derivatives which were successfully synthesised in high yield within continuous flow system C2.

4.8 SYNTHESIS OF DEUTERATED BIPHENYL DERIVATIVES

Table 26. Summary of the results achieved when synthesising penta-deuterio substituted biphenyls within reactor C2 at a flow rate of $10 \mu\text{l min}^{-1}$ and temperature of 100°C .

Biphenyl Product	Residence Time ^a (s)	Throughput (mg hr^{-1})	Conversion ^b (%)	Yield ^c (%)
 162	1800	4.2	90.0 (91.1)	88
 165	1800	5.0	100.0 (95.9)	91
 163	1800	5.5	100.0 (97.9)	97
 164	1800	5.0	97.5 (95.0)	96
 166	1800	6.1	100.0 (97.2)	99

^a Estimated based upon the internal volume of the packed column ($300 \mu\text{l}$) and flow rate. The true residence time will fluctuate depending on the individual path of the flow stream over the catalyst.

^b Number in parentheses represents the % conversion obtained under optimal conditions when using phenylboronic acid **20**.

^c Isolated Yield.

of the isotopically substituted compounds could be confirmed. In the case of 4-(D₅)phenylbenzotrile **165** and 1-nitro-4-(D₅)phenylbenzene **166** it was also necessary to conduct elemental and IR analysis as these particular compounds were previously unreported within the literature.

4.9 Summary

Once again moderate to excellent isolated yields ($\geq 88\%$) were obtained when undertaking the synthesis of isotopically modified biphenyl derivatives under continuous flow at sufficient levels of throughput ($\geq 4.2 \text{ mg hr}^{-1}$) for the purposes of isotope labelling. This was a pleasing result and although the conditions differed somewhat when compared to those reported in the literature, the heating regime was more robust with respect to long term use. In addition the Pd EnCat™40 **149** catalyst proved itself viable for long term use with minimal leaching observed (0.002% w/w) and a high re-usability, employed for a total of ~ 150 hr without any noticeable decrease in activity, an observation that is attributed to the minimal catalyst degradation observed in a flow system compared to a batch reactor.

CHAPTER 5

CONCLUSIONS

5.1 Summary

A number of continuous flow reactions have been presented which were optimised using isotopically unmodified starting materials to the point where it was possible to undertake isotope labelling, in high yield, demonstrated by the substitution of small molecular precursors for their deuterated isotopologues.

In order to demonstrate the feasibility of using micro reactor systems for isotope labelling, the successful acetylation and methylation of phenols was repeated under optimised conditions by the substitution of acetyl chloride **58** and MeI **47** for their tri-deuterated equivalents (D₃)acetyl chloride **59** and (D₃)MeI **106** respectively. In all but one case, the methylation of 4-nitrophenol **62**, high conversions ($\geq 92.3\%$), corresponding to isolated yields of $\geq 92\%$ and throughputs of $\geq 6.6 \text{ mg hr}^{-1}$ were obtained. The deuterated compound (D₃)acetyl chloride **59** was also employed to bring about the synthesis of isotopically modified secondary amides which were once again optimised to achieve conversions $\geq 95.0\%$, isolated yields of $\geq 92\%$ and throughputs of $\geq 7.6 \text{ mg hr}^{-1}$. The residence time for the aforementioned flow syntheses was of the order $< 12.0 \text{ s}$ indicating the expedient nature of undertaking synthesis within micro reactor systems. Additionally, the successful incorporation of deuterium isotopes into a number of biphenyl derivatives was also achieved by the substitution of phenylboronic acid **20** for

the penta-deuterated compound, (D₅)phenylboronic acid **152**. Repeating the successfully optimised experiments in this way furnished excellent conversions of $\geq 90.0\%$ and isolated yields of $\geq 88\%$ at levels of throughput in the range 4.2 mg hr^{-1} to 6.1 mg hr^{-1} .

The practice of undertaking the work presented herein demonstrates the real life applicability of using, and continuing to develop, flow techniques for synthesis involving isotopes on an extremely cost effective scale. Resulting yields were high (88% to 98%) and achieved at excellent throughputs (4.2 mg hr^{-1} to 26.6 mg hr^{-1}) demonstrating that continuous flow technology has a great deal to contribute to the many areas of science that rely upon the use, or synthesis of, isotopically modified compounds.

The labelling procedures presented herein offer superiority over traditional synthesis techniques as the developed methods allow the use of stoichiometric quantities of reagents to produce high yields, provide a highly contained reaction system and allow the reactions to be undertaken using generic methodology for numerous derivatives. Whilst commercially produced devices capable of undertaking small scale flow synthesis with isotopes are not currently available, this work has clearly demonstrated the potential of applying this technology to the manufacture of such units, which would result in significantly reduced costs (when compared with alternative automated synthetic units currently available), and dramatically alter the many areas of science that rely on such techniques.

5.2 Future Work

A theme that has been referred to throughout is the need to develop in-line clean up protocols whereby an isotopically labelled compound would be delivered in a suitably pure state its application. For the reactions presented herein there are of many ways to achieve this which are dependant upon the end use. For example, when considering the methylation of sodium aryloxides, the only by-product is NaCl and the product contains a small percentage of un-reacted starting material. In order to obtain the isotopic target in pure form the implementation of an

in-line purification protocol is necessary. One option is a phase separation ‘chip’, capable of dissolving the NaCl in an aqueous stream, and achieving separation of the two immiscible laminar flow streams. The solvent could then be separated from the organic portion under high vacuum, leaving behind the enriched isotopically modified target molecule. Practically however the resolution of control that is required to achieve this within pressure driven systems is difficult to achieve since perturbations caused by the pulsed nature of the driving technology require correction to obtain a truly efficient separation. In such cases coupling to a preparative HPLC or bringing about chromatographic separation by other techniques could provide the simplest method of on-line purification.

5.2.1 Potential Applications

The acetylation and methylation reactions that were optimised using micro reactor systems are well suited to undertaking isotopic labelling with more than just deuterium. In particular isotopologues of MeI **47** are often employed as a tool for radiolabelling since [¹³C]MeI **45** may be rapidly prepared after cyclotron bombardment of a suitable target. Thus it should be a simple task to undertake the synthesis of many important radiolabelled molecules by employing the micro reactor systems optimised for deuterium labelling. As the radiolabelled precursor is prepared in much lower concentrations than the example reactions herein were optimised for, the migration to lower concentrations should, theoretically produce analogous results.

In contrast it should be noted that the continuous flow systems, C₁ and C₂, presented within Chapter 4 are mainly useful for syntheses involving stable isotopes as the holding volume within the reactor column is much larger, when compared to the other micro reactor systems that were developed herein (*e.g.* 300.0 μl* *cf.* 1.4 μl†). As a direct consequence of this, the ‘priming time’ required to ensure a stable and high yielding synthesis of isotopically modified compound is much greater, as is the residence time at the optimal flow rate (30 min at 10 μl min⁻¹). Therefore, the ability to carry out time dependent carbon-carbon

*Calculated as an average based on five weights when the column was filled with MeOH.

†Calculated as an average volume of all the micro reactors detailed within Appendix A.

couplings on the nanomolar scale, as would be required in order to undertake a radiosynthetic preparation, is somewhat diminished. In order to make these reactions suitable for synthesis on this scale it is suggested that the method be transferred to a micro reactor based system which incorporates a packed bed channel, capable of holding the catalyst and affecting transformations to an equivalent extent. In lieu of this, the developed methodology is well suited to situations where a large isotopic mass increase is required since coupling of (D₅)phenylboronic acid **152** to an aryl iodide will furnish a product which is 5 Da heavier than its isotopically unmodified isotopologue, a more than acceptable increase in molecular weight in a number of situations, as was discussed earlier within Chapter 1.

The use of isotopes to undertake biosynthetic studies serves to highlight that within this particular area of research it is advantageous to have the ability to generate a ready supply of structurally diverse labelled molecules from less expensive labelled precursors, with which to perform biosynthetic evaluation. It may be envisaged that in the future this need will be met with the use of combinatorial micro reactors which would facilitate a diversity of labelled compounds at speed and low cost, greatly enhancing the productivity of such studies.

CHAPTER 6

EXPERIMENTAL DETAILS

6.1 Materials

(D₃)MeI **106** (+99% D) was purchased from Acros Organics (Loughborough, UK). All other reagents were purchased from Sigma Aldrich (Gillingham, UK). NaH **78** (60% as a suspension in mineral oil) was washed with hexane prior to use whilst 4-methoxyphenol **67** (98%), 4-methoxyaniline **122** (98%) and 1-(3-aminophenyl)ethanone **123** (> 99%) were recrystallised from DCM/hexane prior to use. 4-Phenoxyphenol **69** was recrystallised from ether/hexane. All other chemicals were of suitable purity (> 99%) to be used as received and stabiliser free, anhydrous THF (99.9%, H₂O < 0.002%) was used when carrying out micro reactor acylations. Solvents used for micro reactions of amines were puriss grade (≥ 99.5%) over molecular sieves (H₂O ≤ 0.005%) purchased from Fluka (Gillingham, UK). MeCN and DMF used for all other micro reactions were of purity > 99.0% with a water content of < 0.3%. All other solvents were HPLC grade purchased from Fischer Scientific (Loughborough, UK). Water purity was 5 MΩ cm⁻¹, prepared by reverse osmosis and ion exchange using an Elgast (High Wycomb, UK) water purifier fitted with an Option 4 cartridge. Pd EnCat™40 **149** had a specified Pd loading of 0.46 mmol g⁻¹ and a 174 μm particle size. Crown white borosilicate glass pre-coated with chrome and photoresist manufactured by TELIC (Valencia, USA) was used to fabricate all micro reactors employed herein.

6.2 Instrumentation and Apparatus

Elemental analysis was carried out using a Fisons Carlo Erba Instruments EA1108 elemental analyser manufactured by CE Elantech, Inc. (Lakewood, USA). Infra-red spectra (thin film, DCM) were recorded on a Paragon 1000 FT-IR spectrometer manufactured by Perkin Elmer, Inc. (Massachusetts, USA) in the range 4000 cm^{-1} to 500 cm^{-1} and peaks (λ_{max}) reported in wavenumbers (cm^{-1}). NMR spectra were recorded on a Jeol GX400 spectrometer manufactured by JEOL (UK) Ltd. (Welwyn Garden City, UK) operating at room temperature in solutions of trichloro-deuteriomethane (CDCl_3) doped with trimethylsilicon (TMS, 0.03 %) as an internal standard. Chemical shifts are quoted in parts per million (ppm) and coupling constants in Hertz (Hz). Mass spectra were recorded on a Varian GC CP-3800 coupled to a Varian MS Saturn 2000 manufactured by Varian, Inc. (Oxford, UK) with a CP-Sil 8 (30 m) Zebron ZB-5 column manufactured by Phenomenex (Macclesfield, UK) using He (99.9999 %) as the carrier gas. Inductively Coupled Plasma Mass Spectrometry (ICP-MS) measurements were made at $\lambda = 340.46\text{ nm}$ using a Perkin Elmer Optima 5300DV instrument. The melting point (mp) of compounds are reported uncorrected and were recorded using Gallenkamp (UK) melting point apparatus. Characterisation and naming of all compounds is reported in accordance with the current Royal Society of Chemistry (RSC) and IUPAC guidelines.¹⁶⁰

The GC-FID used for the routine analysis of biphenyl and its derivatives was a Shimadzu GC-17A manufactured by Shimadzu UK Ltd. (Milton Keynes, UK) equipped with a CP-Sil 8 (30 m) Zebron ZB-5 column manufactured by Phenomenex using He as the carrier gas and a 50 : 50 mix of air and hydrogen as the detector fuel. In all other cases the HPLC set up used for experimental analysis was a Shimadzu (LC-10AD) pump coupled to an in-line Shimadzu DGU-14A degasser and an appropriate HPLC column. Analyte detection was carried out at $\lambda = 254\text{ nm}$ using a Polymer Laboratories LC 1210 UV/Vis detector manufactured by ICI Instruments (London, UK).

Unless otherwise stated the syringe driver was an MD-1001 connected to a MD-

1000 syringe pump controller which were manufactured by Bioanalytical Systems, Inc. (West Lafayette, USA) and could operate at set flow rates ranging between $1\ \mu\text{l min}^{-1}$ to $20\ \mu\text{l min}^{-1}$. The syringe pump used for the flow reactions of biphenyl and its derivatives was a Harvard PhD 2000 manufactured by Harvard Apparatus Ltd. (Edenbridge, UK) whilst the column heater was a 7971 Jones chromatography column heater manufactured by Jones Chromatography Ltd. (Hengoed, UK). The dimensions and characteristics of all micro reactors used may be found within Appendix A. PEEK™ tubing ($360\ \mu\text{m}$ o.d., $150\ \mu\text{m}$ i.d.) used to connect the micro reactors and syringes was purchased from Anachem (Luton, UK). Glass luer lock syringes, HPLC fittings ($1/16''$), PTFE tubing ($584\ \mu\text{m}$ i.d., $1/16''$ o.d.) and female-female luers were all purchased from Supelco (Gillingham, UK). Ominfit connectors and O-rings were purchased from Kinesis (Cambridge, UK). The thermocouple (2063750) used to monitor heated micro reactions was manufactured by RS components (Corby, UK). The optical microscope used for micro reactor imaging was an Axiovert S100 manufactured by Carl Zeiss MicroImaging Inc. (Welwyn Garden City, UK) fitted with a $20\times$ magnification lens and a coupled CCD camera. The automatic mixing carousel used to undertake small scale batch studies was a Stuart Rotator SB2 manufactured by Bibby Sterilin Ltd. (Stone, UK).

6.3 Instrumental Methodology

6.3.1 GC-MS

All compounds were analysed with an injector volume of $1\ \mu\text{l}$ at a temperature of 200°C and He flow rate of $1\ \text{ml min}^{-1}$. Oven temperature was set to 50°C for 4.0 min and then increased to 250°C at a rate of $30^\circ\text{C min}^{-1}$ and held for 9.3 min with a 3.0 min filament delay. The injector volume was set to $1\ \mu\text{l}$ in all cases and the ion range of the mass spectrometer was set to 50 Da to 650 Da.

6.3.2 GC-FID

Reactions involving biphenyl derivatives were monitored using an injector volume of 1 μl set to 250 $^{\circ}\text{C}$ using He as the carrier gas at a flow rate of 1 ml min^{-1} . The oven temperature was set to 50 $^{\circ}\text{C}$ for 5 min then increased at a rate of 10 $^{\circ}\text{C min}^{-1}$ to 250 $^{\circ}\text{C}$ where it was held for a further 5 min.

6.3.3 HPLC

Method A A Jupiter 10 μm C18 300 \AA (4.6 mm \times 250 mm) column manufactured by Phenomenex was used to conduct all analyses at room temperature in isocratic mode using MeCN and water in a 9 : 11 ratio as the mobile phase, delivered at a flow rate of 1.5 ml min^{-1} . Samples were introduced through a 20 μl sample loop.

Method B Analysis was conducted using a 5 μl sample loop at room temperature using a Jupiter 10 μm C18 300 \AA (4.6 mm \times 250 mm) column manufactured by Phenomenex, run in isocratic mode using MeCN and water in a 7 : 3 ratio as the mobile phase delivered at a flow rate of 1.5 ml min^{-1} .

Method C Using a Prodigy 5 μm ODS-2 (4.6 mm \times 250 mm) column, manufactured by Phenomenex, analysis was carried out at room temperature in isocratic mode with MeCN containing 0.1% TFA and water as the mobile phase, delivered in a ratio of 9 : 1 at a flow rate of 2.0 ml min^{-1} . A 20 μl sample loop was used for the analysis of acetamide derivatives and a 5 μl sample loop was used to analyse benzamide derivatives.

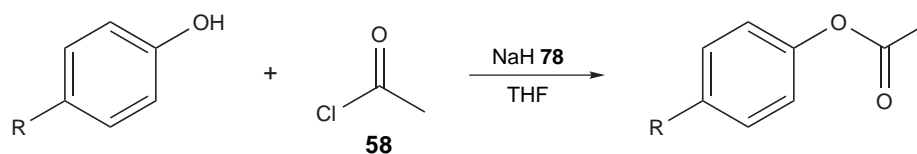
6.4 Batch Procedures

General Procedure 1: Washing NaH

Sodium hydride **78** (~ 2 g, 50.0 mmol) as a 60% dispersion in mineral oil was added to hexane (30.0 ml), the mixture stirred and then the solvent decanted.

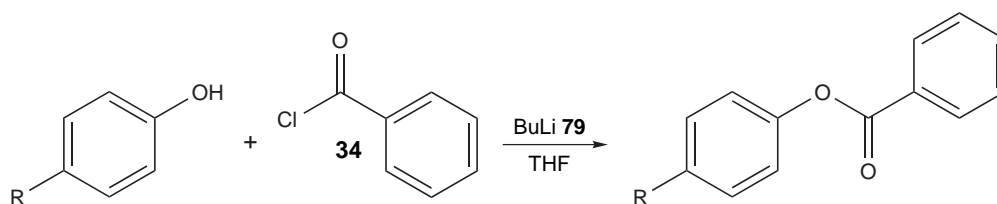
The process was repeated 5 times and the remaining solvent removed *in-vacuo* to afford the dried NaH **78** (typically ~ 1.13 g, 94.2%) which was stored under nitrogen.

General Procedure 2: Acetylation of Phenols



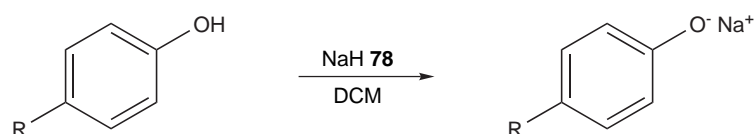
Dried NaH **78** (2.00 eq.) was added with care to a stirred mixture of phenol adduct dissolved in THF (5.0 ml mmol⁻¹). Upon complete addition the mixture was stirred for 15 minutes and acetyl chloride **58** (2.00 eq.) added dropwise. The mixture became hot and was allowed to stir for a further 15 hours. Volatiles were removed *in-vacuo* and the crude product dissolved in DCM (100.0 ml), washed with water (3 \times 50.0 ml) and the organic portion dried over MgSO₄. Filtration and evaporation of the DCM *in-vacuo* afforded the corresponding phenyl acetate derivative.

General Procedure 3: Benzoylation of Phenols



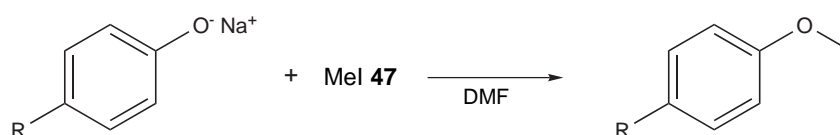
BuLi **79** (1.00 eq.) as a solution in hexanes (2.5 M) was added to a stirred solution of phenol derivative in THF (5.0 ml mmol⁻¹) under nitrogen. Benzoyl chloride **34** (1.05 eq.) was added after 15 min and stirring was continued for a further 3 hr. After this time the solvent was removed *in-vacuo*, DCM (150.0 ml) added and the resulting solution was washed with brine (100.0 ml) and water (3 \times 100.0 ml) before drying over MgSO₄. Filtration and subsequent concentration *in-vacuo* afforded the corresponding phenyl benzoate derivatives which were recrystallised from hot MeOH.

General Procedure 4: Preparation of Sodium Aryloxides



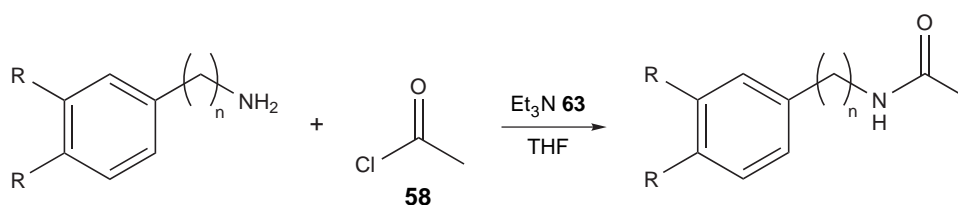
Sodium aryloxides were prepared by the addition of dried NaH **78** (0.24g, 10.0 mmol) to a stirred solution of phenol derivative (10.1 mmol, 1.01 eq.) dissolved in DCM (50.0 ml). Upon precipitation (~ 5 min) filtration and washing with DCM (3 × 50.0 ml) afforded the corresponding sodium aryloxides in excellent yield which was then dried under vacuum prior to storage under nitrogen.

General Procedure 5: Methylation of Phenol Derivatives



MeI **47** (1.10 eq.) was added to a stirred solution of sodium phenoxide derivative in DMF (10.0 ml mmol⁻¹). Stirring was continued for 1 hr after which time water (50.0 ml) was added. The solution was extracted with hexane (3 × 50.0 ml) and the washings combined before further washing with water (2 × 50.0 ml). The organic extract was dried over MgSO₄, filtered and the solvent removed *in-vacuo* to afford the corresponding methoxybenzene derivative.

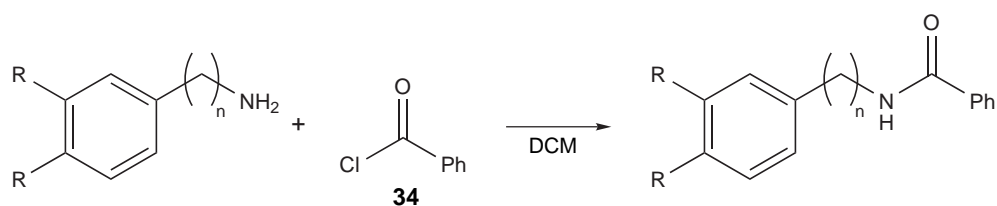
General Procedure 6: Acetylation of Amines



Et₃N **63** (1.00 eq.) was added to a stirred solution of amine dissolved in THF (23.0 ml mmol⁻¹) and after 15 min acetyl chloride **58** (1.10 eq.) was added with care. After 2 hr of continued stirring at room temperature the solvent was removed

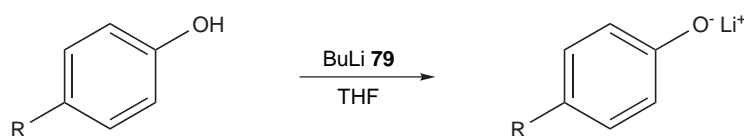
in-vacuo, DCM (150.0 ml) added and the resulting mixture washed with sat. NH_4Cl solution (3×50.0 ml). The organic layer was dried over anhydrous MgSO_4 , filtered and concentrated *in-vacuo*. Subsequent recrystallisation from DCM/hexane or ether/hexane (for aliphatic derivatives) yielded the corresponding amide, confirmed by comparison with data in the literature.

General Procedure 7: Benzoylation of Amines



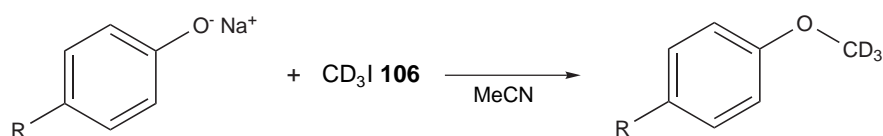
Benzoyl chloride **167** (1.00 eq.) was added to a solution of amine in DCM ($30.0 \text{ ml mmol}^{-1}$) and the mixture was stirred for 2 hr. The resulting ammonium salt precipitate was removed by filtration and organic solvent then removed *in-vacuo*. The remaining residue was recrystallised (DCM/hexane) to afford the corresponding benzamide product.

General Procedure 8: Preparation of Lithium Aryloxides



Lithium aryloxides were prepared as ready to use solutions in the following way; a solution of BuLi **79** (2.50 M in hexanes, 0.4 ml, 1.0 mmol) was added to a solution of phenol derivative (1.0 mmol) in anhydrous THF (9.4 ml) under an inert (N_2) atmosphere. The resulting 0.10 M solution was allowed to stir for 5 min and was used immediately without further treatment or purification.

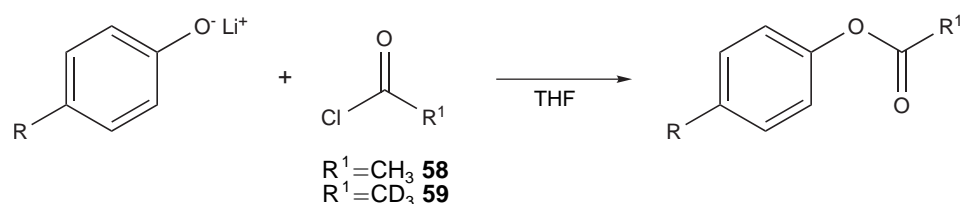
General Procedure 9: Synthesis of Deuterium Labelled Phenyl Ethers



Freshly prepared and dried sodium phenoxide derivative (1.0 mmol) was dissolved in MeCN (50.0 ml) and (D₃)MeI **106** (75 μ l, 1.2 mmol, 1.20 eq.) was added. The mixture was stirred under reflux for 3 hr, the solvent removed *in-vacuo* and the crude product then dissolved in ether (150.0 ml). This was washed with dilute NaOH **100** (3 \times 200.0 ml), dried over MgSO₄, filtered and concentrated *in-vacuo* to afford the corresponding, purified phenyl ether product.

6.5 Micro Reactions

General Procedure 10: Acetylation of Lithium Aryloxides



(a) A solution of lithium phenoxide derivative prepared in THF (0.10 M) was introduced to micro reactor S₃ (Figure 44) through inlet A and acetyl chloride **58** solution (0.10 M, THF) was introduced to inlet B using two 1000 μ l syringes. The resulting product stream was collected from the outlet (C) *via* a 5 cm length of PEEK™ tubing and analysed using HPLC method A by comparison to prepared synthetic standards. The procedure was optimised by evaluating 10 μ l samples over a range of flow rates (20 μ l min⁻¹ to 1 μ l min⁻¹).

(b) Once optimised (D₃)acetyl chloride **59** was employed and with the syringe pump set to a flow rate of 20 μ l min⁻¹ the product stream directed into a flask for sufficient time to obtain \sim 50 mg of product for characterisation. The solvent

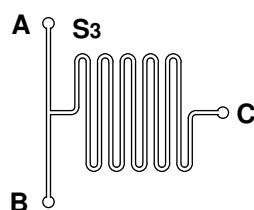
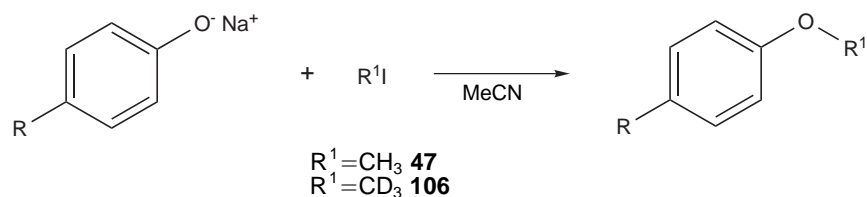


Figure 44. The micro reactor used to synthesise phenyl acetate derivatives.

was then removed *in-vacuo*, the crude product combined with DCM (50.0 ml) which was washed with water (3×50.0 ml), dried over MgSO_4 , filtered and removed *in-vacuo* to afford the corresponding isotopically substituted phenyl acetate derivatives which were analysed without further purification.

General Procedure 11: Methylation of Sodium Aryloxides



(a) Utilising set up $\text{T}_1\text{-R}_\text{T}\text{U}$ (Figure 45) a solution of sodium phenoxide derivative (0.10 M in DMF) was introduced to inlet A of T_1 and a solution of MeI **47** (0.10 M, DMF) into inlet B. The outlet of T_1 was connected *via* a 5 cm length of PEEK™ tubing to the inlet $\text{R}_\text{T}\text{U}$. Heating *via* a hot plate was undertaken by placement of the reactors into a shallow silicon oil bath. The final solution was collected from the outlet (C) of $\text{R}_\text{T}\text{U}$ *via* a 5 cm length of PEEK™ tubing and 10 μl samples were analysed using HPLC by comparison to synthetic standards over a range of flow rates (20 $\mu\text{l min}^{-1}$ to 1 $\mu\text{l min}^{-1}$).

(b) Under optimised conditions (20 $\mu\text{l min}^{-1}$, 100 °C) MeI **47** was employed and the product stream collected for sufficient time to afford ~ 50 mg of product. The micro reactor set up was flushed with water (1.0 ml), acetone (1.0 ml) and DMF (1.0 ml) every 1.5 hr to prevent channel blockages caused by precipitates. Post collection sat. brine solution (50.0 ml) was added and the mixture was

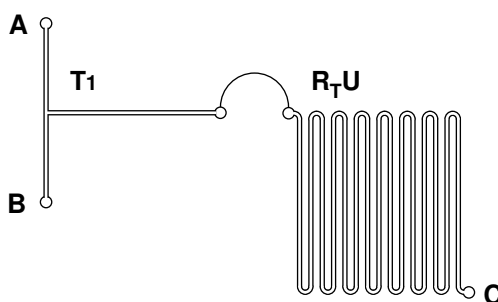
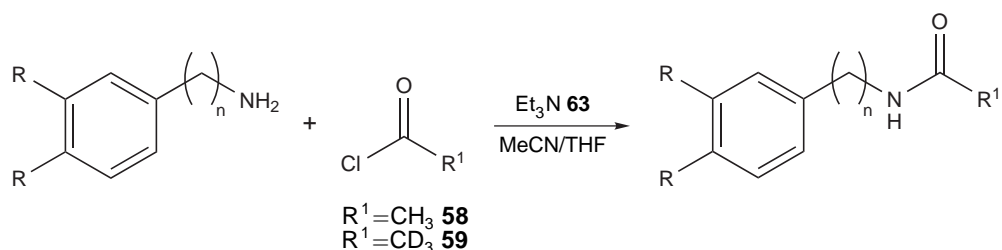


Figure 45. The set up employed in the synthesis of phenyl ethers.

washed with hexane (3×20.0 ml). The combined organic extracts were further washed with water (2×20.0 ml), dried over MgSO_4 and concentrated *in-vacuo* to afford isotopically substituted phenyl acetate derivatives which were analysed without further purification.

General Procedure 12: Acetylation of Amines



(a) Micro reactor set up T_I-T₂ or T_I-S₃ (Figure 46) was used for the preparation of amides by introducing solutions of amine (0.1 M) and Et₃N **63** (0.1 M) in MeCN into micro reactor T_I (inlets A and B). The outlet of this micro reactor was connected *via* a 2.5 cm length of PEEK™ tubing to one inlet of a second micro reactor, either T₂ or S₃, where acetyl chloride **58** was also introduced (inlet C). The resulting product stream was collected from the outlet (D) *via* a further 5 cm length of PEEK™ tubing and 10 μl samples analysed using HPLC by comparison to synthetic standards at a variety of flow rates ($20 \mu\text{l min}^{-1}$ to $1 \mu\text{l min}^{-1}$).

(b) Upon substitution of isotopically unmodified acetyl chloride **58** with its tri-deuterated isotopomer **106** it was necessary to run the system at $20 \mu\text{l min}^{-1}$ for a sufficient amount of time in order to prepare ~ 20 mg of product for characterisation. Post collection the reaction products were concentrated *in-vacuo*,

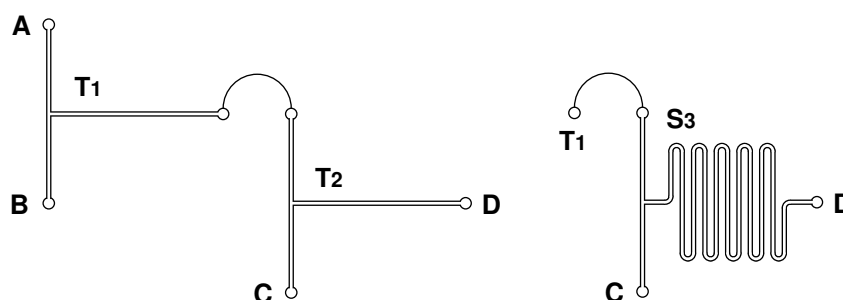
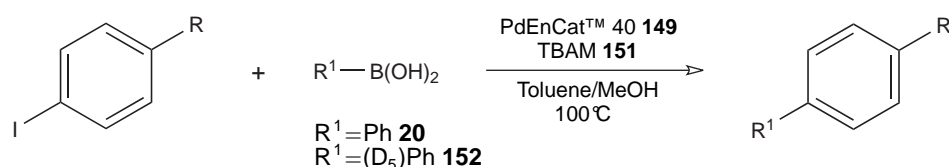


Figure 46. The micro reactor set ups employed to synthesise secondary amides.

dissolved in DCM (25.0 ml) and washed with sat. NH_4Cl solution (3×30.0 ml). Drying over MgSO_4 , filtration, concentration *in-vacuo* and recrystallisation (DCM/hexane) afforded the final product for characterisation.

General Procedure 13: Synthesis of Biphenyl Derivatives



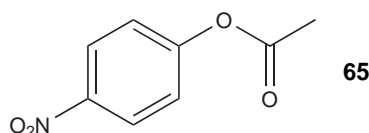
(a) A micro capillary column (3 mm i.d. \times 10 mm length) was packed with Pd EnCat™40 **149** (0.35 g) and secured at the outlet with an Omnifit® connector, containing a small plug of cotton wool. PTFE tubing was attached to the connector allowing for collection from the outlet and the column inlet was interfaced to a syringe *via* another Omnifit® connector and further length of PTFE tubing. A column heater was employed to apply heat to the column, which was held in place by aluminium blocks. The reaction mixture consisted of phenylboronic acid **20**, the iodobenzene derivative and TBAM **151** (0.05 M in 9 : 1 toluene/MeOH) and was infused through the column at flow rates ranging between $200 \mu\text{l min}^{-1}$ and $10 \mu\text{l min}^{-1}$ at temperatures ranging from 70°C to 100°C . In order to optimise the reaction conditions $50 \mu\text{l}$ samples were collected from the reactor outlet and analysed by GC-FID.

(b) The synthesis of deuterium substituted biphenyl derivatives was achieved by substituting phenylboronic acid **20** for its penta-deuterated isotopologue (D_5)phenylboronic acid **152** and operating the set up described above under optimal conditions ($10 \mu\text{l min}^{-1}$, 100°C). The syringe driver was run for the required amount of time to synthesise ~ 20 mg of product, with the column being flushed with a 9 : 1 mixture of toluene/MeOH for a further 60 min post reaction. Following this the reaction solvent was removed *in-vacuo* and the residue dissolved in DCM (50.0 ml), washed with water (3×50.0 ml), dried over MgSO_4 and evaporated to dryness under vacuum. Without any further purification successful synthesis of the resulting product was then confirmed

using conventional analytical techniques.

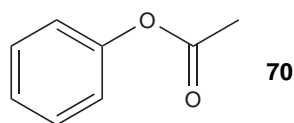
6.6 Preparation of Synthetic Standards

4-Nitrophenyl acetate **65**^{161,162}

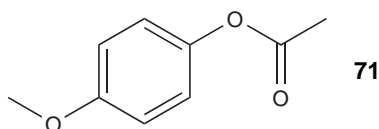


Following general procedure 2, 4-nitrophenol **62** (3.84 g, 27.6 mmol) NaH **78** (1.32 g, 55.2 mmol) and acetyl chloride **58** (3.9 ml, 54.9 mmol) were reacted which, upon recrystallisation (DCM/hexane), formed 4-nitrophenyl acetate **65** (3.04 g, 61%) as faint yellow crystals; mp 78–80°C (lit.,¹⁶¹ 78–79°C); δ_{H} (400 MHz; CDCl₃; TMS) 2.35 (3H, s, CH₃), 7.29 (2H, d, *J* 9.3, 2 × Ar H) and 8.28 (2H, d, *J* 9.3, 2 × Ar H); δ_{C} (100 MHz; CDCl₃; TMS) 21.1 (CH₃), 122.5 (2 × CH), 125.3 (2 × CH), 145.2 (C₀), 155.4 (C₀NO₂) and 168.4 (CO); *m/z* (EI) 182 (M⁺ + 1, 23%), 181 (5), 139 (12), 109 (20) and 43 (100); GC-MS R_T = 9.9 min, HPLC (method A) R_T = 3.5 min.

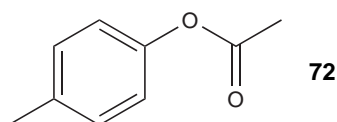
Phenyl acetate **70**^{163,164}



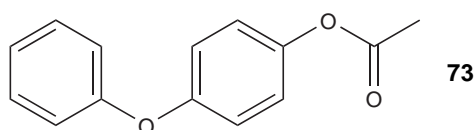
Following general procedure 2, phenol **61** (3.45 g, 36.7 mmol) was reacted with NaH **78** (1.77 g, 73.8 mmol) and acetyl chloride **58** (5.2 ml, 73.1 mmol) to afford phenyl acetate **70** (4.84 g, 97%) as a light yellow oil; δ_{H} (400 MHz; CDCl₃; TMS) 2.29 (3H, s, CH₃), 7.08 (2H, m_u, 2 × Ar H), 7.22 (1H, m_u, Ar H) and 7.37 (2H, m_u, 2 × Ar H); δ_{C} (100 MHz; CDCl₃; TMS) 21.1 (CH₃), 121.6 (2 × CH), 125.8 (CH), 129.4 (2 × CH), 150.7 (C₀) and 169.5 (CO); *m/z* (EI) 137 (M⁺ + 1, 62%), 136 (58), 94 (100), 65 (13) and 43(1); GC-MS R_T = 7.7 min; HPLC (method A) R_T = 4.2 min.

4-Methoxyphenyl acetate **71**^{165,166}

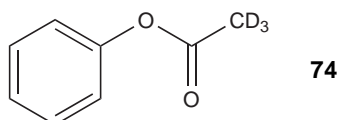
According to general procedure 2, 4-methoxyphenol **67** (3.75 g, 30.2 mmol) was reacted with NaH **78** (1.45 g, 60.4 mmol) and acetyl chloride **58** (4.3 ml, 60.5 mmol) to yield 4-methoxyphenyl acetate **71** (4.47 g, 89%) as a light amber solid; mp 28–29 °C (lit.,¹⁶⁷ 32 °C); δ_{H} (400 MHz; CDCl₃; TMS) 2.28 (3H, s, CH₃), 3.80 (3H, s, OCH₃), 6.89 (2H, d, *J* 9.0, 2 × Ar H) and 7.00 (2H, d, *J* 9.0, 2 × Ar H); δ_{C} (100 MHz; CDCl₃; TMS) 21.1 (CH₃), 55.6 (OCH₃), 114.5 (2 × CH), 122.3 (2 × CH), 144.2 (C₀), 157.3 (C₀) and 169.1 (CO); *m/z* (EI) 167 (M⁺ + 1, 100%), 166 (20), 124 (70), 108 (40) and 95 (2); GC-MS R_T = 9.1 min; HPLC (method A) R_T = 5.8 min.

4-Methylphenyl acetate **72**^{168–170}

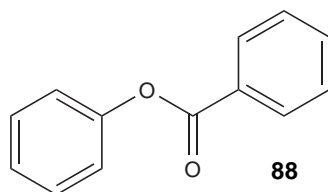
According to general procedure 2 4-methylphenol **68** (3.60 g, 33.3 mmol) was reacted with NaH **78** (1.63 g, 68.0 mmol) and acetyl chloride **58** (4.8 ml, 67.5 mmol) to afford 4-methylphenyl acetate **72** (4.04 g, 81%) as a light yellow oil; δ_{H} (400 MHz; CDCl₃; TMS) 2.28 (3H, s, CH₃), 2.34 (3H, s, CH₃), 6.88 (2H, d, *J* 9.0, 2 × Ar H) and 7.00 (2H, d, *J* 9.0, 2 × Ar H); δ_{C} (100 MHz; CDCl₃; TMS) 20.9 (CH₃), 21.1 (CH₃), 121.3 (2 × CH), 130.0 (2 × CH), 135.5 (C₀), 148.5 (C₀) and 169.8 (CO); *m/z* (EI) 151 (M⁺ + 1, 20%), 150 (13), 108 (100), 80 (13) and 43 (13); GC-MS R_T = 8.4 min; HPLC (method A) R_T = 5.8 min.

4-Phenoxyphenyl acetate **73**

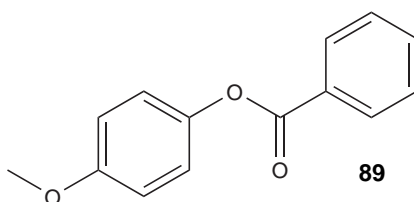
Following general procedure 2 the reaction of 4-phenoxyphenol **69** (4.08 g, 21.9 mmol) with NaH **78** (1.05 g, 43.8 mmol) and acetyl chloride **58** (3.1 ml, 43.8 mmol) was undertaken to afford 4-phenoxyphenyl acetate **73** (3.50 g, 70 %) as a pale yellow oil; Found C, 73.89; H, 5.50 C₁₄H₁₂O₃ requires C, 73.67; H, 5.30 %; ν_{max}/cm^{-1} 3030, 2924, 2864, 1611, 1584, 1510, 1456, 1292, 1254, 1177, 1111, 997, 956, 817 and 703; δ_{H} (400 MHz; CDCl₃; TMS) 2.29 (3H, s, CH₃), 6.93 (2H, m_u, 2 × Ar H), 7.00 (2H, d, *J* 9.0, 2 × Ar H), 7.05 (2H, d, *J* 9.0, 2 × Ar H), 7.11 (1H, m_u, Ar H), 7.34 (2H, m_u, 2 × Ar H); δ_{C} (100 MHz; CDCl₃; TMS) 21.0 (CH₃), 118.8 (2 × CH), 119.5 (2 × CH), 122.7 (2 × CH), 123.4 (CH), 129.8 (2 × CH), 146.0 (C₀), 154.8 (C₀), 157.1 (C₀), 169.6 (CO); *m/z* (EI) 229 (M⁺ + 1, 7 %), 228 (10), 186 (100), 158 (10); GC-MS R_T = 11.3 min; HPLC (method 6.3) R_T = 0. min

Phenyl (D₃)acetate **74**^{171,172}

According to general procedure 10b the micro reactor system was run for 180 min to afford phenyl (D₃)acetate **74** (46 mg, 93 %) as a light yellow oil; δ_{H} (400 MHz; CDCl₃; TMS) 7.00 (2H, m_u, 2 × Ar H), 7.14 (1H, m_u, Ar H) and 7.30 (2H, m_u, 2 × Ar H); δ_{C} (100 MHz; CDCl₃; TMS) 20.4 (CD₃, sep, *J* 20.0), 121.5 (2 × CH), 125.8 (CH), 129.4 (2 × CH), 150.6 (C₀) and 169.4 (CO); *m/z* (EI) 140 (M⁺ + 1, 88 %), 139 (75), 95 (100) and 66 (11); GC-MS R_T = 7.5 min; HPLC (method A) R_T = 4.8 min.

Phenyl benzoate **88**¹⁷³

The reaction of phenol **61** (0.94 g, 10.0 mmol) with BuLi **79** solution (4.0 ml, 2.5 M, 10.0 mmol) and benzoyl chloride **34** (1.2 ml, 10.5 mmol) was carried out according to general procedure 3 which afforded phenyl benzoate **88** (1.03 g, 52 %) as a single, clear cubic crystal; mp 66–68 °C (lit.,¹⁷³ 68–70 °C); δ_{H} (400 MHz; CDCl₃; TMS) 7.23 (2H, m_u, 2 × Ar H), 7.28 (1H, m_u, Ar H), 7.44 (2H, m_u, 2 × Ar H), 7.52 (2H, m_u, 2 × Ar H), 7.64 (1H, m_u, Ar H) and 8.22 (2H, m_u, 2 × Ar H); δ_{C} (100 MHz; CDCl₃; TMS) 121.7 (2 × CH), 125.8 (CH), 128.5 (2 × CH), 129.4 (2 × CH), 129.6 (C₀), 130.1 (2 × CH), 133.5 (CH), 150.9 (C₀) and 165.1 (CO); m/z (EI) 199 (M⁺ + 1, 1%), 198 (2), 106 (23), 105 (100), 94 (10) and 63 (1); GC-MS R_T = 10.2 min; HPLC (method B) R_T = 3.9 min.

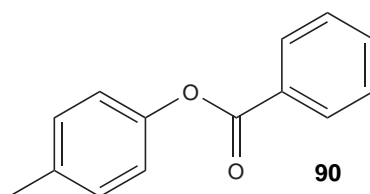
4-Methoxyphenyl benzoate **89**¹⁷⁴

According to general procedure 3, 4-methoxyphenol **67** (1.24 g, 10.0 mmol) was reacted with BuLi **79** solution (4.0 ml, 2.5 M, 10.0 mmol) and benzoyl chloride **34** (1.2 ml, 10.5 mmol) to afford the corresponding product, 4-methoxyphenyl benzoate **89** (1.65 g, 73 %) as fine white needles; mp 85–88 °C (lit.,¹⁷⁵ 87–88 °C); δ_{H} (400 MHz; CDCl₃; TMS) 3.81 (3H, s, OCH₃), 6.93 (2H, d, J 9.0, 2 × Ar H), 7.12 (2H, d, J 9.0, 2 × Ar H), 7.49 (2H, m_u, 2 × Ar H), 7.62 (1H, m_u, Ar H) and 8.19 (2H, m_u, 2 × Ar H); δ_{C} (100 MHz; CDCl₃; TMS) 55.6 (CH₃), 114.5 (2 × CH), 122.4 (2 × CH), 128.5 (2 × CH), 129.6 (C₀), 130.1 (2 × CH), 133.5

6.6 PREPARATION OF SYNTHETIC STANDARDS

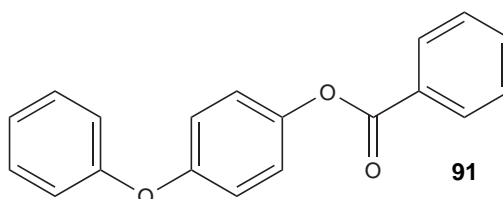
(CH), 144.4 (C₀), 157.3 (C₀) and 165.5 (CO); *m/z* (EI) 229 (M⁺ + 1, 10%), 228 (37), 106 (15), 105 (100), 94 (3) and 63 (1); GC-MS R_T = 11.2 min, HPLC (method B) R_T = 3.8 min.

4-Methylphenyl benzoate **90**¹⁷⁵⁻¹⁷⁷



Following general procedure 3, 4-methylphenol **68** (1.08 g, 10.0 mmol) was reacted with BuLi **79** solution (4.0 ml, 2.5 M, 10.0 mmol) and benzoyl chloride **34** (1.2 ml, 10.5 mmol) to afford 4-methylphenyl benzoate **90** (1.54 g, 73%) as a white crystals; mp 69–71°C (lit.,¹⁷⁵ 71–72°C); δ_{H} (400 MHz; CDCl₃; TMS) 2.38 (3H, s, CH₃), 7.10 (2H, d, *J* 8.4, 2 × Ar H), 7.23 (2H, d, *J* 8.4, 2 × Ar H), 7.51 (2H, m_U, 2 × Ar H), 7.63 (1H, m_U, Ar H) and 8.21 (2H, m_U, Ar H); δ_{C} (100 MHz; CDCl₃; TMS) 20.9 (CH₃), 121.3 (2 × CH), 128.5 (2 × CH), 129.7 (C₀), 130.0 (2 × CH), 130.1 (2 × CH), 1335 (CH), 135.5 (C₀), 148.7 (C₀) and 165.4 (CO); *m/z* (EI) 213 (M⁺ + 1, 10%), 212 (9), 105 (100), 76 (2) and 64 (1); GC-MS R_T = 10.9 min; HPLC (method B) R_T = 4.6 min.

4-Phenoxyphenyl benzoate **91**

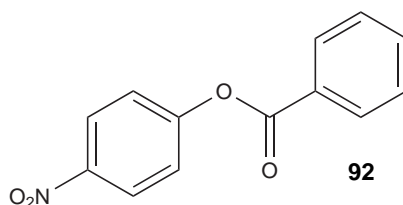


Following general procedure 3, 4-phenoxyphenol **69** (1.86 g, 10.0 mmol), BuLi **79** solution (4.0 ml, 2.5 M, 10.0 mmol) and benzoyl chloride **34** (1.2 ml, 10.5 mmol) were reacted to afford 4-phenoxyphenyl benzoate **91** (1.87 g, 65%) as white needles; mp 96–99°C; Found C, 78.37; H, 4.89 C₁₉H₁₄O₃ requires C, 78.61; H, 4.86%; ν_{max} /cm⁻¹ 3061, 1732, 1589, 1488, 1449, 1263, 1263, 1242, 1184,

6.6 PREPARATION OF SYNTHETIC STANDARDS

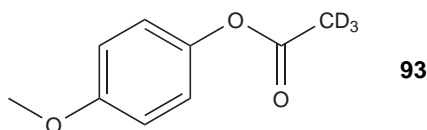
1082, 1061, 1022, 870, 811, 785, 740 and 706; δ_{H} (400 MHz; CDCl_3 ; TMS) 7.05 (2H, m_v, 2 × Ar H), 7.07 (2H, d, *J* 9.0, 2 × Ar H), 7.13 (1H, m_v, Ar H), 7.19 (2H, d, *J* 9.0, 2 × Ar H), 7.36 (2H, m_v, 2 × Ar H), 7.52 (2H, m_v, 2 × Ar H), 7.65 (1H, m_v, Ar H) and 8.22 (2H, m_v, 2 × Ar H); δ_{C} (100 MHz; CDCl_3 ; TMS) 118.8 (2 × CH), 119.6 (2 × CH), 122.8 (2 × CH), 123.4 (CH), 128.6 (2 × CH), 129.4 (C₀), 129.8 (2 × CH), 130.1 (2 × CH), 133.6 (CH), 146.3 (C₀), 154.8 (C₀), 157.2 (C₀) and 165.3 (CO); *m/z* (EI) 291 (M⁺ + 1, 11%), 290 (45), 105 (100) and 63 (1); GC-MS R_T = 15.2 min; HPLC (method B) R_T = 6.3 min.

4-Nitrophenyl benzoate **92**¹⁷⁸



According to general procedure 3, 4-nitrophenol **62** (1.39 g, 10.0 mmol), BuLi **79** solution (4.0 ml, 2.5 M, 10.0 mmol) and benzoyl chloride **34** (1.2 ml, 10.5 mmol) were reacted to afford 4-nitrophenyl benzoate **92** (1.25 g, 52%) as pale yellow crystals; mp 137–138 °C (lit.,¹⁷⁸ 132–133 °C); δ_{H} (400 MHz; CDCl_3 ; TMS) 7.41 (2H, d, *J* 8.8, 2 × Ar H), 7.53 (2H, m_v, 2 × Ar H), 7.67 (1H, m_v, Ar H), 8.19 (2H, m_v, 2 × Ar H) and 8.31 (2H, d, *J* 8.8, 2 × Ar H); δ_{C} (100 MHz; CDCl_3 ; TMS) 122.6 (2 × CH), 125.2 (2 × CH), 128.5 (C₀), 128.8 (2 × CH), 130.3 (2 × CH), 134.2 (CH), 145.4 (C₀), 155.7 (CO) and 164.2 (C₀); *m/z* (EI) 244 (M⁺ + 1, 2%), 243 (1), 105 (100), 77 (8), 63 (6) and 51 (5); GC-MS R_T = 12.6 min; HPLC (method B) R_T = 3.7 min.

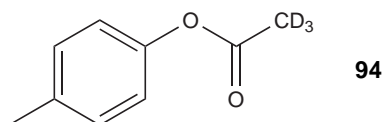
4-Methoxyphenyl (D₃)acetate **93**



6.6 PREPARATION OF SYNTHETIC STANDARDS

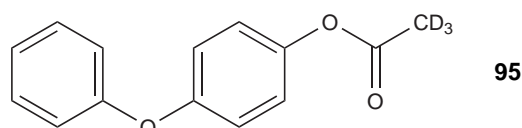
The micro reactor system was run according to general procedure 10b for 148 min to afford 4-methoxyphenyl (D₃)acetate **93** (48 mg, 95 %) as a solid; mp 27–31 °C; Found C, 64.09; H, 6.24 C₉H₇D₃O₃ requires C, 63.89; H, 5.96 %; ν_{max}/cm^{-1} 2955, 2837, 1752, 1507, 1229, 1195, 1061, 1030 and 828; δ_{H} (400 MHz; CDCl₃; TMS) 3.73 (3H, s, OCH₃), 6.86 (2H, d, *J* 9.0, 2 × Ar H) and 6.98 (2H, d, *J* 9.0, 2 × Ar H); δ_{C} (100 MHz; CDCl₃; TMS) 20.2 (CD₃, sep, *J* 19.9), 55.5 (OCH₃), 114.4 (2 × CH), 122.3 (2 × CH), 144.2 (C₀), 157.3 (C₀) and 169.9 (CO); m/z (EI) 170 (M⁺ + 1, 100 %), 169 (29), 125 (37), 95 (2) and 64(4); GC-MS R_T = 8.9 min; HPLC (method A) R_T = 4.4 min.

4-Methylphenyl (D₃)acetate **94**



In accordance with general procedure 10b the micro reactor system was run for 163 min to afford 4-methylphenyl (D₃)acetate **94** (47 mg, 93 %) of light yellow oil; Found C, 70.65; H, 6.67 C₉H₇D₃O₂ requires C, 70.56; H, 6.58 %; ν_{max}/cm^{-1} 3037, 2921, 1757, 1508, 1232, 1198, 1061 and 816; δ_{H} (400 MHz; CDCl₃; TMS) 2.33 (3H, s, CH₃), 6.96 (2H, d, *J* 8.4, 2 × Ar H) and 7.16 (2H, d, *J* 8.4, 2 × Ar H); δ_{C} (100 MHz; CDCl₃; TMS) 18.9 (CD₃, sep, *J* 20.0), 19.3 (CH₃), 119.7 (2 × CH), 128.4 (2 × CH), 133.9 (C₀), 146.9 (C₀) and 168.2 (CO); m/z (EI) 154 (M⁺ + 1, 75 %), 153 (45), 109 (100), 81 (3) and 63 (3); GC-MS R_T = 8.2 min; HPLC (method A) R_T = 5.8 min.

4-Phenoxyphenyl (D₃)acetate **95**

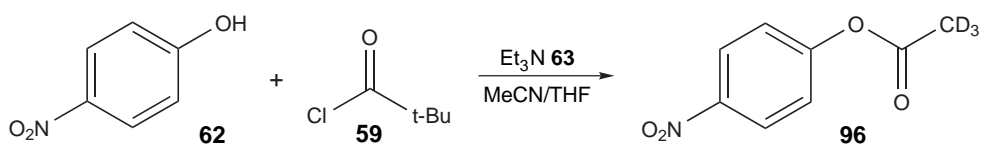


The micro reactor system was run in accordance with general procedure 10b for 108 min to afford 4-phenoxyphenyl (D₃)acetate **95** (48 mg, 96 %) of product as

6.6 PREPARATION OF SYNTHETIC STANDARDS

a faint yellow oil; Found C, 72.92; H, 5.22 $C_{14}H_9D_3O_3$ requires C, 72.71; H, 5.23%; ν_{max}/cm^{-1} 3064, 3045, 1759, 1588, 1499, 1487, 1222, 1184, 1058, 857, 833, 753 and 692; δ_H (400 MHz; $CDCl_3$; TMS) 6.98 (2H, d, J 9.0, $2 \times$ Ar H), 6.99 (2H, m_u, $2 \times$ Ar H), 7.03 (2H, d, J 9.0, $2 \times$ Ar H), 7.07 (1H, m_u, Ar H), 7.31 (2H, m_u, $2 \times$ Ar H); δ_C (100 MHz; $CDCl_3$; TMS) 20.4 (CD_3 , sep, J 20.0), 118.8 ($2 \times$ CH), 119.5 ($2 \times$ CH), 122.7 ($2 \times$ CH), 123.4 (CH), 129.8 ($2 \times$ CH), 146.0 (C_0), 154.8 (C_0), 157.2 (C_0), 169.6 (CO); m/z (EI) 232 ($M^+ + 1$, 35%), 231 (34), 187 (100), 153 (10), 127 (3), 90 (1), 78 (2) and 64 (10); GC-MS $R_T = 11.1$ min; HPLC (method A) $R_T = 12.0$ min.

4-Nitrophenyl (D_3)acetate **96**



Following reaction optimisation with isotopically unmodified acetyl chloride **58** micro reactor set up S1-S2 (Figure 47) was employed to synthesise 4-nitrophenyl (D_3)acetate **96**. Solutions of 4-nitrophenol **62** and Et_3N **63** (0.1M, MeCN) in 500 μ l syringes were introduced to inlets A and B of S1, the outlet of which was connected *via* 5 cm of PEEK™ tubing to the inlet of S2. A solution of (D_3)acetyl chloride **59** (0.05M, THF) was introduced to inlet C from a 1000 μ l syringe and the product stream collected from the outlet (D) of S2 *via* 5 cm of PEEK™ tubing. The set up was run for 272 min and the resulting final solution freed of solvent *in-vacuo*, the residue dissolved in DCM (50.0 ml), washed with water (3×50.0 ml) and dried over $MgSO_4$. Removal of the solvent *in-vacuo* afforded

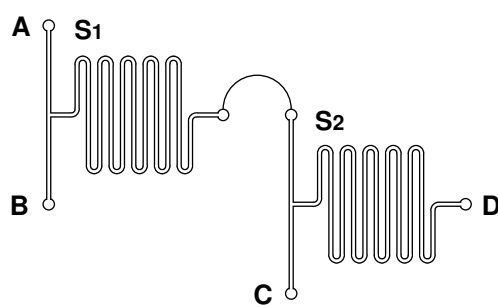
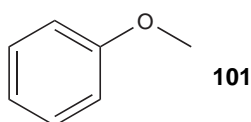


Figure 47. The reactor set up used to synthesise 4-nitrophenyl (D_3)acetate **96**.

6.6 PREPARATION OF SYNTHETIC STANDARDS

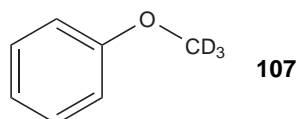
4-nitrophenyl (D₃)acetate **96** (46 mg, 92%) as an off white solid; mp 78–80 °C; Found C, 52.33; H, 3.70; N, 7.50 C₉H₇D₃O₃ Requires C, 52.17; H, 3.83; N, 7.61%; ν_{max}/cm^{-1} 3114, 3886, 1762, 1520, 1347, 1204, 1158, 1060, 743 and 695; δ_{H} (400 MHz; CDCl₃; TMS) 7.20 (2H, d, *J* 9.3, 2 × Ar H) and 8.17 (2H, d, *J* 9.3, 2 × Ar H); δ_{C} (100 MHz; CDCl₃; TMS) 20.3 (CD₃, sep, *J* 20.0), 122.4 (2 × CH), 125.0 (2 × CH), 145.2 (C₀), 155.3 (C₀NO₂) and 168.3 (CO); *m/z* (EI) 185 (M⁺ + 1, 18%), 184 (17), 142 (100), 123 (53), 63 (82) and 46 (49); GC-MS R_T = 9.8 min; HPLC (method A) R_T = 4.6 min.

Methoxybenzene **101**^{179,180}



Following general procedure 5, sodium phenoxide **80** (0.58 g, 5.0 mmol) was reacted with MeI **47** (0.3 ml, 5.5 mmol) to afford methoxybenzene **101** (0.38 g, 70%) as a colourless oil; δ_{H} (400 MHz; CDCl₃; TMS) 3.80 (3H, s, OCH₃), 6.91 (2H, m_v, 2 × Ar H), 6.94 (1H, m_v, Ar H) and 7.29 (2H, m_v, 2 × Ar H); δ_{C} (100 MHz; CDCl₃; TMS) 55.1 (OCH₃), 113.9 (2 × CH), 120.6 (CH), 129.4 (2 × CH) and 159.5 (C₀); *m/z* (EI) 109 (M⁺ + 1, 16%), 108 (100), 91 (1) and 63 (4); GC-MS R_T = 6.4 min; HPLC (method A) R_T = 5.5 min.

(D₃)Methoxybenzene **107**^{181,182}

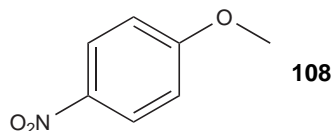


Following general procedure 9, sodium phenoxide **80** (0.12 g, 1.0 mmol) was reacted with (D₃)MeI **106** (75 μl, 1.2 mmol) to afford (D₃)methoxybenzene **107** (79 mg, 71%) as a clear oil; δ_{H} (400 MHz; CDCl₃; TMS) 7.00 (2H, m_v, 2 × Ar H), 7.04 (1H, m_v, Ar H) and 7.38 (2H, m_v, 2 × Ar H); δ_{C} (100 MHz; CDCl₃; TMS) 54.0 (OCD₃, sep, *J* 21.5), 113.7 (2 × CH), 120.5 (CH), 129.3 (2 × CH) and 159.4 (C₀); *m/z* (EI) 112 (M⁺ + 1, 13%), 111 (100) and 63 (2) ;

6.6 PREPARATION OF SYNTHETIC STANDARDS

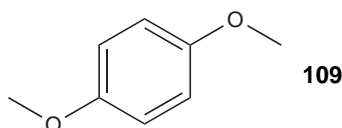
GC-MS $R_T = 6.4$ min; HPLC (method A) $R_T = 5.7$ min.

1-Methoxy-4-nitrobenzene **108**¹⁸³



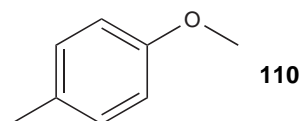
General procedure 5 was followed by reacting sodium 4-nitrophenoxide **102** (0.81 g, 5.0 mol) with MeI **47** (0.3 ml, 5.5 mmol) to afford the product, 1-methoxy-4-nitrobenzene **108** (0.15 g, 19%), as a faint yellow solid; mp 49–51 °C (lit.,¹²⁰ 52–54 °C); δ_H (400 MHz; CDCl₃; TMS) 3.92 (3H, s, OCH₃), 6.96 (2H, d, J 9.3, 2 × Ar H) and 8.22 (2H, d, J 9.3, 2 × Ar H); δ_C (100 MHz; CDCl₃; TMS) 55.9 (OCH₃), 114.0 (2 × CH), 125.9 (2 × CH), 141.6 (C₀) and 164.6 (C₀NO₂); m/z (EI) 154 (M⁺ + 1, 17%), 153 (100), 123 (80), 91 (27) and 63 (30); GC-MS $R_T = 9.4$ min; HPLC (method A) $R_T = 5.4$ min.

1,4-Dimethoxybenzene **109**¹⁸⁴⁻¹⁸⁶



Sodium 4-methoxyphenoxide **103** (0.73 g, 5.0 mmol) was reacted with MeI **47** (0.3 ml, 5.5 mmol) in accordance with general procedure 5 to afford 1,4-dimethoxybenzene **109** (0.49 g, 72%) as a white crystalline solid; mp 51–53 °C (lit.,¹⁸⁷ 49–52 °C); δ_H (400 MHz; CDCl₃; TMS) 3.77 (6H, s, 2 × OCH₃) and 6.84 (4H, s, 4 × Ar H); δ_C (100 MHz; CDCl₃; TMS) 55.7 (2 × OCH₃), 114.7 (4 × CH) and 153.8 (2 × C₀); m/z (EI) 139 (M⁺ + 1, 12%), 138 (100), 95 (22) and 63 (5); GC-MS $R_T = 8.2$ min; HPLC (method A) $R_T = 5.1$ min.

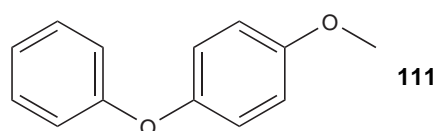
1-Methoxy-4-methylbenzene **110**¹⁸⁸



6.6 PREPARATION OF SYNTHETIC STANDARDS

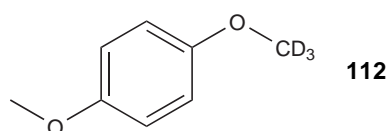
Using general procedure 5, sodium 4-methylphenoxide **104** (0.65 g, 5.0 mmol) and MeI **47** (0.3 ml, 5.5 mmol) were reacted to give 1-methoxy-4-methylbenzene **110** (0.45 g, 73 %) as a colourless oil; δ_{H} (400 MHz; CDCl_3 ; TMS) 2.28 (3H, s, CH_3), 3.76 (3H, s, OCH_3), 6.79 (2H, d, J 8.7, $2 \times \text{Ar H}$) and 7.07 (2H, d, J 8.7, $2 \times \text{Ar H}$); δ_{C} (100 MHz; CDCl_3 ; TMS) 20.4 (CH_3), 55.2 (OCH_3), 113.6 ($2 \times \text{CH}$), 129.8 (C_0), 129.8 ($2 \times \text{CH}$) and 157.4 (C_0); m/z (EI) 123 ($\text{M}^+ + 1$, 14 %), 122 (100), 107 (5), 91 (5), 76 (1) and 63 (2); GC-MS $R_{\text{T}} = 7.2$ min; HPLC (method A) $R_{\text{T}} = 7.7$ min.

1-Methoxy-4-phenoxybenzene **111**¹⁸⁹



According to general procedure 5 the reaction of sodium 4-phenoxyphenoxide **105** (1.04 g, 5.0 mmol) with MeI **47** (3.4 ml, 5.5 mmol) was undertaken to afford 1-methoxy-4-phenoxybenzene **111** (0.86 g, 86 %) as a colourless oil; δ_{H} (400 MHz; CDCl_3 ; TMS) 3.80 (3H, s, OCH_3), 6.88 (2H, d, J 9.0, $2 \times \text{Ar H}$), 6.94 (2H, m_{U} , $2 \times \text{Ar H}$), 6.98 (2H, d, J 9.0, $2 \times \text{Ar H}$), 7.04 (1H, m_{U} , Ar H) and 7.29 (2H, m_{U} , $2 \times \text{Ar H}$); δ_{C} (100 MHz; CDCl_3 ; TMS) 55.6 (OCH_3), 114.8 ($2 \times \text{CH}$), 117.6 ($2 \times \text{CH}$), 120.8 ($2 \times \text{CH}$), 122.4 (CH), 129.6 ($2 \times \text{CH}$), 150.1 (C_0), 155.9 (C_0) and 158.5 (C_0); m/z (EI) 201 ($\text{M}^+ + 1$, 29 %), 200 (100), 185 (27), 171 (1), 129 (12) and 95 (4); GC-MS $R_{\text{T}} = 10.6$ min; HPLC (method A) $R_{\text{T}} = 17.8$ min.

1-(D_3)Methoxy-4-methoxybenzene **112**¹⁹⁰

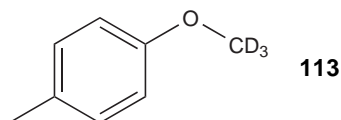


The micro reactor set up described in general procedure 11b was run for 177 min to afford 1-(D_3)-methoxy-4-methoxybenzene **112** (46 mg, 92 %) as a white crystalline solid; mp 52–55 °C; δ_{H} (400 MHz; CDCl_3 ; TMS) 3.68 (3H, s, OCH_3)

6.6 PREPARATION OF SYNTHETIC STANDARDS

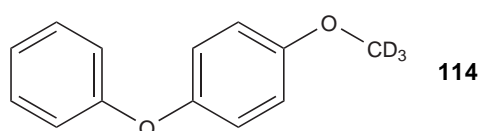
and 6.75 (4H, s, 4 × Ar H); δ_c (100 MHz; CDCl₃; TMS) 54.8 (OCD₃, sep, *J* 21.5), 55.7 (OCH₃), 114.6 (2 × CH), 114.7 (2 × CH) and 153.7 (2 × C₀); *m/z* (EI) 142 (M⁺ + 1, 9%), 141 (100), 95 (6) and 63 (3); GC-MS R_T = 8.2 min; HPLC (method A) R_T = 5.0 min.

1-(D₃)Methoxy-4-methylbenzene **113**¹⁹¹



In accordance with general procedure 9 sodium 4-methylphenoxide **104** (0.13 g, 1.0 mmol) and (D₃)MeI **106** (75 μl, 1.2 mmol) were reacted to afford 1-(D₃)-methoxy-4-methylbenzene **113** (85 mg, 68%) as a clear oil; δ_H (400 MHz; CDCl₃; TMS) 2.30 (3H, s, CH₃), 6.82 (2H, d, *J* 8.4, 2 × Ar H) and 7.10 (2H, d, *J* 8.4, 2 × Ar H); δ_c (100 MHz; CDCl₃; TMS) 19.7 (CH₃), 53.7 (OCD₃, sep, *J* 21.9), 113.0 (2 × CH), 129.1 (C₀), 129.2 (2 × CH) and 156.8 (C₀); *m/z* (EI) 126 (M⁺ + 1, 12%), 125 (100), 107 (5), 87 (4), 76 (2) and 63 (1); GC-MS R_T = 11.0 min; HPLC (method A) R_T = 7.8 min.

1-(D₃)Methoxy-4-phenoxybenzene **114**

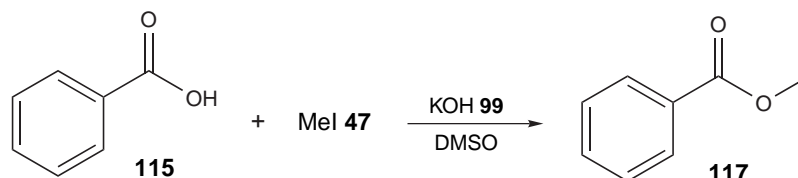


General procedure 11b was followed with the micro reactor set up being run for 123 min to afford 1-(D₃)-methoxy-4-phenoxybenzene **114** (46 mg, 92%) as a clear oil; Found C, 77.04; H, 6.21 C₁₃H₉D₃O₂ requires C, 76.82; H, 5.95%; ν_{max}/cm^{-1} 3042, 1590, 1487, 1293, 1225, 1163, 1109, 995, 957, 870, 840, 758 and 692; δ_H (400 MHz; CDCl₃; TMS) 6.79 (2H, d, *J* 9.3, 2 × Ar H), 6.86 (2H, m_U, 2 × Ar H), 6.90 (2H, d, *J* 9.3, 2 × Ar H), 6.95 (1H, m_U, Ar H) and 7.20 (2H, m_U, 2 × Ar H); δ_c (100 MHz; CDCl₃; TMS) 54.1 (OCD₃, sep, *J* 21.9), 114.1 (2 × CH), 116.9 (2 × CH), 120.1 (2 × CH), 121.7 (CH), 128.9 (2 × CH),

6.6 PREPARATION OF SYNTHETIC STANDARDS

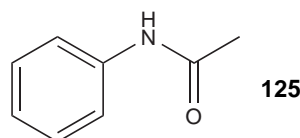
149.4 (C_0), 155.2 (C_0) and 157.8 (C_0); m/z (EI) 204 ($M^+ + 1$, 30%), 203 (100), 149 (2) and 64 (3); GC-MS R_T = 10.5 min; HPLC (method A) R_T = 17.1 min.

Methyl benzoate **117**^{192,193}



Powdered KOH **99** (1.20 eq.) was stirred in DMSO (20 ml) for 20 min and benzoic acid **115** (0.61 g, 5.0 mmol) was then added. Stirring was continued for a further 30 min upon which time MeI **47** (0.6 ml, 10.0 mmol, 2.00 eq.) was added. The reaction flask was covered and after an additional 2 hr stirring water (100.0 ml) was added and the mixture washed with EtOAc (3×20.0 ml). The combined organic extracts were then further washed with water (4×150.0 ml), dried over $MgSO_4$, filtered and removed of solvent *in-vacuo* to afford methyl benzoate **117** (0.47 g, 69%) as a clear oil which was analysed using GC-MS method A and HPLC method A; δ_H (400 MHz; $CDCl_3$; TMS) 3.88 (3H, s, CH_3), 7.40 (2H, m_U , $2 \times Ar H$), 7.51 (1H, m_U , Ar H) and 8.01 (2H, m_U , $2 \times Ar H$); δ_C (100 MHz; $CDCl_3$; TMS) 52.0 (CH_3), 128.2 ($2 \times CH$), 129.4 ($2 \times CH$), 130.0 (C_0), 132.8 (CH) and 167.0 (CO); m/z (EI) 137 ($M^+ + 1$, 45%), 136 (15), 105 (100) and 63 (1); GC-MS R_T = 7.8 min; HPLC (method A) R_T = 4.9 min.

N-Phenylacetamide **125**^{194,195}

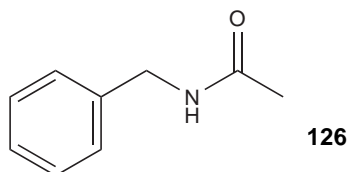


The reaction was carried out in accordance with general procedure 6 using aniline **15** (0.7 ml, 7.4 mmol), Et_3N **63** (1.0 ml, 7.4 mmol) and acetyl chloride **58** (0.6 ml, 8.1 mmol) to give *N*-phenylacetamide **125** (0.27 g, 27%) as a fine white crystalline solid; mp 114–116 °C (lit.,¹⁹⁴ 113–114 °C); δ_H (400 MHz; $CDCl_3$; TMS) 2.18 (3H, s, CH_3), 7.10 (1H, m_U , Ar H), 7.31 (2H, m_U , $2 \times Ar H$), 7.36 (1H, br s,

6.6 PREPARATION OF SYNTHETIC STANDARDS

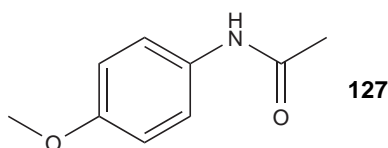
NH) and 7.50 (2H, m_u , $2 \times \text{Ar H}$); δ_c (100 MHz; CDCl_3 ; TMS) 24.6 (CH_3), 119.9 (CH), 124.3 ($2 \times \text{CH}$), 129.0 ($2 \times \text{CH}$), 137.9 (C_0) and 168.3 (CO); m/z (EI) 136 ($\text{M}^+ + 1$, 30%), 135 (84), 93 (100) and 65 (6); GC-MS $R_T = 9.5$ min; HPLC (method C) $R_T = 1.6$ min.

N-(Phenylmethyl)acetamide **126**^{196,197}



According to general procedure 6 phenylmethanamine **55** (0.8 ml, 6.7 mmol), Et_3N **63** (0.9 ml, 6.7 mmol) and acetyl chloride **58** (0.5 ml, 7.4 mmol) were reacted to afford *N*-(phenylmethyl)acetamide **126** (0.13 g, 13%) as white crystals; mp 60–62 °C (lit.,¹⁹⁸ 61–63 °C); δ_H (400 MHz; CDCl_3 ; TMS) 2.02 (3H, s, CH_3), 4.43 (2H, d, J 5.6, CH_2), 5.85 (1H, br s, NH), 7.28 (3H, m_u , $3 \times \text{Ar H}$) and 7.34 (2H, m_u , $2 \times \text{Ar H}$); δ_c (100 MHz; CDCl_3 ; TMS) 23.3 (CH_3), 43.8 (CH_2), 127.5 (CH), 127.9 ($2 \times \text{CH}$), 128.7 ($2 \times \text{CH}$), 138.2 (C_0) and 169.8 (CO); m/z (EI) 150 ($\text{M}^+ + 1$, 100%), 149 (35), 106 (90), 91 (20), 77 (6) and 51 (5); GC-MS $R_T = 9.8$ min; HPLC (method C) $R_T = 1.5$ min.

N-(4-Methoxyphenyl)acetamide **127**¹⁹⁹

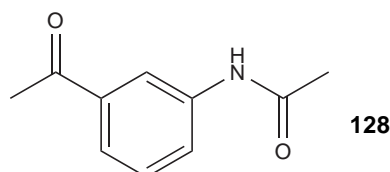


The reaction was carried out in accordance with general procedure 6 using 4-methoxyaniline **122** (0.75 g, 6.1 mmol), Et_3N **63** (0.8 ml, 6.1 mmol) and acetyl chloride **58** (0.5 ml, 6.7 mmol) to afford *N*-(4-methoxyphenyl)acetamide **127** (0.21 g, 21%) as a white crystalline solid; mp 127–128 °C (lit.,¹⁹⁴ 130–130.6 °C); δ_H (400 MHz; CDCl_3 ; TMS) 2.15 (3H, s, CH_3), 3.78 (3H, s, OCH_3), 6.85 (2H, d, J 9.0, $2 \times \text{Ar H}$), 7.19 (1H, br s, NH) and 7.38 (2H, d, J 9.0, $2 \times \text{Ar H}$);

6.6 PREPARATION OF SYNTHETIC STANDARDS

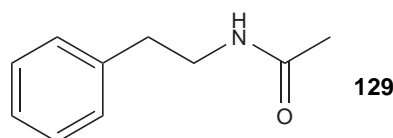
δ_c (100 MHz; CDCl_3 ; TMS) 24.3 (CH_3), 55.5 (CH_3), 114.1 ($2 \times \text{CH}$), 121.9 ($2 \times \text{CH}$), 130.9 (C_0), 156.4 (C_0) and 168.1 (CO); m/z (EI) 166 ($\text{M}^+ + 1$, 100%), 165 (90), 119 (16) and 108 (20); GC-MS $R_T = 10.6$ min; HPLC (method C) $R_T = 1.5$ min.

N-(3-Acetylphenyl)acetamide **128**²⁰⁰



The reaction was carried out in accordance with general procedure 6 using 1-(3-aminophenyl)ethanone **123** (0.76 g, 5.6 mmol), Et_3N **63** (0.8 ml, 5.6 mmol) and acetyl chloride **58** (0.4 ml, 6.2 mmol) to afford *N*-(3-acetylphenyl)acetamide **128** (0.16 g, 16%) as white crystals; mp 127–129°C; δ_H (400 MHz; CDCl_3 ; TMS) 2.22 (3H, s, CH_3), 2.61 (3H, s, CH_3), 7.41 (1H, br s, NH), 7.43 (1H, m_u , Ar H), 7.70 (1H, m_u , Ar H), 7.90 (1H, m_u , Ar H) and 7.99 (1H, m_u , Ar H); δ_c (100 MHz; CDCl_3 ; TMS) 24.6 (CH_3), 26.7 (CH_3), 119.2 (CH), 124.2 (CH), 124.5 (CH), 129.4 (CH), 137.7 (C_0), 138.4 (C_0), 168.5 (CO) and 197.9 (CO); m/z (EI) 178 ($\text{M}^+ + 1$, 48%), 177 (100), 135 (55), 120 (70), 87 (15) and 63 (15); GC-MS $R_T = 8.2$ min; HPLC (method C) $R_T = 1.6$ min.

N,N-(2-Phenylethyl)acetamide **129**¹⁹⁶

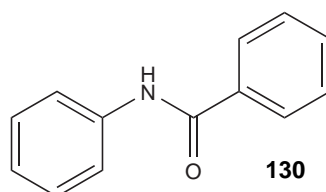


According to general procedure 6 2-phenylethanamine **124** (0.8 ml, 6.1 mmol), Et_3N **63** (0.8 ml, 6.1 mmol) and acetyl chloride **58** (0.5 ml, 6.7 mmol) were reacted to afford *N,N*-(2-phenylethyl)acetamide **129** (0.51 g, 51%) as a white crystalline solid; mp 53–54°C (lit.,²⁰¹ 53.5–54.0°C); δ_H (400 MHz; CDCl_3 ; TMS) 1.93 (3H, s, CH_3), 2.81 (2H, t, J 7.0, CH_2), 3.52 (2H, q, J 7.0, CH_2NH), 5.50

6.6 PREPARATION OF SYNTHETIC STANDARDS

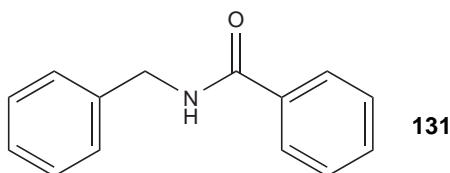
(1H, br s, NH), 7.19 (2H, m_u, 2 × Ar H), 7.24 (1H, m_u, Ar H) and 7.32 (2H, m_u, 2 × Ar H); δ_c (100 MHz; CDCl₃; TMS) 23.3 (CH₃), 35.6 (CH₂), 40.6 (CH₂), 126.5 (CH), 128.6 (2 × CH), 128.7 (2 × CH), 138.8 (C₀) and 170.0 (CO); m/z (EI) 164 (M⁺ + 1, 100%), 163 (24), 104 (37) and 65 (6); GC-MS R_T = 10.1 min; HPLC (method C) R_T = 1.5 min.

N-Phenylbenzamide **130**^{202,203}



The reaction was carried out according to general procedure 7 using aniline **15** (0.5 ml, 5.1 mmol) and benzoyl chloride **34** (0.6 ml, 5.1 mmol) to afford *N*-phenylbenzamide **130** (0.37 g, 37%) as fine white crystals; mp 163–165 °C (lit.,²⁰⁴ 163.0–163.5 °C); δ_H (400 MHz; CDCl₃; TMS) 7.16 (1H, m_u, Ar H), 7.38 (2H, m_u, 2 × Ar H), 7.50 (2H, m_u, 2 × Ar H), 7.56 (1H, m_u, Ar H), 7.65 (2H, m_u, 2 × Ar H), 7.79 (1H, br s, NH) and 7.88 (2H, m_u, 2 × Ar H); δ_c (100 MHz; CDCl₃; TMS) 120.2 (2 × CH), 124.6 (CH), 127.0 (2 × CH), 128.9 (2 × CH), 129.1 (2 × CH), 131.9 (CH), 135.0 (C₀), 137.9 (C₀) and 165.7 (CO); m/z (EI) 198 (M⁺ + 1, 46%), 197 (100), 105 (68) and 51 (4); GC-MS R_T = 11.4 min; HPLC (method C) R_T = 1.8 min.

N-(Phenylmethyl)benzamide **131**²⁰⁵

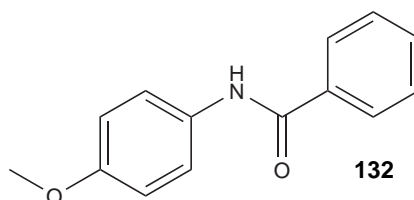


According to general procedure 7 phenylmethanamine **55** (0.5 ml, 4.7 mmol) and benzoyl chloride **34** (0.6 ml, 4.7 mmol) were reacted to afford the product, *N*-(phenylmethyl)benzamide **131** (0.11 g, 11%), as fine white crystals; mp 106–

6.6 PREPARATION OF SYNTHETIC STANDARDS

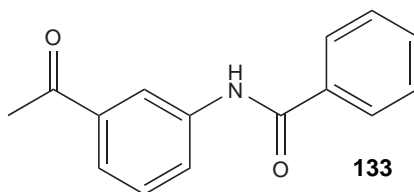
107°C (lit.,²⁰⁶ 106–107°C); δ_{H} (400 MHz; CDCl_3 ; TMS) 4.64 (2H, d, J 6.0, CH_2), 6.46 (1H, br s, NH), 7.31 (1H, m_{U} , Ar H), 7.35 (4H, m_{U} , $4 \times$ Ar H), 7.42 (2H, m_{U} , $2 \times$ Ar H), 7.50 (1H, m_{U} , Ar H) and 7.79 (2H, m_{U} , $2 \times$ Ar H); δ_{C} (100 MHz; CDCl_3 ; TMS) 44.1 (CH_2), 126.9 ($2 \times$ CH), 127.6 (CH), 127.9 ($2 \times$ CH), 128.6 ($2 \times$ CH), 128.8 ($2 \times$ CH), 131.5 (CH), 134.4 (C_0), 138.2 (C_0) and 167.3 (CO); m/z (EI) 212 ($\text{M}^+ + 1$, 26%), 211 (100), 105 (96), 77 (80) and 51 (28); GC-MS $R_{\text{T}} = 12.5$ min; HPLC (method C) $R_{\text{T}} = 1.6$ min.

N-(4-Methoxyphenyl)benzamide **132**^{195,207}



In accordance with general procedure 7 4-methoxyaniline **122** (0.54 g, 4.4 mmol) and benzoyl chloride **34** (0.5 ml, 4.4 mmol) were reacted to afford the product, *N*-(4-methoxyphenyl)benzamide **132** (0.22 g, 22%), as white crystals; mp 160–161°C (lit.,²⁰⁸ 158–160°C); δ_{H} (400 MHz; CDCl_3 ; TMS) 3.81 (3H, s, CH_3), 6.91 (2H, m_{U} , $2 \times$ Ar H), 7.47 (2H, m_{U} , $2 \times$ Ar H), 7.54 (3H, m_{U} , $3 \times$ Ar H), 7.76 (1H, br s, NH) and 7.86 (2H, m_{U} , $2 \times$ Ar H); δ_{C} (100 MHz; CDCl_3 ; TMS) 55.5 (CH_3), 114.2 ($2 \times$ CH), 122.1 ($2 \times$ CH), 127.0 ($2 \times$ CH), 128.7 ($2 \times$ CH), 131.0 (C_0), 131.7 (C_0), 135.0 (CH), 156.6 (C_0) and 165.6 (CO); m/z (EI) 228 ($\text{M}^+ + 1$, 15%), 227 (93), 105 (100), 77 (57) and 51 (19); GC-MS $R_{\text{T}} = 14.1$ min; HPLC (method C) $R_{\text{T}} = 1.7$ min.

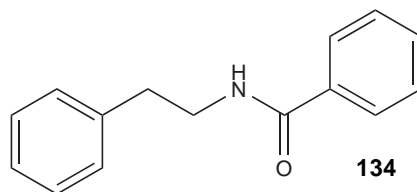
N-(3-Acetylphenyl)benzamide **133**^{200,209}



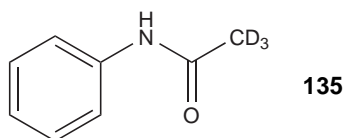
6.6 PREPARATION OF SYNTHETIC STANDARDS

The reaction of 1-(3-aminophenyl)ethanone **123** (0.56 g, 4.2 mmol) with benzoyl chloride **34** (0.5 ml, 4.2 mmol) was carried out according to general procedure 7 to afford *N*-(3-acetylphenyl)benzamide **133** (0.28 g, 28%) as faint pink crystals; mp 110–111 °C (lit.,²¹⁰ 108 °C); δ_{H} (400 MHz; CDCl₃; TMS) 2.61 (3H, s, CH₃), 7.49 (3H, m_U, 3 × Ar H), 7.57 (1H, m_U, Ar H), 7.73 (1H, m_U, Ar H), 7.91 (2H, m_U, 2 × Ar H), 8.07 (1H, m_U, Ar H), 8.17 (1H, m_U, Ar H) and 8.19 (1H, br s, NH); δ_{C} (100 MHz; CDCl₃; TMS) 26.7 (CH₃), 119.6 (CH), 124.4 (CH), 124.8 (CH), 127.1 (2 × CH), 128.8 (2 × CH), 129.4 (CH), 132.1 (CH), 134.6 (C₀), 137.8 (C₀), 138.5 (C₀), 165.9 (CO) and 197.9 (CO); m/z (EI) 240 (M⁺ + 1, 10%), 239 (65), 105 (100), 77 (57) and 51 (15); GC-MS R_T = 15.6 min; HPLC (method C) R_T = 1.7 min.

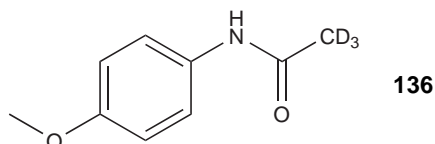
N-(2-Phenylethyl)benzamide **134**^{196,211}



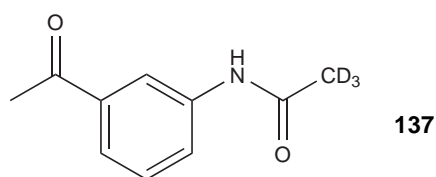
Following general procedure 7, 2-phenylethanamine **124** (0.6 ml, 4.4 mmol) was reacted with benzoyl chloride **34** (0.5 ml, 4.4 mmol) to afford the product, *N*-(2-phenylethyl)benzamide **134** (0.27 g, 27%) as fine white crystals; mp 116–117 °C (lit.,²¹² 116–118 °C); δ_{H} (400 MHz; CDCl₃; TMS) 2.94 (2H, t, *J* 7.0, CH₂), 3.73 (2H, q, *J* 7.0, CH₂NH), 6.15 (1H, br s, NH), 7.25 (3H, m_U, 3 × Ar H), 7.33 (2H, m_U, 2 × Ar H), 7.40 (2H, m_U, 2 × Ar H), 7.48 (1H, m_U, Ar H) and 7.68 (2H, m_U, 2 × Ar H); δ_{C} (100 MHz; CDCl₃; TMS) 35.7 (CH₂), 41.1 (CH₂), 126.6 (CH), 126.8 (2 × CH), 128.5 (2 × CH), 128.7 (2 × CH), 128.8 (2 × CH), 131.4 (CH), 134.7 (C₀), 138.9 (C₀) and 167.4 (CO); m/z (EI) 226 (M⁺ + 1, 10%), 225 (40), 134 (20), 105 (100), 77 (46) and 51 (18); GC-MS R_T = 12.9 min; HPLC (method C) R_T = 1.8 min.

N-Phenyl(D₃)acetamide **135**

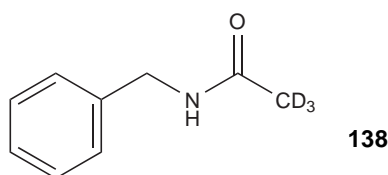
Micro reactor set up Ti-S3 was employed in accordance with general procedure 12 for a total of 145 min to afford *N*-phenyl(D₃)acetamide **135** (18 mg, 92 %) as fine white needles; mp 114–115 °C; Found C, 69.76; H, 6.97; N, 10.11 C₈H₆D₃NO requires C, 69.54; H, 6.57; N, 10.14 %; ν_{max}/cm^{-1} 3300, 3196, 3137, 3080, 1667, 1599, 1434, 1320, 759 and 694; δ_{H} (400 MHz; CDCl₃; TMS) 7.10 (1H, m_u, Ar H), 7.25 (1H, br s, NH), 7.32 (2H, m_u, 2 × Ar H) and 7.50 (2H, m_u, 2 × Ar H); δ_{C} (100 MHz; CDCl₃; TMS) 24.0 (CD₃, sep, *J* 19.5), 119.9 (CH), 124.4 (2 × CH), 129.1 (2 × CH), 137.9 (C₀) and 168.4 (CO); *m/z* (EI) 139 (M⁺ + 1, 30 %), 138 (63), 94 (100) and 65 (7); GC-MS R_T = 9.5 min; HPLC (method C) R_T = 1.6 min.

N-(4-Methoxyphenyl)-(D₃)acetamide **136**

General procedure 12 was followed using micro reactor set up Ti-T2 for 119 min to afford *N*-(4-methoxyphenyl)-(D₃)acetamide **136** (20 mg, 98 %) as a white crystalline solid; mp 128–129 °C; Found C, 64.54; H, 6.70; N, 8.27 C₉H₈D₃NO₂ requires C, 64.26; H, 6.59; N 8.33 %; ν_{max}/cm^{-1} 3266, 2835, 1646, 1605, 1512, 1334, 1246, 1027 and 840; δ_{H} (400 MHz; CDCl₃; TMS) 3.78 (3H, s, OCH₃), 6.83 (2H, d, *J* 9.0, 2 × Ar H), 7.39 (2H, d, *J* 9.0, 2 × Ar H) and 7.65 (1H, br s, NH); δ_{C} (100 MHz; CDCl₃; TMS) 23.5 (CD₃, sep, *J* 19.5), 55.5 (CH₃), 114.1 (2 × CH), 122.0 (2 × CH), 131.0 (C₀), 156.4 (C₀) and 168.6 (CO); *m/z* (EI) 169 (M⁺ + 1, 30 %), 168 (100), 124 (33) and 108 (15); GC-MS R_T = 10.6 min; HPLC (method C) R_T = 1.8 min.

N-(3-Acetylphenyl)-(D₃)acetamide **137**

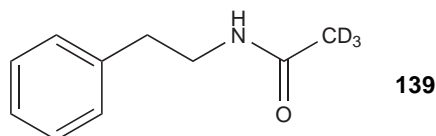
Micro reactor set up T_I-S₃ was run for 111 min according to general procedure 12 to afford *N*-(3-acetylphenyl)-(D₃)acetamide **137** (18 mg, 92%) as white crystals; mp 126–127 °C; Found C, 66.54; H, 6.12; N, 7.95 C₁₀H₈D₃NO₂ requires C, 66.65; H, 6.15; N, 7.77%; ν_{max}/cm^{-1} 3351, 2923, 1672, 1593, 1547, 1432, 1273, 792 and 687; δ_{H} (400 MHz; CDCl₃; TMS) 2.60 (3H, s, CH₃), 7.42 (1H, m_U, Ar H), 7.68 (1H, m_U, Ar H), 7.96 (1H, m_U, Ar H), 7.99 (1H, br s, NH) and 8.02 (1H, m_U, Ar H); δ_{C} (100 MHz; CDCl₃; TMS) 23.8 (CD₃, sep, *J* 19.3), 26.7 (CH₃), 119.2 (CH), 124.1 (CH), 124.6 (CH), 129.3 (CH), 137.6 (C₀), 138.6 (C₀), 168.9 (CO) and 198.1 (CO); m/z (EI) 181 (M⁺ + 1, 75%), 180 (100), 136 (30), 121 (57) and 64 (5); GC-MS R_T = 8.3 min; HPLC (method C) R_T = 1.6 min.

N-(Phenylmethyl)-(D₃)acetamide **138**

General procedure 12 was followed using micro reactor set up T_I-T₂ for 131 min to afford *N*-(phenylmethyl)-(D₃)acetamide **138** (20 mg, 98%) as a white crystalline solid; mp 63–64 °C; Found C, 71.17; H, 7.67; N, 9.15 C₉H₈D₃NO requires C, 71.02; H, 7.28; N, 9.20%; ν_{max}/cm^{-1} 3293, 3087, 2928, 1627, 1552, 1454, 1320, 746 and 694; δ_{H} (400 MHz; CDCl₃; TMS) 4.44 (2H, d, *J* 5.6, CH₂), 5.74 (1H, br s, NH), 7.28 (3H, m_U, 3 × Ar H) and 7.34 (2H, m_U, 2 × Ar H); δ_{C} (100 MHz; CDCl₃; TMS) 22.6 (CD₃, sep, *J* 19.5), 43.8 (CH₂), 127.6 (CH), 127.9 (2 × CH), 128.7 (2 × CH), 138.2 (C₀) and 169.9 (CO); m/z (EI) 153 (M⁺ + 1, 100%), 152 (25) and 107 (45); GC-MS R_T = 9.8 min; HPLC (method

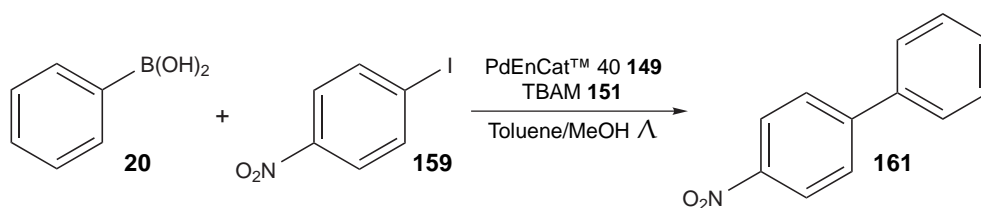
C) $R_T = 1.5$ min.

N-(2-phenylethyl)-(D₃)acetamide **139**



Micro reactor set up T₁-T₂ was run for 120 min in accordance with general procedure 12 to afford *N*-(2-phenylethyl)-(D₃)acetamide **139** (19 mg, 96%) as white needles; mp 53–54 °C; Found C, 72.49; H, 8.33; N, 8.31 C₁₀H₁₀D₃NO requires C, 72.25; H, 7.88; N, 8.43%; ν_{max}/cm^{-1} 3291, 3086, 2930, 1646, 1558, 1451, 1314, 748 and 700; δ_H (400 MHz; CDCl₃; TMS) 2.82 (2H, t, *J* 7.0, CH₂), 3.52 (2H, q, *J* 7.0, CH₂NH), 5.50 (1H, br s, NH), 7.20 (2H, m_u, 2 × Ar H), 7.24 (1H, m_u, Ar H) and 7.32 (2H, m_u, 2 × Ar H); δ_C (100 MHz; CDCl₃; TMS) 22.6 (CD₃, sep, *J* 19.4), 35.6 (CH₂), 40.6 (CH₂), 126.5 (CH), 128.7 (2 × CH), 128.8 (2 × CH), 138.9 (C₀) and 170.1 (CO); *m/z* (EI) 167 (M⁺ + 1, 100%), 166 (30) and 103 (11); GC-MS $R_T = 9.6$ min; HPLC (method C) $R_T = 11.5$ min.

4-Nitrobiphenyl **161**

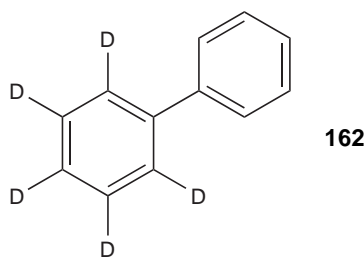


A mixture of phenylboronic acid **20** (0.61 g, 5.0 mmol), 1-iodo-4-nitrobenzene **159** (1.25 g, 5.0 mmol) and TBAM **151** (8.2 ml, 20% in MeOH, 5 mmol) were combined with a 9 : 1 mixture of toluene/MeOH (100 ml). Pd EnCat™ 40 **149** (0.1 g) was added and the mixture held at reflux for 24 hr after which time the volatiles were removed *in-vacuo*. The residue was subsequently dissolved in DCM (150 ml), washed with water (5 × 200 ml), dried over MgSO₄ and evaporated to dryness *in-vacuo*. The resultant crude product was then recrystallised from DCM/hexane to afford the product, 4-nitrobiphenyl **161** (0.55 g, 55%), as an

6.6 PREPARATION OF SYNTHETIC STANDARDS

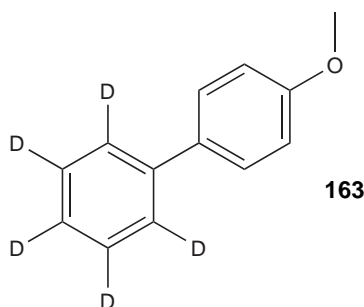
orange crystalline solid; mp 112–114 °C; Found C, 72.61; H, 4.64; N, 6.74 $C_{12}H_9NO_2$ requires C, 72.35; H, 4.55; N 7.03%; ν_{max}/cm^{-1} 1597, 1517, 1350, 854, 740 and 699; δ_H (400 MHz; $CDCl_3$; TMS) 7.60 (3H, m_U, 3 × Ar H), 7.68 (2H, m_U, 2 × Ar H), 7.73 (2H, d, *J* 9.0, 2 × Ar H) and 8.28 (2H, d, *J* 9.0, 2 × Ar H); δ_C (100 MHz; $CDCl_3$; TMS) 124.1 (2 × CH), 127.4 (2 × CH), 127.8 (2 × CH), 129.0 (CH), 129.1 (2 × CH), 138.3 (C_0NO_2), 147.0 (C_0) and 147.8 (C_0); *m/z* (EI) 200 ($M^+ + 1$, 16%), 199 (100), 183 (33), 169 (51), 153 (41), 142 (30), 126 (6), 115 (14), 102 (3), 89 (2), 77 (2) and 63 (3); GC-MS R_T = 11.1 min; GC-FID R_T = 24.0 min.

(D₅)Phenylbenzene **162**^{213,214}



Following general procedure 13 for 250 min using reactor C2 afforded the product, (D₅)phenylbenzene **162** (18 mg, 88%) as white crystals; mp 69–71 °C (lit.,²¹⁴ 63–66 °C); δ_H (400 MHz; $CDCl_3$; TMS) 7.37 (1H, m_U, Ar H), 7.46 (2H, m_U, 2 × Ar H) and 7.63 (2H, m_U, 2 × Ar H); δ_C (100 MHz; $CDCl_3$; TMS) 126.6 (3 × CD, t, *J* 23.8), 127.1 (2 × CH), 127.2 (CH), 128.2 (2 × CD, t, *J* 23.8), 128.7 (2 × CH), 141.0 (C_0) and 141.2 (C_0); *m/z* (EI) 160 ($M^+ + 1$, 14%), 159 (100), 142 (1), 131 (2), 105 (1), 90 (2), 78 (1), and 66 (2); GC-MS R_T = 9.2 min.

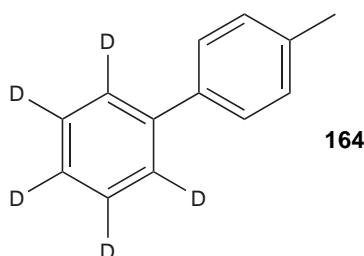
1-Methoxy-4-(D₅)phenylbenzene **163**²¹⁵



6.6 PREPARATION OF SYNTHETIC STANDARDS

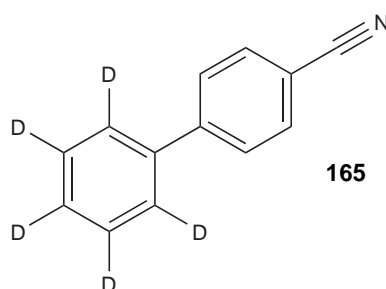
Employing reactor C2 in accordance with general procedure 13 for 211 min afforded 1-methoxy-4-(D₅)phenylbenzene **163** (19 mg, 97 %) as a pale yellow solid; mp 84–85 °C; δ_{H} (400 MHz; CDCl₃; TMS) 3.85 (3H, s, CH₃), 7.00 (2H, d, J 9.0, 2 × Ar H) and 7.55 (2H, d, J 9.0, 2 × Ar H); δ_{C} (100 MHz; CDCl₃; TMS) 55.4 (CH₃), 114.2 (2 × CH), 126.1 (CD, t, J 24.6), 126.3 (2 × CD, J 24.6) 128.1 (2 × CH), 128.2 (2 × CD, J 24.6), 133.8 (C₀), 138.2 (C₀) and 159.2 (C₀); m/z (EI) 190 (M⁺ + 1, 22%), 146 (23), 119 (8), 92 (2) and 65 (2); GC-MS R_T = 10.4 min.

1-Methyl-4-(D₅)phenylbenzene **164**²¹⁵



Reactor C2 was run for 231 min in accordance with general procedure 13 to afford 1-methyl-4-(D₅)phenylbenzene **164** (19 mg, 96 %) as a yellow solid; mp 44–46 °C; δ_{H} (400 MHz; CDCl₃; TMS) 2.32 (3H, s, CH₃), 7.18 (2H, m_v, 2 × Ar H) and 7.42 (2H, m_v, 2 × Ar H); δ_{C} (100 MHz; CDCl₃; TMS) 21.1 (CH₃), 126.4 (CD, t, J 24.1), 126.5 (2 × CD, t, J 24.1), 127.0 (2 × CH), 128.2 (2 × CD, t, J 24.1), 137.0 (C₀), 138.3 (C₀) and 141.0 (C₀); m/z (EI) 174 (M⁺ + 1, 17%), 173 (100), 157 (8), 116 (2), 92 (2) and 65 (1); GC-MS R_T = 9.8 min.

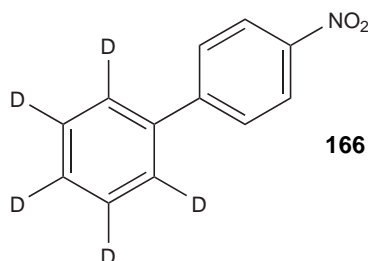
4-(D₅)Phenylbenzotrile **165**



6.6 PREPARATION OF SYNTHETIC STANDARDS

Using reactor C2 general procedure 13 was followed for 217 min to afford 4-(D₅)phenylbenzotrile **165** (18 mg, 91%) as a pale brown crystalline solid; mp 84–86 °C; Found C, 85.58; H, 5.64; N, 7.40 C₁₃H₄D₅N requires C, 84.74; H, 4.92; N 7.60%; ν_{max}/cm^{-1} 3164, 2886, 2170, 1609, 1399, 865, 788, 712 and 540; δ_{H} (400 MHz; CDCl₃; TMS) 7.61 (2H, d, *J* 8.4, 2 × Ar H) and 7.66 (2H, d, *J* 8.4, 2 × Ar H); δ_{C} (100 MHz; CDCl₃; TMS) 110.9 (C₀CN), 118.9 (CN), 126.8 (2 × CD, t, *J* 24.5), 128.3 (CD, t, *J* 24.5), 128.6 (2 × CD, t, *J* 24.5), 132.6 (2 × CH), 138.2 (C₀) and 145.6 (C₀); *m/z* (EI) 185 (M⁺ + 1, 69%), 184 (100), 156 (9), 129 (3), 89 (2) and 65 (3); GC-MS R_T = 10.7 min.

1-Nitro-4-(D₅)phenylbenzene **166**



In accordance with general procedure 13 reactor C2 was run for 196 min to afford 1-nitro-4-(D₅)phenylbenzene **166** (20 mg, 99%) as pale brown crystals; mp 110–112 °C; Found C, 70.68; H, 4.64; N, 6.60 C₁₂H₄D₅NO₂ requires C, 70.57; H, 4.49; N 6.86%; ν_{max}/cm^{-1} 1597, 1511, 1346, 1112, 859, 744, 695, 554 and 448; δ_{H} (400 MHz; CDCl₃; TMS) 7.76 (2H, d, *J* 9.0, 2 × Ar H) and 8.32 (2H, d, *J* 9.0, 2 × Ar H); δ_{C} (100 MHz; CDCl₃; TMS) 124.1 (2 × CH), 126.9 (2 × CD, t, *J* 24.2), 127.8 (2 × CH), 128.4 (CD, t, *J* 24.2), 128.7 (2 × CD, t, *J* 24.2), 138.6 (C₀NO₂), 147.1 (C₀) and 147.6 (C₀); *m/z* (EI) 205 (M⁺ + 1, 17%), 204 (100), 188 (20), 174 (34), 157 (19), 146 (19), 119 (5), 107 (1), 93 (2) and 65 (3); GC-MS R_T = 11.2 min.

REFERENCES

1. R. Van Grieken and M. De Bruin, *Pure Appl. Chem.*, 1994, **66**, 2513–2526, doi:[10.1351/pac199466122513](https://doi.org/10.1351/pac199466122513).
2. S. Okada and N. Momoshima, *Health Phys.*, 1993, **65**, 595–609.
3. International Union of Pure and Applied Physics, *IUPAC Compendium of Chemical Terminology*, <<http://goldbook.iupac.org/I03327.html>>, 2005 (accessed 21st March 2008).
4. P. W. Atkins, *Physical Chemistry*, Oxford University Press, Oxford (UK), 6th edn., 1999.
5. J. M. Brown, *Molecular Spectroscopy*, Oxford University Press Inc., Oxford (UK), 1998.
6. R. R. Wolfe and D. L. Chinkes, *Isotope Tracers in Metabolic Research: Principles and Practice of Kinetic Analysis*, Wiley-VCH, Weinheim (Germany), 2nd edn., 2004.
7. T. A. Baillie, *Pharmacological Reviews*, 1981, **33**, 81–132.
8. H. C. Urey, *Rep. Prog. Phys.*, 1939, **6**, 48–77, doi:[10.1088/0034-4885/6/1/303](https://doi.org/10.1088/0034-4885/6/1/303).
9. G. R. Choppin, J. Rydberg and J.-O. Liljenzin, *Radiochemistry and Nuclear Chemistry*, Butterworth-Heinemann, Woburn (USA), 3rd edn., 2002.
10. A. I. Miller, *Can. Nucl. Soc. Bull.*, 2001, **22**, 1–14.
11. N. A. Matwiyoff, B. B. Mc Inteer and T. R. Mills, *Los Alamos Sci.*, 1983, **4**, 65.
12. N. R. Stevenson, T. S. Bigelow and F. J. Tarallo, *J. Radioanal. Nucl. Chem.*, 2003, **257**, 153–155, doi:[10.1023/A:1024722132332](https://doi.org/10.1023/A:1024722132332).
13. B. Bonnevier, *Plasma Phys.*, 1971, **13**, 763–774, doi:[164](https://doi.org/10.1088/0032-</div><div data-bbox=)

- [1028/13/9/007](#).
14. E. O. Lawrence, in *Nobel Lectures in Physics: 1922–1941*, Elsevier Publishing Company, Amsterdam (Neth.), 1965, vol. 2, pp. 431–443.
 15. A. L. Yergey and A. K. Yergey, *J. Am. Soc. Mass Spectrom.*, 1997, **8**, 943–953, doi:[10.1016/S1044-0305\(97\)00123-2](#).
 16. E. O. Lawrence, *Methods of and apparatus for separating materials*, US Patent: US19440557784 19441009, 1955.
 17. P. Parvin, B. Sajad, K. Silakhori, M. Hooshvar and Z. Zamanipour, *Prog. Nucl. Energy*, 2004, **44**, 331–345, doi:[10.1016/j.pnucene.2004.07.002](#).
 18. I. E. Olivares, A. E. Duarte, E. A. Saravia and F. J. Duarte, *Appl. Opt.*, 2002, **41**, 2973–2977.
 19. E. W. Washburn and H. C. Urey, *Proc. Natl. Acad. Sci. USA*, 1932, **18**, 496–498, doi:[10.1073/pnas.18.7.496](#).
 20. M. P. Malkov, *Atom. Ener.*, 1958, **7**, 613–619, doi:[10.1007/BF01480337](#).
 21. D. Y. Graham and P. D. Klein, *Gastroenterol. Clin. North Am.*, 2000, **29**, 885–893, doi:[10.1016/S0889-8553\(05\)70157-6](#).
 22. D. J. Schlyer, *Annals Acad. Med.*, 2004, **33**, 146–154.
 23. A. K. Paul and H. Abdel-Nabi, *Curr. Med. Imaging Rev.*, 2007, **3**, 178–185, doi:[10.2174/157340507781386997](#).
 24. C. S. Levin, *Eur. J. Nucl. Med. Mol. Imaging*, 2005, **32**, S325–S345, doi:[10.1007/s00259-005-1973-y](#).
 25. U. Scheffel, J. W. Boja and M. J. Kuhar, *Synapse*, 1989, **4**, 390–392.
 26. L. Farde, *Science*, 1986, **231**, 258–261, doi:[10.1126/science.2867601](#).
 27. M. T. Madsen, *J. Nucl. Med.*, 2007, **48**, 661–261, doi:[10.2967/jnumed.106.032680](#).
 28. P. Blower, *Dalton Trans.*, 2006, 1705–1711, doi:[10.1039/b516860k](#).
 29. R. Bentley and J. W. Bennett, *Annu. Rev. Microbiol.*, 1999, **53**, 411–446, doi:[10.1146/annurev.micro.53.1.411](#).
 30. T. J. Simpson, in *Isotopes in the Physical and Biomedical Sciences*, ed. E. Bun- cel and J. R. Jones, Elsevier, Amsterdam (Neth.), 1991, vol. 2, ch. 9, pp. 431–474.
 31. A. J. Birch, R. A. Massey-Westropp and C. J. Moye, *Aust. J. Chem.*, 1955,

- 8**, 539, doi:[10.1071/CH9550539](https://doi.org/10.1071/CH9550539).
32. D. A. Whiting, *Nat. Prod. Rep.*, 2001, **18**, 583–606, doi:[10.1039/b003686m](https://doi.org/10.1039/b003686m).
33. D. S. J. M. Keown, C. M. Nicholas, T. J. Simpson and N. J. Willett, *Chem. Commun.*, 1996, 301–302, doi:[10.1039/CC9960000301](https://doi.org/10.1039/CC9960000301).
34. G. E. Francis, W. Mulligan and A. Wormall, *Isotopic Tracers*, The Athlone Press, London (UK), 1954.
35. N. Lifson, G. B. Gordon, M. B. Visscher and A. O. Nier, *J. Biol. Chem.*, 1949, **180**, 803–811.
36. L. Melander, in *Isotope Effects on Reaction Rates*, ed. B. Crawford Jr., W. D. M. Elroy and C. C. Price, The Ronald Press Company, New York (USA), 1960.
37. M. L. Bender, *J. Am. Chem. Soc.*, 1951, **73**, 1626–1629, doi:[10.1021/ja01148a063](https://doi.org/10.1021/ja01148a063).
38. A. K. Deisingh, *Analyst (Cambridge, UK)*, 2005, **130**, 271–279, doi:[10.1039/b407759h](https://doi.org/10.1039/b407759h).
39. A. Townsend (ed.), *Encyclopedia of Analytical Science*, Academic Press Limited, London (UK), 1995.
40. D. H. Williams and I. Fleming, *Spectroscopic Methods in Organic Chemistry*, M^c Graw Hill, London (UK), 4th edn., 1989.
41. C. J. Jameson, in *Isotopes in the Physical and Biomedical Sciences*, ed. E. Bun- cel and J. R. Jones, Elsevier, Amsterdam (Neth.), 1991, vol. 2, ch. 1, pp. 1–54.
42. R. E. Oosterbroek and A. van den Berg (ed.), *Lab-on-a-Chip Miniaturized Systems for (Bio)Chemical Analysis and Synthesis*, Elsevier, Amsterdam (Neth.), 2003.
43. A. Kirschning, W. Solodenko and K. Mennecke, *Chem. Eur. J.*, 2006, **12**, 5972–5990, doi:[10.1002/chem.200600236](https://doi.org/10.1002/chem.200600236).
44. A. Manz, N. Graber and H. M. Widmer, *Sens. Actuators, B*, 1990, **1**, 244–248, doi:[10.1016/0925-4005\(90\)80209-I](https://doi.org/10.1016/0925-4005(90)80209-I).
45. W. Ehrfeld, V. Hessel and H. Löwe, *Microreactors: New Technology for Modern Chemistry*, Wiley-VCH, Weinheim (Germany), 2000.
46. K. Jähnisch, V. Hessel, H. Löwe and M. Baerns, *Angew. Chem., Int. Ed.*,

- 2004, **43**, 406–446, doi:[10.1002/anie.200300577](https://doi.org/10.1002/anie.200300577).
47. T. M. Creedy, *Anal. Chim. Acta*, 2001, **427**, 39–43, doi:[10.1016/S0003-2670\(00\)01174-0](https://doi.org/10.1016/S0003-2670(00)01174-0).
48. M. A. Roberts, J. S. Rossier, P. Bercier and H. Girault, *Anal. Chem.*, 1997, **69**, 2035–2042, doi:[10.1021/ac961038q](https://doi.org/10.1021/ac961038q).
49. C. G. Khan Malek, *Anal. Bioanal. Chem.*, 2006, **385**, 1351–1361, doi:[10.1007/s00216-006-0514-2](https://doi.org/10.1007/s00216-006-0514-2).
50. X. Li, T. Abe and M. Esashi, *Sens. Actuators, A*, 2001, **87**, 139–145, doi:[10.1016/S0924-4247\(00\)00482-9](https://doi.org/10.1016/S0924-4247(00)00482-9).
51. A. Goyal, V. Hood and S. Tadigadapa, *J. Non-Cryst. Solids*, 2006, **352**, 657–663, doi:[10.1016/j.jnoncrysol.2005.11.063](https://doi.org/10.1016/j.jnoncrysol.2005.11.063).
52. E. Belloy, S. Thurre, E. Walckiers, A. Sarah and M. A. M. Gijs, *Sens. Actuators, A*, 2000, **84**, 330–337, doi:[10.1016/S0924-4247\(00\)00390-3](https://doi.org/10.1016/S0924-4247(00)00390-3).
53. E. Belloy, A. Sayah and M. A. M. Gijs, *Sens. Actuators, A*, 2000, **86**, 231–237, doi:[10.1016/S0924-4247\(00\)00447-7](https://doi.org/10.1016/S0924-4247(00)00447-7).
54. D. Solignac, A. Sayah, S. Constantin, R. Freitag and M. A. M. Gijs, *Sens. Actuators, A*, 2001, **92**, 388–393, doi:[10.1016/S0924-4247\(01\)00577-5](https://doi.org/10.1016/S0924-4247(01)00577-5).
55. D. C. Duffy, J. C. Mc Donald, O. J. A. Schueller and G. M. Whitesides, *Anal. Chem.*, 1998, **70**, 4974–4984, doi:[10.1021/ac980656z](https://doi.org/10.1021/ac980656z).
56. K. Shah, W. C. Shin and R. S. Besser, *Sens. Actuators, B*, 2004, **97**, 157–167, doi:[10.1016/j.snb.2003.08.008](https://doi.org/10.1016/j.snb.2003.08.008).
57. R. Knitter, D. Göhring, P. Risthaus and J. Haußelt, *Microsyst. Technol.*, 2001, **7**, 85–90, doi:[10.1007/s005420100107](https://doi.org/10.1007/s005420100107).
58. R. Knitter and M. A. Liauw, *Lab Chip*, 2004, **4**, 378–383, doi:[10.1039/b403361b](https://doi.org/10.1039/b403361b).
59. W. Ehrfeld and H. Lehr, *Radiat. Phys. Chem.*, 1995, **45**, 349–365, doi:[10.1016/0969-806X\(93\)E0007-R](https://doi.org/10.1016/0969-806X(93)E0007-R).
60. E. W. Becker, W. Ehrfeld, P. Hagmann, A. Maner and D. Münchmeyer, *Microelectron. Eng.*, 1986, **4**, 35–56, doi:[10.1016/0167-9317\(86\)90004-3](https://doi.org/10.1016/0167-9317(86)90004-3).
61. Y. Tanaka, K. Sato, T. Shimizu, M. Yamato, T. Okano and T. Kitamori, *Lab Chip*, 2007, **7**, 207–212, doi:[10.1039/b612082b](https://doi.org/10.1039/b612082b).
62. Z. Yin and A. Prosperetti, *J. Micromech. Microeng.*, 2005, **15**, 643–651,

- doi:[10.1088/0960-1317/15/3/028](https://doi.org/10.1088/0960-1317/15/3/028).
63. M. Zimmermann, H. Schmid, P. Hunziker and E. Delamarche, *Lab Chip*, 2007, **7**, 119–125, doi:[10.1039/b609813d](https://doi.org/10.1039/b609813d).
64. Y. Hiratsuka, M. Miyata, T. Tada and T. Q. P. Uyeda, *Proc. Natl. Acad. Sci. USA*, 2006, **103**, 13618–13623, doi:[10.1073/pnas.0604122103](https://doi.org/10.1073/pnas.0604122103).
65. P. D. I. Fletcher, S. J. Haswell and V. N. Paunov, *Analyst*, 1999, **124**, 1273–1282, doi:[10.1039/a903624e](https://doi.org/10.1039/a903624e).
66. P. D. I. Fletcher, S. J. Haswell, E. Pombo-Villar, B. H. Warrington, P. Watts, S. Y. F. Wong and X. Zhang, *Tetrahedron*, 2002, **58**, 4735–4757, doi:[10.1016/S0040-4020\(02\)00432-5](https://doi.org/10.1016/S0040-4020(02)00432-5).
67. C. Schwer and E. Kenndler, *Anal. Chem.*, 1991, **63**, 1801–1807, doi:[10.1016/S0021-9673\(98\)00794-8](https://doi.org/10.1016/S0021-9673(98)00794-8).
68. V. George, P. Watts, S. J. Haswell and E. Pombo-Villar, *Chem. Commun.*, 2003, 2886–2887, doi:[10.1039/b310744b](https://doi.org/10.1039/b310744b).
69. P. D. Christensen, S. W. P. Johnson, T. M. Creedy, V. Skelton and N. G. Wilson, *Anal. Commun.*, 1998, **35**, 317–348, doi:[10.1039/a806928j](https://doi.org/10.1039/a806928j).
70. P. D. I. Fletcher, S. J. Haswell and X. Zhang, *Lab Chip*, 2001, **1**, 115–121, doi:[10.1039/b106339c](https://doi.org/10.1039/b106339c).
71. K. Seller, Z. H. Fan, K. Fluri and D. J. Harrison, *Anal. Chem.*, 1994, **66**, 3485–3491, doi:[10.1021/ac00092a029](https://doi.org/10.1021/ac00092a029).
72. D. R. Lide and H. P. R. Frederikse (ed.), *CRC Handbook of Chemistry and Physics*, CRC Press Inc., Boca Raton (USA), 72nd edn., 1991–1992.
73. D. Gobby, P. Angeli and A. Gavriilidis, *J. Micromech. Microeng.*, 2001, **11**, 126–132, doi:[10.1088/0960-1317/11/2/307](https://doi.org/10.1088/0960-1317/11/2/307).
74. F. G. Bessoth, A. J. deMello and A. Manz, *Anal. Commun.*, 1999, **36**, 213–215, doi:[10.1039/a902237f](https://doi.org/10.1039/a902237f).
75. H. Salimi-Moosavi, T. Tang and D. J. Harrison, *J. Am. Chem. Soc.*, 1997, **119**, 8716–8717, doi:[10.1021/ja971735f](https://doi.org/10.1021/ja971735f).
76. R. C. R. Wootton, R. Fortt and A. J. de Mello, *Lab Chip*, 2002, **2**, 5–7, doi:[10.1039/b111286d](https://doi.org/10.1039/b111286d).
77. R. Fortt, R. C. R. Wootton and A. J. de Mello, *Org. Process Res. Dev.*, 2003, **7**, 762–768, doi:[10.1021/op025586j](https://doi.org/10.1021/op025586j).

78. G. M. Greenway, S. J. Haswell, D. O. Morgan, V. Skelton and P. Styring, *Sens. Actuators, B*, 2000, **63**, 153–158, doi:[10.1016/S0925-4005\(00\)00352-X](https://doi.org/10.1016/S0925-4005(00)00352-X).
79. T. Schwalbe, D. Kadzimirsz and G. Jas, *QSAR Comb. Sci.*, 2005, **24**, 758–768, doi:[10.1002/qsar.200540005](https://doi.org/10.1002/qsar.200540005).
80. I. R. Baxendale, J. Deeley, C. M. Griffiths-Jones, S. V. Ley, S. Saaby and G. K. Tranmer, *Chem. Commun.*, 2007, 2566–2568, doi:[10.1039/b600382f](https://doi.org/10.1039/b600382f).
81. H. R. Sahoo, J. G. Kralj, and K. F. Jensen, *Angew. Chem., Int. Ed.*, 2007, **46**, 5704–5708, doi:[10.1002/anie.200701434](https://doi.org/10.1002/anie.200701434).
82. T. Curtius, *Chem. Ber.*, 1890, **23**, 3023–3033, doi:[10.1002/cber.189002302232](https://doi.org/10.1002/cber.189002302232).
83. O. Flögel, J. D. C. Codée, D. Seebach and P. H. Seeberger, *Angew. Chem., Int. Ed.*, 2006, **45**, 7000–7003, doi:[10.1002/anie.200602167](https://doi.org/10.1002/anie.200602167).
84. R. D. Chambers, M. A. Fox, D. Holling, T. Nakano, T. Okazoe and G. Sandford, *Lab Chip*, 2005, **5**, 191–198, doi:[10.1039/b416400h](https://doi.org/10.1039/b416400h).
85. R. D. Chambers, M. A. Fox and G. Sandford, *Lab Chip*, 2005, **5**, 1132–1139, doi:[10.1039/b504675k](https://doi.org/10.1039/b504675k).
86. K. Tanaka, S. Motomatsu, K. Koyama, S.-I. Tanaka and K. Fukase, *Org. Lett.*, 2007, **9**, 299–302, doi:[10.1021/ol062777o](https://doi.org/10.1021/ol062777o).
87. F. Brady, S. K. Luthra, J. M. Gillies and N. T. Jeffery, *Use of microfabricated devices*, US Patent: US02267761A1, 2005.
88. S.-Y. Lu, P. Watts, F. T. Chin, J. Hong, J. L. Musachio, E. Briard and V. W. Pike, *Lab Chip*, 2004, **4**, 523–525, doi:[10.1039/b407938h](https://doi.org/10.1039/b407938h).
89. J. M. Gillies, C. Prenant, G. N. Chimon, G. J. Smethurst, W. Perrie, I. Hamblett, B. Dekker and J. Zweit, *Appl. Radiat. Isot.*, 2006, **64**, 325–332, doi:[10.1016/j.apradiso.2005.08.007](https://doi.org/10.1016/j.apradiso.2005.08.007).
90. J. M. Gillies, C. Prenant, G. N. Chimon, G. J. Smethurst, B. A. Dekker and J. Zweit, *Appl. Radiat. Isot.*, 2006, **64**, 333–336, doi:[10.1016/j.apradiso.2005.08.009](https://doi.org/10.1016/j.apradiso.2005.08.009).
91. C.-C. Lee, G. Sui, A. Elizarov, C. J. Shu, Y.-S. Shin, A. N. Dooley, J. Huang, A. Daridona, P. Wyatt, D. Stout, H. C. Kolb, O. N. Witte,

- N. Satyamurthy, J. R. Heath, M. E. Phelps, S. R. Quake and H.-R. Tseng, *Science*, 2005, **310**, 1793–1796, doi:[10.1126/science.1118919](https://doi.org/10.1126/science.1118919).
92. P. W. Miller, N. J. Long, A. J. de Mello, R. Vilar, H. Audrain, D. Bender, J. Passchier and A. Gee, *Angew. Chem., Int. Ed.*, 2007, **46**, 2875–2878, doi:[10.1002/anie.200604541](https://doi.org/10.1002/anie.200604541).
93. Z. Rappoport (ed.), *The Chemistry of Phenols*, Wiley-VCH, Chichester (UK), 2003.
94. M. B. Smith and J. March, *March's Advanced Organic Chemistry Reactions, Mechanisms, and Structure*, Wiley-VCH, Toronto (Canada), 5th edn., 2001.
95. J. Otera, *Esterification*, Wiley-VCH, Weinheim (Germany), 2003.
96. T. W. Greene, *Greene's Protective Groups in Organic Synthesis*, John Wiley & Sons, Inc., Hoboken (USA), 4th edn., 2007.
97. E. Fischer and A. Speier, *Ber. Dtsch. Chem. Ges.*, 1895, **28**, 3252–3258, doi:[10.1002/cber.189502803176](https://doi.org/10.1002/cber.189502803176).
98. E. W. Dean and D. D. Stark, *Ind. Eng. Chem.*, 1920, **12**, 486–490, doi:[10.1021/ie50125a025](https://doi.org/10.1021/ie50125a025).
99. S. S. Pizey, *Synthetic Reagents, Vol. 1*, Ellis Horwood Ltd. Chichester (UK), 1974.
100. H. Seçen and A. H. Kaplar, *Turk. J. Chem.*, 1999, **23**, 27–30.
101. M. A. Bigdeli, M. M. Heravi and N. Nahid, *Iran. J. Chem. Chem. Eng.*, 2000, **19**, 37–39.
102. S. Velusamy, S. Borpuzari and T. Punniyamurthy, *Tetrahedron*, 2005, **61**, 2011–2015, doi:[10.1016/j.tet.2005.01.006](https://doi.org/10.1016/j.tet.2005.01.006).
103. M. M. Heravi, M. Bolourtchian, L. Nakhshab and R. Zadmand, *Phosphorus, Sulfur Silicon Relat. Elem.*, 2002, **177**, 2295–2297, doi:[10.1080/10426500214120](https://doi.org/10.1080/10426500214120).
104. V. K. Yadav, K. G. Babu and M. Mittal, *Tetrahedron*, 2001, **57**, 7047–7051, doi:[10.1016/S0040-4020\(01\)00677-9](https://doi.org/10.1016/S0040-4020(01)00677-9).
105. M. H. Sarvari and H. Sharghi, *Tetrahedron*, 2005, **61**, 10903–10907, doi:[10.1016/j.tet.2005.09.002](https://doi.org/10.1016/j.tet.2005.09.002).
106. H.-P. Zhu, F. Yang, J. Tang and M.-Y. He, *Green Chem.*, 2003, **5**, 38–39, doi:[10.1039/b209248b](https://doi.org/10.1039/b209248b).

107. S. Xu, I. Held, B. Kempf, H. Mayr, W. Steglich and H. Zipse, *Chem. Eur. J.*, 2005, **11**, 4751–4757, doi:[10.1002/chem.200500398](https://doi.org/10.1002/chem.200500398).
108. J. Clayden, N. Greeves, S. Warren and P. Wothers, *Organic Chemistry*, Oxford University Press, Oxford (UK), 2001.
109. C. Wiles, P. Watts, S. J. Haswell and E. Pombo-Villar, *Tetrahedron*, 2003, **59**, 10173–10179, doi:[10.1016/j.tet.2003.10.069](https://doi.org/10.1016/j.tet.2003.10.069).
110. D. R. Lide and H. P. R. Frederikse (ed.), *CRC Handbook of Chemistry and Physics*, CRC Press Inc., Boca Raton (USA), 76th edn., 1995.
111. C. Wiles, Ph.D. thesis, The University of Hull, 2003.
112. E. F. V. Scriven, *Chem. Soc. Rev.*, 1983, **12**, 129–161, doi:[10.1039/CS9831200129](https://doi.org/10.1039/CS9831200129).
113. R. Murugan and E. F. V. Scriven, *Aldrichimica Acta*, 2003, **36**, 21–27.
114. A. C. Spivey and S. Arseniyadis, *Angew. Chem., Int. Ed.*, 2004, **43**, 5436–5441, doi:[10.1002/anie.200460373](https://doi.org/10.1002/anie.200460373).
115. R. Schwesinger, J. Willaredt, H. Schlemper, M. Keller, D. Schmitt and H. Fritz, *Chem. Ber.*, 1994, **127**, 2435–2454, doi:[10.1002/cber.19941271215](https://doi.org/10.1002/cber.19941271215).
116. H. B. Bürgi, J. D. Dunitz, J. M. Lehn and G. Wipff, *Tetrahedron*, 1974, **30**, 1563–1572, doi:[10.1016/S0040-4020\(01\)90678-7](https://doi.org/10.1016/S0040-4020(01)90678-7).
117. T. Ando, J. Yamawaki, T. Kawante, S. Sumi and T. Hanafusa, *Bull. Chem. Soc. Jpn.*, 1982, **55**, 2504–2507, doi:[10.1246/bcsj.55.2504](https://doi.org/10.1246/bcsj.55.2504).
118. J. C. Lee, J. Y. Yuk and S. H. Cho, *Synth. Commun.*, 1995, **25**, 1367–1370, doi:[10.1080/00397919508013838](https://doi.org/10.1080/00397919508013838).
119. R. A. W. Johnstone and M. E. Rose, *Tetrahedron*, 1979, **35**, 2169–2173, doi:[10.1016/0040-4020\(79\)87035-0](https://doi.org/10.1016/0040-4020(79)87035-0).
120. N. J. Hales, H. Heaney, J. H. Hollinshead and S. V. Ley, *Tetrahedron*, 1995, **51**, 7741–7754, doi:[10.1016/0040-4020\(95\)00394-N](https://doi.org/10.1016/0040-4020(95)00394-N).
121. J. M. Miller, K. H. So and J. H. Clark, *Can. J. Chem.*, 1979, **57**, 1887–1889, doi:[10.1139/CJC-57-14-1887](https://doi.org/10.1139/CJC-57-14-1887).
122. T. Ando, J. H. Clark, D. G. Cork, T. Hanafusa, J. Ichihara and T. Kimura, *Tetrahedron Lett.*, 1987, **28**, 1421–1424, doi:[10.1016/S0040-4039\(00\)95943-4](https://doi.org/10.1016/S0040-4039(00)95943-4).

123. A. R. MacKenzie, C. J. Moody and C. W. Rees, *Tetrahedron*, 1986, **42**, 3259–3268, doi:[10.1016/S0040-4020\(01\)87390-7](https://doi.org/10.1016/S0040-4020(01)87390-7).
124. C. Wiles, P. Watts, S. J. Haswell and E. Pombo-Villar, *Tetrahedron*, 2005, **61**, 10757–10773, doi:[10.1016/j.tet.2005.08.076](https://doi.org/10.1016/j.tet.2005.08.076).
125. J. Burgess, *Metal Ions in Solution*, Ellis Horwood, New York (USA), 1978.
126. L. I. Kruse, C. W. DeBrosse and C. H. Kruse, *J. Am. Chem. Soc.*, 1985, **107**, 5435–5442, doi:[10.1021/ja00305a018](https://doi.org/10.1021/ja00305a018).
127. M. J. Adam, S. Jivan, J. M. Huser and J. Lu, *Radiochim. Acta*, 2000, **88**, 207–209, doi:[10.1524/ract.2000.88.3-4.207](https://doi.org/10.1524/ract.2000.88.3-4.207).
128. H. Benveniste, J. S. Fowler, W. Rooney, Y.-S. Ding, A. L. Baumann, D. H. Moller, C. Du, W. Backus, J. Logan, P. Carter, J. D. Coplan, A. Biegon, L. Rosenblum, B. Scharf, J. S. Gately and N. D. Volkow, *J. Nuc. Med.*, 2005, **46**, 312–320.
129. D. P. Cox, J. Terpinski and W. Lawrynowicz, *J. Org. Chem.*, 1984, **49**, 3216–3219, doi:[10.1021/jo00191a035](https://doi.org/10.1021/jo00191a035).
130. A. Hassner and V. Alexanian, *Tetrahedron Lett.*, 1978, **19**, 4475–4478, doi:[10.1016/S0040-4039\(01\)95256-6](https://doi.org/10.1016/S0040-4039(01)95256-6).
131. M. C. Wani, H. L. Taylor, M. E. Wall, P. Coggon and A. T. M. Phail, *J. Am. Chem. Soc.*, 1971, **93**, 2325–2327, doi:[10.1021/ja00738a045](https://doi.org/10.1021/ja00738a045).
132. M. D. de Jong, T. T. Thanh, T. H. Khanh, V. M. Hien, G. J. Smith, N. V. Chau, B. V. Cam, P. T. Qui, D. Q. Ha, Y. Guan, J. M. Peiris, T. T. Hien and J. Farrar, *New Eng. J. Med.*, 2005, **353**, 2667–2672.
133. O. Itsenko, T. Kihlberg and B. Långström, *J. Org. Chem.*, 2004, **69**, 4356–4360, doi:[10.1021/jo049934m](https://doi.org/10.1021/jo049934m).
134. E. A. Almeida, C. F. Klitzke, G. R. Martinez, M. H. G. Medeiros and P. D. Mascio, *J. Pineal Res.*, 2004, **36**, 64–71, doi:[10.1046/j.1600-079X.2003.00098.x](https://doi.org/10.1046/j.1600-079X.2003.00098.x).
135. J. Courty, B. Cornelissen, R. Oltenfreiter, M. Vandecapelle, G. Slegers and K. Strijckmans, *Nucl. Med. Biol.*, 2004, **31**, 649–654, doi:[10.1016/j.nucmedbio.2003.11.001](https://doi.org/10.1016/j.nucmedbio.2003.11.001).
136. V. P. Shevchenko, I. Y. Nagaev and N. F. Myasoedov, *Radiochemistry*, 2004, **46**, 72–77, doi:[10.1023/B:RACH.0000024641.49263.14](https://doi.org/10.1023/B:RACH.0000024641.49263.14).

137. C. Schotten, *Chem. Ber.*, 1884, **17**, 2544–2547, doi:[10.1002/cber.188401702178](https://doi.org/10.1002/cber.188401702178).
138. E. Baumann, *Chem. Ber.*, 1886, **19**, 3218–3222, doi:[10.1002/cber.188601902348](https://doi.org/10.1002/cber.188601902348).
139. K. F. Schmidt, *Chem. Ber.*, 1924, **57**, 704–706, doi:[10.1002/cber.19240570423](https://doi.org/10.1002/cber.19240570423).
140. I. Ugi, R. Meyr, U. Fetzer and C. Steinbrückner, *Angew. Chem.*, 1959, **71**, 386, doi:[10.1002/ange.19590711110](https://doi.org/10.1002/ange.19590711110).
141. M. F. Bodroux, *Bull. Soc. Chim. Fra.*, 1905, **33**, 831–835.
142. A. W. Chapman, *J. Chem. Soc., Trans.*, 1925, **127**, 1992–1997, doi:[10.1039/CT9252701992](https://doi.org/10.1039/CT9252701992).
143. E. Beckmann, *Chem. Ber.*, 1886, **19**, 988–993, doi:[10.1002/cber.188601901222](https://doi.org/10.1002/cber.188601901222).
144. Y. Kikutani, A. Hibar, K. Uchiyama, H. Hisamoto, M. Tokeshia and T. Kitamori, *Lab Chip*, 2002, **2**, 193–196, doi:[10.1039/b208383n](https://doi.org/10.1039/b208383n).
145. N. Miyaura, K. Yamada and A. Suzuki, *Tetrahedron Lett.*, 1979, **20**, 3437–3440, doi:[10.1016/S0040-4039\(01\)95429-2](https://doi.org/10.1016/S0040-4039(01)95429-2).
146. N. Miyaura and A. Suzuki, *J. Chem. Soc., Chem. Commun.*, 1979, 866–867, doi:[10.1039/C39790000866](https://doi.org/10.1039/C39790000866).
147. A. Suzuki, *Pure Appl. Chem.*, 1991, **63**, 419–422, doi:[10.1016/S0969-8043\(02\)00183-5](https://doi.org/10.1016/S0969-8043(02)00183-5).
148. N. Miyaura and A. Suzuki, *Chem. Rev.*, 1995, **95**, 2457–2483, doi:[10.1021/cr00039a007](https://doi.org/10.1021/cr00039a007).
149. A. Suzuki, *J. Organomet. Chem.*, 1999, **576**, 147–168, doi:[10.1016/S0022-328X\(98\)01055-9](https://doi.org/10.1016/S0022-328X(98)01055-9).
150. K. Matos and J. A. Soderquist, *J. Org. Chem.*, 1998, **63**, 461–470, doi:[10.1021/jo971681s](https://doi.org/10.1021/jo971681s).
151. G. B. Smith, G. C. Dezeny, D. L. Hughes, A. O. King and T. R. Verhoeven, *J. Org. Chem.*, 1999, **59**, 8151–8156, doi:[10.1021/jo00105a036](https://doi.org/10.1021/jo00105a036).
152. Y. Uozumi, Y. M. A. Yamada, T. Beppu, N. Fukuyama, M. Ueno and T. Kitamori, *J. Am. Chem. Soc.*, 2006, **128**, 15994–15995, doi:[10.1021/ja066697r](https://doi.org/10.1021/ja066697r).
153. N. T. Phan, J. Khan and P. Styring, *Tetrahedron*, 2005, **61**, 12065–12073,

- doi:10.1016/j.tet.2005.07.109.
154. E. Comer and M. G. Organ, *J. Am. Chem. Soc.*, 2005, **157**, 8160–8167, doi:10.1021/ja0512069.
155. E. Comer and M. G. Organ, *Chem. Eur. J.*, 2005, **11**, 7223–7227, doi:10.1002/chem.200500820.
156. R. K. Arvela, N. E. Leadbeater and M. J. Collins Jr. *Tetrahedron*, 2005, **61**, 9349–9355, doi:10.1016/j.tet.2005.07.063.
157. P. He, S. J. Haswell and P. D. I. Fletcher, *Appl. Catal., A*, 2004, **274**, 111–114, doi:10.1016/j.apcata.2004.05.042.
158. I. R. Baxendale, C. M. Griffiths-Jones, S. V. Ley and G. K. Tranmer, *Chem. Eur. J.*, 2006, **12**, 4407–4416, doi:10.1002/chem.200501400.
159. C. K. Y. Lee, A. B. Holmes, S. V. Ley, I. F. M. Convey, B. Al-Duri, G. A. Leeke, R. C. D. Santos and J. P. K. Seville, *Chem. Commun.*, 2005, 2175–2177, doi:10.1039/b418669a.
160. RSC, *Article Layout*, <<http://www.rsc.org/Publishing/ReSource/AuthorGuidelines/ArticleLayout/sect3.asp>>, 2008 (accessed 21st March 2008).
161. U. Ghosh, D. Ganessunker, V. J. Sattigeri, K. E. Carlson, D. J. Mortensen, B. S. Katzenellenbogen and J. A. Katzenellenbogen, *Bioorg. Med. Chem.*, 2003, **11**, 629–657, doi:10.1016/S0968-0896(02)00309-7.
162. H. Neuvonen, K. Neuvonen, A. Koch, E. Kleinpeter and P. Pasanen, *J. Org. Chem.*, 2002, **67**, 6995–7003, doi:10.1021/jo020121c.
163. M. Gonzalez-Nunez, R. Mello, A. Olmos and G. Asensio, *J. Org. Chem.*, 2006, **71**, 6432–6436, doi:10.1021/jo060753pp.
164. J. Raap, S. Nieuwenhuis, A. Creemers, S. Hexspoor, U. Kragl and J. Lugtenburg, *Eur. J. Org. Chem.*, 1999, 2609–2621, doi:10.1002/(SICI)1099-0690(199910)1999:10<2609::AID-EJOC2609>3.0.CO;2-P.
165. R. S. Bargota, M. Akhtar, K. Biggadike, D. Gani and R. K. Allemann, *Bioorg. Med. Chem. Lett.*, 2003, **13**, 1623–1626, doi:10.1016/S0960-894X(03)00290-7.
166. C. B. Thomas, *J. Chem. Soc. B*, 1970, 430–436, doi:10.1039/J29700000430.

167. K. Fujimoto, Y. Tokuda, H. Maekawa, Y. Matsubara, T. Mizuno and I. Nishiguchi, *Tetrahedron*, 1996, **52**, 3889–3896, doi:[10.1016/S0040-4020\(96\)00056-7](https://doi.org/10.1016/S0040-4020(96)00056-7).
168. B. J. Hall, M. Chebib, J. R. Hanrahan and G. A. Johnston, *Eur. J. Pharmacol.*, 2005, **512**, 97–104, doi:[10.1016/j.ejphar.2005.02.034](https://doi.org/10.1016/j.ejphar.2005.02.034).
169. R. T. C. Brownlee and M. Sadek, *Aust. J. Chem.*, 1981, **34**, 1593–1602, doi:[10.1071/CH9811593](https://doi.org/10.1071/CH9811593).
170. D. H. Russell, B. S. Freiser, E. H. M. Bay and D. C. Canada, *Org. Mass Spectrom.*, 1983, **18**, 474–485, doi:[10.1002/oms.1210181105](https://doi.org/10.1002/oms.1210181105).
171. C. H. Arrowsmith and A. J. Kresge, *J. Am. Chem. Soc.*, 1986, **108**, 7918–7920, doi:[10.1021/ja00285a006](https://doi.org/10.1021/ja00285a006).
172. D. J. Underwood and J. H. Bowie, *J. Chem. Soc., Perkin Trans. 2*, 1977, 1670–1674, doi:[10.1039/P29770001670](https://doi.org/10.1039/P29770001670).
173. S. Tasadaque, A. Shah, K. M. Khan, H. Hussain, M. U. Anwar, M. Feckera and W. Voelter, *Tetrahedron*, 2005, **61**, 6652–6656, doi:[10.1016/j.tet.2005.03.126](https://doi.org/10.1016/j.tet.2005.03.126).
174. C.-T. Chen and Y. S. Munot, *J. Org. Chem.*, 2005, **70**, 8627–8627, doi:[10.1021/jo051337s](https://doi.org/10.1021/jo051337s).
175. H. Neuvonen, K. Neuvonen and P. Pasanen, *J. Org. Chem.*, 2004, **69**, 3794–3800, doi:[10.1021/jo035521u](https://doi.org/10.1021/jo035521u).
176. D. Hellwinkel, F. Lämmerzahl and G. Hofmann, *Chem. Ber.*, 1983, **116**, 3375–3405, doi:[10.1002/cber.19831161014](https://doi.org/10.1002/cber.19831161014).
177. A. Procopio, R. Dalpozzo, A. D. Nino, L. Maiuolo, B. Russo and G. Sindonab, *Adv. Synth. Catal.*, 2004, **346**, 1465–1470, doi:[10.1002/adsc.200404132](https://doi.org/10.1002/adsc.200404132).
178. K. J. P. Yoon, C. L. Morton, P. M. Potter, M. K. Danksa and R. E. Lee, *Bioorg. Med. Chem.*, 2003, **11**, 3237–3244, doi:[10.1016/S0968-0896\(03\)00302-X](https://doi.org/10.1016/S0968-0896(03)00302-X).
179. T. Shintou and T. Mukaiyama, *J. Am. Chem. Soc.*, 2004, **126**, 7359–7367, doi:[10.1021/ja0487877](https://doi.org/10.1021/ja0487877).
180. B. Torto, D. Obeng-Ofori, P. G. N. Njagi, A. Hassanali and H. Amiani, *J. Chem. Ecol.*, 1994, **20**, 1749–1761, doi:[10.1007/BF02059896](https://doi.org/10.1007/BF02059896).

181. J. R. L. Smith and P. R. Sleath, *J. Chem. Soc., Perkin Trans. 2*, 1983, 621–628, doi:[10.1039/P29830000621](https://doi.org/10.1039/P29830000621).
182. T. A. Molenaar-Langeveld, S. Ingemann and N. M. M. Nibbering, *Org. Mass Spectrom.*, 1993, **28**, 1167–1178, doi:[10.1002/oms.1210281031](https://doi.org/10.1002/oms.1210281031).
183. W.-B. Pan, F.-R. Chang, L.-M. Wei, M.-J. Wu and Y.-C. Wu, *Tetrahedron Lett.*, 2003, **44**, 331–334, doi:[10.1016/S0040-4039\(02\)02578-9](https://doi.org/10.1016/S0040-4039(02)02578-9).
184. J. Yoon, C. Sheu, K. N. Houk, C. B. Knobler and D. J. Cram, *J. Org. Chem.*, 1996, **61**, 9323–9339, doi:[10.1021/jo9612786](https://doi.org/10.1021/jo9612786).
185. A. Makriyannis and S. Fesik, *J. Am. Chem. Soc.*, 1982, **104**, 6462–6463, doi:[10.1021/ja00387a058](https://doi.org/10.1021/ja00387a058).
186. G. J. Van-Berkel and K. G. Asano, *Anal. Chem.*, 1994, **66**, 2096–2102, doi:[10.1021/ac00085a027](https://doi.org/10.1021/ac00085a027).
187. H. Ulrich, D. V. Rao, B. Tucker and A. A. R. Sayigh, *J. Org. Chem.*, 1974, **39**, 2437–2438, doi:[10.1021/jo00930a032](https://doi.org/10.1021/jo00930a032).
188. K. A. Agrios and M. Srebnik, *J. Org. Chem.*, 1993, **58**, 6908–6910, doi:[10.1021/jo00076a066](https://doi.org/10.1021/jo00076a066).
189. E. Elhalem, B. Bailey, R. Docampo, I. Ujvary, S. Szajnman and J. Rodriguez, *J. Med. Chem.*, 2002, **45**, 3984–3999, doi:[10.1021/jm0201518](https://doi.org/10.1021/jm0201518).
190. Y. Watanabe, S. Oae and T. Iyanagi, *Bull. Chem. Soc. Jpn.*, 1982, **55**, 188–195, doi:[10.1246/bcsj.55.188](https://doi.org/10.1246/bcsj.55.188).
191. P. Brown, *Org. Mass Spec.*, 1969, **2**, 1085–1101, doi:[10.1002/oms.1210021107](https://doi.org/10.1002/oms.1210021107).
192. J. M. Nulty, A. Capretta, V. Laritchev, J. Dyck and A. J. Robertson, *J. Org. Chem.*, 2003, **68**, 1597–1600, doi:[10.1021/jo026639y](https://doi.org/10.1021/jo026639y).
193. G. C. Galletti, G. Dinelli and G. Chiavari, *J. Mass Spectrom.*, 1995, **30**, 333–338, doi:[10.1002/jms.1190300216](https://doi.org/10.1002/jms.1190300216).
194. W. Su and H. Cai, *J. Chem. Res.*, 2004, 414–415.
195. Y. A. Ibrahim, K. Kaul and N. A. Al-Awadi, *Tetrahedron*, 2001, **57**, 10171–10176, doi:[10.1016/S0040-4020\(01\)01040-7](https://doi.org/10.1016/S0040-4020(01)01040-7).
196. C.-T. Chen, J.-H. Kuo, V. D. Pawar, Y. S. Munot, S.-S. Weng, C.-H. Ku and C.-Y. Liu, *J. Org. Chem.*, 2005, **70**, 1188–1197, doi:[10.1021/jo048363v](https://doi.org/10.1021/jo048363v).
197. K. Kobayashi, E. Koyama, C. Kono, K. Namatame, K. Nakamura and N. Fu-

- rukawa, *J. Org. Chem.*, 2001, **66**, 2085–2090, doi:[10.1021/jo001645k](https://doi.org/10.1021/jo001645k).
198. A. L. Maycock and G. A. Berchtold, *J. Org. Chem.*, 1970, **35**, 2532–2538, doi:[10.1021/jo00833a014](https://doi.org/10.1021/jo00833a014).
199. C. J. Bennett, S. T. Caldwell, D. B. M. Phail, P. C. Morrice, G. G. Duthie and R. C. Hartley, *Bioorg. Med. Chem.*, 2004, **12**, 2079–2098, doi:[10.1016/j.bmc.2004.02.031](https://doi.org/10.1016/j.bmc.2004.02.031).
200. T. Yuzuri, H. Suezawa and M. Hirota, *Bull. Chem. Soc. Jpn.*, 1994, **67**, 1664–1673, doi:[10.1246/bcsj.67.1664](https://doi.org/10.1246/bcsj.67.1664).
201. M. E. Smith and H. Adkins, *J. Am. Chem. Soc.*, 1938, **60**, 657–663, doi:[10.1021/ja01270a048](https://doi.org/10.1021/ja01270a048).
202. N. A. Al-Awadi, B. J. George, H. H. Dib, M. R. Ibrahim, Y. A. Ibrahim and O. M. El-Dusouqui, *Tetrahedron*, 2005, **61**, 8257–8263, doi:[10.1016/j.tet.2005.06.028](https://doi.org/10.1016/j.tet.2005.06.028).
203. C. A. Faler and M. M. Joullié, *Tetrahedron Lett.*, 2006, **47**, 7229–7231, doi:[10.1016/j.tetlet.2006.07.136](https://doi.org/10.1016/j.tetlet.2006.07.136).
204. I. Azumaya, H. Kagechika, Y. Fujiwara, M. Itoh, K. Yamaguchi and K. Shudo, *J. Am. Chem. Soc.*, 1991, **113**, 2833–2838, doi:[10.1021/ja00008a005](https://doi.org/10.1021/ja00008a005).
205. Y. Wan, M. Alterman, M. Larhed and A. Hallberg, *J. Org. Chem.*, 2002, **67**, 6232–6235, doi:[10.1021/jo025965a](https://doi.org/10.1021/jo025965a).
206. D. Dubé and A. A. Scholte, *Tetrahedron Lett.*, 1999, **40**, 2295–2298, doi:[10.1016/S0040-4039\(99\)00211-7](https://doi.org/10.1016/S0040-4039(99)00211-7).
207. M. W. Khan and A. M. Reza, *Tetrahedron*, 2005, **61**, 11204–11210, doi:[10.1016/j.tet.2005.09.032](https://doi.org/10.1016/j.tet.2005.09.032).
208. P. A. S. Smith and E. P. Antoniades, *Tetrahedron*, 1960, **9**, 210–229, doi:[10.1016/0040-4020\(60\)80010-5](https://doi.org/10.1016/0040-4020(60)80010-5).
209. G. C. G. Pais, X. Zhang, C. Marchand, N. Neamati, K. Cowansage, E. S. Svarovskaia, V. K. Pathak, Y. Tang, M. Nicklaus, Y. Pommier and J. Terrence R. Burke, *J. Med. Chem.*, 2002, **45**, 3184–3194, doi:[10.1021/jm020037p](https://doi.org/10.1021/jm020037p).
210. D. A. Peak and T. I. Watkins, *J. Chem. Soc.*, 1950, 445–452, doi:[10.1039/JR9500000445](https://doi.org/10.1039/JR9500000445).
211. M. Kunishima, C. Kawachi, J. Monta, K. Terao, F. Iwasaki and S. Tani,

- Tetrahedron*, 1999, **55**, 13159–13170, doi:[10.1016/S0040-4020\(99\)00809-1](https://doi.org/10.1016/S0040-4020(99)00809-1).
212. G. R. Pettut and R. E. Kadunce, *J. Org. Chem.*, 1962, **27**, 4566–4570, doi:[10.1021/jo01059a106](https://doi.org/10.1021/jo01059a106).
213. R. E. Mayo and J. H. Goldstein, *Mol. Phys.*, 1966, **10**, 301–307, doi:[10.1080/00268976600100411](https://doi.org/10.1080/00268976600100411).
214. R. G. Cooks, I. Howe, S. W. Tam and D. H. Williams, *J. Am. Chem. Soc.*, 1968, **90**, 4064–4069, doi:[10.1021/ja01017a025](https://doi.org/10.1021/ja01017a025).
215. S. Safe, *Org. Mass Spectrom.*, 1971, **5**, 1221–1226, doi:[10.1002/oms.1210051011](https://doi.org/10.1002/oms.1210051011).

APPENDIX A

REACTOR CHARACTERISTICS

The following Appendix provides a reference of the most significant characteristics of the the micro reactors and PEEK™ tubing used for the work contained within this thesis. Detailed listings are provided within Section A.5 which follows the example calculations below.

A.1 Dimensions and Characteristics

In order to clarify the methods of calculation employed, which give rise to the data given in Section A.5, example calculations using the dimensions of micro reactor T1 are given below. The mask width was 50 μm and flow rate taken as 1 μl min⁻¹ for all calculations. The channel length, L_c , refers to the channel which has one of its end points connected to the other at a 90° angle.

According to Figure 48 which illustrates an ideal isotropically etched channel the depth, σ_c , may be calculated as half of the difference between the mask width, w_M and the measured channel width, w_C , as follows:

$$\begin{aligned}\sigma_c &= \frac{1}{2}(w_C - w_M) \\ &= \frac{1}{2} \times (201 \times 10^{-6} \text{ m} - 50 \times 10^{-6} \text{ m}) \\ &= 75.5 \times 10^{-6} \text{ m} = 75.5 \mu\text{m}\end{aligned}\tag{34}$$

From this is then possible to calculate the cross sectional area, A_c , which will be

equal to half the area of a circle with radius $r = \sigma_c$, plus the product of the depth, σ_c , and the mask width, w_M as follows:

$$\begin{aligned}
 A_c &= (w_M \sigma_c) + (1/2 \pi \sigma_c^2) & (35) \\
 &= (50 \times 10^{-6} \text{ m} \times 7.55 \times 10^{-5} \text{ m}) + (1/2 \times \pi \times (7.55 \times 10^{-5} \text{ m})^2) \\
 &= (3.78 \times 10^{-9} \text{ m}^2) + (8.95 \times 10^{-9} \text{ m}^2) \\
 &= 1.27 \times 10^{-8} \text{ m}^2 = 12\,729 \mu\text{m}^2
 \end{aligned}$$

Thus the volume of the micro reactor channel, V_c , is the product of its length, L_c , and the cross sectional area, A_c , given by:

$$\begin{aligned}
 V_c &= A_c L_c & (36) \\
 &= 1.27 \times 10^{-8} \text{ m}^2 \times 0.02 \text{ m} \\
 &= 2.55 \times 10^{-10} \text{ m}^3 = 2.55 \times 10^{-7} \text{ dm} = 255 \text{ nl}
 \end{aligned}$$

In order to determine the surface to volume ratio (S/V) the wetted perimeter, Θ_c , of the channel cross section must first be calculated, as shown below:

$$\begin{aligned}
 \Theta_c &= w_c + w_M + \pi \sigma_c & (37) \\
 &= 201 \times 10^{-6} \text{ m} + 50 \times 10^{-6} \text{ m} + (\pi \times 75.5 \times 10^{-6} \text{ m}) \\
 &= 4.88 \times 10^{-4} \text{ m} = 488 \mu\text{m}
 \end{aligned}$$

The surface to volume ratio, S/V , may then be calculated by dividing the product

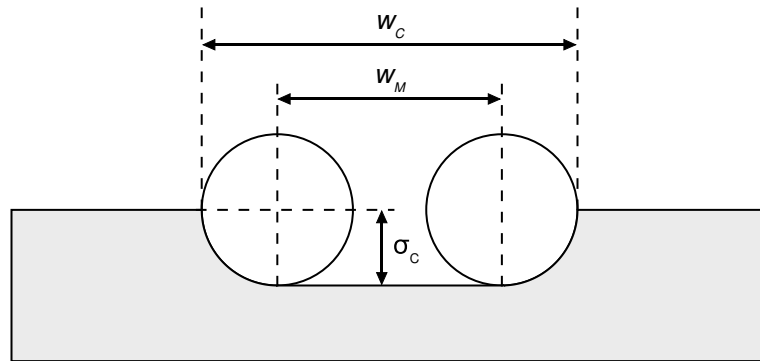


Figure 48. Schematic diagram illustrating the relationship between mask width (w_M), channel width (w_c) and channel depth (σ_c), employed for the calculation of characteristic micro reactor variables.

of the wetted perimeter, Θ_c , and channel length, L_c , with the channel volume, V_c , in the following way:

$$s/V = \frac{\Theta_c L_c}{V_c} \quad (38)$$

$$= \frac{4.88 \times 10^{-4} \text{ m} \times 0.02 \text{ m}}{2.55 \times 10^{-10} \text{ m}^3} = 38\,274.5 \text{ m}^{-1} = 382.7 \text{ cm}^{-1}$$

The linear flow rate, Φ_L , may also be calculated using the cross sectional area, A_c , for a given flow rate, Φ_v , demonstrated below for a flow rate of $1 \mu\text{l min}^{-1}$, which is equal to $1/60 \times 10^{-9} \text{ m}^3 \text{ s}^{-1}$:

$$\Phi_L = \frac{\Phi_v}{A_c} \quad (39)$$

$$= \frac{1/60 \times 10^{-9} \text{ m}^3 \text{ s}^{-1}}{1.27 \times 10^{-8} \text{ m}^2} = 1.31 \times 10^{-3} \text{ m s}^{-1} = 1.31 \text{ mm s}^{-1}$$

Finally the residence time, R_T , at a given flow rate is simply calculated by dividing the mixing channel length, L_c , into the linear flow rate, Φ_L :

$$R_T = \frac{L_c}{\Phi_L} \quad (40)$$

$$= \frac{0.02 \text{ m}}{1.31 \times 10^{-3} \text{ m s}^{-1}} = 15.24 \text{ s}$$

A.2 Reynolds Numbers

Equation 22 provides a way to calculate Reynolds numbers for cylindrical geometries however in the case of an isotropically etched micro reactor channel it is necessary to derive the hydraulic diameter, δ_r , as a function of the area and wetted perimeter. Since the cross sectional area of a circular tube, A_r , is given by:

$$A_r = 1/4 \pi \delta_r^2 \quad (41)$$

where δ_r is the diameter (m) and the circumference, or wetted perimeter, Θ_r , is given by:

$$\Theta_r = \pi \delta_r \quad (42)$$

combination of the two equations gives rise to the modified expression for the diameter of a no-circular cross section, δ_c , to be:

$$\delta_c = \frac{4A_c}{\Theta_c} \quad (43)$$

By substituting this expression into Equation 22 Reynolds numbers for the micro reactors were calculated. As an example the Reynolds number for DMF ($\rho = 0.949 \text{ g ml}^{-1}$) within micro reactor T1 at a flow rate of $1 \mu\text{l min}^{-1}$ may be determined as follows:

$$\begin{aligned} Re(DMF) &= \frac{\rho(\frac{4A_c}{C_c})\Phi_L}{\eta} \quad (44) \\ &= \frac{949 \text{ kg m}^{-3} \times (\frac{4 \times 1.27 \times 10^{-8} \text{ m}^2}{4.88 \times 10^{-4} \text{ m}}) \times 1.31 \times 10^{-3} \text{ m s}^{-1}}{9.2 \times 10^{-4} \text{ kg m}^{-1} \text{ s}^{-1}} = 0.14 \end{aligned}$$

All of the Reynolds numbers quoted within this Appendix were calculated in an analogous way using their related values.

A.3 Back Pressures

Back pressures were calculated using Equation 30, introduced in Section 1.2.5. The following example calculation is the pressure change across the mixing channel of micro reactor T1 when DMF is infused at a flow rate of $1 \mu\text{l min}^{-1}$:

$$\begin{aligned} P &= \frac{\Phi_v \eta L_c \Theta_c^4}{2\pi A_c^4} \quad (30) \\ P &= \frac{1/60 \times 10^{-9} \text{ m}^3 \text{ s}^{-1} \times 9.2 \times 10^{-4} \text{ kg m}^{-1} \text{ s}^{-1} \times 0.02 \text{ m} \times (4.88 \times 10^{-4} \text{ m})^4}{2 \times \pi \times (1.27 \times 10^{-8} \text{ m}^2)^4} \\ &= 106 \text{ kg m}^{-1} \text{ s}^{-2} \quad (45) \end{aligned}$$

A.4 Fourier Numbers

Fourier numbers for all micro reactors and PEEK™ tubing have been calculated using Equation 24 and the diffusion coefficients of acetic acid in EtOAc ($2.18 \times 10^{-9} \text{ m}^2 \text{ s}^{-1}$ at 20°C) and aniline **15** in benzene ($1.97 \times 10^{-9} \text{ m}^2 \text{ s}^{-1}$ at 25°C) as examples. The value for the time, t , used in the calculations was taken as the residence time, R_T , at a volumetric flow rate, Φ_v , of $1 \mu\text{l min}^{-1}$ and the characteristic distance as half of the channel width, w_c . The following example uses the values previously determined for micro reactor T1 and the diffusion coefficient of acetic acid in EtOAc.

$$Fo = \frac{Dt}{x^2} = \frac{DR_T}{(\frac{1}{2}w_c)^2} \quad (46)$$

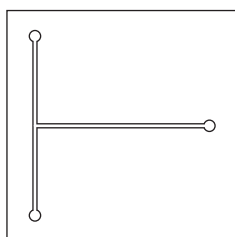
$$= \frac{2.18 \times 10^{-9} \text{ m}^2 \text{ s}^{-1} \times 15.24 \text{ s}}{(100.5 \times 10^{-6} \text{ m})^2} = 3.3$$

Further Fourier numbers provided within the following section were calculated in an analogous way.

A.5 Micro Reactor Data

The data given below for each micro reactor has been calculated using the methods outlined above based on a mask width, w_m , of $50 \mu\text{m}$. Where more than one channel is present in the design the channel lengths, L_c , given refer to the mixing channels (*i.e.* the distance from the point of confluence between two channels which are 90° apart and the end of the adjoining channel, or point at which another channel intersects). Related values were calculated assuming an overall flow rate of $1 \mu\text{l min}^{-1}$ for ease of scaling, against which the residence times of micro reactors were determined. Solvents for which Reynolds numbers (Re) and back pressures (P) are given were selected based upon the occurrence within the text, and are provided to confirm the laminar profile of reagent streams when mobilised through the micro reactors described.

Micro Reactor T1

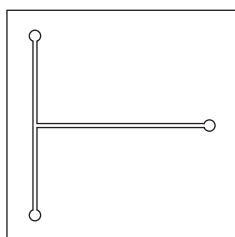


Width 201 μm
 Height 76 μm
 Length 2.0 cm
 Volume 255 nl
 Θ_c 488 μm
 A_c 12 729 μm^2

Solvent	η (cPas)	Re	P (Pa)
DMF	0.92	0.14	106
MeCN	0.37	0.29	42
THF	0.55	0.22	63
H ₂ O	0.89	0.15	103

Surface/Volume Ratio 384 cm^{-1}
 Linear Flow Rate 1.3 mm s^{-1}
 Residence Time 15 s
 Fo Acetic acid in EtOAc 3.3
 Fo Aniline **15** in Benzene 3.0

Micro Reactor T2

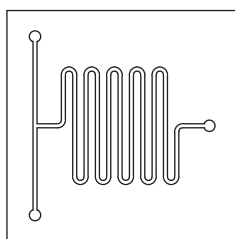


Width 158 μm
 Height 54 μm
 Length 1.5 cm
 Volume 109 nl
 Θ_c 378 μm
 A_c 7280 μm^2

Solvent	η (cPas)	Re	P (Pa)
DMF	0.92	0.18	265
MeCN	0.37	0.38	107
THF	0.55	0.29	158
H ₂ O	0.89	0.20	258

Surface/Volume Ratio 519 cm^{-1}
 Linear Flow Rate 2.3 mm s^{-1}
 Residence Time 7 s
 Fo Acetic acid in EtOAc 2.3
 Fo Aniline **15** in Benzene 2.1

Micro Reactor S1

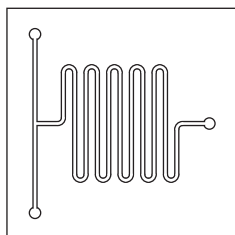


Width 150 μm
 Height 50 μm
 Length 12.1 cm
 Volume 778 nl
 Θ_c 357 μm
 A_c 6427 μm^2

Solvent	η (cPas)	Re	P (Pa)
DMF	0.92	0.19	2814
MeCN	0.37	0.40	1132
THF	0.55	0.30	1682
H ₂ O	0.89	0.21	2734

Surface/Volume Ratio 556 cm^{-1}
 Linear Flow Rate 2.6 mm s^{-1}
 Residence Time 47 s
 Fo Acetic acid in EtOAc 18.1
 Fo Aniline **15** in Benzene 16.3

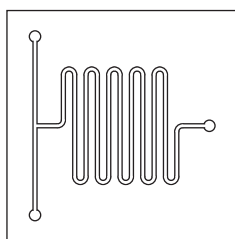
Micro Reactor S2



Width 176 μm
 Height 63 μm
 Length 12.1 cm
 Volume 1136 nl
 Θ_c 424 μm
 A_c 9384 μm^2

Solvent	η (cPas)	Re	P (Pa)
DMF	0.92	0.16	1230
MeCN	0.37	0.33	494
THF	0.55	0.25	735
H ₂ O	0.89	0.18	1195

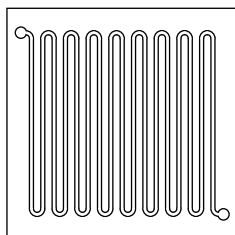
Surface/Volume Ratio 452 cm^{-1}
 Linear Flow Rate 1.8 mm s^{-1}
 Residence Time 68 s
 Fo Acetic acid in EtOAc 19.2
 Fo Aniline **15** in Benzene 17.3

Micro Reactor S₃

Width 170 μm
 Height 60 μm
 Length 23.6 cm
 Volume 2043 nl
 Θ_c 408 μm
 A_c 8655 μm^2

Solvent	η (cPas)	Re	P (Pa)
DMF	0.92	0.17	2858
MeCN	0.37	0.35	1149
THF	0.55	0.26	1709
H ₂ O	0.89	0.18	2777

Surface/Volume Ratio 472 cm^{-1}
 Linear Flow Rate 1.9 mm s^{-1}
 Residence Time 123 s
 Fo Acetic acid in EtOAc 37.0
 Fo Aniline **15** in Benzene 33.4

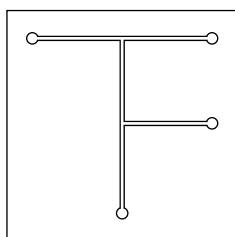
Micro Reactor R_TU

Width 195 μm
 Height 73 μm
 Length 45.1 cm
 Volume 5359 nl
 Θ_c 398 μm
 A_c 11 882 μm^2

Solvent	η (cPas)	Re	P (Pa)
DMF	0.92	0.15	2759
MeCN	0.37	0.30	1110
THF	0.55	0.23	1649
H ₂ O	0.89	0.16	2681

Surface/Volume Ratio 398 cm^{-1}
 Linear Flow Rate 1.4 mm s^{-1}
 Residence Time 322 s
 Fo Acetic acid in EtOAc 73.7
 Fo Aniline **15** in Benzene 66.6

Micro Reactor dT



Width 150 μm
 Height 50 μm
 Length 0.7 cm
 Volume 45 nl
 Θ_c 357 μm
 A_c 6427 μm^2

Solvent	η (cPas)	Re	P (Pa)
DMF	0.92	0.19	163
MeCN	0.37	0.40	66
THF	0.55	0.30	97
H ₂ O	0.89	0.21	158

Surface/Volume Ratio 556 cm^{-1}
 Linear Flow Rate 2.6 mm s^{-1}
 Residence Time 3 s
 Fo Acetic acid in EtOAc 1.1
 Fo Aniline **15** in Benzene 1.0

PEEK™ Tubing



I.d. 150 μm
 Length 1.0 cm
 Volume 177 nl
 Θ_r 471 μm
 A_r 17 672 μm^2

Solvent	η (cPas)	Re	P (Pa)
DMF	0.92	0.15	12
MeCN	0.37	0.30	5
THF	0.55	0.23	7
H ₂ O	0.89	0.16	12

Surface/Volume Ratio 267 cm^{-1}
 Linear Flow Rate 0.9 mm s^{-1}
 Residence Time 11 s
 Fo Acetic acid in EtOAc 4.1
 Fo Aniline **15** in Benzene 3.7

APPENDIX B

CHN ANALYSIS

There follows reproduction of an email received on 21st September 2006 from the engineer, Paul Hemming of Exeter Analytical Limited (UK), who services the CE440 combustion analysis instrument, housed within The Department of Chemistry at the University of Hull. It explains how to calculate the expected CHN values for a compound that contains a mixture of hydrogen and deuterium atoms when undertaking combustion analysis using the CE440.

THE ANALYSIS OF DEUTERIUM COMPOUNDS ON THE CE440

- INTRODUCTION

The hydrogen atom and molecule are an important part of theoretical chemistry. The fundamental differences between hydrogen and deuterium or their compounds stem from their differences in mass. This in turn affects their fundamental vibration frequencies and hence their zero point energies, these plays an important role in the identification of deuterium compounds.

The determination of the deuterium content of a partially deuterated substance can be made by mass spectroscopy, infra red spectroscopy or density measurement (after conversion to water).

- PROCEDURE

You will note that at no time did we mention the CE440 as a means of determining

the deuterium content of a partially deuterated compounds. This is simply because the CE440 is unable to differentiate between hydrogen and deuterium. The CE440 measures both hydrogen and its most common isotope deuterium as hydrogen.

To calculate the relevant amounts of hydrogen and deuterium in a compound *via* CHN analysis on the CE440 you have to make some assumptions that could be wrong and hence this calculation should only be carried out if all parties concerned are aware of this.

Hydrogen has a mass of 1.0078 Deuterium has a mass of 2.0141

As a good approximation any hydrogen determined *via* the CE440 that is in fact deuterium needs to be doubled in value. It actually calculates out to be 1.9985 but for this illustration we shall use 2.

As an example if a compound had the theoretical values of C 55.10 % H 4.20 % N 8.20 % and D 2.10 % when the analysis were carried out and if the compound is likely to be pure we would in ideal circumstances find C 55.10 % H 5.25 % and N 8.20 % if this were the case it would be a reasonable assumption to assume that the compound is likely to be pure and to calculate the content of D, to do this we would do the following calculation.

$$\text{D content} = (\% \text{ H found} - \% \text{ Theoretical H content}) \times 2 \quad (47)$$

For the above example this would, in ideal circumstances, be:

$$(5.25 - 4.20) \times 2 = 2.10 \quad (48)$$

which, in this case, represents the theoretical content of deuterium.

Under these circumstances this is likely to be an accurate representation of the deuterium content but CHN analysis alone is not enough to be sure that this assumption is correct. It is possible to obtain CHN analysis figures that agree with theoretical values for a specific compound but unfortunately there is no guarantee that this is the only compound that these figures agree with you could

have another pure compound that has the same theoretical figures or an impure compound with the same figures. To confirm the structural determination of a compound CHN analysis must be used in association with other analytical techniques such as NMR and mass spectroscopy. A simple analogy is that of a jigsaw, until you have all the pieces the picture is not complete.

APPENDIX C

PUBLICATIONS

1. J. Hooper, P. Watts and C. Wiles, 15th International Isotope Society (UK group) Symposium, *J. Labelled Compd. Radiopharm.*, 2006, **49**, 377–420, doi:[10.1002/jlcr.1056](https://doi.org/10.1002/jlcr.1056).
2. J. Hooper and P. Watts, Expedient synthesis of deuterium-labelled amides within micro-reactors, *J. Labelled Compd. Radiopharm.*, 2007, **50**, 189–196, doi:[10.1002/jlcr.1254](https://doi.org/10.1002/jlcr.1254).
3. J. Hooper, P. Watts and C. Wiles, Deuterated isotope labelling of phenol derivatives within micro reactors, *Micro Nano Fluid.*, 2008, In Press, doi:[10.1007/s10404-008-0274-8](https://doi.org/10.1007/s10404-008-0274-8).